Parameter identification based on artificial intelligence optimization and distributed tracking control of fractional-order multi-agent systems

Wei Hu

N^o *d'ordre*: | 3 | 7 | 6 |

CENTRALE LILLE

THESE

Présentée en vue
d'obtenir le grade de

DOCTEUR

En

Spécialité : Automatique, Géie informatique, Traitement du Signal et des Images

Par

Wei HU

DOCTORAT DELIVRE PAR CENTRALE LILLE

Titre de la thèse :

Identification de Paramètre basée sur l'Optimisation de l'Intelligence Artificielle et le Contrôle de Suivi Distribué des Systèmes Multi-agents d'Ordre Fractionnaire

Parameter Identification based on Artificial Intelligence Optimization and Distributed Tracking Control of Fractional-order Multi-agent Systems

---

Soutenue le 10 Juillet 2019 devant le jury d'examen :

Président	Mme. Nathalie MITTON	Directrice de Recherche, INRIA Lille-Nord Europe
Rapporteur	M. Pierre MELCHIOR	Professeur, University of Bordeaux, France
Rapporteur	M. Yangquan CHEN	Professeur, University of California, Merced, USA
Membre	Mme. Nathalie MITTON	Directrice de Recherche, INRIA Lille-Nord Europe
Membre	M. Yongguang YU	Professeur, Beijing Jiaotong University, China
Membre	M. Guoguang WEN	Professeur Associé, Beijing Jiaotong University, China
Membre	Mme. Zhaoxia PENG	Professeur Associée, Beihang University, China
Directeur de thèse	M. Ahmed RAHMANI	Professeur, Centrale Lille, France

Thèse préparée au Centre de Recherche en Informatique Signal et Automatique de Lille
CRIStAL, UMR CNRS 9189 - Centrale Lille
Ecole Doctorale SPI 072

À mes parents,

à toute ma famille,

à mes professeurs,

et à mes chèr(e)s ami(e)s.

Acknowledgements

This research work has been realized in Centrale Lille, in "Centre de Recherche en Informatique, Signal et Automatique de Lille (CRIStAL)", with the research team "Méthodes & Outils pour la Conception Intégrée de Systèmes (MOCIS)".

First of all, I would like to express my sincere appreciation and thanks to my supervisor Mr. Ahmed RAHMANI, who has offered his continuous advice and insight throughout the course of this thesis. With his guidance, patience and understanding, I have obtained a lot of experiences in research, these will be invaluable on both my future study as well as my career, and encourage me to grow as an independent thinker. I thank him for everything he has done for me.

Besides, I also would like to thank all the members of jury for their valuable time to review this thesis. Their invaluable comments and objective criticisms which shed a light on my drawbacks and the research road in future. Meanwhile, I would like to thank Mr. Belkacem Ould Bouamama, who is the leader of the group MOCIS in CRIStAL Lab, for providing many opportunities to exchange academic ideas with other group members.

In particular, I would like to gratefully thank my master supervisor Mr. Yongguang YU in China, he gives me much help and advice in research. In addition, I am very grateful for the help of Mr. Guoguang WEN, he has provided me much guidance and suggestions during my thesis.

In addition, I would like to thank my Ph.D. colleagues Xing CHU, Yan WEI, Wei JIANG, Thanh Binh Do, Yunlong ZHANG, etc. And I also want to express my great thanks to the staff at Centrale Lille, Brigitte FONCEZ, Patrick GALLAIS and Vanessa FLEURY for their kindly help.

My Ph.D. study was supported and funded by CSC (China Scholarship Council). Therefore, I would like to thank all the people who have contributed to select candidates for this interesting project and given me this precious opportunity.

ACKNOWLEDGEMENTS

Finally, and most importantly, I would like to thank my parents and my wife Wenjuan GU for their love and support.

Villeneuve d'Ascq, France *Wei HU*
July, 2019

Contents

List of Figures

List of Tables

Abbreviations and notations

List of abbreviations

MASs	multi-agent systems
FOMASs	fractional-order multi-agent systems
HFOMASs	heterogeneous fractional-order multi-agent systems
AIOAs	artificial intelligence optimization algorithms
ABC	artificial bee colony
mABC	modified artificial bee colony
DE	differential evolution
PSO	particle swarm optimization
CS	cuckoo search
UUB	uniformly ultimately bounded
LMI	linear matrix inequality
OBL	opposition-based learning
OGJ	opposition-based generation jumping
J_r	jumping rate
PID	proportional-integral-derivative
FOPID	fractional-order proportional-integral-derivative

Abbreviations and notations

List of notations

C	the set of complex numbers
R	the set of real numbers
R^n	the n-dimensional Euclidean real vector space
$R^{m\times n}$	the $m \times n$ real matrix space
I_n	n-dimensional identity matrix
$\mathbf{1}_n(\mathbf{0}_n)$	N-dimensional column vector with each element being 1(0)
$\otimes$	Kronecker product
$\lVert \cdot \rVert$	Euclidian norm
$\lvert m\rvert$	the absolute value of a scaler m
$M > 0$	M is symmetric positive definite matrix
$\lambda(M)$	the eigenvalues of a matrix M
$\lambda_i(M)$	the ith eigenvalue of a matrix M
$\lambda_{min}(M)$	the minimal eigenvalue of a matrix M
$\lambda_{max}(M)$	the maximal eigenvalue of a matrix M
$*$	symmetric part in a symmetric matrix
M^T	the transpose of matrix M
M^{-1}	the inversion of square matrix M
$diag\{a_1, \cdots, a_n\}$	the diagonal matrix with diagonal elements being $a_1, \cdots, a_n$
$det(M)$	determinant of square matrix M

Chapter 1

Introduction

Contents

1.1 Background and motivation

In the past two decades, **multi-agent systems (MASs)** have attracted increasing attention from researchers in various fields, such as physics, mathematics, engineering, biology, sociology and control theory. This is partly due to its potential applications, including biological systems, vehicle formation, and group decision making problems, to name a few (see Fig. 1.1). The advancements are that a group of networked autonomous agents can perform tasks more efficiently than a single agent or can accomplish tasks not executable by a single one.

Moreover, networked MASs have advantages like increasing tolerance to possible vehicle fault, providing flexibility to the task execution or taking advantage of distributed sensing and actuation.

(a)

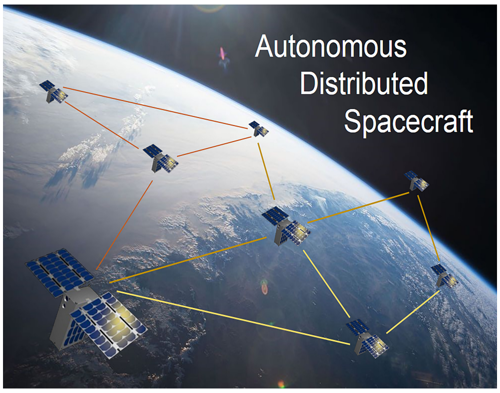

(b)

(c)

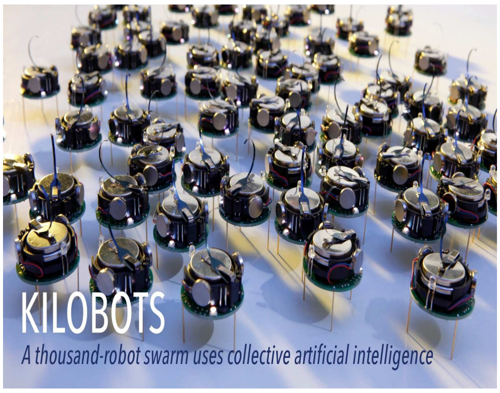

(d)

Fig. 1.1. Examples of multi-agent systems in practice applications

Considering the advantages of the MASs, the control of the MASs has received increasing demands. Currently, two approaches are commonly used for controlling MASs: the centralized approach and the distributed coordination approach (Cao *et al.*, 2013). **The centralized approach** is based on the assumption that a central station is available and sufficiently powerful to control a whole group of vehicles which can be described as Fig. 1.2a. Essentially, the centralized approach is a direct extension of the traditional single-agent-based control philosophy and strategy. On the contrary, as shown in Fig. 1.2b, **the distributed coordination approach** does not require a central station for control, at the cost of becoming far more complex in structure and organization. Although both approaches are considered to be practical depending on the situations and conditions of the real applications, the distributed coordination approach is believed more promising due to many inevitable physical constraints such as limited resources and energy, short wireless communication ranges, narrow bandwidths, and large sizes of vehicles to manage and control. Besides, the distributed coordination owns many advantages, such as low operational costs, less system requirement, high robustness, more adaptive and flexible scalability (Cao *et al.*, 2013). Thus, the distributed coordination of MASs has been applied to many fields in the control community, such as the rendezvous (Lin *et al.*, 2007), robot teams (Peng *et al.*, 2013, 2016), flocking (Olfati-Saber, 2006), formation control (Consolini *et al.*, 2008), consensus (Tian & Liu, 2008) and so on. One challenge in distributed coordination is that the collective group behaviours are achieved only through the interacting of the local information.

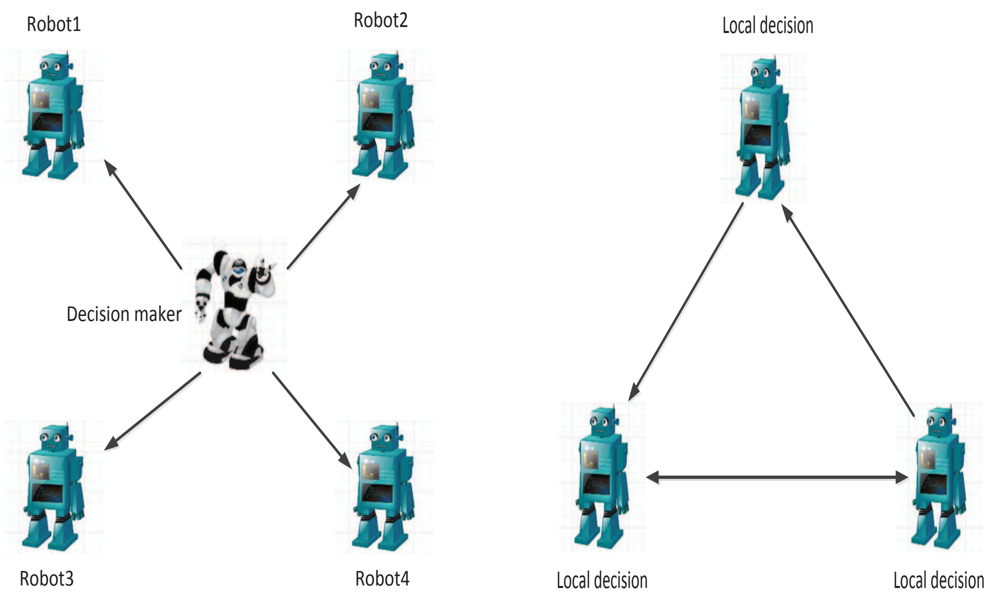

(a) The centralized control **(b)** The distributed coordination control

Fig. 1.2. Two approaches for controlling MASs.

In the last few decades, as a generalization of the ordinary differentiation and integration to arbitrary non-integer order, **fractional calculus** has attracted great attention of many scientists. In fact, the first appearance of the concept of a fractional derivative was found in a letter by the famous mathematician Leibniz in 1695 to Guillaume de l'Hôpital. As far as the existence of such a theory was concerned, the foundation of the subject was laid by Liouville in a paper from 1832.

(a) Leibniz **(b)** Guillaume de l'Hôpital **(c)** Liouville

Fig. 1.3. The important scientists in the history of fractional calculus.

Compared with the classical integer-order systems, **fractional-order systems** provide an excellent instrument for the description of memory and hereditary properties of various materials and processes. In fact, the real-world processes generally or most likely are fractional-order systems, such as phenomenological description of viscoelastic liquids, diffusion and wave propagation, electromagnetic waves, dielectric relaxation phenomena in polymeric material and so on (Podlubny, 1998). In other words, there are many phenomena that cannot or are hard to be interpreted accurately by integer-order dynamics. For example, the consensus motion of agents performs in viscoelastic materials such as macromolecule fluid, porous media, and complicated environments, underwater vehicles operate in lentic lakes composed of microbes and viscoelastic materials, flying vehicles operate in an environment where the influence of particles in air can not be ignored (e.g. high-speed flight in duststorm, rain or snow), and ground vehicles move on top of carpet, sand, muddy road or grass (Cao & Ren, 2010). Therefore, it is more interesting and significant to investigate the distributed coordination of fractional-order multi-agent systems (FOMASs).

Thus, the combination of the distributed coordination control of MASs and fractional calculus leads to a new interdisciplinary subject, namely the **distributed coordination of fractional-order multi-agent systems (FOMASs)**. The objective of this subject is to develop new distributed algorithms for networked FOMASs according to different situations, and improve the effectiveness of MASs from the viewpoint of performance both in accomplishing certain tasks and in the robustness and reliability of the system.

1.2 Overview of distributed coordination of FOMASs

The recent researches on distributed coordination of FOMASs mainly focus on the consensus and formation control. The following subsections will introduce these directions in terms of definition and state of the arts.

1.2.1 Consensus problem

Consensus problem, one of the most important and fundamental issues in the distributed coordination for MASs, has attracted much attention from the researchers in recent years. Among the research topics in consensus of MASs, there are mainly three classes, i.e., leaderless consensus, leader-following consensus and containment consensus problem. To define these three cases clearly, we first introduce a leader (reference state).

Leader: a leader denotes a control objective or a common interest of the whole multi-agent group, a leader is also regraded as a reference state.

Leaderless consensus: if multi-agents are not required to track a leader, the consensus problem is called leaderless consensus or consensus producing (see as Fig. 1.4).

Leader-following consensus: if multi-agents are required to track a leader, the consensus problem is called leader-following consensus or consensus tracking or synchronization (see as Fig. 1.5).

Fig. 1.4. Leaderless consensus problem

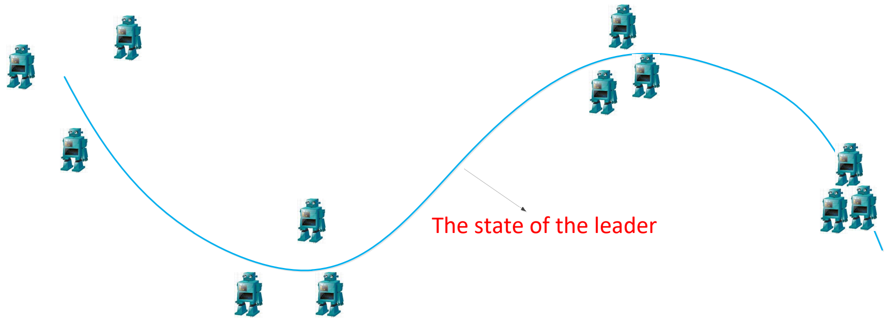

Fig. 1.5. Leader-following consensus problem

Containment consensus: if multi-agents are required to converge to the convex hull spanned by multiple leaders, the consensus problem is called containment consensus (see as Fig. 1.6).

1.2.1.1 Leaderless consensus/consensus producing

For leaderless consensus of MASs, the aim is to design a network distributed control protocol by only using the neighbors' information, such that all agents achieve the desired common goal, which maybe represent attitude, position, ve-

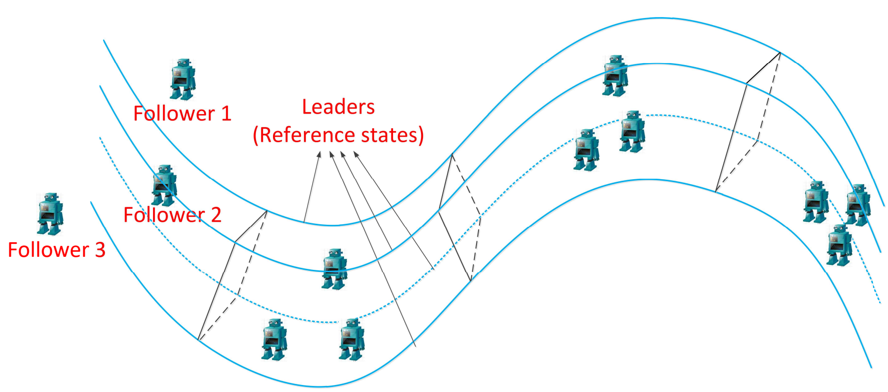

Fig. 1.6. Containment consensus problem

locity, temperature, voltage and so on. Until now, the study of consensus problem for MASs has made great achievements. For example, different kinds of control methods have been proposed to achieve the consensus problem, such as event-triggered control (Dimarogonas *et al.*, 2012), output feedback control (Du *et al.*, 2014) and sliding mode control (Zhao *et al.*, 2012). Besides, different kinds of limited conditions have been considered when agents work in different environment, such as the time delay (Tian & Liu, 2008), parameter uncertainty (Lin & Jia, 2010), external disturbances (Du *et al.*, 2012) and so on.

To the best of our knowledge, the consensus of FOMASs with single integrator was first studied in Cao & Ren (2010) under fixed directed communication topology, where it has been stated that the convergence speed can be improved by using a varying-order fractional-order strategy. Then until now, many results have been obtained by considering different situations and using different kinds of control, which can be summarized as follows.

In many cases, **time delays** occur in practical systems due to the finite switching speed of amplifiers, finite signal propagation time in biological networks, finite chemical reaction times, memory effects, and so on. The existence of time delays in a dynamic system is frequently a source of instability and poor performance. Therefore, stability testing and stabilization of time-delay systems is a problem of practical and theoretical interests. In Shen & Cao (2012), leaderless consensus of single integrator FOMASs under fixed undirected/directed communication topology was studied, where the identical/heterogeneous input delay was considered. In Shen *et al.* (2012), the leaderless consensus of single integrator FOMASs with nonuniform input delays and communication delays were considered separately or together over fixed undirected/directed communication topology. Yang *et al.* (2013b) studied the leaderless consensus of compound-order FOMASs with communication delays under fixed directed communication topology, where there were two groups of MASs with integer-order and fraction-order single integrator dynamics. In Yang *et al.* (2014b), leaderless consensus of single integrator FOMASs with communication delays under fixed directed communication topology was addressed. In Soorki & Tavazoei (2017), leaderless consensus of a generalized linear form of FOMASs with self state and communication uniform time-delays was considered under fixed undirected/directed communication topology. In Liu *et al.* (2017b), leaderless consensus of single integrator FOMASs under fixed directed communication topology was studied, where the state fractional-order derivative was introduced into the existing traditional leaderless consensus protocol and the communication channels with time delay and without time delay cases were considered. In Zhu *et al.* (2017), under fixed directed communication topology, the leaderless consensus of FOMASs with general linear and nonlinear dynamics under input delay was investigated by evaluating the error states. In Liu *et al.* (2018b,d,e), leaderless consensus of single/double/high-order integrator FOMASs with nonuniform input delays was investigated respectively, where the FOMASs with symmetric time delays under fixed undirected communication topology and FOMASs with asymmetric time delays under fixed directed communication topology were considered. In Liu *et al.* (2018c), a state derivative feedback was added into the designed control protocol and the leaderless consensus of FOMASs with symmetric time delays under fixed undirected communication topology and FOMASs with asymmetric time delays under fixed directed communication topology was studied. In Liu *et al.* (2018f), leaderless consensus of a double integrator FOMASs containing two state variables with different fractional orders was researched under symmetric time delays with fixed undirected communication topology and asymmetric time delays with fixed directed communication topology. In Liu *et al.* (2019e), leaderless consensus of nonlinear FOMASs with self state time delay was investigated under fixed directed communication topology by employing the fractional Razumikhin theorem and linear matrix inequalities. In Shi *et al.* (2019b), leaderless consensus of a class of linear FOMASs with input time delay was studied under fixed directed communication topology.

In terms of the control approach, most of the results about the time delays mentioned above are based on the frequency domain analysis and generalized Nyquist stability criterion (Liu *et al.*, 2018b,c,d,e,f, 2017b; Shen & Cao, 2012; Shen *et al.*, 2012; Shi *et al.*, 2019b; Soorki & Tavazoei, 2017; Yang *et al.*, 2013b, 2014b). Besides, Zhu *et al.* (2017) studied the leaderless consensus of FOMASs with input time delays based on the properties of Mittag-Leffler function, matrix theory, stability theory of fractional-order differential equations. Liu *et al.* (2019e) addressed the leaderless consensus of FOMASs with time delay based on the fractional Razumikhin theorem.

In terms of the system dynamics, most of the results are based on the single integrator dynamics (Liu *et al.*, 2018b,c, 2017b; Shen & Cao, 2012; Shen *et al.*, 2012; Shi *et al.*, 2019b; Soorki & Tavazoei, 2017; Yang *et al.*, 2013b, 2014b). Besides, Liu *et al.* (2018e,f) studied the double integrator dynamics, Liu *et al.* (2018d) studied the high-order dynamics. Shi *et al.* (2019b); Zhu *et al.* (2017) studied the FOMASs with nonlinearity.

In some real systems, **parameter uncertainty** is inevitable. In Li (2012), an observer-type leaderless consensus protocol was proposed to deal with the uncertain FOMASs with general linear node dynamics over fixed directed communication topology. In Yin & Hu (2013), leaderless consensus of uncertain FOMASs with general linear node dynamics was investigated based on output feedback under fixed undirected communication topology. In Song *et al.* (2015), leaderless consensus of uncertain FOMASs with general linear node dynamics was studied under fixed undirected communication topology, where the second-order neighbors information was utilised. In Chen *et al.* (2015a), the group leaderless consensus of uncertain FOMASs with general linear node dynamics was investigated based on output feedback under fixed directed communication topology. In summary, all the results were based on the general linear dynamics and the uncertainties were denoted as time-invariant matrices.

External disturbances, such as stochastic noises, external interferences always impacts the system performance and causes the system instability. In Ren & Yu (2016, 2017b), robust leaderless consensus of linear /nonlinear FOMASs with external disturbances was studied based on fixed directed communication topology, where linear control protocol was utilised.

Sometimes, the **unknown nonlinear term and the external disturbance term** cannot usually be observed. Therefore, it is significant to design the valid control laws, which are not necessary to know the specific information, such as the Lipschitz condition of the nonlinearity and the boundedness of the external disturbances. In Bai & Yu (2018); Mo *et al.* (2019), leaderless consensus of uncertain FOMASs was studied under fixed undirected communication topology, where the radial basis function neural networks (RBFNNs) method was proposed to compensate the unknown nonlinear term and the external disturbance term, and the corresponding fractional-order/integer-order adaptation laws were designed respectively to approach the ideal neural network weight matrix of the unknown nonlinear term.

In practice, the control input subjected to the **bounded situation** is very prevalent. In Soorki & Tavazoei (2016), leaderless consensus of FOMASs with general linear dynamics was studied based on undirected/directed communication topology, where two constraints were considered: the input constraint and the restriction on distance of the agents from final destination which should be less than a desired value.

In Yin & Hu (2013), leaderless consensus of **heterogenous** FOMASs modelled by two kinds of general linear dynamics was addressed under fixed directed communication topology.

All of the aforementioned works are concerned with continuous-time FOMASs, some results have been obtained based on **discrete-time systems**. For example, in Yang *et al.* (2013a), leaderless consensus of single integrator FOMASs via sampled control and sampling delay was investigated based on fixed directed communication topology, where the FOMASs was reformulated as discrete-time dynamics by using the definition of Grünwald-Letnikov (GL) fractional derivative. In Malinowska & Odzijewicz (2018), leaderless consensus of discrete-time FOMASs with single/double integrators was studied using optimal control strategy based on fixed undirected communication topology.

In Yang *et al.* (2017), leaderless consensus of FOMAS with **double-integrator** dynamics was studied over fixed directed communication topology. In Shen *et al.* (2017), under switching topologies, leaderless consensus of FOMAS with double-integrator dynamics was studied by applying Mittag-Leffler function, Laplace transform and dwell time technique.

It is known that **sliding mode control** is an effective way to deal with model uncertainty and disturbance in the control of fractional-order systems. In Soorki & Tavazoei (2018), under fixed directed communication topology, leaderless consensus of general linear FOMAS with model uncertainties and external disturbances was investigated based on an adaptive robust sliding mode control, where a fractional-integral sliding manifold was constructed. In Liu *et al.* (2018a), exponential finite-time leaderless consensus of single integrator FOMASs was studied by using the fast sliding mode control over fixed strongly connected communication topology/directed communication topology containing spanning tree. In Bai *et al.* (2017a, 2018), leaderless consensus of single/double integrators FOMASs without/with inherent nonlinearity was addressed based on sliding mode control under fixed directed communication topology.

In practice, continuous control may be infeasible since the controllers are subjected to enormous load of continuously updated information. Besides, in practical of digital sensors and controllers, although the system is always continuous, only the discrete sampled-data at some sampling instances can be used in the control process. Compared with the continuous-time control, continuous-time systems via **sampled-data control** have series of excellent properties such as robustness, flexibility and low cost. Therefore, sampled-data control is more practicable in applications. In Yu *et al.* (2017b), leaderless consensus of single integrator FOMASs was studied via periodic sampled-data control over fixed undirected/directed communication topology. In Liu *et al.* (2019a), leaderless consensus of double integrator FOMASs was investigated over fixed directed communication topology, where periodic sampled-data control was proposed for absolute and relative damping cases.

However, it is pointed out that periodical sampling still leads to a large amount of energy-cost and it may reduce system lifespan consequently. Thus the **event-triggered control strategy** is proposed to solve this problem. In Chen *et al.* (2018c), leaderless consensus of single integrator FOMASs over fixed undirected communication topology was investigated via periodic sampled-data event-triggered control. Besides, in Xu *et al.* (2014), leaderless consensus of single integrator FOMASs based on fixed undirected communication topology was studied using centralized/distributed event-triggered sampled-data control, where the exclusion of the Zeno behavior was not guaranteed. In Ren *et al.* (2019), leaderless consensus of general linear FOMASs over fixed undirected communication topology was investigated through distributed event-triggered strategy, where the Zeno behavior could be precluded to ensure the feasibility of the devised event-triggered strategy.

Most of the works on leaderless consensus of FOMASs were devoted to design the state feedback control protocol using the state information of agents directly. However, during practical implementation, under some circumstance, some agents' states can not be directly measured, while only the output information is available. Therefore, the **control protocol based on output informa-**

tion is more effective. Fox example, in Yin & Hu (2013), leaderless consensus of uncertain FOMASs with general linear node dynamics was investigated based on static output feedback under fixed undirected communication topology. In Chen *et al.* (2015a), the group leaderless consensus of uncertain FOMASs with general linear node dynamics was investigated based on static output feedback under fixed directed communication topology.

Besides the static output feedback, in Li *et al.* (2014); Ma *et al.* (2017), under fixed directed topology, a fractional-order **observer**-type leaderless consensus protocol based on relative output measurements was proposed to achieve the leaderless consensus of general linear FOMASs. In addition, in large scale networks, the absolute output measurement of each agent is not often completely available. In Zhu *et al.* (2017), under fixed directed commmunication topology, leaderless consensus of general linear FOMASs was studied, where a distributed observer-type protocol was proposed to utilize the estimated states by available measurements.

1.2.1.2 Leader-following consensus/consensus tracking

The consensus of a group of agents with a (virtual) leader has become a particularly interesting topic, where the leader is a special agent whose motion is independent of all the other agents and thus is followed by all the other ones. Such a consensus problem with a dynamic (virtual) leader is commonly called leader-following consensus or consensus tracking problem (see Fig. 1.5). It was reported that the leader-following configuration was an energy saving mechanism (Hummel, 1995), which was found in many biological systems, and could also enhance the communication and orientation of the flock (Andersson & Wallander, 2004). So far, for the leader-following consensus of FOMASs, many results have been obtained considering different conditions with different control methods.

Based on the stability theory of fractional-order linear system (Matignon, 1996), Bai *et al.* (2016, 2017a); Zhu *et al.* (2014) studied the leader-following consensus of single integrator/general linear FOMASs under fixed directed communication topology. **By using the fractional-order Lyapunov direct method** (Li *et al.*, 2010a), Gong (2017); Ren *et al.* (2015); Yu *et al.* (2015) investigated the leader-following consensus of single/double integrators FOMASs with inherent nonlinearities under fixed undirected/directed communication topology, where different kinds of Lyapunov functions were constructed. **Based on the Lyapunov indirect method**, Ye & Su (2019) studied the leader-following consensus of general linear FOMASs with inherent nonlinearities under fixed directed communication topology, where the explicit solution of the tracking errors system was solved and evaluated by utilizing the Mittag-Leffler function, the Laplace transform, and the inequality technique.

Time delay is a universal phenomenon in real dynamical system, which has distinct effects on dynamical behavior of systems and even makes systems unstable. In Zhu *et al.* (2017), leader-following consensus of general linear FOMASs with input delay was studied over fixed directed communication topology by evaluating error states, where the explicit solution of the tracking errors system was obtained. In Yang *et al.* (2019b), over fixed directed weighted graph, leader-following consensus of nonlinear FOMASs with distributed and input delays was investigated by using the fractional-order Razumikhin approach (Wen *et al.*, 2015) and algebraic graph theory. Similarly, by using a modified fractional-order Razumikhin approach, Liu *et al.* (2019e) studied the leader-following consensus of nonlinear FOMASs under fixed directed communication topology, where state time delay existed in the nonlinearity. Note that for the above results, the fractional orders between the leader and followers are all homogeneous, while in some complex environment, the fractional orders for the leader and followers may be heterogeneous, which can be more accurate and flexible in describing the dynamics of the leader-following FOMASs. Therefore, in **Chapter 2** the leader-following consensus of FOMASs with heterogenous fractional orders between leader and followers under input delays is investigated.

In practical applications, **the external disturbances** may be inevitable which always affect the stability performance of the systems. In Ren & Yu (2016), leader-following consensus of nonlinear FOMASs with external disturbances was investigated over fixed directed communication topology, where a distributed linear control protocol was proposed and the ultimately uniformly bounded tracking errors were obtained. In Chen *et al.* (2018b), leader-following consensus of general linear FOMASs with bounded matched disturbances was studied, where the control input was subjected to bounded saturation and the tracking errors were ultimately uniformly bounded, where the performances were not satisfying. Therefore, in order to improve the consensus performance of the FOMASs with external disturbances, two more efficient nonlinear control algorithms will be designed in **Chapter 3**, which can speed up the convergence process and get a better convergence effect.

In many cases, it is very difficult to measure the exact values of all the agents' states due to sensor constraints, communication limits, noise perturbations or data drop-out. Therefore **observer design** for consensus in MASs has been widely discussed. For instance, in Yu *et al.* (2017a), under fixed directed communication topology, to track the states of the leader described by second-order dynamics, observers for the followers were designed by the FOMASs where the relative velocity information was unavailable. In Pan *et al.* (2018), leader-following consensus of singular general linear FOMASs was investigated under fixed undirected communication topology, where a distributed consensus protocol was proposed based on the information of observer. In Wen *et al.* (2019), under fixed directed communication topology, the observer-based output consensus of leader-following heterogeneous linear/nonlinear FOMASs with potentially different state dimensions and different dynamics was studied.

In some cases, the dynamics of the agent have **unknown nonlinearities and disturbances**. To tackle this situation, the neural networks-based (NNs-based) adaptive approach has been widely used to approximate the unknown functions. Gong & Lan (2018a,b) studied the leader-following consensus of uncertain nonlinear FOMASs with double integrators under fixed undirected/directed communication topology, where NNs were used in the designed controller to approximate the unknown nonlinearities. In Shi *et al.* (2019a), the distributed adaptive cooperative control algorithms for second-order agents to track a leader with unknown fractional-order dynamics were investigated, where linearly parameterized NNs were used to approximate the unknown functions.

All of the aforementioned works are concerned with continuous communication and continuous control updates which mean that the agents propagate their information all the time. However, for the networks with limited resources, it is necessary to use the **intermittent communication technique** to reduce the frequency of the control update and communication of agents. At present, the event-triggered sampling strategy has been displayed to be an effective way to reduce the frequency of control updates in MASs. For FOMASs, over fixed undirected communication topology, based on fractional Lyapunov approach, Shi *et al.*

(2018); Wang & Yang (2017a) studied the leader-following consensus of FOMASs via centralized/distributed event-triggered control respectively, where the agents were modeled as single integrator dynamics with nonlinearities or general linear system. Based on evaluating the explicit solution of the errors systems, Ye & Su (2018); Ye *et al.* (2018) investigated the leader-following consensus of general linear FOMASs without/with input delay via distributed event-triggered control over fixed undirected/directed communication topologies. By using the generalized Nyquist stability criterion, over fixed directed communication topology, a necessary and sufficient condition for the observer tracking consensus of the second-order leader systems via periodic sampled-based event-triggered control was derived in Wang *et al.* (2018a).

Compared with the existing continuous control method mentioned above, **impulsive control** is an efficient methods to deal with the dynamical systems which can be controlled by continuous control methods. In Wang & Yang (2017b), over fixed undirected communication topology, leader-following exponential consensus of nonlinear FOMASs with hybrid time-varying delay was investigated by a heterogenous impulsive control. In Ma *et al.* (2018), over fixed directed communication topology, leader-following consensus of nonlinear FOMASs was investigated through distributed impulsive control.

All the above works are concerned with the continuous-time FOMASs, while some results about the **discrete-time FOMASs** have been obtained using the Grünwald-Letnikov fractional derivative definition. For example, Shi & Zhang (2015) studied the leader-following consensus of discrete-time FOMASs with sampling delay by using Hermite-Biehler theorem and the change of bilinearity under symmetrical and directly weighted networks. Girejko *et al.* (2018); Shahamatkhah & Tabatabaei (2018); Wyrwas *et al.* (2018) addressed the leader-following consensus of single/double summator FOMASs over fixed communication topology.

Adaptive strategies are also utilised in the leader-following consensus of FOMASs. For examples, in Gong (2016), leader-following consensus of nonlinear FOMASs with adaptive feedback control protocols was studied over fixed directed communication topology. Soorki & Tavazoei (2014) presented an adaptive controller to achieve consensus tracking of general linear FOMASs over fixed directed communication topology. Yu *et al.* (2015) studied the leader-following consensus of general linear FOAMSs without/with nonlinearities via adaptive pinning control over fixed directed communication topology. Zhang *et al.* (2018b) addressed the group multiple lag consensus of leader-following nonlinear FOMASs via adaptive control over fixed directed communication topology. In addition, Bai *et al.* (2017c) investigated the distributed consensus tracking of linear/nonlinear FOMASs based on the sliding mode control method over fixed undirected communication topology.

1.2.1.3 Containment consensus with multiple leaders

The main objective of containment control is to design appropriate protocol such that all followers can converge to the convex hull spanned by the leaders.

In Liu & Xu (2012); Liu *et al.* (2012), over fixed directed topology, distributed containment control of single integrator FOMASs with input delay was investigated by using the algebraic graph theory, matrix theory, Nyquist stability criterion and frequency domain method. In Chen *et al.* (2016), over fixed undirected communication topology, containment control of general linear FOMASs with parameter uncertainty was studied based on the stability theory of fractional-order systems and matrix theory. In Gong (2017), over fixed undirected communication topology, by using the fractional Lyapunov direct method, the distributed robust containment control problem for a class of FOMASs with heterogeneous unknown nonlinearities and external disturbances was studied based on the neural networks-based adaptive control. In Zou & Xiang (2017), over fixed directed communication topology, the containment control problem of nonlinear FOMASs was addressed by using the fractional-order Lyapunov function method. In Yang *et al.* (2018), containment control of single integrator FOMASs without/with time delays was analyzed in a directed/undirected communication topology by using Laplace transform and frequency domain theorem. In Liu *et al.* (2019b), over fixed directed communication topology, periodic sampling-data control was applied to the containment control of FOMASs, where single integrator FOMAS without/with time delays and double integrator FOMASs were considered. In Yang *et al.* (2019a), containment control of FOMAS without/with input delays under fixed directed weighted communication topology was studied by applying frequency domain analysis theory, where the FOMASs were formulated with diverse dynamical equations. In Yuan *et al.* (2019), observer-based quasi-containment of general linear FOMASs was investigated via event-triggered control strategy based on fixed directed communication topology.

1.2.2 Consensus-based formation control

Consensus algorithms normally guarantee the agreement of a team of agents on some common states without taking group formation into consideration. To reflect many practical applications where a group of agents are normally required to form some preferred geometric structures, it is desirable to consider a task-oriented formation control problem for a group of mobile agents, which motivates the study of formation control presented in this subsection.

Compared with the consensus problem where the final states of all agents typically reach a singleton, the final states of all agents can be more diversified under the formation control scenario. Indeed, formation control is more desirable in many practical applications such as formation flying, cooperative transportation, sensor networks, as well as combat intelligence, surveillance, and reconnaissance. In addition, the performance of a team of agents working cooperatively often exceeds the simple integration of the performance of all individual agents. For its broad applications and advantages, formation control has been a very active research subject in the control systems community, where a certain geometric pattern is aimed to form with or without a group reference. More precisely, the main objective of formation control is to coordinate a group of agents such that they can achieve some desired formation so that some tasks can be finished by the collaboration of the agents.

Generally speaking, formation control can be categorized according to the group reference.

Formation producing: if multi-agents are not required to track a leader, the formation problem is called formation producing (see Fig. 1.7).

Formation tracking: if multi-agents are required to track a leader, the formation problem is called formation tracking (see Fig. 1.8).

Formation control without a group reference, called formation producing, refers to the algorithm designed for a group of agents to reach some pre-desired geometric pattern in the absence of a group reference, which can also be considered as the control objective. Formation control with a group reference, called

Fig. 1.7. Formation producing problem

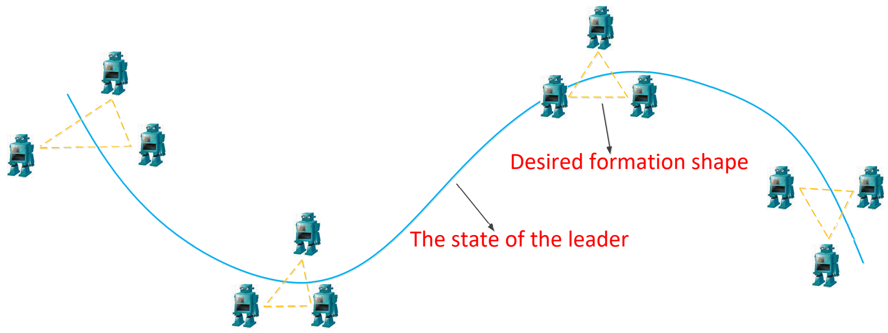

Fig. 1.8. Formation tracking problem

formation tracking, refers to the same task but following the predesigned group reference. Due to the existence of the group reference, formation tracking is usually much more challenging than formation producing and control algorithms for the latter might not be useful for the former. As for today, there are still many open questions in solving the formation control problem. Some more detailed descriptions can refer to Cao *et al.* (2013).

Up to now, formation control has been extensively studied by numerous researches (Cao *et al.*, 2013), and the existing results of formation control primarily assume an integer-order dynamics, such as single integrator dynamics and double ones. However, many practical engineering systems can't be explained by integer-order systems, and some more well reflections to the systems properties can be given by fractional-order systems.

Currently, for the formation control of FOMASs, a few results have been obtained. In Cao *et al.* (2010), the distributed formation producing for fractional-order multi-agent systems was firstly studied under the dynamic interaction and absolute/relative damping. In Bai *et al.* (2015a, 2017c), over fixed directed communication topology, the distributed formation producing for fractional-order multi-agent systems with communication delay and absolute/relative damping was investigated respectively. In Bai *et al.* (2015b), formation tracking of fractional-order multi-agent systems was considered based on error predictor. In Luo *et al.* (2018), over fixed directed communication topology, two iterative learning control schemes (P-type and PI-type) were employed to fulfill the formation producing of general linear FOMASs. In Liu *et al.* (2019c,d), formation producing of single integrator or double integrators FOMASs in the case of relative damping and nonuniform time-delays was studied respectively, where symmetric time-delays and relative damping were studied under an undirected network topology, and asymmetric time-delays and relative damping were studied under a directed network topology. Besides, different from the above mentioned literatures considering the time-invariant formation control, in Gong *et al.* (2019), observer-based time-varying formation producing of general linear FOMASs was investigated over fixed and switching directed communication topologies.

1.3 Overview of parameter identification problem

Most control methods mentioned in Section 1.2 are valid only for the FOMASs whose system parameters and fractional orders are known in advance. However, in some situations, the dynamics of FOMASs are usually partly known. That is, the structure of the fractional-order differential equations are known, while some or all of the fractional orders and system parameters are unknown. Therefore, in order to control the FOMASs, identifying the unknown fractional orders and system parameters are really important.

Currently, for parameter identification of nonlinear systems, there are mainly two methods. The first one is **synchronization-based method**, which was first put forward by Parlitz (Parlitz, 1996). After that this method has been sufficiently applied to the unknown parameter identification of different kinds of nonlinear systems (Gu *et al.*, 2017; Konnur, 2003). But it is not easy to be applied because it is sensitive to the considered systems for designing the controllers and updating laws. The second one is **optimization-based method by using artificial intelligence optimization algorithms (AIOAs)**. In the second method, the parameter identification issue can be converted into a functional optimization problem. Contrasted with the synchronization-based method, the second method does not need the differentiable information of the considered systems and is more flexible to be applied. Currently, many kinds of AIOAs have been applied for the second parameter identification method, such as differential evolution (DE) (Guedes *et al.*, 2018) and Cuckoo search (CS) (Wei & Yu, 2018).

In the past few decades, AIOAs based on evolutionary and swarm principles have achieved considerable success in handling complex function optimization problems as they do not depend on the differentiability, continuity, and convexity of the objective function. For instance, most of the traditional optimization methods, such as steepest decent, conjugate gradient method and Newton method, require gradient information of the objective function which make it impossible for them to deal with the non-differentiable functions. Therefore, the AIOAs have attracted more and more attention. In the family of AIOAs, the most popular methods are genetic algorithms (GA) (Tam, 1992), differential evolution (DE) (Storn & Price, 1997), particle swarm optimization (PSO) (Kennedy, 2010), biogeography-based optimization (BBO) (Simon, 2008), ant colony optimization (ACO) (Socha & Dorigo, 2008), and artificial bee colony (ABC) algorithm (Karaboga *et al.*, 2014).

In the following, the problem formulation of parameter identification problem with AIOAs is introduced.

Assume the original system is described as

$$ {}_0D_t^q Y(t) = f(Y(t), Y_0, \theta), \tag{1.1} $$

where $Y(t) = [y_1(t), y_2(t), \cdots, y_n(t)]^T \in R^n$ denotes the state vector, $Y_0 = Y(0)$ denotes the initial value, $\theta = [\theta_1, \theta_2, \cdots, \theta_m]^T$ is a set of original systematic parameters, $q = [q_1, q_2, \cdots, q_n]$ $(0 < q_i < 1, i = 1, 2, \cdots, n)$ is the fractional derivative orders, and the function $f(Y(t), Y_0, \theta) = [f_1(Y(t), Y_0, \theta), f_2(Y(t), Y_0, \theta), \cdots, f_n(Y(t), Y_0, \theta)]^T$.

Suppose the structure of system (1.1) is known, then the corresponding identified system can be written as

$$ {}_0D_t^{\tilde{q}} \tilde{Y}(t) = f(\tilde{Y}(t), Y_0, \tilde{\theta}), \tag{1.2} $$

where $\tilde{Y}(t) = [\tilde{y}_1(t), \tilde{y}_2(t), \cdots, \tilde{y}_n(t)]^T \in R^n$ is the state vector of the identified system, $\tilde{\theta} = [\tilde{\theta}_1, \tilde{\theta}_2, \cdots, \tilde{\theta}_m]^T$ is a set of identified system parameters and $\tilde{q} =$

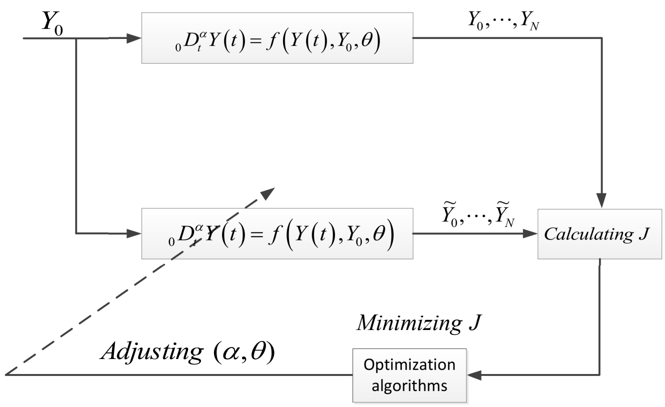

Fig. 1.9. The general principle of parameter identification by AIOAs

$[\tilde{q}_1, \tilde{q}_2, \cdots, \tilde{q}_n]^T$ is the identified fractional orders. Besides, systems (1.1) and (1.2) have the same initial conditions Y_0.

Based on the measurable state vector $Y(t) = [y_1(t), y_2(t), \cdots, y_n(t)]^T \in R^n$, to identify the fractional-order system (1.1), the following objective function is defined as

$$J(\tilde{q}, \tilde{\theta}) = arg \min_{(\tilde{q},\tilde{\theta})\in\Omega} F = arg \min_{(\tilde{q},\tilde{\theta})\in\Omega} \sum_{k=1}^{N} \|Y_k - \tilde{Y}_k\|_2, \tag{1.3}$$

where $k = 1, 2, \cdots, N$ is the sampling time point and N denotes the length of data used for parameter identification. Y_k and $\tilde{Y}_k$ respectively denote the state vector of the original system (1.1) and the identified system (1.2) at time kh. h is the step size introduced in the predictor-corrector approach for the numerical solutions of fractional differential equations. $\|\cdot\|$ is Euclid norm. Ω is the searching area admitted for parameters $\tilde{\theta}$, where the fractional orders $\tilde{q}$ are considered as special variables. The parameter identification of system (1.1) can be achieved by searching suitable $\tilde{\theta}$ and $\tilde{q}$ in the searching space Ω such that the objective function (1.3) is minimized. In other words, the main task is to find the best combination of the independent variables $\tilde{q}$ and $\tilde{\theta}$ for the objective function (1.3). The general principle of parameter identification can be illustrated as Fig. 1.9.

In this thesis, we will identify the unknown FOMASs based on AIOAs. More specifically, in **Chapters 4 and 5**, the ABC and DE algorithms will be employed respectively to identify the unknown nonlinear delayed FOMASs, then the identified parameters are applied to the distributed consensus tracking of the delayed nonlinear FOMASs. In **Chapter 6**, in order to improve the performance of the original ABC algorithm, a modified artificial bee colony (mABC) algorithm will be proposed to identify the unknown nonlinear FOMASs.

1.4 Preliminaries

1.4.1 Graph Theory

In this thesis, the fixed undirected/directed communication graph with N agents is considered. In graph $\mathcal{G} = (\mathcal{V}, \mathcal{E}, \mathcal{A})$, $\mathcal{V} = \{v_1, v_2, \cdots, v_N\}$ and $\mathcal{E} \subseteq \mathcal{V} \times \mathcal{V}$ denote nodes set and edges set respectively, and $\mathcal{A} = [a_{ij}]_{N\times N} \in R^{N\times N}$ denotes a weighted adjacency matrix where all the elements $a_{ij} \geq 0$ and $a_{ii} = 0$ due to the no existence of the self-loops. $e_{ij} = (v_j, v_i)$ denotes the edge of $\mathcal{G}$, and if agent i can receive information from agent j, it can be denoted by $e_{ij} \in \mathcal{E}$ which is equal to $a_{ij} > 0$. For undirected communication graph, if $e_{ij} \in \mathcal{E}$, it implies $e_{ji} = (v_i, v_j) \in \mathcal{E}$. Denote $\mathcal{N}_i = \{v_j | (v_j, v_i) \in \mathcal{E}\}$ as the neighbour set of agent i. $(v_1, v_2), (v_2, v_3), \cdots$ represents a path. For undirected communication graph, if there exists an undirected path between each pair of distinct nodes, the corresponding undirected graph is **connected**. For directed communication graph, if at least one node has a directed path to all other nodes, we say that the directed graph has a **directed spanning tree**. Define the in-degree of the ith agent as $d_i = \sum_{j=1}^{N} a_{ij}$ and the in-degree matrix as $\mathcal{D} = diag\{d_i\} \in R^{N\times N}$ which is a diagonal matrix with diagonal elements $d_i (i = 1, \cdots, N)$. Defined $\mathcal{L} = \mathcal{D} - \mathcal{A} = [l_{ij}]_{N\times N} \in R^{N\times N}$ as the Laplace matrix, which means that $l_{ij} = -a_{ij} (i \neq j)$ and $l_{ii} = d_i = \sum_{j=1}^{N} a_{ij}$.

In this thesis, let vertex v_0 denote the leader in the communication graph and x_0 represent its state. Then, the graph $\bar{\mathcal{G}}$ is defined, which includes the graph $\mathcal{G}$ and leader v_0. For distributed coordination, the leader is independent, which means it doesn't obtain the information from its neighbors. The diagonal matrix $\mathcal{B} \in R^{N\times N}$ denotes the leader's adjacency matrix and when the leader is a neighbor of agent i, the diagonal elements $b_i = a_{i0} > 0$ and $b_i = 0$, otherwise. Similarly, in graph $\bar{\mathcal{G}}$, the in-degree of the ith agent can be defined as $d_i = \sum_{j=0}^{N} a_{ij}$ $(i = 1, \cdots, N)$.

In order to utilize the communication topology, the following lemmas are guaranteed.

Lemma 1.1 *(Ren & Beard, 2008) Suppose the undirected communication topology $\bar{\mathcal{G}}$ which contains N followers and one leader is connected, then $M = \mathcal{L} + \mathcal{B}$ is symmetric and positive definite.*

Lemma 1.2 *(Li et al., 2015) Suppose the directed communication topology $\bar{\mathcal{G}}$ among the followers and leader has a directed spanning tree with the leader as the root node, then all the eigenvalues of matrix $M = \mathcal{L} + \mathcal{B}$ own positive real parts. Let*

$$\begin{aligned} &g = [g_1, g_2, \cdots, g_N]^T = M^{-T}\mathbf{1}_N, \\ &G = diag\{g_1, g_2, \cdots, g_N\}, \\ &Q = GM + M^T G, \end{aligned}$$

then $G > 0$ and $Q > 0$.

Remark 1.3 *In this thesis, we assume that the fixed undirected/directed communication topologies have 0-1 weight.*

In the following, two examples with fixed undirected/directed communication topologies will be given to show the definitions of adjacency matrixes $\mathcal{A}$ and $\mathcal{B}$, in-degree matrix $\mathcal{D}$, and Laplace matrix $\mathcal{L}$.

Example 1.4 *Consider the fixed undirected communication topology as Fig. 1.10, its adjacency matrixes $\mathcal{A}$ and $\mathcal{B}$, in-degree matrix $\mathcal{D}$, and Laplace matrix $\mathcal{L}$ can be given as follows:*

$$\mathcal{A} = \begin{bmatrix} 0 & 1 & 1 & 0 \\ 1 & 0 & 0 & 1 \\ 1 & 0 & 0 & 0 \\ 0 & 1 & 0 & 0 \end{bmatrix}, \mathcal{D} = \begin{bmatrix} 2 & 0 & 0 & 0 \\ 0 & 2 & 0 & 0 \\ 0 & 0 & 1 & 0 \\ 0 & 0 & 0 & 1 \end{bmatrix},$$

$$\mathcal{B} = \begin{bmatrix} 1 & 0 & 0 & 0 \\ 0 & 0 & 0 & 0 \\ 0 & 0 & 0 & 0 \\ 0 & 0 & 0 & 0 \end{bmatrix}, \mathcal{L} = \mathcal{D} - \mathcal{A} = \begin{bmatrix} 2 & -1 & -1 & 0 \\ -1 & 2 & 0 & -1 \\ -1 & 0 & 1 & 0 \\ 0 & -1 & 0 & 1 \end{bmatrix}.$$

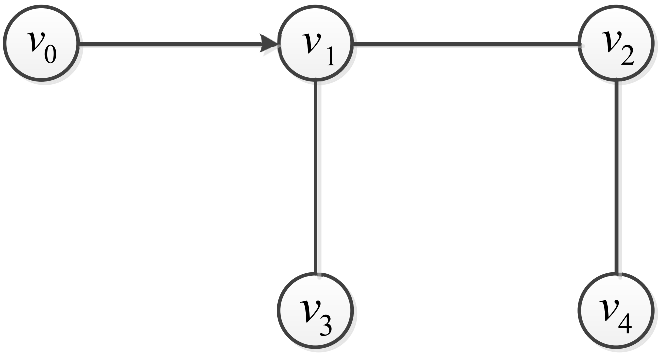

Fig. 1.10. A fixed **undirected** communication topology with one leader v_0 and four followers $v_i (i = 1, \cdots, 4)$

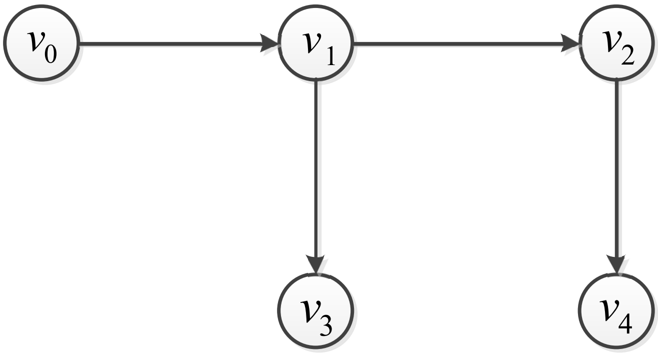

Fig. 1.11. A fixed **directed** communication topology with one leader v_0 and four followers $v_i (i = 1, \cdots, 4)$

Example 1.5 *Consider the fixed directed communication topology as Fig. 1.11, its adjacency matrixes $\mathcal{A}$ and $\mathcal{B}$, in-degree matrix $\mathcal{D}$, and Laplace matrix $\mathcal{L}$ can be given as follows:*

$$\mathcal{A} = \begin{bmatrix} 0 & 0 & 0 & 0 \\ 1 & 0 & 0 & 0 \\ 1 & 0 & 0 & 0 \\ 0 & 1 & 0 & 0 \end{bmatrix}, \mathcal{D} = \begin{bmatrix} 0 & 0 & 0 & 0 \\ 0 & 1 & 0 & 0 \\ 0 & 0 & 1 & 0 \\ 0 & 0 & 0 & 1 \end{bmatrix},$$

$$\mathcal{B} = \begin{bmatrix} 1 & 0 & 0 & 0 \\ 0 & 0 & 0 & 0 \\ 0 & 0 & 0 & 0 \\ 0 & 0 & 0 & 0 \end{bmatrix}, \mathcal{L} = \mathcal{D} - \mathcal{A} = \begin{bmatrix} 0 & 0 & 0 & 0 \\ -1 & 1 & 0 & 0 \\ -1 & 0 & 1 & 0 \\ 0 & -1 & 0 & 1 \end{bmatrix}.$$

1.4.2 Caputo fractional-order derivative

In general, three best-known definitions of fractional-order derivatives are widely used: Grunwald-Letnikov, Riemann-Liouville and Caputo definitions (Podlubny, 1998). In particular, the main advantage of Caputo fractional-order derivative is that it owns same initial conditions with integer-order derivatives, which has well-understood features of physical situations and more applicable to real world problems.Thus, the Caputo fractional-order derivative is employed in this thesis.

Definition 1.6 *(Caputo fractional-order derivative) The Caputo fractional-order derivative of order α for a function $f(t)$ is defined as*

$$ {}_{t_0}D_t^{\alpha} f(t) = \frac{1}{\Gamma(n-\alpha)} \int_{t_0}^{t} \frac{f^{(n)}(\tau)}{(t-\tau)^{\alpha+1-n}} d\tau, \tag{1.4}$$

where $\alpha > 0$ and $\alpha \in (n-1, n)$, $\Gamma(\cdot)$ represents the gamma function. When $\alpha = n$, it holds that ${}_{t_0}D_t^{\alpha} f(t) = f^{(n)}(t)$. Particularly, when $\alpha \in (0,1)$, it holds that

$$ {}_{t_0}D_t^{\alpha} f(t) = \frac{1}{\Gamma(1-\alpha)} \int_{t_0}^{t} \frac{f'(\tau)}{(t-\tau)^{\alpha}} d\tau. $$

The corresponding Laplace transform is

$$ \mathcal{L}\{{}_{t_0}D_t^{\alpha} f(t); s\} = s^{\alpha} F(s) - \sum_{k=0}^{n-1} s^{\alpha-k-1} f^{(k)}(t_0), \tag{1.5}$$

where $\alpha \in (n-1, n)$, $\mathcal{L}\{\cdot\}$ is the Laplace transform, s is the variable in Laplace domain and $F(s)$ is the Laplace transform of $f(t)$, and $F(s) = \mathcal{L}\{f(t); s\} = \int_0^{+\infty} e^{-st} f(t) dt$. In this thesis, we assume that $\alpha \in (0, 1]$, so the Laplace transform of Caputo fractional derivative can be written as follows:

$$ \mathcal{L}\{{}_{t_0}D_t^{\alpha} x(t); s\} = s^{\alpha} X(s) - s^{\alpha-1} x(0), $$

Property 1.7 *If C is a constant, then ${}_{t_0}D_t^{\alpha} C = 0$.*

Property 1.8 *The linearity of Caputo fractional-order derivative can be depicted as*

$$ {}_{t_0}D_t^{\alpha}(\mu f(t) + \nu g(t)) = \mu \; {}_{t_0}D_t^{\alpha} f(t) + \nu \; {}_{t_0}D_t^{\alpha} g(t). $$

where μ and ν are arbitrary constants.

Analogous to the exponential function appearing in the solution of integer-order differential equations, the Mittag-Leffler function is used frequently in the solutions of fractional-order differential equations.

Definition 1.9 *The Mittag-Leffler function with two parameters is*

$$E_{\alpha,\beta}(z) = \sum_{k=0}^{\infty} \frac{z^k}{\Gamma(k\alpha+\beta)}. \tag{1.6}$$

Where $\alpha, \beta \in C$. As a special case, if $\beta = 1$, and $\alpha > 0$, then (1.6) can be rewritten as $E_\alpha(z) = \sum_{k=0}^{\infty} \frac{z^k}{\Gamma(k\alpha+1)}$. Especially, $E_{1,1}(z) = e^z$.

The corresponding Laplace transform is

$$\mathcal{L}\{t^{\beta-1}E_{\alpha,\beta}(-\lambda t^\alpha); s\} = \frac{s^{\alpha-\beta}}{s^\alpha+\lambda}, \qquad (t \geq 0, Re(s) > |\lambda|^{\frac{1}{\alpha}}),$$

where $\lambda \in R$, and $Re(s)$ is the real part of the variable s.

Consider the following n-dimensional Caputo fractional-order system

$$\begin{cases} {}_{t_0}D_t^\alpha x(t) = f(t, x(t)), \\ x(t_0) = x_{t_0}, \end{cases} \tag{1.7}$$

where $\alpha \in (0,1), x = (x_1, x_2, \cdots, x_n) \in R^n, t_0 \geq 0,\ f : [0, +\infty) \times R^n \to R^n$ is piecewise continuous on t and satisfies locally Lipschitz conditions on x.

Definition 1.10 *(Li et al., 2010a) The constant $\bar{x}$ is an equilibrium point of Caputo fractional dynamic system (1.7) if and only if $f(t, \bar{x}) = 0$.*

Remark 1.11 *According to Properties (1.7) and (1.8), any equilibrium point can be converted to the origin through change of variables. When the equilibrium point in (1.7) is $\bar{x} \neq 0$, by using the change of variable $y(t) = x(t) - \bar{x}$, system (1.7) can be rewritten as*

$$\begin{aligned} {}_{t_0}D_t^\alpha y(t) &= {}_{t_0}D_t^\alpha (x(t) - \bar{x}) = f(t, x(t)), \\ &= f(t, y(t) + \bar{x}) = g(t, y(t)), \end{aligned}$$

where $g(t, 0)$ and $\bar{y} = 0$ is the equilibrium of the new system for variable y. Therefore, without loss of generality, the only case that the equilibrium point is the origin is considered in Definition 1.10.

Lemma 1.12 *(Existence and uniqueness theorem (Li et al., 2010a)) There exists a unique solution of system (1.7) for any initial value, if $f(t, x)$ satisfies locally Lipschitz condition on x.*

Definition 1.13 *(Mittag-Leffler stability (Li et al., 2010a)) If $\bar{x} = 0$ is an equilibrium point of Caputo fractional dynamic system (1.7), the solution of system (1.7) is said to be Mittag-Leffler stable if*

$$\|x(t)\| \leq [m(x_{t_0})E_\alpha(-\lambda(t-t_0)^\alpha)]^b \tag{1.8}$$

where $\lambda > 0, b > 0, m(0) = 0$, $\|\cdot\|$ denotes an arbitrary norm and $m(x) \geq 0$ satisfies locally Lipschitz condition on $x \in R^n$ with Lipschitz constant m_0.

Remark 1.14 *Mittag-Leffler stability implies asymptotic stability for fractional-order systems, i.e., $\|x(t)\| \to 0$ with $t \to +\infty$.*

To judge the system stability, the following lemmas are introduced.

Lemma 1.15 *(Stability theory for fractional-order linear system (Matignon, 1996)) The following autonomous system*

$${}_{t_0}D_t^\alpha x(t) = Ax(t), \quad \alpha \in (0, 1], \tag{1.9}$$

is asymptotically stable if and only if $|arg(\rho(A))| > \alpha\pi/2$, where $\rho(A)$ denotes the eigenvalue of matrix A, $arg(\cdot)$ denotes the argument principle value of a complex number.

Lemma 1.16 *(Fractional-order Lyapunov direct method (Li et al., 2010a)) The equilibrium point $\bar{x} = 0$ of fractional-order system is Mittag-Leffler stable if there exist positive constants $\alpha_1, \alpha_2, \alpha_3, a, b$ and a continuously differentiable function $V(t, x(t))$ satisfying*

$$\alpha_1\|x(t)\|^a \leq V(t, x(t)) \leq \alpha_2\|x(t)\|^{ab}, \tag{1.10}$$

$${}_{t_0}D_t^\beta V(t, x(t)) \leq -\alpha_3\|x(t)\|^{ab}, \tag{1.11}$$

where $t \geq 0, \beta \in (0, 1)$, and $V(t, x(t)) : [t_0, \infty) \times D \to R$ satisfies the local Lipschitz condition on x, and $D \in R^n$ is a domain including the origin. If the assumptions are satisfied globally on R^n, then $\bar{x} = 0$ is globally Mittag-Leffler stable.

Lemma 1.17 *(Comparison principle of linear fractional equation with delay (Wang et al., 2015)) Consider the following delayed fractional-order differential inequality*

$$\begin{cases} {}_{t_0}D_t^{\alpha} x(t) \leq -\lambda x(t) + \delta x(t-\tau), & \alpha \in (0,1], \\ x(t) = \phi(t), t \in [-\tau, 0], \end{cases} \tag{1.12}$$

and the following linear delayed fractional-order differential system

$$\begin{cases} {}_{t_0}D_t^{\alpha} z(t) = -\lambda z(t) + \delta z(t-\tau), & \alpha \in (0,1], \\ z(t) = \phi(t), t \in [-\tau, 0], \end{cases} \tag{1.13}$$

where $x(t)$ and $z(t)$ are continuous and nonnegative in $(0, +\infty)$, and $\phi(t) \geq 0, t \in [-\tau, 0]$. If $\lambda > 0$ and $\delta > 0$, then $x(t) \leq z(t), t \in [0, +\infty)$.

Lemma 1.18 *(Stability theory of linear fractional equation with delay (Chen et al., 2015b)) For system (1.13), the Lyapunov globally asymptotically stable can be achieved for the zero solution of system (1.13), if $\lambda > \delta$ and there has no purely imaginary root for the characteristic equation $s^{\alpha} + \lambda - \delta e^{-s\tau} = 0$ of system (1.13).*

Lemma 1.19 *(Fractional derivative inequality (Duarte-Mermoud et al., 2015)) Denote $x(t) \in R^n$ as a vector of differentiable functions. Then*

$$\frac{1}{2}\,{}_{t_0}D_t^{\alpha}(x^T(t)Px(t)) \leq x^T(t)P\,{}_{t_0}D_t^{\alpha} x(t), \qquad \forall\ \alpha \in (0,1], \quad \forall\ t \geq t_0, \tag{1.14}$$

where the constant square matrix $P \in R^{n\times n}$ is symmetric and positive definite.

Remark 1.20 *In the following Chapters, in order to study simply, ${}_{t_0}D_t^{\alpha} x(t)$ is replaced by $x^{(\alpha)}(t)$.*

1.4.3 Mathematical knowledge

If A is an $m \times n$ matrix and B is a $p \times q$ matrix, then the Kronecker product $A \otimes B$ is an $mp \times nq$ block matrix as follows:

$$A \otimes B = \begin{bmatrix} a_{11}B & \cdots & a_{1n}B \\ \vdots & \ddots & \vdots \\ a_{m1}B & \cdots & a_{mn}B \end{bmatrix}.$$

The properties of Kronecker product are:

- $A \otimes (B + C) = A \otimes B + A \otimes C$;
- $(A \otimes B)(C \otimes D) = (AC) \otimes (BD)$;
- $(A + B)^T = A^T + B^T$;
- $(A + B)^{-1} = A^{-1} + B^{-1}$;
- $\lambda_{max}(A \otimes B) = \lambda_{max}(A)\lambda_{max}(B)$.

Lemma 1.21 *(Schur complement (Crabtree & Haynsworth, 1969)) For given matrices A, B, C, the following holds:*

$$D = \begin{bmatrix} A & B \\ B^T & C \end{bmatrix} < 0 \Longleftrightarrow C < 0 \ \& \ A - BC^{-1}B^T < 0, \qquad\qquad \Longleftrightarrow A < 0 \ \& \ C - B^T A^{-1} B < 0. \tag{1.15}$$

Lemma 1.22 *(Cao et al., 2005) For any real matrixes X, Y, $\Xi = \Xi^T > 0$ and scalar $\xi > 0$, it holds*

$$X^T Y + Y^T X \leq \xi X^T \Xi X + \xi^{-1} Y^T \Xi^{-1} Y. \tag{1.16}$$

Lemma 1.23 *(Gerschgorin's disc theory (Horn et al., 1990)) For any matrix $M = [m_{ij}] \in R^{N \times N}$, all the eigenvalue of M are located in the union of N Gerschgorin's disc as*

$$Ger(M) = \bigcup_{i=1}^{N} \big\{ z \in C, |z - m_{ii}| \leq \Sigma_{j \neq i} |m_{ij}| \big\}. \tag{1.17}$$

1.5 Contributions and outline of dissertation

This dissertation presents parameter identification based on artificial intelligent optimization and distributed tracking control of fractional-order multi-agent systems (FOMASs) under fixed communication topology. The main contributions are summarized as follows.

Chapter 2: In many physical systems, the **time delays** universally exist because the signal propagation speed is limited, the sensor needs extra time to obtain the measurement information, the controller needs additional computation and execution time to produce and implement the control inputs. The undesirable instability and poor performance can easily happen due to the existence of time delays. Secondly, note that for most existing results about the leader-following consensus of fractional-order multi-agent systems (FOMASs), the fractional orders between the leader and followers are all homogeneous, while in some complex environment, **the fractional orders for the leader and followers may be heterogeneous**, which can be more accurate and flexible in describing the dynamics of the leader-following FOMASs. Therefore, it is interesting and significant to learn the leader-following consensus of FOMASs with heterogenous fractional orders between leader and followers, which can be viewed as HFOMASs.

Therefore, in this Chapter, over fixed directed communication graph, the leader-following consensus of heterogenous HFOMASs is investigated with respect to input delays, where the fractional orders between leader and followers are heterogenous, which is more general. Firstly, a control algorithm with a fractional-order estimator is proposed to guarantee the leader-following consensus of the HFOMASs. Then, the identical input delays are taken into account in the above control algorithm, and the leader-following consensus of the HFOMASs can be achieved under the derived sufficient and necessary condition. Thirdly, the diverse input delays are further considered in the HFOMASs, and a sufficient condition is put forward under the designed control algorithm. Finally, simulations are conducted to make the results be convinced.

The main contributions are as follows: firstly, different from the leaderless consensus of FOMASs and leader-following consensus of FOMASs with homogeneous orders between leader and followers, the leader-following consensus of FOMASs with heterogenous orders between leader and followers is investigated and a novel control algorithm with a fractional-order estimator is designed. Secondly, in contrast with leaderless consensus of delayed FOMASs and leader-following consensus of FOMASs without time delays, the leader-following consensus of HFOMASs under input delays is considered based on the proposed control algorithm.

Chapter 3: Note that the results studied in Chapter 2 are based on single integrator systems. In practice, more complex intrinsic **nonlinear dynamics** may exist in mobile agents. However, due to the complexity of the FOMASs, stability of the nonlinear FOMASs is difficult to be verified. Besides, in real applications, **unknown external disturbances** arising from environment and communication are usually unavoidable. External disturbances can easily lead to instability or bad performance.

Therefore, in this Chapter, over fixed undirected communication topology and based on the fractional Lyapunov direct method, the distributed consensus tracking of nonlinear FOMASs with external disturbances is addressed. Firstly, a nonlinear discontinuous distributed control protocol is put forward to solve the distributed consensus tracking when some conditions are satisfied. Secondly, a nonlinear continuous distributed control algorithm is further proposed to suppress the chattering behavior of the discontinuous controller, where the upper bound of the tracking error is uniformly ultimately bounded and can be made small enough by choosing the parameters properly. Finally, some simulations are provided to validate the advantages of the obtained results.

Compared with the existing results, There are four main differences. Firstly, different from the most results studying the integer-order models, the MASs with fractional dynamics are studied. Secondly, in contrast with most results about the consensus tracking of FOMASs without considering the external disturbances, the external disturbances are considered into the FOMASs in this Chapter. Thirdly, different from most results where the style of the external disturbances are known, in this Chapter we do not known the style of the external disturbances beforehand. Fourthly, different from most results using a linear control protocol, we propose two effective nonlinear control algorithms.

Chapter 4: As mentioned in Chapter 2, **time delays** are unavoidable in many applications. In Chapter 2, several results with time delays have been achieved based on linear case. However, in practice, more complex intrinsic nonlinear dynamics may exist in mobile agents. Unfortunately, the consensus control algorithms and conditions designed for linear delayed FOMASs are not applicable to the **nonlinear case**. Thus, it is significant to investigate the distributed consensus tracking of nonlinear FOMASs with state time delays, which is full of challenges and not well investigated. In addition, as mentioned in Chapter 3, the effects of **unknown external disturbances** arising from environment and communication are usually unavoidable in practice. Undesirable instability or bad performance can easily happen because of the external disturbances. Thus, for the study of MASs, taking the effects of the external disturbances into account is essential and reasonable. On the other hand, note that most existing results are under the assumption that the fractional orders and system parameters of the FOMASs are known beforehand. However in the real applications, **the fractional orders and system parameters are usually partly or all unknown**, which need to be identified in advance.

Therefore, in this Chapter, over fixed undirected communication topology, the distributed consensus tracking of unknown nonlinear delayed FOMASs with external disturbances is investigated, where the fractional orders and system parameters are unknown. Firstly, in order to identify the unknown parameters of the delayed nonlinear FOMASs, an efficient artificial bee colony algorithm (ABC)-based parameter identification approach is put forward. Secondly, based on the identified parameters, by using fractional derivative inequality and comparison principle of linear fractional equation with delay, a discontinuous distributed control protocol is proposed to make the tracking errors converge to zero asymptotically. Thirdly, to overcome the undesirable chattering phenomenon caused by the discontinuous controller, a continuous distributed control algorithm is further designed and uniformly ultimately bounded (UUB) tracking errors can be obtained and reduced as small as desired. Finally, numerical simulations are given to test the effectiveness of the proposed parameter identification scheme and the deigned control algorithms.

Compared with the existing works, the contributions are as follows. Firstly, compared with most results concerning the integer-order MASs, the delayed MASs with fractional-order dynamics, external disturbances are considered. Secondly, different from the results about the time delays with linear case, the time delay under nonlinear case is further investigated. Thirdly, most results about the FOMASs only considered the external disturbances, but have not taken the time delays into account at the same time. Fourthly, most existing results are supposed that the fractional orders and system parameters of the nonlinear FOMASs are known beforehand, while in this Chapter, the parameters are considered to be unknown, and the ABC algorithm is employed to identify the unknown parameters of the unknown delayed FOMASs. Furthermore, it should be pointed out that this Chapter provides a promising link between the artificial intelligent technique and distributed cooperative control of FOMASs or other control fields.

Chapter 5: The results obtained in above Chapters 2, 3 and 4 assume that the control input of a leader is either equal to zero or available to all the followers, which has some limitations and lacks flexibility. More specifically, for the purpose of leading the followers to achieve special tasks, **the leader's input need to be nonzero or time-varying**. Furthermore, it is impossible for all the followers to know the leader's control input, when they are in an uncooperative scenario. Therefore, it is significant and essential to consider the leader with nonzero input, although it is difficult to address because of the limited information accessibility. In addition, recently, the investigation of heterogeneous MASs has become a hot topic in distributed cooperative control. Heterogeneity may occur because of the diverse designs and operating factors. For example, some results considered heterogeneous input disturbances in the rendezvous problem. Some researchers studied the formation control of multi-vehicles with heterogenous control gains. In addition, MASs with heterogenous dynamics were also investigated. However, most results about the heterogeneous MASs were based on the integer-order models, a few results have been obtained based on the fractional-order models. Therefore, in this Chapter, we consider the delayed nonlinear FOMASs with **heterogenous control gains**, which is more reasonable and practical. Besides, as mentioned in Chapters 2 and 4, **time delays** are unavoidable in many applications. What's more, as mentioned in Chapter 4, in some situations, the structure of the MASs may be known and **the differential orders and system parameters are unknown**, which need to be identified beforehand.

Therefore, in this Chapter, under a fixed directed graph, the distributed cooperative synchronization of heterogenous uncertain nonlinear delayed FOMASs with a leader of bounded unknown input is investigated, where the fractional orders and system parameters are uncertain and the controller gains are heterogenous due to imperfect implementation. It should be noted that the study is more general by considering the FOMASs with time delays, unknown leader, heterogeneity and unknown nonlinear dynamics. Firstly, a differential evolution (DE)-based parameter identification method is proposed to identify the uncertain parameters. Then based on the identified parameters, by using the matrix theory, graph theory, fractional derivative inequality and comparison principle of linear fractional equation with delay, a heterogenous discontinuous controller is designed to achieve the distributed cooperative synchronization asymptotically. Thirdly, a heterogenous continuous controller is further constructed to suppress the undesirable chattering behaviour, where uniformly ultimately bounded (UUB) synchronization tracking errors can be achieved and tuned as small as desired. Finally, numerical simulations are provided to validate the effectiveness of the proposed parameter identification scheme and the designed control algorithms.

Compared with the existing works, our contribution are as follows. Firstly, compared with most results concerning the integer-order MASs, the delayed MASs with fractional-order dynamics, unknown leaders and parameters, and heterogenous control gains are involved. Secondly, different from some results studied the time delays with linear FOMASs, the time delay with nonlinear dynamics is further studied; Thirdly, different from most results without considering the leader's control input, we assume that the leader owns bounded unknown input, which could be more flexible and general in the distributed cooperative synchronization. Fourthly, different from most results, where the differential orders are assumed to be known, while in this Chapter, differential orders and system parameters are both considered to be unknown, and a DE-based parameter estimation method is proposed to identity the unknown parameters of the delayed heterogenous nonlinear FOMASs.

Chapter 6: As mentioned in Chapters 4 and 5, most consensus control algorithms are valid only for the FOMASs whose system parameters and fractional orders are known in advance. However, in practice, **the FOMASs are usually partly known**. That is, the form of the fractional-order differential equations are known, while some or all the fractional orders and system parameters are unknown. Therefore, in order to control and utilize the FOMASs, identifying the unknown fractional orders and system parameters is really important. In Chapter 4, an efficient artificial bee colony algorithm (ABC) is used to identify the unknown FOMASs. In Chapter 5, the differential evolution (DE) is selected to identify the unknown FOMASs. However, although the AIOAs, such as ABC and DE, have demonstrated superior features compared to other traditional methods, there is no specific algorithm that can achieve the best solution for all optimization problems. Namely, as far as most algorithms are concerned, it is difficult to simultaneously **manage the tradeoff between exploration and exploitation** successfully for all the optimization problems. Similarly, there are no exceptions for ABC and DE.

Therefore, in this Chapter, **to enhance the exploration and the exploitation abilities**, a modified artificial bee colony algorithm, named as mABC algorithm, is put forward. In mABC algorithm, the opposite population is generated using opposite numbers based on perturbation rate to jump out from the local optima. Secondly, two new searching equations are proposed and self-adaptive component is added to explore all the promising search regions. Thirdly, the random numbers in the searching equations are generated based on a chaotic map. Then, the proposed mABC algorithm is applied to the parameter identification of nonlinear FOMASs. Simulation results demonstrate that the proposed hybrid algorithm is effective and comparative to identify the unknown parameters when compared with some other typical population-based evolutionary algorithms.

Compared with the existing works, our contributions are as follows. Firstly, a new modified ABC algorithm is proposed. Secondly, a novel parameter identification scheme based on the modified ABC algorithm is put forward. Thirdly, non-parametric statistic tests are employed to demonstrate the performance of the proposed algorithm.

Conclusions and perspectives: In this chapter, the results are summarized and several possible directions for our future research are shared.

Papers accepted:

- **Wei Hu**, Guoguang Wen, Ahmed Rahmani, Jing Bai and Yongguang Yu. Leader-following consensus of heterogenous fractional-order multi-agent systems under input delays. *Asian journal of control*, DOI:10.1002/asjc.2137 (Hu *et al.*, 2019a)

- **Wei Hu**, Guoguang Wen, Ahmed Rahmani, and Yongguang Yu. Distributed consensus tracking of unknown nonlinear chaotic delayed fractional-order multi-agent systems with external disturbances based on ABC algorithm. *Communications in nonlinear science and numerical simulation*, 71, 101-117 (2019) (Hu *et al.*, 2019c)

- **Wei Hu**, Guoguang Wen, Ahmed Rahmani, and Yongguang Yu. Differential evolution-based parameter estimation and synchronization of heterogenous uncertain nonlinear delayed fractional-order multi-agent systems with unknown leader. *Nonlinear Dynamics*, 97(2), 1087-1105 (2019) (Hu *et al.*, 2019b)

- **Wei Hu**, Guoguang Wen, Ahmed Rahmani, and Yongguang Yu. Parameters estimation using mABC algorithm applied to distributed tracking control of unknown nonlinear fractional-order multi-agent systems with external disturbances. *Communications in nonlinear science and numerical simulation*, 79, 104933, (2019). (Hu *et al.*, 2019d)

- **Wei Hu**, Yongguang Yu, Ahmed Rahmani, and Guoguang Wen. Robust consensus tracking based on DE with parameters identification for uncertain nonlinear fractional-order multi-agent systems with external disturbances. *2019 International Conference on Fractional Calculus Theory and Applications (ICFCTA)*, 25-26 April 2019, Bourges, France. (Hu *et al.*, 2019e)

Chapter 2

Leader-following consensus of heterogenous FOMASs under input delays

Contents

2.1 Introduction

As mentioned in Chapter 1, the consensus of MASs with a (virtual) leader has become a particularly interesting topic, which is commonly named as leader-following consensus or consensus tracking. So far, for the leader-following consensus of FOMASs, some results have been obtained. For example, in Yu *et al.* (2015), leader-following consensus of FOMASs has been studied with algebraic graph theory and Lyapunov method. In Gong (2017), the nonlinear FOMASs with an unknown leader and heterogenous control gains were studied and consensus tracking was guaranteed. Bai *et al.* (2017b) proposed a sliding mode control method to fulfill the leader-following consensus of FOMASs. Ma *et al.* (2018) applied an impulsive controller to achieve the consensus tracking of nonlinear FOMASs. Note that for all the above results, the fractional orders between the leader and followers are all homogeneous, while in some complex environment, the fractional orders for the leader and followers may be heterogeneous, which can be more accurate and flexible in describing the dynamics of the leader-following MASs. Therefore, it is interesting and significant to learn the leader-following consensus of FOMASs with heterogenous fractional orders between leader and followers, which can be viewed as HFOMASs.

In many physical systems, the time delays universally exist because the signal propagation speed is limited, the sensor needs extra time to obtain the measurement information, the controller needs additional computation and execution time to produce and implement the control inputs. The undesirable instability and poor performance can easily happen due to the existence of time delays. Nowadays, many results about the leader-following consensus of integer-order delayed MASs have been obtained, which can be referred to Ni *et al.* (2017); Shariati & Tavakoli (2017); Wang & Su (2018); Wang *et al.* (2018b). Some results about the consensus of delayed FOMASs have been obtained (Shen & Cao, 2012; Yang *et al.*, 2014a; Zhu *et al.*, 2017). However, most of the works in Shen & Cao (2012); Yang *et al.* (2014a); Zhu *et al.* (2017) mainly deal with the leaderless consensus of delayed FOMASs. For leader-following consensus of delayed FOMASs with heterogenous fractional orders between leader and followers, little research has been done.

Given above discussion, in this Chapter, the HFOMASs without delays are considered firstly, where a control algorithm with a fractional-order estimator is proposed. Then, the identical input delays are considered in the above proposed control algorithm and the leader-following consensus of HFOMASs can be also achieved under the given condition. Thirdly, the control algorithm with diverse input delays is further studied, leader-following consensus of the HFOMASs can be guaranteed under the derived condition. Finally, the obtained results are verified with some simulations.

The main contributions are as following: firstly, different from the leaderless consensus of FOMASs (Bai *et al.*, 2018; Cao & Ren, 2010; Liu *et al.*, 2018a; Ren & Yu, 2017a; Song *et al.*, 2015; Yin *et al.*, 2013) and leader-following consensus of FOMASs with homogeneous orders between leader and followers (Bai *et al.*, 2017b; Gong, 2017; Ma *et al.*, 2018; Yu *et al.*, 2015), the leader-following consensus of FOMASs with heterogenous orders between leader and followers is investigated and a novel control algorithm with a fractional-order estimator is designed. Secondly, in contrast with leaderless consensus of delayed FOMASs (Shen & Cao, 2012; Yang *et al.*, 2014a; Zhu *et al.*, 2017) and leader-following consensus of FOMASs without time delays (Bai *et al.*, 2017b; Gong, 2017; Ma *et al.*, 2018; Yu *et al.*, 2015), the leader-following consensus of HFOMASs under input delays is considered based on the proposed control algorithm.

The rest parts of this chapter is organized as follows. Section 2.2 introduces the problem formulation. In Section 2.3, main results are introduced. In Section 2.4, the obtained results are convinced by some simulations. Section 2.5 is the conclusions.

2.2 Problem formulation

The leader is modeled as

$$x_0^{(\alpha)}(t) = u_0(t), \tag{2.1}$$

where $\alpha \in (0, 1]$, $x_0(t) \in R^n$ is the leader's state and $u_0(t) \in R^n$ is the leader's control input.

The followers are formulated as

$$x_i^{(\beta)}(t) = u_i(t) + \overline{u}_i(t), \quad i \in \mathcal{N} = \{1, 2, \cdots, N\}, \tag{2.2}$$

where $\beta \in (0, 1]$, $x_i(t) \in R^n$ is the ith follower's state vector. The ith follower's control input consists of $u_i(t)$ and $\overline{u}_i(t)$, and $\overline{u}_i(t)$ is related to $u_0(t)$ which can be viewed as an estimator of $u_0(t)$.

Remark 2.1 *Without loss of generality, a one-dimensional space is considered for all agents in this chapter, which can be easily extended to n-dimensional ($n > 1$) case with Kronecker product.*

Assumption 2.2 *The fixed communication graph $\bar{\mathcal{G}}$ contains a directed spanning tree with leader as the root node.*

Assumption 2.3 *For each follower $i \in \mathcal{N}$, if $u_0(t)$ is given, there has $\overline{u}_i(t)$ such that $s^{-\alpha}\mathcal{L}\{u_0(t); s\} = s^{-\beta}\mathcal{L}\{\overline{u}_i(t); s\}$, where $u_0(t)$ and $\overline{u}_i(t)$ are defined in (2.1) and (2.2).*

Remark 2.4 *If $u_0(t)$ is set, $\overline{u}_i(t)$ can be calculated by the inverse Laplace transform such that $s^{-\alpha}\mathcal{L}\{u_0(t); s\} = s^{-\beta}\mathcal{L}\{\overline{u}_i(t); s\}$. Thus, the Assumption 2.3 is reasonable.*

Definition 2.5 *For any initial conditions, the MASs (2.1) and (2.2) are said to achieve leader-following consensus if*

$$\lim_{t\to\infty} \big(x_i(t) - x_0(t)\big) = 0, \quad \forall\, i \in \mathcal{N}.$$

2.3 Main results

2.3.1 Case without input delays

In this subsection, the leader-follower consensus of HFOMASs (2.1) and (2.2) without input delays is investigated.

The ith follower's control input $u_i(t)$ in (2.2) is designed as

$$u_i(t) = -\gamma\Sigma_{j=0}^{N} a_{ij}\big(x_i(t) - x_j(t)\big), \tag{2.3}$$

where γ is a positive constant.

Theorem 2.6 *(Hu et al., 2019a) Given Assumptions 2.2 and 2.3, the HFOMASs (2.1) and (2.2) can achieve leader-following consensus.*

Proof: Performing Laplace transform of (2.1), it can be given as: $s^\alpha X_0(s) - s^{\alpha-1}x_0(0) = \mathcal{L}\{u_0(t); s\}$, where $X_0(s) = \mathcal{L}\{x_0(t); s\}$, it is easy to see that

$$X_0(s) = s^{-1}x_0(0) + s^{-\alpha}\mathcal{L}\{u_0(t); s\}. \tag{2.4}$$

Similarly, with the Laplace transform of (2.2), one has

$$\begin{aligned} & s^\beta X_i(s) - s^{\beta-1}x_i(0) \\ & \quad = -\gamma\Sigma_{j=0}^{N} a_{ij}\big(X_i(s) - X_j(s)\big) + \mathcal{L}\{\overline{u}_i(t); s\}, \end{aligned}$$

where $X_i(s) = \mathcal{L}\{x_i(t); s\}, i \in \mathcal{N}$. Then we can obtain

$$\begin{aligned} X_i(s) = s^{-1}x_i(0) - s^{-\beta}\gamma\Sigma_{j=0}^{N}a_{ij}\big(X_i(s) - X_j(s)\big) \\ + s^{-\beta}\mathcal{L}\{\overline{u}_i(t); s\}. \end{aligned} \tag{2.5}$$

Denote error vector as $e_i(t) = x_i(t) - x_0(t)$. The Laplace transform of $e_i(t)$ is $E_i(s) = \mathcal{L}\{e_i(t); s\} = X_i(s) - X_0(s)$. Subtracting (2.4) from (2.5) gets the error system:

$$E_i(s) = s^{-1}e_i(0) - s^{-\beta}\gamma\Sigma_{j=0}^{N}a_{ij}\big(E_i(s) - E_j(s)\big),$$

which can be rewritten as

$$E(s) = s^{-1}e(0) - s^{-\beta}\gamma M E(s), \tag{2.6}$$

where $E(s)$ and $e(0)$ denote the column vectors of $E_i(s)$ and $e_i(0)$ respectively. From (2.6), it can be calculated that

$$E(s) = (s^{\beta}I_N + \gamma M)^{-1}\big(s^{\beta-1}e(0)\big). \tag{2.7}$$

The characteristic equation of (2.7) is

$$det(s^{\beta}I_N + \gamma M) = 0, \tag{2.8}$$

which can be viewed as the characteristic equation of the following system

$$e^{\beta}(t) = -\gamma M e(t). \tag{2.9}$$

Therefore, the achievement of leader-following consensus of HFOMASs (2.1) and (2.2) is equivalent to the asymptotically stable problem of system (2.9). Based on Assumption 2.2 and Lemma 1.1, one has

$$min_{i\in\mathcal{N}}|arg\big(\lambda_i(-\gamma M)\big)| > \pi/2 > \beta\pi/2, \quad \beta \in (0, 1].$$

According to Lemma 1.15, system (2.9) is asymptotically stable. This completes the proof. ■

Based on Lemma 1.15, a more general condition for the leader-following consensus of HFOMASs (2.1) and (2.2) can be easily obtained as following:

Corollary 2.7 *(Hu et al., 2019a) Given Assumptions 2.2 and 2.3, the HFOMASs (2.1) and (2.2) can achieve leader-following consensus if and only if*

$$min_{i\in\mathcal{N}}|arg\big(\lambda_i(-\gamma M)\big)| > \beta\pi/2, \quad \beta \in (0, 1],$$

where $\lambda_i(-\gamma M)$ represent the eigenvalues of $-\gamma M$.

Proof: Based on system (2.9) and Lemma 1.15, the above Corollary 2.7 can be easily derived. ■

2.3.2 Case with identical input delays

In this subsection, a control algorithm with identical input delays is proposed to achieve the leader-following consensus of HFOMASs, and a necessary and sufficient condition is obtained, which has closed relationship with the eigenvalue of the directed graph $\bar{\mathcal{G}}$ and the followers' fractional order β.

The dynamics of the followers with identical input delays are described as

$$x_i^{(\beta)}(t) = u_i(t-\tau) + \overline{u}_i(t), \ i \in \mathcal{N} = \{1, \cdots, N\}, \tag{2.10}$$

where $u_i(t-\tau) = -\gamma\Sigma_{j=0}^{N} a_{ij}\big(x_i(t-\tau) - x_j(t-\tau)\big)$, τ is the input delay with identical value for each follower, the definitions of other parameters and variables in (2.10) are the same as those of (2.2) and (2.3).

Theorem 2.8 *(Hu et al., 2019a) Given Assumptions 2.2 and 2.3, the leader-following consensus of HFOMASs (2.1) and (2.10) can be achieved if and only if*

$$\tau < \min_{i\in\mathcal{N}} \frac{\pi - \pi\beta/2 + arg(\mu_i)}{(\gamma|\mu_i|)^{1/\beta}}, \tag{2.11}$$

where μ_i is the eigenvalue of M.

Proof: Conducting Laplace transform of (2.10) yields

$$\begin{aligned} &s^\beta X_i(s) - s^{\beta-1}x_i(0) \\ &\quad = -\gamma\Sigma_{j=0}^{N} a_{ij} e^{-\tau s}\big(X_i(s) - X_j(s)\big) + \mathcal{L}\{\overline{u}_i(t); s\}, \end{aligned} \tag{2.12}$$

where $X_i(s) = \mathcal{L}\{x_i(t); s\}, i \in \mathcal{N}$. Then, through simple calculation, the following formula can be obtained as:

$$\begin{aligned} X_i(s) =& - s^{-\beta}\gamma e^{-\tau s}\Sigma_{j=0}^{N} a_{ij}\big(X_i(s) - X_j(s)\big) + s^{-1}x_i(0) \\ &+ s^{-\beta}\mathcal{L}\{\overline{u}_i(t); s\}. \end{aligned} \tag{2.13}$$

Let $e_i(t) = x_i(t) - x_0(t)$ be the error vector, the corresponding Laplace transform is $E_i(s) = \mathcal{L}\{e_i(t); s\} = X_i(s) - X_0(s)$. Subtracting (2.4) from (2.13), the error system can be obtained as

$$E_i(s) = s^{-1}e_i(0) - s^{-\beta}\gamma e^{-\tau s}\Sigma_{j=0}^{N} a_{ij}\big(E_i(s) - E_j(s)\big),$$

which can be rewritten as

$$E(s) = s^{-1}e(0) - s^{-\beta}\gamma e^{-\tau s}ME(s), \tag{2.14}$$

where $E(s)$ and $e(0)$ are the column vectors of $E_i(s)$ and $e_i(0)$ respectively. $E(s)$ can be obtained as

$$E(s) = (s^{\beta}I_N + \gamma e^{-\tau s}M)^{-1}\big(s^{\beta-1}e(0)\big). \tag{2.15}$$

The characteristic equation of (2.15) is

$$det(s^{\beta}I_N + \gamma e^{-\tau s}M) = 0. \tag{2.16}$$

Since $det(s^{\beta}I_N + \gamma e^{-\tau s}M) = \prod_{i=1}^{N}(s^{\beta} + \gamma e^{-\tau s}\mu_i)$ and the real part of the eigenvalue μ_i of M are positive based on Lemma 1.1, therefore all the characteristic roots of (2.16) are nonzero. With generalized Nyquist stability criterion (Desoer & Wang, 1980), all of the roots of $s^{\beta} + \gamma e^{-\tau s}\mu_i = 0$ are on the open left half plane if and only if the Nyquist plot of $G_i(\omega) = \gamma e^{-j\omega\tau}\mu_i/(j\omega)^{\beta}$ neither encircle nor touches the point $(-1, j\omega)$ for all $\omega \in (-\infty, +\infty)$. Because the Nyquist plot is symmetric, the case of $\omega \in (0, +\infty)$ is only considered. In the following, the bound of the input delays is derived. By some calculation of $G_i(\omega)$, we can obtain that:

$$\begin{aligned} G_i(\omega) &= \frac{\gamma e^{-j\omega\tau}|\mu_i|e^{jarg(\mu_i)}}{\omega^\beta e^{j\pi\beta/2}} \\ &= \frac{\gamma|\mu_i|}{\omega^\beta}e^{j\left(arg(\mu_i)-\omega\tau-\pi\beta/2\right)} \\ &= \frac{\gamma|\mu_i|}{\omega^\beta}\Big(\cos\left(\omega\tau+\pi\beta/2-arg(\mu_i)\right)-j\sin\left(\omega\tau+\pi\beta/2-arg(\mu_i)\right)\Big). \end{aligned}$$

Fig. 2.1 shows the Nyquist plot of $G_i(\omega)$, which does not enclose $(-1, j0)$ if and only if the intersection point, where the real axis is intersected with $G_i(\omega)$ for the first time as ω varies from 0 to $+\infty$, is on the right side of (-1, j0). This means

$$\omega\tau + \pi\beta/2 - arg(\mu_i) = \pi, \ \ and \ \gamma|\mu_i|/\omega^\beta < 1,$$

which implies

$$\tau < \min_{i\in\mathcal{N}} \frac{\pi - \pi\beta/2 + arg(\mu_i)}{(\gamma|\mu_i|)^{1/\beta}}.$$

Therefore, under condition (2.11), error system (2.15) is asymptotically stable. This completes the proof. ■

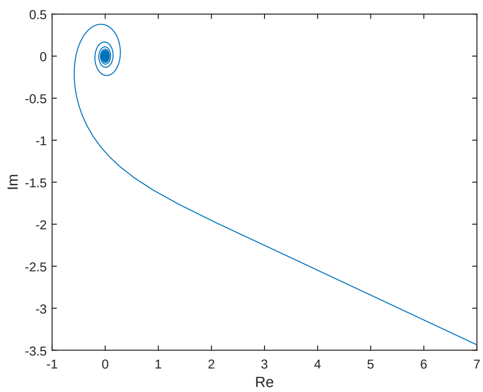

Fig. 2.1. Nyquist plot of $G_i(\omega)$ for $\mu_i = 1+2i, \beta = 0.9, \tau = 0.6$

Remark 2.9 *Theorem 2.8 demonstrates that the followers' fractional order β, the control gain γ and the eigenvalues μ_i of matrix M paly important roles in the threshold of the input delay τ.*

2.3.3 Case with diverse input delays

In this subsection, a control algorithm with diverse input delays is considered and leader-following consensus of HFOMASs can be achieved under the proposed sufficient condition.

The dynamics of the followers with diverse input delays are described as

$$x_i^{(\beta)}(t) = u_i(t-\tau_i) + \overline{u}_i(t),\ i \in \mathcal{N} = \{1, \cdots, N\}, \tag{2.17}$$

where $u_i(t-\tau_i) = -\gamma\Sigma_{j=0}^{N} a_{ij}\big(x_i(t-\tau_i) - x_j(t-\tau_i)\big)$, τ_i is the ith follower's input delay which is different from each follower, the definitions of other parameters and variables are the same as those of (2.2) and (2.3).

Theorem 2.10 *(Hu et al., 2019a) Given Assumptions 2.2 and 2.3, the leader-following consensus of HFOMASs (2.1) and (2.17) can be achieved if*

$$\tau_i < \frac{(2-\beta)\pi}{2(2\gamma d_i)^{1/\beta}},\quad i \in \mathcal{N}, \tag{2.18}$$

where $d_i = \sum_{k=0}^{N} a_{ik}$, which is the in-degree of the ith follower in graph $\bar{\mathcal{G}}$.

Proof: Performing Laplace transform of system (2.17), one has

$$\begin{aligned} &s^{\beta}X_i(s) - s^{\beta-1}x_i(0) \\ &= -\gamma\Sigma_{j=0}^{N} a_{ij}e^{-\tau_i s}\big(X_i(s) - X_j(s)\big) + \mathcal{L}\{\overline{u}_i(t); s\}, \end{aligned} \tag{2.19}$$

where $X_i(s) = \mathcal{L}\{x_i(t); s\}, i \in \mathcal{N}$. Then, after simple calculation, (2.19) can be written as

$$\begin{aligned} X_i(s) = &- s^{-\beta}\gamma\Sigma_{j=0}^{N} a_{ij}e^{-\tau_i s}\big(X_i(s) - X_j(s)\big) \\ &+ s^{-1}x_i(0) + s^{-\beta}\mathcal{L}\{\overline{u}_i(t); s\}. \end{aligned} \tag{2.20}$$

Let $e_i(t) = x_i(t) - x_0(t)$ be the error vector, then the corresponding Laplace transform is $E_i(s) = \mathcal{L}\{e_i(t); s\} = X_i(s) - X_0(s)$. Subtracting (2.4) from (2.20), the error system can be obtained as

$$E_i(s) = s^{-1}e_i(0) - s^{-\beta}\gamma\Sigma_{j=0}^{N} a_{ij}e^{-\tau_i s}\big(E_i(s) - E_j(s)\big),$$

which can be rewritten as

$$E(s) = s^{-1}e(0) - s^{-\beta}\gamma\Lambda(s)ME(s), \tag{2.21}$$

where $E(s)$ and $e(0)$ are the column vectors of $E_i(s)$ and $e_i(0)$ respectively, $\Lambda(s) = diag\{e^{-\tau_1 s}, e^{-\tau_2 s}, \cdots, e^{-\tau_N s}\}$. From (2.21), it can be obtained as

$$E(s) = \big(s^{\beta}I_N + \gamma\Lambda(s)M\big)^{-1}\big(s^{\beta-1}e(0)\big). \tag{2.22}$$

Then the characteristic equations is

$$det\big(s^{\beta}I + \gamma\Lambda(s)M\big) = 0. \tag{2.23}$$

Due to $det\big(s^{\beta}I_N + \gamma\Lambda(s)M\big) = \prod_{i=1}^{N}(s^{\beta} + \gamma e^{-\tau_i s}\mu_i)$ and all the eigenvalue μ_i of M have positive real part based on Lemma 1.1, therefore all the characteristic roots of the characteristic equation (2.23) are nonzero. Then let $F(s) = det(I_N + s^{-\beta}\gamma\Lambda(s)M)$, in the next step, we will proof all the zeros of $F(s) = 0$ are on the left half plane.

Let $G(s) = s^{-\beta}\gamma\Lambda(s)M$, $s = j\omega$ with j denoting complex number unit. With generalized Nyquist stability criterion (Desoer & Wang, 1980), the zeros of the $F(s)$ are all on the left half plane if the eigenvalue of the $G(j\omega)$, i.e., $\lambda\big((j\omega)^{-\beta}\gamma\Lambda(j\omega)M\big)$, neither enclose nor touch the point $(-1, j0)$ for $\omega \in (-\infty, +\infty)$. After simple calculation, one obtains

$$G(j\omega) = \gamma\omega^{-\beta}diag\{e^{-j(\omega\tau_1+\beta\pi/2)}, e^{-j(\omega\tau_2+\beta\pi/2)}, \cdots, e^{-j(\omega\tau_N+\beta\pi/2)}\}M. \tag{2.24}$$

Here, to estimate the eigenvalue of the matrix $G(j\omega)$ denoted as $\lambda(G(j\omega))$, the Gerschgorin's disc theory introduced in Lemma 1.23 is used, and one has

$$\lambda\big(G(j\omega)\big) \in \cup_{i\in\mathbb{N}}G_i, \tag{2.25}$$

where for $i \in \mathcal{N}$,

$$\begin{aligned} G_i = \{\delta \in \mathrm{C}, &|\delta - \gamma\omega^{-\beta} d_i e^{-j(\omega\tau_i + \beta\pi/2)}| \\ &\leq \gamma\omega^{-\beta} \sum_{k=1}^{N} |a_{ik} e^{-j(\omega\tau_i+\beta\pi/2)}| \\ &\leq \gamma\omega^{-\beta} \sum_{k=0}^{N} |a_{ik} e^{-j(\omega\tau_i+\beta\pi/2)}|\}, \end{aligned} \tag{2.26}$$

with $d_i = \sum_{k=0}^{N} a_{ik}$. After sorting, one has

$$G_i = \{\delta \in \mathrm{C}, |\delta - \gamma\omega^{-\beta} d_i e^{-j(\omega\tau_i+\beta\pi/2)}| \leq \gamma\omega^{-\beta} d_i\}. \tag{2.27}$$

From (2.27), it is clearly seen that G_i is a disc, and the origin of the disc G_i is $\gamma\omega^{-\beta} d_i e^{-j(\omega\tau_i+\beta\pi/2)}$ and the radius of the disc G_i is $\gamma\omega^{-\beta} d_i$. Then, we will proof that arbitrary point $(-a, j0)(a \geq 1)$ is not in the disc $G_i(i \in \mathcal{N})$, i.e., the distance between the point $(-a, j0)(a \geq 1)$ and the origin of the disc G_i is larger than the radius of the disc G_i. Thus, let

$$\triangle = |(-a + j0) - \gamma\omega^{-\beta} d_i e^{-j(\omega\tau_i+\beta\pi/2)}|^2 - (\gamma\omega^{-\beta} d_i)^2.$$

After simple calculation, it can be obtained as

$$\triangle = a\big(a + 2\gamma\omega^{-\beta} d_i \cos(\omega\tau_i + \beta\pi/2)\big).$$

Let $\omega_c\tau_i + \beta\pi/2 = \pi$, then $\cos(\omega_c\tau_i + \beta\pi/2) = -1$. Thus we can get $\triangle \geq a(a - 2\gamma\omega_c^{-\beta} d_i)$, where $\omega_c = (2-\beta)\pi/(2\tau_i)$. According to the condition (2.18) in Theorem 2.10, we can get that $2\gamma\omega_c^{-\beta} d_i = 2\gamma\big((2-\beta)\pi/(2\tau_i)\big)^{-\beta} d_i < 1$. Based on the hypothesis $a \geq 1$, we can get $\triangle \geq a(a - 2\gamma\omega_c^{-\beta} d_i) > 0$. Then we have

$$|(-a + j0) - \gamma\omega^{-\beta} d_i e^{-j(\omega\tau_i+\beta\pi/2)}| > \gamma\omega^{-\beta} d_i,$$

which means that the point $(-a, j0)(a \geq 1)$ is not in the disc G_i. Thus the point $(-1, j0)$ is neither enclosed nor touched by the curves of eigenvalue $\lambda(G(j\omega))$ of matrix $G(j\omega)$. Therefore, all zero points of $F(s)$ have negative real parts. This completes the proof. ■

Remark 2.11 *The condition (2.18) in Theorem 2.10 indicates that the upper*

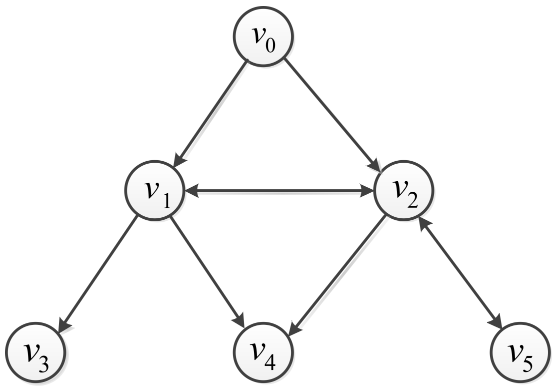

Fig. 2.2. Graph $\bar{\mathcal{G}}$ for case 1

bound of the input delay τ_i for follower i is related with the followers' fractional order β, control gain γ and in-degree of follower i. More specially, if the fractional order β and control gain γ are fixed for all the followers, the higher in-degree the agent i has, the less tolerance for the input delay the follower i has.

2.4 Simulations

Here we give three examples to verify Theorems 2.6-2.10. The directed graph with 0-1 weights is used.

1) Case without input delays: To verify Theorem 2.6, graph $\bar{\mathcal{G}}$ in Fig. 2.2 is employed. We randomly assume the order of the leader $\alpha = 0.8$ and the order of the followers $\beta = 0.9$, the dynamic of leader is $x_0^{(\alpha)}(t) = -0.01t^2$, the initial values are $[x_1(0), x_2(0), x_3(0), x_4(0), x_5(0), x_0(0)] = [2, -10, -8, 5, 7, 3]$. Choose $\gamma = 1, 2, 3$, the state trajectories of leader-follower consensus with one leader and five followers under different control gains γ are displayed in Fig. 2.3, which can verify Theorem 2.6. In addition, as the value γ increases, the convergence speed of achieving consensus becomes faster.

2) Case with identical input delays: Here, the MASs with one leader x_0 and four followers $x_i (i = 1, 2, 3, 4)$ is considered. Graph $\bar{\mathcal{G}}$ in Fig. 2.4 is used. Based on condition (2.11) in Theorem 2.8, the relationship between the upper bound of input delays and the control gains γ under different derivative orders β is illustrated in Fig. 2.5. Fig. 2.5 shows that the smaller the value of the derivative order β is, the faster the upper bound of the input delays change. Besides, based on condition (2.11) in Theorem 2.8, the relationship between the

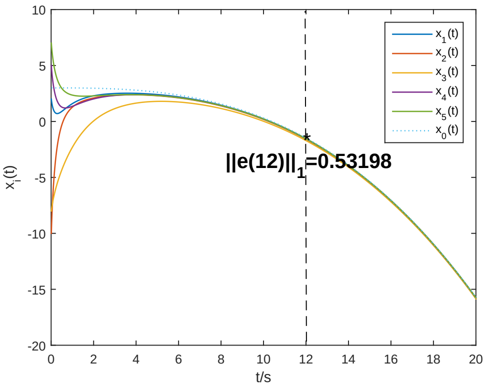

(a) Under $\gamma = 1$

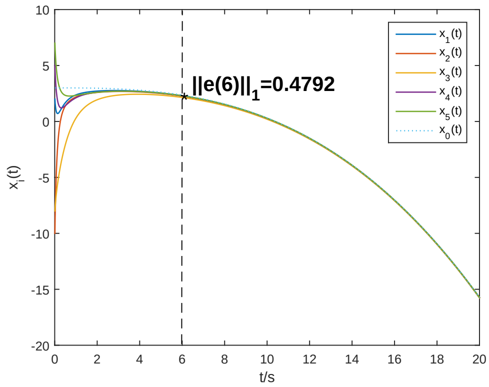

(b) Under $\gamma = 2$

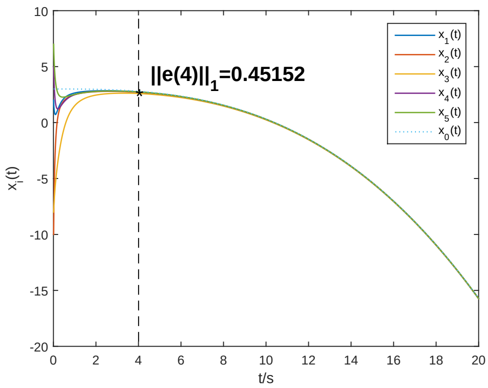

(c) Under $\gamma = 3$

Fig. 2.3. State trajectories of leader-follower consensus for case 1 under different values of γ

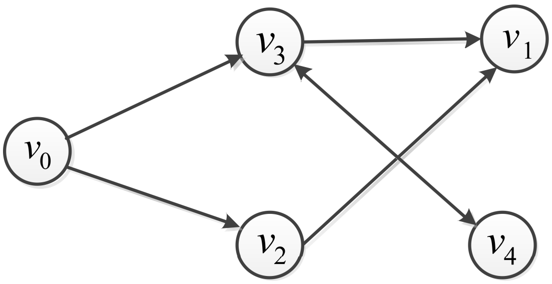

Fig. 2.4. Graph $\bar{\mathcal{G}}$ for case 2

upper bound of input delays and derivative orders β under different control gains is given in Fig. 2.6. Fig. 2.6 shows that under lower control gains, the agents with fractional orders are more tolerant than those with integer orders, while under high control gains, the agents with integer orders are more tolerant than those with fractional orders.

Here, the order of the leader is assumed as $\alpha = 0.8$, the order of the follower is assumed as $\beta = 0.9$, the control gain is chosen as $\gamma = 1$, the dynamic of leader is $x_0^{(\alpha)}(t) = 0.01t$, the initial values are $[x_1(0), x_2(0), x_3(0), x_4(0), x_0(0)] = [2, -10, -8, 5, 3]$. Based on condition (2.11) in Theorem 2.8, the leader-following consensus of HFOMASs (2.1) and (2.10) can be guaranteed if and only if $\tau < 0.59$. In the following, the different values of the input delays are choose as $\tau = 0.2, 0.5, 0.59, 0.8$ in respect. Fig. 2.7 depicts the states trajectories of the HFOMASs (2.1) and (2.10), which can verify the correctness of Theorem 2.8. Besides, Fig. 2.7 shows that if the input delay increases, the time to fulfill leader-following consensus of the HFOMASs (2.1) and (2.10) will increase. When $\tau = 0.59$, as the critical case, an oscillatory behavior happens. When $\tau = 0.8$, the leader-following consensus of the HFOMASs (2.1) and (2.10) can not be achieved which can confirm our derived results.

3) Case with diverse input delays: Consider MASs with one leader x_0 and five followers $x_i (i = 1, 2, \cdots, 5)$. Graph $\bar{\mathcal{G}}$ in Fig. 2.8 is considered. According to condition (2.18) in Theorem 2.10, the relationship between the upper bound of input delays and control gain γ for each agent with various derivative orders β can be obtained and illustrated as Fig. 2.9, where agent 1 is randomly selected as an example to show the corresponding relationship. Similarly, the relationship between the upper bound of input delays and derivative orders under different control gains for agent 1 is shown in Fig. 2.10, which indicates that under low

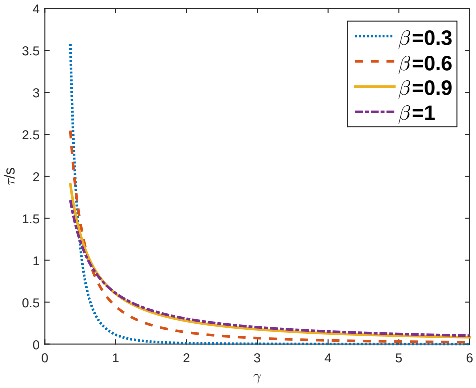

(a) Under large scale control gain

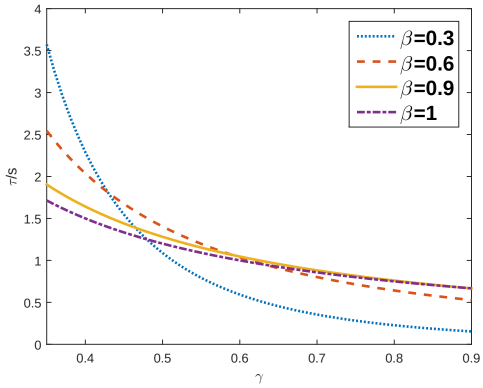

(b) Under small scale control gain

Fig. 2.5. Relationship between the upper bound of the input delay and the control gain

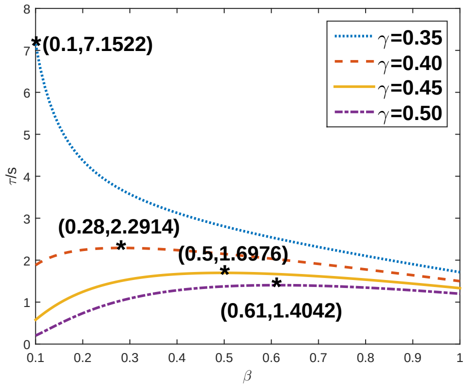

(a) Under low control gain

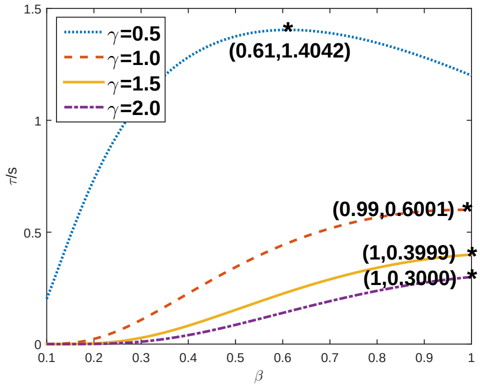

(b) Under high control gain

Fig. 2.6. Relationship between the upper bound of the input delay and the followers' derivative order

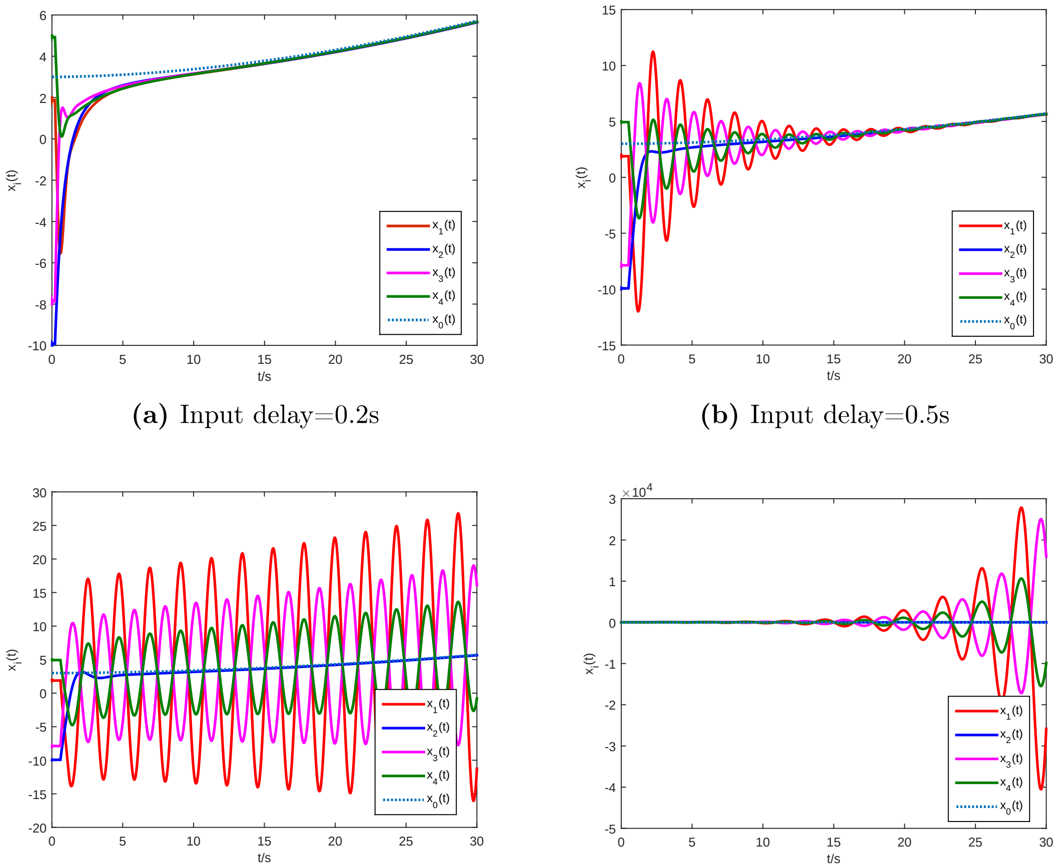

(a) Input delay=0.2s

(b) Input delay=0.5s

(c) Input delay=0.59s

(d) Input delay=0.8s

Fig. 2.7. State trajectories of leader-follower consensus for case 2 under identical input delays

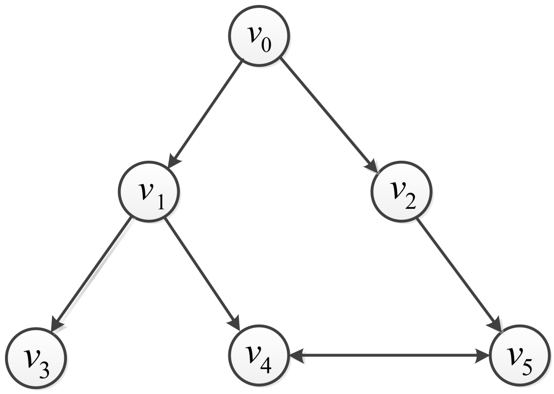

Fig. 2.8. Graph $\bar{\mathcal{G}}$ for case 3

control gains, the agents with fractional orders have more tolerance than those with integer orders, while under high control gains, the agents with integer orders have more tolerance than those with fractional orders.

In this example, the leader's order is assumed as $\alpha = 0.85$, the order of the followers is assumed as $\beta = 0.95$, the control gain is chosen as $\gamma = 1$, the dynamic of leader is $x_0^{(\alpha)}(t) = -0.03t^2 + 0.5t$, the initial values are $[x_1(0), x_2(0), x_3(0), x_4(0), x_5(0), x_0(0)] = [3, -6, 2, 8, -4, 5]$. Based on Theorem 2.10, it can be obtained that the consensus conditions requires $\tau_1 < 0.7951, \tau_2 < 0.7951, \tau_3 < 0.7951, \tau_4 < 0.3833, \tau_5 < 0.3833$. It should be noted that due to agents 1-3 have the same in-degrees which can be observed in Fig. 2.8, therefore based on condition (2.18), they have the same upper limit of input delays. With the same reason, agents 4 and 5 also own the same upper limits of the input delays. We randomly choose $\tau_1 = 0.79, \tau_2 = 0.79, \tau_3 = 0.79, \tau_4 = 0.38, \tau_5 = 0.38$. The state trajectories of the leader and followers are described in Fig. 2.11, which proves our theoretical results in Theorem 2.10.

2.5 Conclusion

This chapter addresses the leader-following consensus of HFOMASs with input delays, where the fractional orders between leader and followers are heterogenous and a control algorithm with a fractional-order estimator is designed. Firstly, the leader-following consensus of HFOMASs without input delays is studied, and a sufficient condition is obtained based on fractional-order stability theory. Secondly, the proposed control algorithm with the identical input delays is consid-

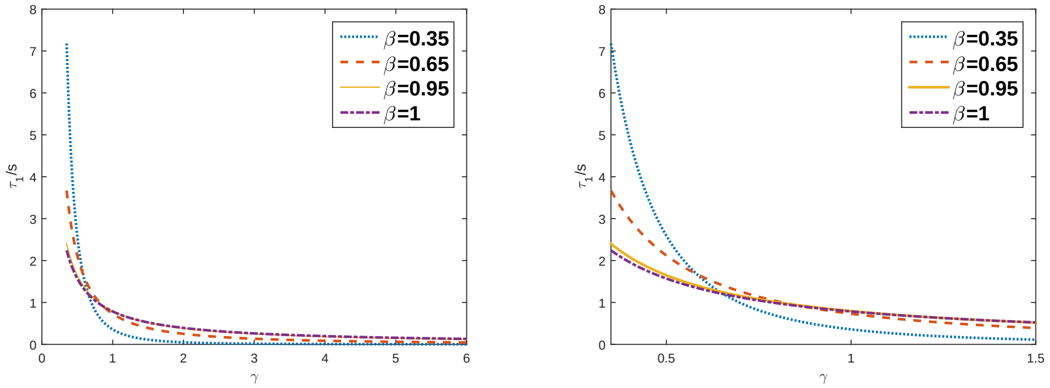

(a) Under large scale control gain (b) Under small scale control gain

Fig. 2.9. Relationship between the upper bound of the input delay and the control gain

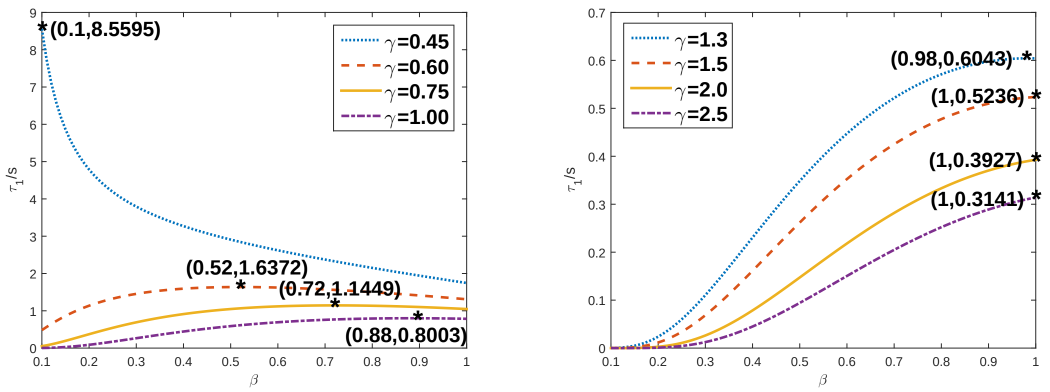

(a) Under low control gain (b) Under high control gain

Fig. 2.10. Relationship between the upper bound of the input delay and the followers' derivative order

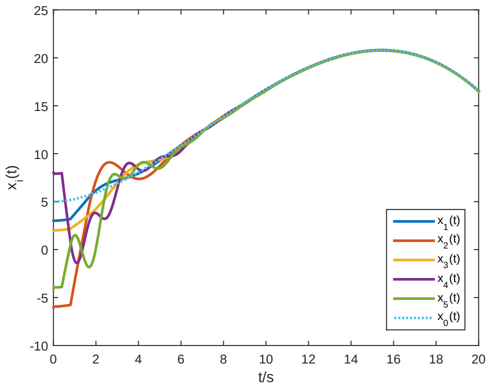

Fig. 2.11. State trajectories of leader-follower consensus for case 3 under diverse input delays

ered, with the generalized Nyquist stability theory, the HFOMASs can achieve leader-following consensus within a certain bound of input delays. Furthermore, the diverse input delays are further taken into account in the proposed control algorithm, leader-following consensus of the HFOMASs can be guaranteed under the derived sufficient condition. Finally, simulations are given to validate our results.

Chapter 3

Distributed consensus tracking of nonlinear FOMASs with external disturbances based on nonlinear algorithms

Contents

3.1 Introduction

Note that the results studied in Chapter 2 are based on single integrator systems without considering the external disturbances. However, in real applications, unknown external disturbances arising from environment and communication are usually unavoidable. External disturbances can easily lead to instability or bad performance. Thus, for the study of MASs, taking the external disturbances into account is much more important and significant. In recent years, many results about the mentioned topics have been developed. For instance, in Yu & Long (2015), consensus of second-order MASs with disturbances was studied based on integral sliding mode. In Liu *et al.* (2017a), a discontinuous observer was proposed to solve the consensus of MASs with external disturbances. In Dong & Wang (2018), a distributed observer was designed for the consensus of nonlinear MASs with unknown external disturbance. However, most existing results are only based on the integer-order MASs, few results have been obtained by considering the external disturbances into the FOMASs. In Yang *et al.* (2014a), consensus of FOMASs with external disturbance was studied, where the external disturbance was generated with a fractional linear systems. In Ren & Yu (2016, 2017b), consensus problem for linear and nonlinear FOMASs with external disturbances was investigated based on linear control protocol, where the control performances were not satisfying. Therefore, in order to improve the consensus performance of the FOMASs with external disturbances, it is very significant and promising to investigate the consensus problem of FOMASs with nonlinear control algorithms, which can accelerate the convergence speed and achieve a better convergence effect (Bai *et al.*, 2017b).

Note that most of the results for the consensus of FOMASs mentioned above are mainly based on single or double integrator systems. In practice, more complicated intrinsic dynamics may exist in mobile agents. However, due to the complexity of the FOMASs, stability of the nonlinear FOMASs is difficult to be verified. In Li *et al.* (2010a) and Duarte-Mermoud *et al.* (2015), the Lyapunov direct method for fractional-order systems has been investigated, where an efficient tool was proposed to verify the stability problem. But it is still difficult to design an ideal Lyapunov candidate function for the FOMAs due to the existence of the communication topology.

Based on the above discussions, the distributed consensus tracking of nonlinear FOMASs with external disturbances is investigated based on nonlinear algorithms. Firstly, a nonlinear discontinuous control protocol is put forward to deal with the distributed consensus tracking problem. Then, in order to eliminate the chattering phenomenon resulting from the discontinuity, a nonlinear continuous distributed algorithm is further designed to make the tracking error asymptotically converge to a bounded set which is given clearly and can be made small enough through selecting the parameters appropriately.

Compared with the existed results, There are four main differences. Firstly, different from Dong & Wang (2018); Liu *et al.* (2017a); Sun *et al.* (2016); Yu & Long (2015), the MASs with fractional dynamics are studied. Secondly, in contrast with Bai *et al.* (2017b); Cao & Ren (2010); Gong (2017); Sun *et al.* (2011); Yu *et al.* (2017b); Zhu *et al.* (2017), the external disturbances are considered into the FOMASs. Thirdly, different from Yang *et al.* (2014a), in this chapter we do not known the style of the external disturbances beforehand. What is more, different from Ren & Yu (2016, 2017b) where a linear control protocol was used, we propose two effective nonlinear control algorithms.

The rest of this chapter is organised as follows. In Section 3.2, the problem formulation is introduced. In Sections 3.3, to deal with the distributed consensus tracking of nonlinear FOMASs with external disturbances, a nonlinear discontinuous and continuous control algorithms are given respectively. In Section 3.4, several simulation results are performed to validate the proposed controllers. Finally, a short conclusion is drawn in Section 3.5.

3.2 Problem formulation

Consider the nonlinear FOMASs with N followers described as

$$x_i^{(\alpha)}(t) = Ax_i(t) + f(x_i(t)) + u_i(t) + w_i(t), \qquad i \in \mathcal{N} = \{1, 2, \cdots, N\}, \tag{3.1}$$

where $\alpha \in (0, 1]$, $x_i(t) \in R^n$ and $u_i(t) \in R^n$ are the state and control input of the ith follower respectively. $f(x_i(t)) \in R^n$ is the corresponding intrinsic nonlinear dynamics, and $w_i(t) \in R^n$ denotes the external disturbances.

The leader's dynamic is

$$x_0^{(\alpha)}(t) = Ax_0(t) + f(x_0(t)), \tag{3.2}$$

where $\alpha \in (0, 1]$, $x_0(t) \in R^n$ and $f(x_0(t)) \in R^n$ represent the state vector and the intrinsic nonlinear dynamics for the leader respectively. It can be treated as an exosystem or a command generator, which produces the desired target trajectory.

Definition 3.1 *The distributed consensus tracking for MASs (3.1) and (3.2) are said to be achieved if for any initial conditions, the following condition is satisfied*

$$\lim_{t\to\infty} \|x_i(t) - x_0(t)\| = 0, \quad \forall\, i \in \mathcal{N}.$$

Before moving forward, the following assumptions are needed.

Assumption 3.2 *The communication topology $\bar{\mathcal{G}}$ among the followers and leader is undirected and connected.*

Assumption 3.3 *The nonlinear function f is continuous and satisfies the following local Lipschitz condition*

$$\|f(x(t)) - f(y(t))\| \leq l\|x(t) - y(t)\|, \qquad \forall\, x(t), y(t) \in R^n, \tag{3.3}$$

where $l > 0$ is the Lipschitz constant.

Assumption 3.4 *The external disturbances $w_i(t)$ satisfy $\|w_i(t)\| \leq \rho < +\infty, \forall\, i \in \mathcal{N}$.*

For the sake of convenience, denote that $e_{x_i} = x_i - x_0$, $e_{f_i} = f(x_i(t)) - f(x_0(t))$. Let $e_x, e_f, u(t)$ and $w(t)$ be the column vector of $e_{x_i}, e_{f_i}, u_i(t)$ and $w_i(t)$ respectively. Subtracting system (3.2) from system (3.1), the tracking errors e_x can be obtained as

$$e_x^{(\alpha)}(t) = (I_N \otimes A)e_x + e_f + u(t) + w(t). \tag{3.4}$$

Based on Assumption 3.2, v_0 is a global reachable node. Let $M = \mathcal{L} + \mathcal{B} = [m_{ij}]_{N\times N}$, then M is a symmetric positive definite matrix based on Lemma 1.1.

3.3 Main results

3.3.1 Nonlinear discontinuous tracking control algorithm

In this subsection, a nonlinear discontinuous control algorithm is proposed to tackle the problem of consensus tracking of nonlinear FOMASs considering external disturbances.

The following nonlinear discontinuous control protocol is designed for each follower:

$$u_i(t) = -ay_i - \beta h(y_i), \qquad i \in \mathcal{N} = \{1, 2, \cdots, N\}, \tag{3.5}$$

where $y_i = \sum_{j=0}^{N} a_{i,j}(x_i - x_j)$, and a, β are positive constant coupling gains, $h(y_i)$ is a nonlinear discontinuous function defined as

$$h(y_i) = \begin{cases} \frac{y_i}{\|y_i\|}, & \|y_i\| \neq 0, \\ \mathbf{0}_n, & \|y_i\| = 0. \end{cases} \tag{3.6}$$

Based on the graph theory introduced in Subsection 1.4.1, we can obtain that $y_i = \sum_{j=0}^{N} a_{i,j}(e_{x_i} - e_{x_j}) = \sum_{j=1}^{N} m_{ij}e_{x_j}$, which means $y = (M \otimes I_n)e_x = \tilde{M}e_x$, where y is the column vector of y_i.

Theorem 3.5 *(Hu et al., 2019d) Suppose that Assumptions 3.2-3.4 hold, if $a > \frac{\lambda_{max}(A+A^T)+2l}{2\lambda_{min}(\tilde{M})}$ and $\beta \geq \rho$, then the distributed consensus tracking of nonlinear FO-MASs (3.1) and (3.2) can be achieved under the nonlinear discontinuous control algorithm (3.5).*

Proof: Substituting the protocol (3.5) into tracking errors system (3.4) as

$$e_x^{(\alpha)}(t) = (I_N \otimes A)e_x + e_f - ay - \beta H(y) + w(t), \tag{3.7}$$

where $H(y)$ is the column vector of $h(y_i)$.

Construct the following Lyapunov function as

$$V(t) = e_x^T(M \otimes I_n)e_x = e_x^T\tilde{M}e_x. \tag{3.8}$$

Then based on Lemma 1.19, the fractional-order derivative of (3.8) with respect to time t along the trajectories of system (3.7) is

$$\begin{aligned} V^{(\alpha)}(t) &\leq 2e_x^T\tilde{M}e_x^{(\alpha)} \\ &= 2e_x^T\tilde{M}\big((I_N \otimes A)e_x + e_f - ay - \beta H(y) + w(t)\big) \\ &= 2e_x^T\tilde{M}(I_N \otimes A)e_x + 2e_x^T\tilde{M}e_f - 2ae_x^T\tilde{M}y - 2\beta e_x^T\tilde{M}H(y) + 2e_x^T\tilde{M}w(t). \end{aligned} \tag{3.9}$$

Based on the properties of Kronecker product introduced in Subsection 1.4.3 , we have

$$\begin{aligned} 2e_x^T \tilde{M}(I_N \otimes A)e_x &= 2e_x^T(M \otimes A)e_x \\ &= e_x^T(M \otimes A)e_x + e_x^T(M \otimes A)^T e_x \\ &= e_x^T\big(M \otimes (A + A^T)\big)e_x \\ &\leq \lambda_{max}(A + A^T)e_x^T \tilde{M} e_x. \end{aligned} \tag{3.10}$$

Based on Assumption 3.3, we have

$$2e_x^T \tilde{M} e_f \leq 2l e_x^T \tilde{M}^T e_x. \tag{3.11}$$

Due to $y = \tilde{M}e_x$, we have

$$-2ae_x^T \tilde{M} y = -2ae_x^T \tilde{M}\tilde{M}e_x \leq -2a\lambda_{min}(\tilde{M})e_x^T \tilde{M} e_x. \tag{3.12}$$

Due to $y = \tilde{M}e_x$ and $y_i^T h(y_i) = \|y_i\|$, we have

$$-2\beta e_x^T \tilde{M} H(y) = -2\beta y^T H(y) = -2\beta \sum_{i=1}^{N} \|y_i\|. \tag{3.13}$$

Due to $y = \tilde{M}e_x$ and $y_i^T w_i(t) \leq \|y_i\|\|w_i(t)\|$, combining with Assumption 3.4, we have

$$2e_x^T \tilde{M} w(t) = 2\sum_{i=1}^{N} y_i^T w_i(t) \leq 2\sum_{i=1}^{N} \|y_i\|\|w_i(t)\| \leq 2\rho \sum_{i=1}^{N} \|y_i\|. \tag{3.14}$$

Thus, based on (3.10)-(3.14) and $\beta > \rho$, we have

$$\begin{aligned} V^{(\alpha)}(t) \leq& -\big(2a\lambda_{min}(\tilde{M}) - \lambda_{max}(A + A^T) - 2l\big)e_x^T \tilde{M} e_x \\ &+ 2(\rho - \beta)\sum_{i=1}^{N} \|y_i\| \\ <& -\big(2a\lambda_{min}(\tilde{M}) - \lambda_{max}(A + A^T) - 2l\big)V(t). \end{aligned} \tag{3.15}$$

Because $a > \frac{\lambda_{max}(A+A^T)+2l}{2\lambda_{min}(\tilde{M})}$, i.e. $2a\lambda_{min}(\tilde{M}) - \lambda_{max}(A + A^T) - 2l > 0$, thus based on Lemma 1.16, the tracking error dynamics (3.7) is asymptotically stable. Therefore, the distributed consensus tracking problem is achieved in systems (3.1) and (3.2) with the control protocol (3.5). ■

3.3.2 Nonlinear continuous tracking control algorithm

In the last subsection, the $h(\cdot)$ in protocol (3.5) is discontinuous, which may generate the undesirable chattering behavior and restrict its application. Therefore, it is significant and interesting to design a continuous distributed protocol without undesirable chattering problem to solve the distributed consensus tracking.

In order to overcoming the chattering problem, by using the boundary layer technique (Slotine & Sastry, 1983), the following nonlinear continuous control protocol is proposed as

$$u_i(t) = -ay_i - \beta \bar{h}_i(y_i), \qquad i \in \mathcal{N} = \{1, 2, \cdots, N\}, \tag{3.16}$$

where

$$\bar{h}_i(y_i) = \begin{cases} \frac{y_i}{\|y_i\|}, & \|y_i\| > d_i, \\ \frac{y_i}{d_i}, & \|y_i\| \le d_i, \end{cases} \tag{3.17}$$

and $d_i > 0$ $(i = 1, 2, \cdots, N)$ are small constants, denoting the widths of the boundary layers. $y_i = \sum_{j=0}^{N} a_{i,j}(x_i - x_j)$, a, β are positive constant coupling gains.

Theorem 3.6 *(Hu et al., 2019e) Suppose that Assumptions 3.2-3.4 hold, the tracking errors of nonlinear FOMASs (3.1) and (3.2) are uniformly ultimately bounded (UUB) under the nonlinear continuous control algorithm (3.16), if $a > \frac{\lambda_{max}(A+A^T)+2l}{2\lambda_{min}(\tilde{M})}$ and $\beta \ge \rho$. Moreover, e_x asymptotically converges to the following bounded set*

$$\mathcal{D} = \left\{ e_x : \|e_x\|^2 \le \frac{2(\beta+\rho)\sum_{i=1}^{N} d_i}{\lambda_{min}(\tilde{M})\big(2a\lambda_{min}(\tilde{M}) - \lambda_{max}(A+A^T) - 2l\big)} \right\}. \tag{3.18}$$

Proof: Substituting the protocol (3.16) into tracking errors system (3.4), we can obtain that

$$e_x^{(\alpha)}(t) = (I_N \otimes A)e_x + e_f - ay - \beta \bar{H}(y) + w(t), \tag{3.19}$$

where $\bar{H}(y)$ is the column vector of $\bar{h}_i(y)$.

Consider the Lyapunov function candidate as (3.8), based on Lemma 1.19, its fractional-order derivative satisfies the following inequality

$$\begin{aligned} V^{(\alpha)}(t) &\leq e_x^T \tilde{M} e_x^{(\alpha)} \\ &= 2e_x^T \tilde{M}\big((I_N \otimes A)e_x + e_f - ay - \beta \bar{H}(y) + w(t)\big). \end{aligned} \tag{3.20}$$

Due to the virtue of (3.17), the following three cases are discussed.

(i) $\|y_i\| > d_i, i = 1, 2, \cdots, N$.

In this case, based on (3.13) and (3.14), one can obtained that

$$2e_x^T \tilde{M}\big(-\beta \bar{H}(y) + w(t)\big) = 2(-\beta + \rho)\sum_{i=1}^{N} \|y_i\| < 0. \tag{3.21}$$

Substituting (3.10)-(3.12) and (3.21) into(3.20) yields

$$V^{(\bar{\alpha})}(t) < -\big(2a\lambda_{min}(\tilde{M}) - \lambda_{max}(A + A^T) - 2l\big)V(t). \tag{3.22}$$

(ii) $\|y_i\| \leq d_i, i = 1, 2, \cdots, N$.

In this case, due to $y_i^T \bar{h}_i(y_i) = \|y_i\|^2/d_i \leq d_i$, one has

$$2e_x^T \tilde{M}\big(-\beta \bar{H}(y)\big) = -2\beta \sum_{i=1}^{N} y_i^T \bar{h}_i(y_i) = -2\beta \sum_{i=1}^{N} \|y_i\|^2/d_i \leq 2\beta \sum_{i=1}^{N} d_i. \tag{3.23}$$

Due to $y_i^T w_i(t) \leq \|y_i\|\|w_i(t)\| \leq \rho\|y_i\| \leq \rho d_i$, one has

$$2e_x^T \tilde{M} w(t) = 2\sum_{i=1}^{N} y_i^T w_i(t) \leq 2\sum_{i=1}^{N} \|y_i\|\|w_i(t)\| \leq 2\rho \sum_{i=1}^{N} \|y_i\| \leq 2\rho \sum_{i=1}^{N} d_i. \tag{3.24}$$

Therefore, one can deduce that

$$2e_x^T \tilde{M}\big(-\beta \bar{H}(y) + w(t)\big) \leq 2(\beta + \rho)\sum_{i=1}^{N} d_i. \tag{3.25}$$

Substituting (3.10)-(3.12) and (3.25) into Eq. (3.20) yields

$$\begin{aligned} V^{(\bar{\alpha})}(t) < &-\big(2a\lambda_{min}(\tilde{M}) - \lambda_{max}(A + A^T) - 2l\big)V(t) \\ &+ 2(\beta + \rho)\sum_{i=1}^{N} d_i. \end{aligned} \tag{3.26}$$

(iii) y satisfies neither Case (i) nor Case (ii).

Without loss of generality, suppose that $\|y_i\| > d_i, i = 1, 2, \cdots, k$, and $\|y_i\| \leq d_i, i = k+1, k+2, \cdots, N$, where $1 < k < N$. In this case, from (3.22) and (3.26), one can get that

$$\begin{aligned} V^{(\bar{\alpha})}(t) < &- \big(2a\lambda_{min}(\tilde{M}) - \lambda_{max}(A + A^T) - 2l\big)V(t) \\ &+ 2(\beta + \rho)\sum_{i=k+1}^{N} d_i. \end{aligned} \tag{3.27}$$

Therefore, by analyzing the above three cases, it can be easily deduced that

$$\begin{aligned} V^{(\bar{\alpha})}(t) < &- \big(2a\lambda_{min}(\tilde{M}) - \lambda_{max}(A + A^T) - 2l\big)V(t) \\ &+ 2(\beta + \rho)\sum_{i=1}^{N} d_i. \end{aligned} \tag{3.28}$$

Denote $\eta = 2a\lambda_{min}(\tilde{M}) - \lambda_{max}(A + A^T) - 2l$, let $z(t) = V(t) - \frac{2(\beta+\rho)\sum_{i=1}^{N} d_i}{\eta}$, this together with (3.28) implies that

$$z^{(\alpha)}(t) \leq -\eta z(t). \tag{3.29}$$

Then, there exists a nonnegative function $m(t)$ satisfying

$$z^{(\alpha)}(t) + m(t) = -\eta z(t). \tag{3.30}$$

Taking the Laplace transform of (3.30) gives

$$s^{\alpha}Z(s) - z(0)s^{\alpha-1} + M(s) = -\eta Z(s), \tag{3.31}$$

where $Z(s) = \mathcal{L}\{z(t); s\}$ and $M(s) = \mathcal{L}\{m(t); s\}$. Thus, we have

$$Z(s) = \frac{z(0)s^{\alpha-1} - M(s)}{s^{\alpha} + \eta}. \tag{3.32}$$

For (3.30), there exists a unique solution. By the inverse Laplace transform, we can achieve that

$$z(t) = z(0)E_{\alpha}(-\eta t^{\alpha}) - m(t) * \left(t^{\alpha-1}E_{\alpha,\alpha}(-\eta t^{\alpha})\right), \tag{3.33}$$

where $*$ is a convolution operator. Because $t^{\alpha-1}$ and $E_{\alpha,\alpha}(-\eta t^{\alpha})$ are nonnegative functions, thus the above Eq. (3.33) becomes

$$z(t) = V(t, e_x) - \frac{2(\beta+\rho)\sum_{i=1}^{N} d_i}{\eta} \leq z(0)E_{\alpha}(-\eta t^{\alpha}) \longrightarrow 0, \tag{3.34}$$

when $t \to +\infty$. Note that $V(t) \geq \lambda_{min}(\tilde{M})\|e_x\|^2$ and let t converge to infinity, then one has

$$\lim_{t\to+\infty} \|e_x\|^2 \leq \frac{2(\beta+\rho)\sum_{i=1}^{N} d_i}{\lambda_{min}(\tilde{M})\big(2a\lambda_{min}(\tilde{M}) - \lambda_{max}(A + A^T) - 2l\big)}. \tag{3.35}$$

Thus, one can obtain from Eq. (3.35) that tracking error e_x asymptotically converges to the bounded set $\mathcal{D}$ in Eq. (3.14). ■

Corollary 3.7 *If the widths d_i of the boundary layers are the same, i.e., $d_1 = d_2 = \cdots = d_N = d$, the bounded set can be simplified as*

$$\mathcal{D} = \left\{ e_x : \|e_x\|^2 \leq \frac{2(\beta+\rho)Nd}{\lambda_{min}(\tilde{M})\big(2a\lambda_{min}(\tilde{M}) - \lambda_{max}(A + A^T) - 2l\big)} \right\}. \tag{3.36}$$

Remark 3.8 *In virtue of Eqs. (3.14) and (3.36), the upper bound of the tracking errors e_x asymptotically converges to a bounded set which depends on the width d_i of the boundary layers. Thus, a sufficiently small acceptable tracking errors e_x with the nonlinear continuous algorithm (3.16) can be obtained asymptotically if a small enough d_i is chosen.*

3.4 Simulations

In the following simulation, we assume that the undirected graph has 0-1 weights for simplicity. Consider the FOMASs consisting of one leader and five followers. The communication topology is displayed in Fig. 3.1. Assume the FOMASs are modeled by fractional-order neural network with three neurons as

$$x_i^{(\alpha)}(t) = Ax_i(t) + f(x_i(t)), \quad i = 0, 1, \cdots, 5, \tag{3.37}$$

where $A = diag\{a_1, a_2, a_3\}$, $f(x_i(t)) = Btanh(x_i(t))$. When $\alpha = 0.98$, $A = -I_3$,

$$B = [b_{ij}]_{3\times 3} = \begin{bmatrix} 2 & -1.2 & 0 \\ 1.8 & 1.71 & 1.15 \\ -4.75 & 0 & 1.1 \end{bmatrix},$$

the system has a chaotic attractor. It can be easily obtained that $\lambda_{max}(A+A^T) = -2$, $l = 5.5$.

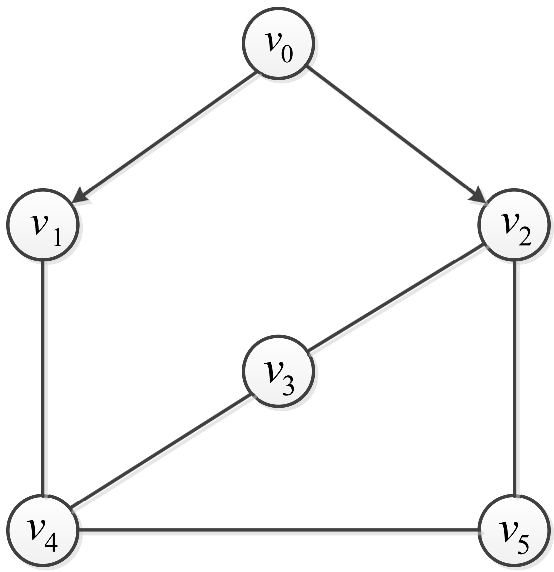

Fig. 3.1. The communication topology with one leader and five followers

The initial conditions are selected as $x_0(0) = [1, 2, 0.5]^T$, $x_1(0) = [3, 1.5, -1.2]^T$, $x_2(0) = [3, 0.3, -1.5]^T$, $x_3(0) = [4.5, -3.5, 0.5]^T$, $x_4(0) = [1.2, 1, -3]^T$, $x_5(0) = [2, -0.5, -2.5]^T$. The external disturbances are given as: $w_1(t) = 0.65sin(t+2), w_2(t) = 0.8cos(5t-6), w_3(t) = 0.35sin(3t+5), w_4(t) = 0.9sin(t+4), w_5(t) = 0.5cos(-7t+1)$. According to Theorems 3.5 and 3.6, we choose $a = 15 > 14.7, \beta = 1.5 > 1.3 = \rho$.

Firstly, for the nonlinear discontinuous control protocol (3.5), the state trajectories of consensus tracking are illustrated in Fig. 3.2, where five followers track the leader quickly within very short time. The phase portraits are also given in Fig. 3.3, which shows that the followers can tracking the chaotic attractor of the leader successfully. The control inputs are also provided in Fig. 3.4. Therefore, the feasibility of Theorem 3.5 is verified.

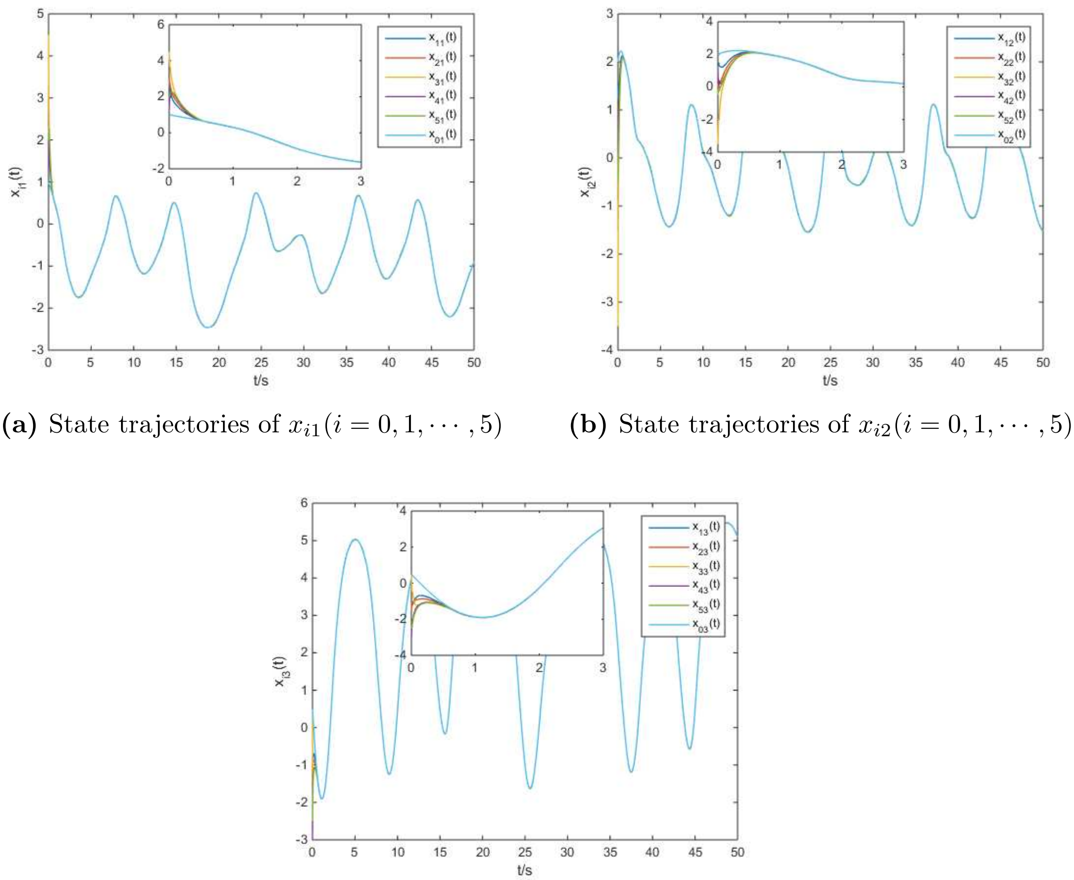

(a) State trajectories of $x_{i1}(i = 0, 1, \cdots, 5)$

(b) State trajectories of $x_{i2}(i = 0, 1, \cdots, 5)$

(c) State trajectories of $x_{i3}(i = 0, 1, \cdots, 5)$

Fig. 3.2. State trajectories of FOMASs (3.1) and (3.2) by control algorithm (3.5)

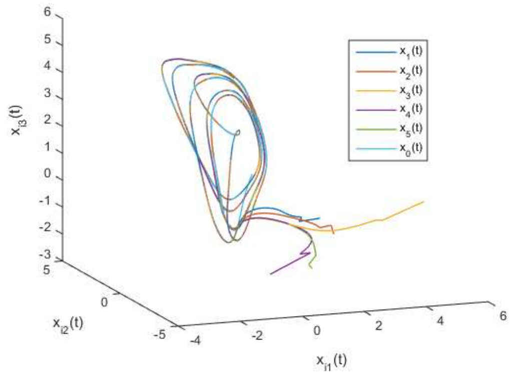

(a) Phase portrait in 3D

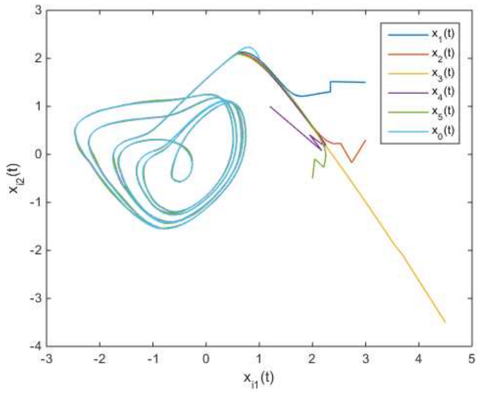

(b) Phase portrait in 2D

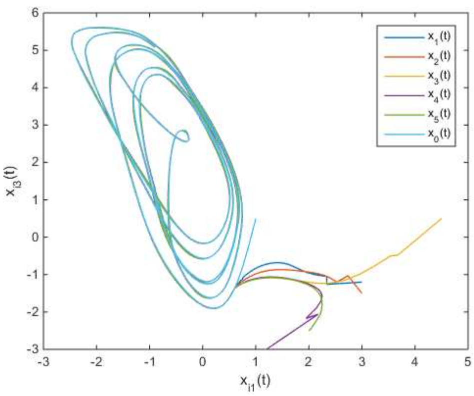

(c) Phase portrait in 2D

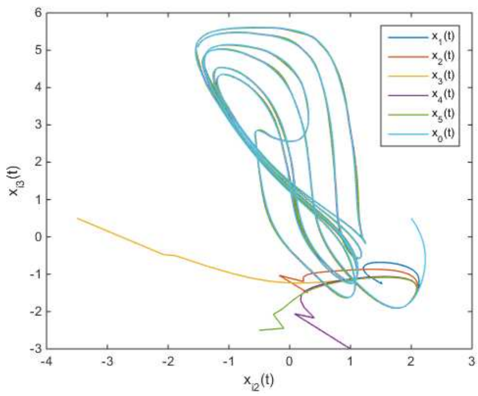

(d) Phase portrait in 2D

Fig. 3.3. Phase portraits for all agents ($i = 0, 1, \cdots, 5$) by control algorithm (3.5)

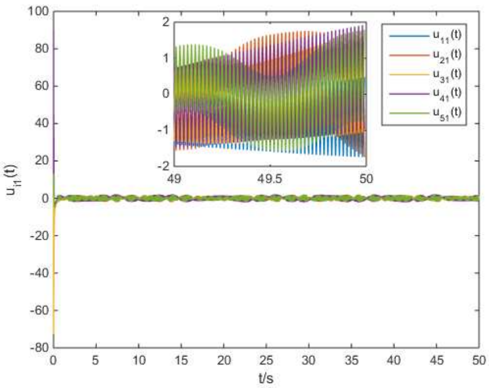

(a) Control inputs of $u_{i1}(i = 1, \cdots, 5)$

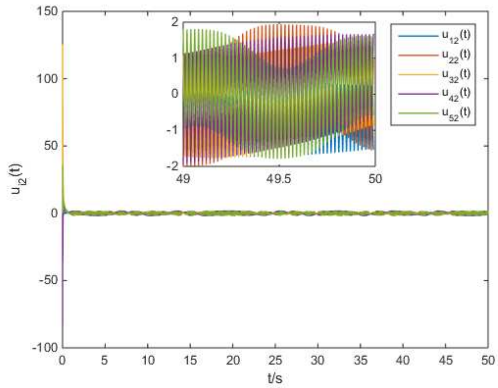

(b) Control inputs of $u_{i2}(i = 1, \cdots, 5)$

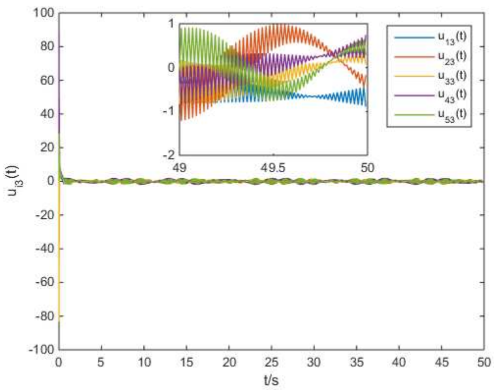

(c) Control inputs of $u_{i3}(i = 1, \cdots, 5)$

Fig. 3.4. Control inputs for control algorithm (3.5)

Then, for the nonlinear continuous control protocol (3.16), two cases are considered in terms of boundary layers widths d_i given in Eq. (3.17) as: $d_i = 0.2, (i = 1, 2, \cdots, 5)$ and $d_i = 2, (i = 1, 2, \cdots, 5)$. The state trajectories of consensus tracking are displayed in Figs. 3.5 and 3.8 respectively, where it can be concluded that the consensus tracking errors can asymptotically converge a sufficiently small neighborhood of zero if one can choose a sufficient small d_i. The phase portraits are also given in Figs. 3.6 and 3.9. Besides, chattering behavior can be avoided by the control protocol (3.16), which can be verified in Figs. 3.7 and 3.10. Therefore, the feasibility of Theorem 3.6 is proved as well.

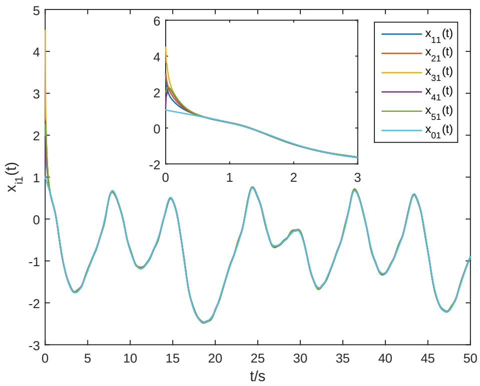

(a) State trajectories of $x_{i1}(i = 0, 1, \cdots, 5)$

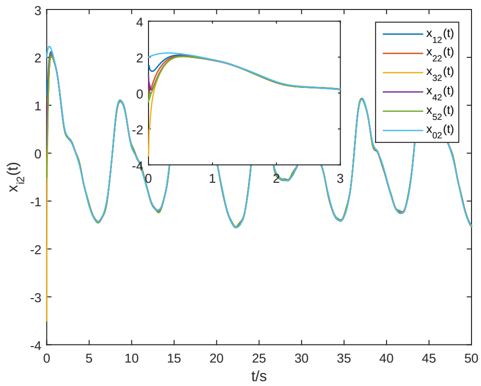

(b) State trajectories of $x_{i2}(i = 0, 1, \cdots, 5)$

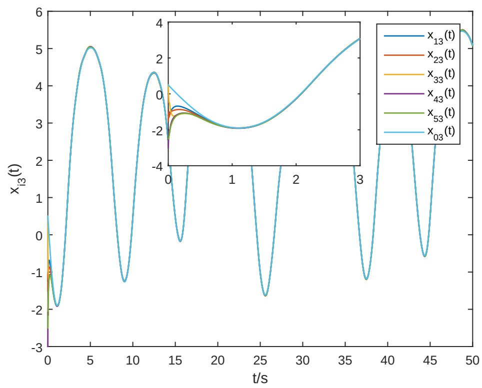

(c) State trajectories of $x_{i3}(i = 0, 1, \cdots, 5)$

Fig. 3.5. State trajectories of FOMASs (3.1) and (3.2) by control algorithm (3.16) with $d_i = 0.2$

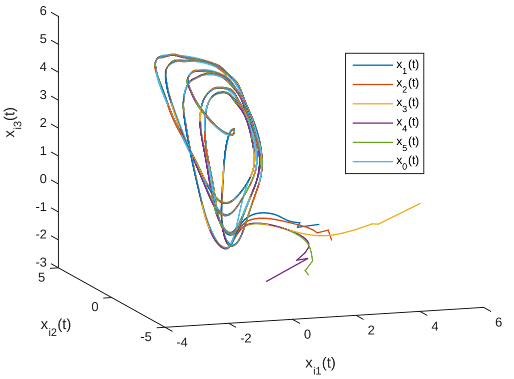

(a) Phase portrait in 3D

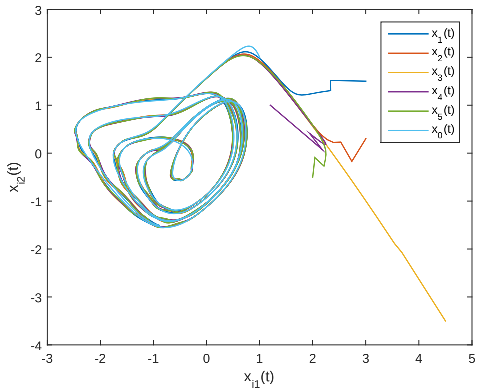

(b) Phase portrait in 2D

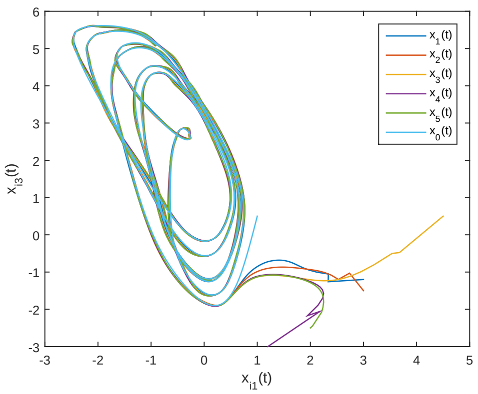

(c) Phase portrait in 2D

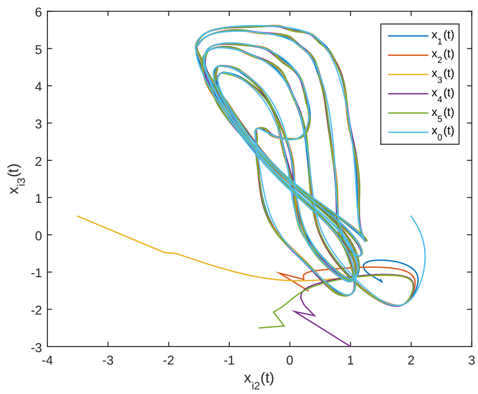

(d) Phase portrait in 2D

Fig. 3.6. Phase portraits for all agents ($i = 0, 1, \cdots, 5$) by control algorithm (3.16) with $d_i = 0.2$

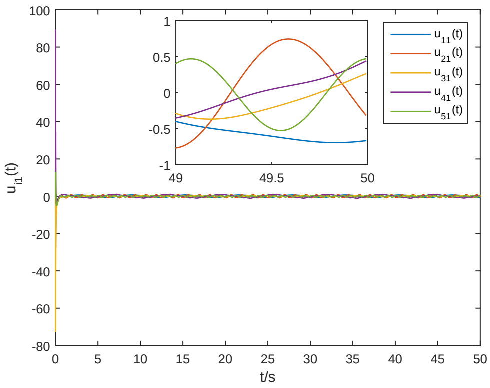

(a) Control inputs of $u_{i1}(i=1,\cdots,5)$

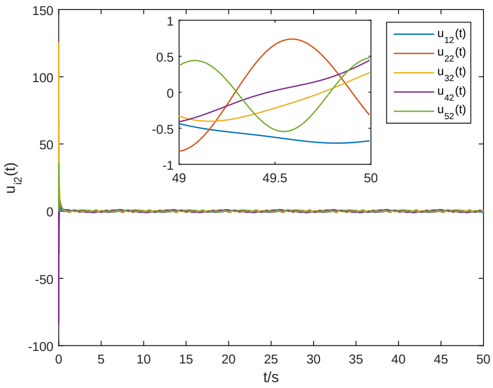

(b) Control inputs of $u_{i2}(i=1,\cdots,5)$

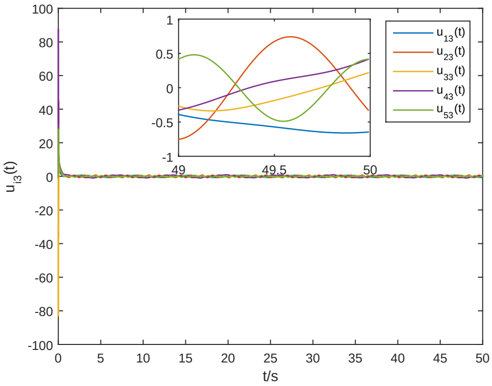

(c) Control inputs of $u_{i3}(i=1,\cdots,5)$

Fig. 3.7. Control inputs for control algorithm (3.16) with $d_i = 0.2$

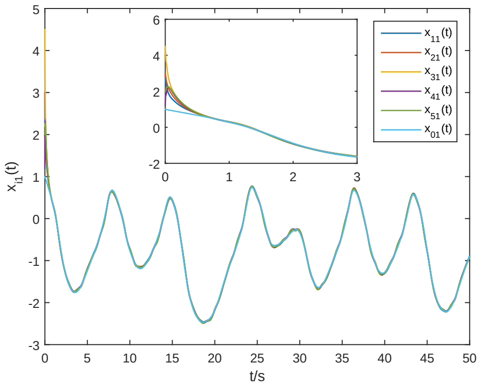

(a) State trajectories of $x_{i1}(i = 0, 1, \cdots, 5)$

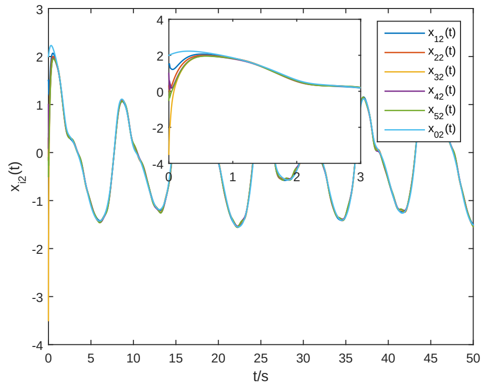

(b) State trajectories of $x_{i2}(i = 0, 1, \cdots, 5)$

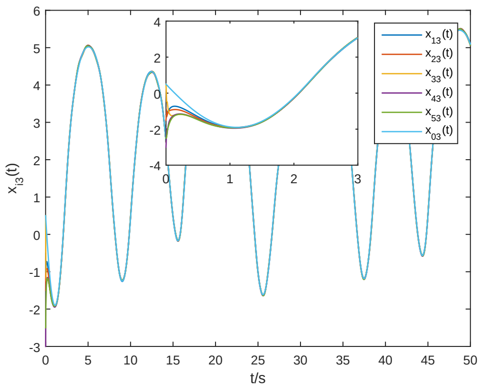

(c) State trajectories of $x_{i3}(i = 0, 1, \cdots, 5)$

Fig. 3.8. State trajectories of FOMASs (3.1) and (3.2) by control algorithm (3.16) with $d_i = 2$

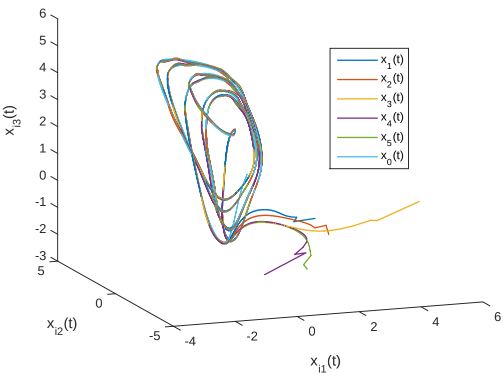

(a) Phase portrait in 3D

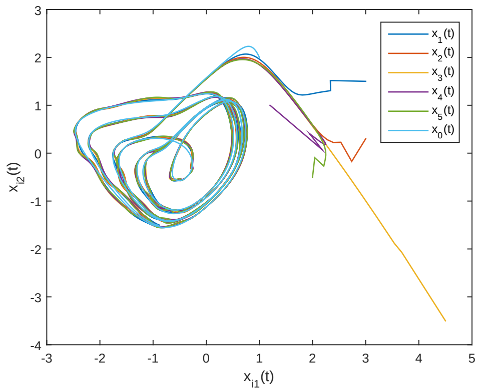

(b) Phase portrait in 2D

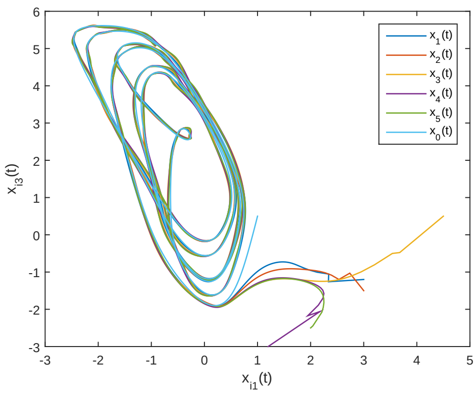

(c) Phase portrait in 2D

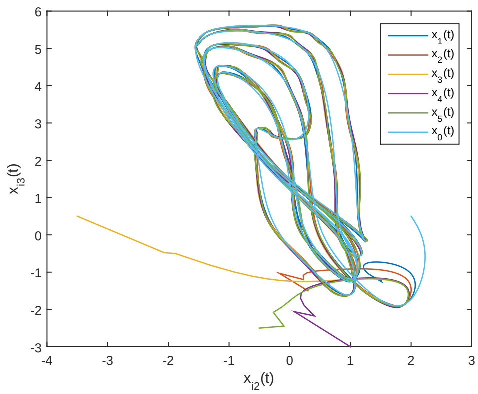

(d) Phase portrait in 2D

Fig. 3.9. Phase portraits for all agents ($i = 0, 1, \cdots, 5$) by control algorithm (3.16) with $d_i = 2$

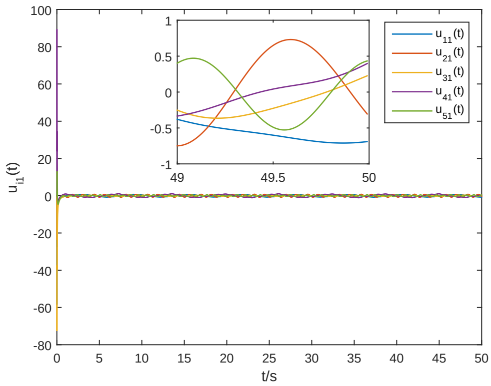

(a) Control inputs of $u_{i1}(i = 1, \cdots, 5)$

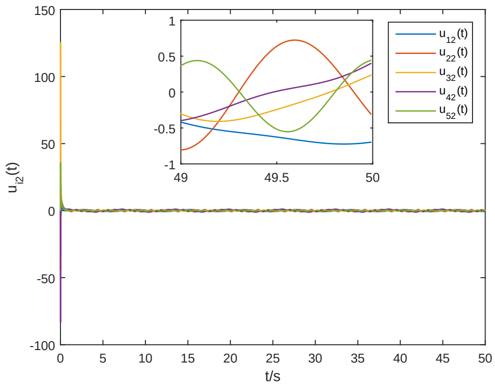

(b) Control inputs of $u_{i2}(i = 1, \cdots, 5)$

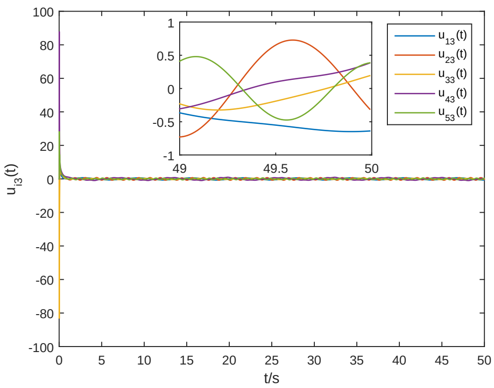

(c) Control inputs of $u_{i3}(i = 1, \cdots, 5)$

Fig. 3.10. Control inputs for control algorithm (3.16) with $d_i = 2$

3.5 Conclusion

In this chapter, the distributed consensus tracking problem of nonlinear FOMASs is studied, and the external disturbances are considered at the same time. A nonlinear discontinuous and a nonlinear continuous distributed control protocols are proposed to solve the consensus tracking problem respectively. By using the Lyapunov direct method, firstly a nonlinear discontinuous control protocol is proposed to solve the consensus tracking problem successfully under the demanded conditions. Then a nonlinear continuous control algorithm is further designed without chattering behavior, and it is proved that the tracking error can reach to a uniformly bounded region which can be made small enough by selecting the parameters appropriately. Finally, the simulations are conducted to illustrate the effectiveness and advantage of our results.

Chapter 4

Distributed consensus tracking of unknown nonlinear delayed FOMASs with external disturbances based on ABC algorithm

Contents

4.1 Introduction

As mentioned in Chapter 2, time delays are unavoidable in many applications. Thus in Chapter 2, several results with time delays have been achieved based on linear case. However, in practice, more complex intrinsic nonlinear dynamics may exist in mobile agents. Unfortunately, the consensus control algorithms and conditions designed for linear delayed FOMASs are not be extended to the nonlinear case. Currently, a few results have been obtained for the consensus of nonlinear delayed FOMASs (Zhu *et al.*, 2017). Thus, it is significant to investigate the distributed consensus tracking of nonlinear FOMASs with time delays, which is full of challenges and not well investigated.

In addition, as mentioned in Chapter 3, the effects of unknown external disturbances arising from environment and communication are usually unavoidable in the real world. Undesirable instability or bad performance can easily happen because of the external disturbances. Thus, for the study of MASs, taking the effects of the external disturbances into account is essential and reasonable.

On the other hand, note that most of the existing results about the distributed coordination of the FOMASs are under the assumption that the fractional orders and system parameters of the FOMASs are known beforehand. However in the real applications, the fractional orders and system parameters are usually partly or all unknown, which need to be identified in advance. Currently, for parameter identification of nonlinear systems, there are mainly two methods. The first one is synchronization-based method, which was first put forward by Parlitz (Parlitz, 1996). This method has been sufficiently applied to the unknown parameters identification of different kinds of nonlinear systems (Gu *et al.*, 2017; Konnur, 2003). But it is not easy to be applied because it is sensitive to the considered systems for designing the controllers and updating laws. The second one is optimization-based method by using artificial intelligence optimization algorithms (AIOAs). In the second method, the parameter identification issue can be converted into a functional optimization problem. Contrasted with the synchronization-based method, the second method does not need the differentiable information of the considered systems and is more flexible to be applied. Currently, many kinds of AIOAs have been applied for the second parameter identification method, such as differential evolution (DE) (Guedes *et al.*, 2018) and Cuckoo search (CS) (Wei & Yu, 2018).

Artificial bee colony (ABC) algorithm, as an efficient AIOAs, was proposed by Karaboga in 2005 and the idea comes from the foraging behavior of honeybee swarm. Lots of studies have revealed that ABC algorithm can successfully solve different kinds of optimization problems appeared in many fields, such as image segmentation, vehicle routing problem and control engineering (Karaboga *et al.*, 2014). Therefore, considering its wonderful performance, the ABC algorithm is chosen to identify the unknown fractional orders and system parameters of the unknown nonlinear delayed FOMASs in this chapter, which can extend the application fields of the ABC algorithm, and can provide a promising parameter identify method for the FOMASs as well.

Given the above discussion, in this chapter, distributed consensus tracking of unknown nonlinear delayed FOMASs with external disturbances is addressed. More specifically, FOMASs with time delays, external disturbances and unknown nonlinear dynamics are considered, which are more general than the existing results about consensus of FOMASs. Firstly, the efficient ABC algorithm-based parameter identify scheme is proposed to identify the unknown nonlinear delayed FOMASs. Secondly, based on the identified fractional orders and system parameters, we design a discontinuous distributed control protocol to achieve the consensus tracking by using the fractional-order comparison principle. Thirdly, for the purpose of suppressing the chattering phenomenon occurring in the discontinuous controller, a continuous control protocol is further proposed, with which the UUB tracking errors can be obtained and regulated small enough with proper parameters.

Compared with the existing works, our contribution are as follows. Firstly, compared with Cui *et al.* (2017); Li *et al.* (2010b); Ma (2015); Ma *et al.* (2016) concerning the integer-order MASs, the delayed MASs with fractional-order dynamics, external disturbances are considered. Secondly, different from Shen & Cao (2012); Yang *et al.* (2014a) with linear case, the time delay under nonlinear case is further investigated. Thirdly, in Ren & Yu (2016); Yang *et al.* (2014a), the authors only considered the external disturbances, but have not taken the time delays into account. Fourthly, all the results mentioned above are supposed that the fractional orders and system parameters of the nonlinear FOMASs are known beforehand, while in this chapter the parameters are considered to be unknown, and the ABC algorithm is employed to identify the unknown parameters of the unknown delayed FOMASs. Furthermore, it should be pointed out that this chapter provides a promising link between the AI technique and distributed cooperative control of FOMASs.

The rest of this chapter is arranged as below. In Section 4.2, the description of consensus tracking problem is given. In Section 4.3, an ABC algorithm-based parameter identification scheme for unknown nonlinear delayed FOMASs is proposed. In Section 4.4, based on the identified parameters, two efficient nonlinear control protocols are put forward to solve the consensus tracking problem. Finally, the efficiencies of the proposed ABC algorithm-based parameter identification method and the designed control algorithms are both verified based on the simulation experiments.

4.2 Problem description for consensus tracking of FOMASs

Consider dynamics of the followers as

$$\begin{aligned} x_i^{(\alpha)}(t) = -Cx_i(t) + Af(x_i(t)) + Bf(x_i(t-\tau)) + u_i(t) + w_i(t), \\ i = 1, 2, \cdots, N, \end{aligned} \tag{4.1}$$

where $\alpha \in (0, 1]$, $x_i(t) = [x_{i1}(t), \cdots, x_{in}(t)]^T \in R^n$ denotes state vector of the ith follower. The nonlinear vector function $f(x_i(t)) = [f_1(x_{i1}(t)), \cdots, f_n(x_{in}(t))]^T \in R^n$ and constant time delay $\tau > 0$. $C = [c_{ij}]_{n\times n}$, $A = [\hat{a}_{ij}]_{n\times n}$ and $B = [\hat{b}_{ij}]_{n\times n}$ denote the corresponding weight matrices. $u_i(t) \in R^n$ is the control input vector for follower i. $w_i(t) \in R^n$ is external disturbance of follower i.

The dynamic of the leader is described as

$$x_0^{(\alpha)}(t) = -Cx_0(t) + Af(x_0(t)) + Bf(x_0(t-\tau)), \tag{4.2}$$

where $x_0(t) = [x_{01}, \cdots, x_{0n}(t)]^T \in R^n$ represents the state vector of the leader, the other definitions are the same as those of systems (4.1).

Remark 4.1 *In this chapter, the authors considered a representative model (Bao et al., 2015; Chen et al., 2018a, 2015b; Fan et al., 2018; Huang et al., 2012; Kaslik & Sivasundaram, 2012; Lakshmanan et al., 2018; Liu et al., 2018g; Rakkiyappan et al., 2015; Wang et al., 2015; Zhang & Yang, 2018; Zhou & Tan, 2019), which can represent a general class of fractional-order nonlinear systems including delayed fractional-order nonlinear systems, such as the fractional-order Hopfield delayed neural networks, fractional-order cellular delayed neural networks, and fractional-order BAM neural networks with or without delays. Some unpredictable behaviours of the model considered in this chapter, such as periodic oscillations, bifurcation and chaotic attractors, and master-slave synchronization have been widely investigated which can be referred to Bao et al. (2015); Chen et al. (2018a, 2015b); Fan et al. (2018); Huang et al. (2012); Kaslik & Sivasundaram (2012); Lakshmanan et al. (2018); Liu et al. (2018g); Rakkiyappan et al. (2015); Wang et al. (2015); Zhang & Yang (2018); Zhou & Tan (2019). Besides, special setting of matrices A,B,C of the model considered in this chapter can include other simpler models. In addition, when the delayed nonlinearity in the considered model (5.1) does not exist, the dynamics will degrade to a class of general nonlinear systems.*

Definition 4.2 *For any initial conditions of FOMASs (4.1) and (4.2), the distributed consensus tracking is achieved, if*

$$\lim_{t\to\infty} \|x_i(t) - x_0(t)\| = 0, \quad \forall\ i = 1, 2, \cdots, N.$$

To achieve the distributed consensus tracking, the following assumptions are needed.

Assumption 4.3 *The nonlinear functions f_i are Lipschitz continuous with Lipschitz constants $\theta_i > 0$, such that*

$$|f_i(\mu) - f_i(\nu)| < \theta_i|\mu - \nu|, \qquad \forall \mu, \nu \in R, i = 1, 2, \cdots, n. \tag{4.3}$$

Assumption 4.4 *The external disturbances $w_i(t)$ satisfy $\|w_i(t)\| \le \rho < +\infty, \forall\ i = 1, 2, \cdots, N$.*

Assumption 4.5 *The communication topology $\bar{\mathcal{G}}$ among the followers and leader is undirected and connected.*

4.3 ABC algorithm-based parameter identification scheme for FOMASs

4.3.1 Problem formulation for parameter identification

For the purpose of identifying the unknown fractional orders and systematic parameters of nonlinear FOMASs (4.1) and (4.2), we consider the following original and identified systems with same initial conditions. The original systems are described as

$$x_i^{(\alpha)}(t) = -Cx_i(t) + Af(x_i(t)) + Bf(x_i(t-\tau)), \quad i = 0, 1, \cdots, N, \tag{4.4}$$

where the definition of the corresponding parameters and variables in (4.4) are the same as those of (4.1) and (4.2).

The corresponding identified systems are

$$\tilde{x}_i^{(\tilde{\alpha})}(t) = -\tilde{C}\tilde{x}_i(t) + \tilde{A}f(\tilde{x}_i(t)) + \tilde{B}f(\tilde{x}_i(t-\tau)), \quad i = 0, 1, \cdots, N, \tag{4.5}$$

where $\tilde{\alpha}$ is the identified fractional order, $\tilde{x}_i(t) = [\tilde{x}_{i1}(t), \cdots, \tilde{x}_{in}(t)]^T \in R^n$ represents the state vector for identified systems (4.5), $\tilde{C} = [\tilde{c}_{ij}]_{n\times n}$, $\tilde{A} = [\tilde{a}_{ij}]_{n\times n}$ and $\tilde{B} = [\tilde{b}_{ij}]_{n\times n}$ are the corresponding matrices of identified system.

To identify the unknown nonlinear FOMASs (4.4), we convert them into the following functional optimization model as

$$\begin{aligned} J_i(\tilde{\alpha}, \tilde{C}, \tilde{A}, \tilde{B}) &= arg \min_{(\tilde{\alpha},\tilde{C},\tilde{A},\tilde{B})\in\Omega} F_i \\ &= arg \min_{(\tilde{\alpha},\tilde{C},\tilde{A},\tilde{B})\in\Omega} \sum_{k=1}^{K} \|x_{ik} - \tilde{x}_{ik}\|, \quad i = 0, 1, \cdots, N, \end{aligned} \tag{4.6}$$

where sampling time point $k = 1, 2, \cdots, K$ and K is data length. x_{ik} and $\tilde{x}_{ik}$ denote respectively the state vectors of original system (4.4) and identified system (4.5) at time kh for agent i, where h is the step size between two sampling time point (Bhalekar & Daftardar-Gejji, 2011). Ω represents searching area predesigned for parameters $\tilde{\alpha}, \tilde{C}, \tilde{A}$ and $\tilde{B}$. Thus, the unknown parameters of FOMASs (4.4) can be identified through finding suitable $\tilde{\alpha}, \tilde{C}, \tilde{A}$ and $\tilde{B}$ in the searching space Ω along with the minimization of objective function (4.6).

4.3.2 The standard ABC algorithm

In 2005, Karaboga proposed the artificial bee colony (ABC) algorithm, which is a competitive population-based AIOAs. The idea comes from the foraging behavior of honeybee swarm (Karaboga *et al.*, 2014). There are three kinds of bees in the standard ABC algorithm, which are employed bees, onlooker bees and scout bees. In fact, half of them are employed bees, others are onlooker bees, which is also equal with the size of food sources or candidate solutions. The standard ABC algorithm can be described as the following phases.

In population initialization phase, several basic parameters are initialized. D and SN represent the dimension and sizes of the solutions (food sources), and $X_i = (x_{i1}, x_{i,2}, \cdots, x_{i,D})$ denotes the ith food source generated by

$$x_{i,j} = x_{min,j} + rand(0,1)(x_{max,j} - x_{min,j}), \tag{4.7}$$

where $i = 1, \cdots, SN/2, j = 1, \cdots, D$, $x_{min,j}$ and $x_{max,j}$ are the lower and upper bounds for the jth dimension in respect. Then the corresponding fitness is calculated as

$$fit_i = \begin{cases} \frac{1}{1+f(X_i)}, & if\ f(X_i) \geq 0, \\ 1 + |f(X_i)|, & if\ f(X_i) < 0, \end{cases}$$

where $f(X_i)$ represents the objective function value with respect to X_i.

In employed bee phase, in order to find a better food source, the employed bee generates a new food source position V_i around the current position X_i with

$$v_{i,j} = x_{i,j} + \phi_{i,j}(x_{i,j} - x_{k,j}), \tag{4.8}$$

where $k = 1, \cdots, SN/2(k \neq i), j = 1, 2, \cdots, D$, $\phi_{i,j}$ denotes a real number randomly selected in [-1,1]. Then if V_i has better fitness than that of X_i, X_i will be replaced by V_i, otherwise X_i is retained.

In onlooker bee phase, the employed bees will share information about amounts and positions of their food sources with onlooker bees. Then the onlooker bees will choose a food source to further search new food sources based on probability value p_i formulated as

$$p_i = fit_i / \sum_{j=1}^{SN} fit_j. \tag{4.9}$$

After that, a modification is made around the chosen food source using (4.8).

In scout bee phase, if the new position in corresponding to X_i is not improved continuously within certain time ($limit$), then the corresponding food source will be abandoned by the employed bee, which will become a scout bee. Then a new food source will be generated by the scout bee using (4.7).

The main flowchart of the ABC algorithm is described in Algorithm 1.

4.3.3 The proposed ABC algorithm-based parameter identification scheme

Based on the above efficient ABC algorithm, the following parameter identification scheme for FOMASs is proposed as Algorithm 2 (Hu *et al.*, 2019c).

Remark 4.6 *In this chapter, the ABC algorithm is specially applied to the parameter identification of unknown nonlinear delayed FOMASs, which can enlarge the applications of the ABC algorithm and can offer a promising method for identifying the unknown nonlinear delayed FOMASs.*

Remark 4.7 *Compared with the synchronized-based parameter identification method studied in (Gu et al., 2017), the proposed ABC algorithm-based parameter identification method in this chapter does not need design the parameter updating laws which are sensitive to the considered systems. Besides, the fractional orders are also considered as unknown parameters, which need to be identified.*

4.4 Distributed consensus tracking of FOMASs based on ABC algorithm

After applying Algorithm 1, assume that fractional order α and system parameters C, A, B of the unknown FOMASs (4.4) are identified as $\bar{\alpha}, \bar{C} = [\bar{C}_{ij}]_{n\times n}$,

Algorithm 1 Framework of the standard ABC algorithm

Step 0) Predefine some parameters: SN (population size number), D (searching dimension), $LOWER$ (lower bound), $UPPER$ (upper bound), $limit$ (control parameter), MCN (maximum cycle number), $trail = 0$.

Step 1) The population initialization phase:

  Step 1.1) Randomly generate $0.5 * SN$ points in the search space to form an initial population via Eq. (4.7).

  Step 1.2) Evaluate the objective function values of population.

  Step 1.3) cycle=1;

Step 2) The employed bees phase:

  For $i = 1$ **to** $0.5 * SN$ **do**

    Step 2.1)

      Step 2.1.1) Generate a candidate solution V_i by Eq. (4.8).

      Step 2.1.2) Evaluate $f(V_i)$.

    Step 2.2) If $f(V_i) < f(X_i)$, set $X_i = V_i$, otherwise, set $trial_i = trial_i + 1$.

  End For

Step 3) Calculating the probability values p_i by Eq. (4.9), set $t = 0, i = 1$.

Step 4) The onlooker bees phase:

  While $t \leq 0.5 *$ SN, **do**

    Step 4.1)

    If $rand(0, 1) < p_i$

      Step 4.1.1) Searching the candidate solution V_i via Eq. (4.8).

      Step 4.1.4) Set $t = t + 1$.

    End If

    Step 4.2) Set $i = i + 1$, if $i = 0.5 * SN$, set $i = 1$.

  End While

Step 5) The scout bees phase:

  If $max(trial_i) > limit$, replace X_i with a new candidate solution generated via Eq. (4.7).

Step 6) Set $cycle = cycle + 1$, and **if** $cycle > MCN$, then stop and output the best solution achieved so far, otherwise, go to **Step 2**.

Algorithm 2 ABC algorithm-based parameter identification scheme

1: Initialize the parameters for Algorithm 1 and FOMASs (4.5)
2: Generate the initial population in the feasible domain Ω defined in subsection 4.3.1
3: **repeat**
4: Optimize the function (4.6) with employed bees
5: Optimize the function (4.6) with onlooker bees
6: Optimize the function (4.6) with scout bees
7: **until** Maximum iteration is met
8: Return the best parameter identification values

$\bar{A} = [\bar{a}_{ij}]_{n\times n}$ and $\bar{B} = [\bar{b}_{ij}]_{n\times n}$, then the dynamics of $N \geq 1$ followers can be modeled as

$$x_i^{(\bar{\alpha})}(t) = -\bar{C}x_i(t) + \bar{A}f(x_i(t)) + \bar{B}f(x_i(t-\tau)) + u_i(t) + w_i(t), \quad i = 1, 2, \cdots, N. \tag{4.10}$$

The dynamic of the leader can be described as

$$x_0^{(\bar{\alpha})}(t) = -\bar{C}x_0(t) + \bar{A}f(x_0(t)) + \bar{B}f(x_0(t-\tau)), \tag{4.11}$$

where $\bar{\alpha}, \bar{C} = [\bar{a}_{ij}]_{n\times n}, \bar{A} = [\bar{a}_{ij}]_{n\times n}$ and $\bar{B} = [\bar{b}_{ij}]_{n\times n}$ are the corresponding estimated values. Other definitions in (4.10) and (4.11) are the same as those of (4.1) and (4.2).

Denote the tracking errors as $e_{x_i} = x_i(t) - x_0(t)$, and $e_{f_i} = f(x_i(t)) - f(x_0(t))$, $e_{x_{i\tau}} = x_i(t-\tau) - x_0(t-\tau)$, $e_{f_{i\tau}} = f(x_i(t-\tau)) - f(x_0(t-\tau))$. Let $e_x, e_f, e_{x_\tau}, e_{f_\tau}, u(t)$ and $w(t)$ be the column vector of $e_{x_i}, e_{f_i}, e_{x_{i\tau}}, e_{f_{i\tau}}, u_i(t)$ and $w_i(t)$, respectively. Subtracting system (4.11) from system (4.10), the tracking errors e_x can be obtained as:

$$e_x^{(\bar{\alpha})}(t) = -(I_N \otimes \bar{C})e_x + (I_N \otimes \bar{A})e_f + (I_N \otimes \bar{B})e_{f_\tau} + u(t) + w(t). \tag{4.12}$$

According to Assumption 4.5, v_0 is a global reachable node. Let $M = \mathcal{L} + \mathcal{B} = [m_{ij}]_{N\times N}$, then matrix M is positive definite based on Lemma 1.1.

Given the identified FOMASs (4.10) and (4.11), two kinds of distributed controllers are designed to deal with the consensus tracking issue.

4.4.1 Discontinuous distributed control algorithm

To guarantee the distributed consensus tracking, a nonlinear discontinuous tracking protocol is designed as following for each follower:

$$u_i(t) = -ay_i - \beta h(y_i), \qquad i = 1, 2, \cdots, N, \tag{4.13}$$

where $y_i = \sum_{j=0}^{N} a_{i,j}(x_i - x_j)$ and $a, \beta > 0$ are constant coupling gains. $h(y_i)$ is a nonlinear discontinuous function defined as

$$h(y_i) = \begin{cases} \frac{y_i}{\|y_i\|}, & \|y_i\| \neq 0, \\ \mathbf{0}_n, & \|y_i\| = 0. \end{cases} \tag{4.14}$$

Based on the graph theory introduced in Chapter 1, it can be easily verified that $y_i = \sum_{j=0}^{N} a_{i,j}(e_{x_i} - e_{x_j}) = \sum_{j=1}^{N} m_{ij} e_{x_j}$, which means $y = (M \otimes I_n)e_x = \tilde{M} e_x$, where y is the column vector of y_i.

Theorem 4.8 *(Hu et al., 2019c) Suppose that Assumptions 4.3-4.5 hold, with the nonlinear discontinuous control algorithm (4.13), the distributed consensus tracking of nonlinear delayed FOMASs (4.10) and (4.11) can be achieved, if $\beta \geq \rho$, and there exist some constants $\lambda > \delta > 0, a > 0$ and positive definite matrixes Ξ_1 and Ξ_2 such the following LMIs hold:*

$$\Phi = \begin{bmatrix} \Phi_1 & I_N \otimes \Theta \\ * & -\Xi_1 \end{bmatrix} < 0, \tag{4.15}$$

$$\Psi = \begin{bmatrix} -\lambda_{min}(\tilde{M})\delta I_{Nn} & I_N \otimes \Theta \\ * & -\Xi_2 \end{bmatrix} < 0, \tag{4.16}$$

where $\Phi_1 = -2M \otimes (\bar{C} + \bar{C}^T) + (M \otimes \bar{A})\Xi_1(M \otimes \bar{A})^T + (M \otimes \bar{B})\Xi_2(M \otimes \bar{B})^T - 2a(M^2 \otimes I_n) + \lambda_{max}(\tilde{M})\lambda I_{Nn}$, $\tilde{M} = M \otimes I_n$. $\Theta = diag\{\theta_1, \cdots, \theta_n\}$ with θ_i defined in Assumption 4.3.

Proof: Substitute the protocol (4.13) into tracking errors system (4.12) as

$$\begin{aligned} e_x^{(\bar{\alpha})}(t) = &-(I_N \otimes \bar{C})e_x + (I_N \otimes \bar{A})e_f + (I_N \otimes \bar{B})e_{f_\tau} \\ &- ay - \beta H(y) + w(t), \end{aligned} \tag{4.17}$$

where $H(y) = \big(h^T(y_1), \cdots, h^T(y_N)\big)^T \in R^{Nn}$.

To verify the stability of the errors system (4.17), construct the Lyapunov function as

$$V(t) = e_x^T \tilde{M} e_x. \tag{4.18}$$

Then based on Lemma 1.19, we have

$$\begin{aligned} V^{(\bar{\alpha})}(t) &\leq 2e_x^T \tilde{M} e_x^{(\bar{\alpha})} \\ &= 2e_x^T \tilde{M}\big(-(I_N \otimes \bar{C})e_x + (I_N \otimes \bar{A})e_f \\ &\quad + (I_N \otimes \bar{B})e_{f_\tau} - ay - \beta H(y) + w(t)\big). \end{aligned} \tag{4.19}$$

According to the properties of Kronecker product, one can obtain

$$\begin{aligned} 2e_x^T \tilde{M}\big(-(I_N \otimes \bar{C})e_x\big) &= -2e_x^T (M \otimes I_n)(I_N \otimes \bar{C})e_x \\ &= -2e_x^T (M \otimes \bar{C})e_x \\ &= -e_x^T (M \otimes \bar{C})e_x - e_x^T (M \otimes \bar{C})^T e_x \\ &= -e_x^T \big(M \otimes (\bar{C} + \bar{C}^T)\big)e_x. \end{aligned} \tag{4.20}$$

According to Lemma 1.22, denoting $\Xi = \Xi_1, \xi = 1$, it yields

$$\begin{aligned} &2e_x^T \tilde{M}(I_N \otimes \bar{A})e_f \\ &\quad \leq e_x^T \tilde{M}(I_N \otimes \bar{A})\Xi_1 (I_N \otimes \bar{A})^T \tilde{M} e_x + e_f^T \Xi_1^{-1} e_f \\ &\quad \leq e_x^T \big((M \otimes \bar{A})\Xi_1 (M \otimes \bar{A})^T + (I_N \otimes \Theta)\Xi_1^{-1}(I_N \otimes \Theta)\big)e_x. \end{aligned} \tag{4.21}$$

According to Lemma 1.22, denoting $\Xi = \Xi_2, \xi = 1$, it yields

$$\begin{aligned} &2e_x^T \tilde{M}(I_N \otimes \bar{B})e_{f_\tau} \\ &\quad \leq e_x^T \tilde{M}(I_N \otimes \bar{B})\Xi_2 (I_N \otimes \bar{B})^T \tilde{M} e_x + e_{f_\tau}^T \Xi_2^{-1} e_{f_\tau} \\ &\quad \leq e_x^T \big((M \otimes \bar{B})\Xi_2 (M \otimes \bar{B})^T\big)e_x + e_{x_\tau}^T \big((I_N \otimes \Theta)\Xi_2^{-1}(I_N \otimes \Theta)\big)e_{x_\tau}. \end{aligned} \tag{4.22}$$

Note that $y_i^T h(y_i) = \|y_i\|$, one has

$$2e_x^T \tilde{M}\big(-\beta H(y)\big) = -2\beta \sum_{i=1}^{N} y_i^T h(y_i) = -2\beta \sum_{i=1}^{N} \|y_i\|. \tag{4.23}$$

Note that $y_i^T w_i(t) \leq \|y_i\|\|w_i(t)\| \leq \rho\|y_i\|$, one has

$$2e_x^T \tilde{M} w(t) = 2\sum_{i=1}^{N} y_i^T w_i(t) \leq 2\sum_{i=1}^{N} \|y_i\|\|w_i(t)\| \leq 2\rho \sum_{i=1}^{N} \|y_i\|. \tag{4.24}$$

Thus based on $\beta > \rho$, (4.15),(4.16), and (4.20)-(4.24), one can obtain that

$$\begin{aligned}
&V^{(\bar{\alpha})}(t) \\
&\leq e_x^T\big(-2(M\otimes\bar{C}) + (M\otimes\bar{A})\Xi_1(M\otimes\bar{A})^T + (I_N\otimes\Theta)\Xi_1^{-1}(I_N\otimes\Theta) \\
&\quad + (M\otimes\bar{B})\Xi_2(M\otimes\bar{B})^T - 2a(M^2\otimes I_n)\big)e_x \\
&\quad + e_{x_\tau}^T\big((I_N\otimes\Theta)\Xi_2^{-1}(I_N\otimes\Theta)\big)e_{x_\tau} - 2\beta\sum_{i=1}^{N}\|y_i\| + 2\rho\sum_{i=1}^{N}\|y_i\| \\
&\leq e_x^T\big(-2(M\otimes\bar{C}) + (M\otimes\bar{A})\Xi_1(M\otimes\bar{A})^T + (I_N\otimes\Theta)\Xi_1^{-1}(I_N\otimes\Theta) \\
&\quad + (M\otimes\bar{B})\Xi_2(M\otimes\bar{B})^T - 2a(M^2\otimes I_n) + \tilde{\lambda}I_{Nn}\big)e_x \\
&\quad + e_{x_\tau}^T\big((I_N\otimes\Theta)\Xi_2^{-1}(I_N\otimes\Theta) - \tilde{\delta}I_{Nn}\big)e_{x_\tau} - \tilde{\lambda}e_x^Te_x + \tilde{\delta}e_{x_\tau}^Te_{x_\tau} \\
&= e_x^T\Phi e_x + e_{x_\tau}^T\Psi e_{x_\tau} - \tilde{\lambda}e_x^Te_x + \tilde{\delta}e_{x_\tau}^Te_{x_\tau} \\
&\leq -\tilde{\lambda}e_x^Te_x + \tilde{\delta}e_{x_\tau}^Te_{x_\tau} \\
&\leq -\frac{\tilde{\lambda}}{\lambda_{max}(\tilde{M})}e_x^T\tilde{M}e_x + \frac{\tilde{\delta}}{\lambda_{min}(\tilde{M})}e_{x_\tau}^T\tilde{M}e_{x_\tau} \\
&= -\lambda V(t) + \delta V(t-\tau),
\end{aligned} \tag{4.25}$$

where $\tilde{\lambda} = \lambda_{max}(\tilde{M})\lambda$, $\tilde{\delta} = \lambda_{min}(\tilde{M})\delta$.

Now, consider the following fractional-order linear delayed system

$$\begin{cases} Z^{(\bar{\alpha})}(t) = -\lambda Z(t) + \delta Z(t-\tau), \bar{\alpha} \in (0,1], \\ Z(t) = \phi(t), t \in [-\tau, 0], \end{cases} \tag{4.26}$$

where the initial condition is same as that of system (4.25). Based on Lemma 1.18, if $\lambda > \delta$ and there has no purely imaginary root for the following characteristic equation of system (4.26)

$$s^{\bar{\alpha}} + \lambda - \delta e^{-s\tau} = 0, \tag{4.27}$$

then, the zero solution of system (4.26) is Lyapunov globally asymptotically stable, which means that $Z(t) \to 0$ as $t \to +\infty$. For Eq. (4.27), suppose there exists a pure imaginary root $s = \eta i, \eta \in R$. If $\eta > 0, s = \eta i = |\eta|(\cos\frac{\pi}{2} + i\sin\frac{\pi}{2})$, and if

$\eta < 0, s = \eta i = |\eta|(\cos\frac{\pi}{2} - i\sin\frac{\pi}{2})$. Then substituting $s = \eta i = |\eta|(\cos\frac{\pi}{2} \pm i\sin\frac{\pi}{2})$ into Eq. (4.27) yields

$$|\eta|^{\bar{\alpha}}\big(\cos\frac{\bar{\alpha}\pi}{2} + i\sin(\pm\frac{\bar{\alpha}\pi}{2})\big) + \lambda - \delta\big(\cos(\eta\tau) - i\sin(\eta\tau)\big) = 0. \tag{4.28}$$

Separate Eq. (4.28) into real and imaginary parts as

$$\begin{cases} |\eta|^{\bar{\alpha}}\cos\frac{\bar{\alpha}\pi}{2} + \lambda = \delta\cos(\eta\tau), \\ |\eta|^{\bar{\alpha}}\sin(\pm\frac{\bar{\alpha}\pi}{2}) = -\delta\sin(\eta\tau). \end{cases} \tag{4.29}$$

From Eq. (4.29), it can be deduced as

$$|\eta|^{2\bar{\alpha}} + 2\lambda|\eta|^{\bar{\alpha}}\cos\frac{\bar{\alpha}\pi}{2} + \lambda^2 - \delta^2 = 0. \tag{4.30}$$

Since $|\eta|^{\bar{\alpha}} > 0, \cos\frac{\bar{\alpha}\pi}{2} > 0, \lambda^2 > \delta^2$, so Eq. (4.30) cannot hold. Therefore, the pure imaginary root does not exist in characteristic Eq. (4.27). According to Lamma 1.18, $Z(t)$ is Lyapunov globally asymptotically stable. With Lamma 1.17, one can obtained that $\lambda_{min}(\tilde{M})\|e_x\|^2 \le V(t) \le Z(t) \to 0, t \to +\infty$, which implies that $\|e_x\|^2 \to 0, t \to +\infty$. Therefore, the proof is completed. ■

Remark 4.9 *Theorem 4.8 shows us how to select the coupling gain $a > 0$ in the control protocol (4.13). From the definition of Φ_1 in Theorem 4.8, it can be found that the coupling gain $a > 0$ should be selected large in order to make the LMI (4.15) hold.*

Remark 4.10 *In Theorem 4.8, the coupling gain $\beta > 0$ in the control protocol (4.13) is related to the bound of the external disturbances. The value of the coupling gain $\beta > 0$ must be larger than the bound of the external disturbances. In special, if there are no external disturbances, the value of the coupling gain β can be set as zero.*

Remark 4.11 *Compared with the synchronization of delayed fractional-order neural networks where there are only a single master and a single slave system (Bao et al., 2015; Chen et al., 2015b; Lakshmanan et al., 2018; Vaseghi et al., 2017; Zhang et al., 2018a), in this chapter, the synchronization for a single mater and multiple slaves delayed fractional-order neural networks is considered, where the multiple salves systems are coupled with a connected graph communication topology. Different from Bao et al. (2015); Chen et al. (2015b); Lakshmanan et al.*

(2018); Vaseghi et al. *(2017); Zhang* et al. *(2018a), in this chapter, to prove the efficiency of the proposed synchronization controller in theory, the design of the Lyapunov function should depend on the graph communication topology, which is full of challenge due to the structure of the graph.*

4.4.2 Continuous distributed control algorithm

In subsection 4.4.1, the discontinuous control protocol (4.13) can cause the negative chattering effect in applications. Thus, to overcome this drawback, a continuous distributed control protocol is further designed to deal with the consensus tracking. Based on the boundary layer technique (Young *et al.*, 1999), we propose the following continuous control protocol as

$$u_i(t) = -ay_i - \beta \bar{h}_i(y_i), \qquad i = 1, 2, \cdots, N, \tag{4.31}$$

where $y_i = \sum_{j=0}^{N} a_{i,j}(x_i - x_j)$ and $a, \beta > 0$ are constant coupling gains. $\bar{h}_i(y_i)$ is a nonlinear continuous function defined as

$$\bar{h}_i(y_i) = \begin{cases} \frac{y_i}{\|y_i\|}, & \|y_i\| > d_i, \\ \frac{y_i}{d_i}, & \|y_i\| \leq d_i, \end{cases} \tag{4.32}$$

where $d_i > 0$ represents the width of the boundary layers.

Theorem 4.12 *(Hu* et al.*, 2019c) Suppose that Assumptions 4.3-4.5 hold, the tracking errors of FOMASs (4.10) and (4.11) are UUB with the continuous control algorithm (4.31), if $\beta \geq \rho$, and there exist some constants $\lambda > \delta > 0, a > 0$ and positive definite matrixes Ξ_1 and Ξ_2 such the following LMIs hold:*

$$\Phi = \begin{bmatrix} \Phi_1 & I_N \otimes \Theta \\ * & -\Xi_1 \end{bmatrix} < 0, \tag{4.33}$$

$$\Psi = \begin{bmatrix} -\lambda_{min}(\tilde{M})\delta I_{Nn} & I_N \otimes \Theta \\ * & -\Xi_2 \end{bmatrix} < 0, \tag{4.34}$$

where Φ_1 and $\tilde{M}$ are defined as Theorem 4.8, $\Theta = diag\{\theta_1, \cdots, \theta_n\}$ with θ_i defined as Assumption 4.3. Moreover, the tracking errors e_x asymptotically converge to *the following bounded region*

$$\mathcal{D} = \left\{ e_x : \|e_x\|^2 \le \frac{2(\beta+\rho)\sum_{i=1}^{N} d_i}{\lambda_{min}(\tilde{M})(\lambda-\delta)} \right\}. \tag{4.35}$$

Proof: Substitute the protocol (4.31) into the tracking errors system (4.12), it can be obtained as

$$\begin{aligned} e_x^{(\bar{\alpha})}(t) = &-(I_N \otimes \bar{C})e_x + (I_N \otimes \bar{A})e_f + (I_N \otimes \bar{B})e_{f_\tau} \\ &- ay - \beta \bar{H}(y) + w(t), \end{aligned} \tag{4.36}$$

where $\bar{H}(y) = [\bar{h}_1^T(y_1), \cdots, \bar{h}_N^T(y_N)]^T \in R^{Nn}$.

The $\bar{\alpha}$-order derivative of Lyapunov function candidate (4.18) with errors system (4.36) is

$$\begin{aligned} V^{(\bar{\alpha})}(t) &\le 2e_x^T \tilde{M} e_x^{(\bar{\alpha})} \\ &= 2e_x^T \tilde{M}\big(-(I_N \otimes \bar{C})e_x + (I_N \otimes \bar{A})e_f + (I_N \otimes \bar{B})e_{f_\tau} \\ &\quad - ay - \beta \bar{H}(y) + w(t)\big). \end{aligned} \tag{4.37}$$

According to the property of Eq. (4.31), the following three cases are discussed.

(i) $\|y_i\| > d_i, \quad i = 1, 2, \cdots, N.$

For this case, based on Eqs. (4.23) and (4.24), one can obtained

$$2e_x^T \tilde{M}\big(-\beta \bar{H}(y) + w(t)\big) = 2(-\beta+\rho)\sum_{i=1}^{N} \|y_i\| < 0. \tag{4.38}$$

Substituting Eqs. (4.20)-(4.22) and(4.38) into Eq. (4.37) yields

$$V^{(\bar{\alpha})}(t) < -\lambda V(t) + \delta V(t-\tau). \tag{4.39}$$

(ii) $\|y_i\| \le d_i, \quad i = 1, 2, \cdots, N.$

In this case, note that $y_i^T \bar{h}_i(y_i) = \|y_i\|^2/d_i \le d_i$, one has

$$2e_x^T \tilde{M}\big(-\beta \bar{H}(y)\big) = -2\beta \sum_{i=1}^{N} y_i^T \bar{h}_i(y_i) = -2\beta \sum_{i=1}^{N} \|y_i\|^2/d_i \le 2\beta \sum_{i=1}^{N} d_i. \tag{4.40}$$

Note that $y_i^T w_i(t) \leq \|y_i\| \|w_i(t)\| \leq \rho \|y_i\| \leq \rho d_i$, one has

$$2e_x^T \tilde{M} w(t) = 2\sum_{i=1}^{N} y_i^T w_i(t) \leq 2\sum_{i=1}^{N} \|y_i\| \|w_i(t)\| \leq 2\rho \sum_{i=1}^{N} \|y_i\| \leq 2\rho \sum_{i=1}^{N} d_i. \quad (4.41)$$

Therefore, one can deduce that

$$2e_x^T \tilde{M} \big(-\beta \bar{H}(y) + w(t) \big) \leq 2(\beta + \rho) \sum_{i=1}^{N} d_i. \quad (4.42)$$

Substituting Eqs. (4.20)-(4.22), (4.42) into Eq. (4.37) yields

$$V^{(\bar{\alpha})}(t) < -\lambda V(t) + \delta V(t-\tau) + 2(\beta + \rho) \sum_{i=1}^{N} d_i. \quad (4.43)$$

(iii) y satisfies neither Case (i) nor Case (ii).

Without loss of generality, we suppose $|y_i| > d_i, i = 1, 2, \cdots, \kappa$, and $|y_i| \leq d_i, i = \kappa+1, \kappa+2, \cdots, N$, $(1 < \kappa < N)$. For this case, according to (4.38) and (4.42), one can get that

$$2e_x^T \tilde{M} \big(-\beta \bar{H}(y) + w(t) \big) \leq 2(\beta + \rho) \sum_{i=\kappa+1}^{N} d_i. \quad (4.44)$$

Thus, from Eqs. (4.20)-(4.22) and (4.44), one has

$$V^{(\bar{\alpha})}(t) < -\lambda V(t) + \delta V(t-\tau) + 2(\beta + \rho) \sum_{i=\kappa+1}^{N} d_i. \quad (4.45)$$

Therefore, based on the above three discussed cases, for all $y \in R^{Nn}$, we have

$$V^{(\bar{\alpha})}(t) < -\lambda V(t) + \delta V(t-\tau) + d, \quad (4.46)$$

where $d = 2(\beta + \rho) \sum_{i=1}^{N} d_i$.

Consider the following system:

$$Z^{(\bar{\alpha})}(t) = -\lambda Z(t) + \delta Z(t-\tau) + d, \quad (4.47)$$

where $Z(t) \geq 0(Z(t) \in R)$, and has the same initial conditions with $V(t)$. Based on Lemma 1.17, one can obtain that $0 < V(t) < Z(t)$. With Properties 1.7 and 1.8, we have

$$\big(Z(t) - \bar{d}\ \big)^{(\bar{\alpha})}(t) = -\lambda\big(Z(t) - \bar{d}\ \big) + \delta\big(Z(t-\tau) - \bar{d}\ \big), \tag{4.48}$$

where $\bar{d} = d/(\lambda - \delta)$. Taking $\bar{Z}(t) = Z(t) - \bar{d}$, then system (4.48) can be transformed into

$$\bar{Z}^{(\bar{\alpha})}(t) = -\lambda\bar{Z}(t) + \delta\bar{Z}(t-\tau). \tag{4.49}$$

Applying the similar proof procedure in Theorem 4.8, we can obtain that $\bar{Z}(t) = Z(t) - \bar{d} \to 0$, as $t \to +\infty$, which implies that $\lambda_{min}(\tilde{M})\|e_x\|^2 \leq V(t) \leq Z(t) \to \bar{d}$, as $t \to +\infty$. Therefore, the tracking errors can asymptotically converge to the following bounded region

$$\|e_x\|^2 \leq \frac{\bar{d}}{\lambda_{min}(\tilde{M})} = \frac{2(\beta+\rho)\sum_{i=1}^{N} d_i}{\lambda_{min}(\tilde{M})(\lambda-\delta)}, (t \to +\infty), \tag{4.50}$$

which can be made small enough by choosing proper parameter d_i. ■

Corollary 4.13 *If all the widths d_i of the boundary layers are equal in controller (4.31), i.e., $d_1 = d_2 = \cdots = d_N = d$, the bounded region in Theorem 4.12 can be simplified as*

$$\mathcal{D} = \left\{ e_x : \|e_x\|^2 \leq \frac{2(\beta+\rho)Nd}{\lambda_{min}(\tilde{M})(\lambda-\delta)} \right\}. \tag{4.51}$$

Remark 4.14 *In this chapter, the distributed consensus tracking of nonlinear delayed FOMASs with external disturbances is investigated. In fact, the results are also effective for consensus tracking of FOMASs with any nonlinear dynamics as*

$$\begin{cases} x_0^{(\alpha)}(t) = f(x_0(t), x_0(t-\tau)), & leader, \\ x_i^{(\alpha)}(t) = f(x_i(t), x_i(t-\tau)) + u_i(t) + w_i(t), & followers, \end{cases}$$

where nonlinear function $f(\cdot)$ satisfies Assumption 4.3, and external disturbance $w_i(t)$ satisfies Assumption 4.4.

Remark 4.15 *When the number of the followers is chosen as $N = 1$, the consensus tracking methods studied in this chapter will degenerate into the case of single* *mater-single slave synchronization between two delayed fractional-order neural networks (Bao et al., 2015; Chen et al., 2015b; Zhang et al., 2018a). That is to say, this chapter is an extension of the traditional master-slave synchronization to more general case of FOMASs.*

Remark 4.16 *When the fractional order $\bar{\alpha} = 1$, the consensus tracking problem studied in this chapter will reduce to the case of integer-order MASs (Cui et al., 2017; Ma, 2015; Ma et al., 2016) as*

$$\begin{cases} \dot{x}_0(t) = -Cx_0(t) + Af(x_0(t)) + Bf(x_0(t-\tau)), & leader, \\ \dot{x}_i(t) = -Cx_i(t) + Af(x_i(t)) + Bf(x_i(t-\tau)) + u_i(t) + w_i(t), & followers, \end{cases}$$

which is a special case of this chapter.

Remark 4.17 *For the master-slave chaos synchronization, one of the important applications is in terms of the secure communication (Lakshmanan et al., 2018; Vaseghi et al., 2017). In this chapter, the extension provides some interesting viewpoints in the real applications. More specifically, it is the security transmission that plays an important role in the application of chaos synchronization. For single master-multiple slaves case studied in this chapter, the single master system (leader) can avoid sending information directly to all the slave systems (followers), and the single master system (leader) just needs transmit its information to a part of informed followers, and other followers can obtain the leader's information indirectly by interacting with their neighborhoods. Finally, the single master-multiple slaves chaos synchronization can be achieved.*

4.5 Simulations

4.5.1 ABC algorithm-based parameter identification results

For the initialization of Algorithm 2, the number of sample points is chosen as 200 and the step size is 0.01. For ABC algorithm, $SN = 100$, maximum iterations is 200, the control parameter $limit = 15$.

- **Case 1:** $\alpha = 0.97$

Consider FOMASs with one leader and six followers. The communication topology is given as Fig. 4.1. Assume that the leader and followers own homoge-

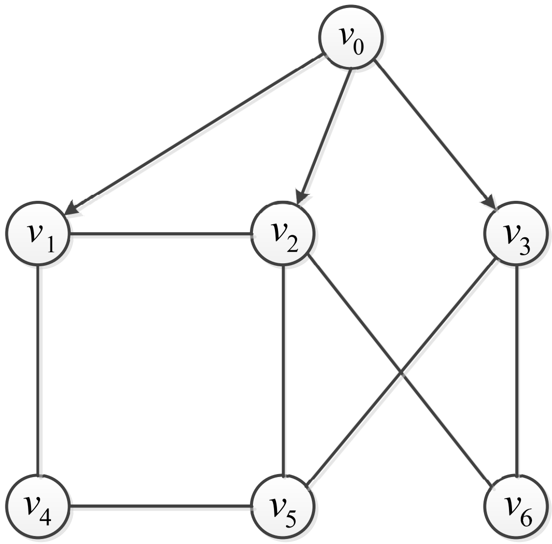

Fig. 4.1. The communication topology with one leader and six followers

nous nonlinear dynamics with two-dimensional fractional-order delayed NNs as

$$x_i^{(\alpha)}(t) = -Cx_i(t) + Af(x_i(t)) + Bf(x_i(t-\tau)), \qquad i = 0, 1, \cdots, 6, \tag{4.52}$$

where $x_i(t) = [x_{i1}(t), x_{i2}(t)]^T, \alpha = 0.97, C = I_2, \tau = 1,\ f(x_i(t)) = tanh(x_i(t))$. Obviously, from Assumption 4.3, it is easily obtained that $\Theta = I_2$. The feedback matrix A and the delay feedback matrix B are respectively given as

$$A = [\hat{a}_{ij}]_{2\times 2} = \begin{bmatrix} 2.0 & -0.1 \\ -5.0 & 2.0 \end{bmatrix}, \qquad B = [\hat{b}_{ij}]_{2\times 2} = \begin{bmatrix} -1.5 & -0.1 \\ -0.2 & -1.5 \end{bmatrix}.$$

Under the above parameters, each agent has a chaotic attractor (Zhang *et al.*, 2018a), which is shown in Fig. 4.2.

Since the nonlinear dynamics of all the agents are homogenous, we just need identify one agent. Without loss of generality, we select agent 1 as the identified object. For the purpose of showing the performance of Algorithm 2 more clearly in terms of tables and figures, we randomly choose the fractional order $\alpha = 0.97$, system parameters $\hat{a}_{11} = 2.0, \hat{b}_{22} = -1.5$ as unknown parameters which need to be identified. Then the corresponding identified system is

$$\tilde{x}_1^{(\tilde{\alpha})}(t) = -\tilde{C}\tilde{x}_1(t) + \tilde{A}f(\tilde{x}_1(t)) + \tilde{B}f(\tilde{x}_1(t-\tau)), \tag{4.53}$$

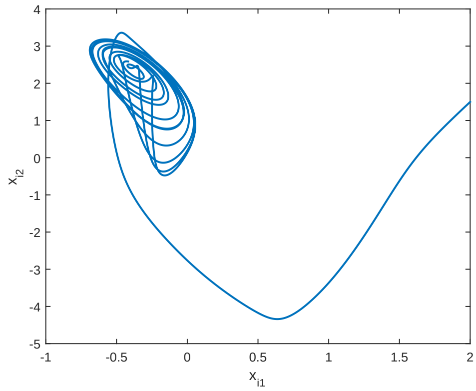

Fig. 4.2. Chaotic behavior of agent i with initial value $[2, 1.5]^T$

with $\tilde{C} = I_2$, and

$$\tilde{A} = [\tilde{a}_{ij}]_{2\times 2} = \begin{bmatrix} \tilde{a}_{11} & -0.1 \\ -5.0 & 2.0 \end{bmatrix}, \quad \tilde{B} = [\tilde{b}_{ij}]_{2\times 2} = \begin{bmatrix} -1.5 & -0.1 \\ -0.2 & \tilde{b}_{22} \end{bmatrix},$$

other definitions in (4.53) are the same as those of (4.52). We set the searching space Ω as $(\tilde{\alpha}, \tilde{a}_{11}, \tilde{b}_{22}) \in [0.01, 1] \times [1, 3] \times [-2, -1]$. The corresponding objective function is

$$F_1(\tilde{\alpha}, \tilde{a}_{11}, \tilde{b}_{22}) = \sum_{k=0}^{K} \|x_{1k} - \tilde{x}_{1k}\|. \tag{4.54}$$

Thus, the parameter identification problem of system (4.52) becomes a functional optimization problem where the objective function is Eq. (4.54). Obviously, the smaller the objective function value F_1 is, the better combination of parameters $(\tilde{\alpha}, \tilde{a}_{11}, \tilde{b}_{22})$ is.

Firstly, the statistical results in terms of the best, the mean and the worst identified parameters obtained by ABC algorithm are given in Table 4.1, where 30 independent runs are operated. Table 4.1 demonstrates that the unknown parameters of system (4.52) can be well identified by ABC algorithm, even though the worst identified values can also have a high accuracy. Figs. 4.3 and 4.4 show the convergence profile of the evolutionary processes in terms of identified values, the corresponding relative error values and the fitness values in a single run, which further demonstrate the effectiveness of the proposed ABC algorithm-based parameter identification method.

Table 4.1: Statistical results for system (4.52) over 30 independent runs in Case 1

	Best	Mean	Worst
$\tilde{\alpha}$	0.969998942018956	0.969999169844999	0.970181112780390
$\lvert\frac{\tilde{\alpha}-0.97}{0.97}\rvert$	1.09E-06	3.26E-05	1.87E-04
$\tilde{a}_{11}$	2.000005093988760	1.999998453254200	1.999682379184920
$\lvert\frac{\tilde{a}_{11}-2}{2}\rvert$	2.55E-06	3.06E-05	1.59E-04
$\tilde{b}_{22}$	-1.500003022791350	-1.500014242901070	-1.501174138236190
$\lvert\frac{\tilde{b}_{22}-(-1.5)}{-1.5}\rvert$	2.02E-06	1.01E-04	7.83E-04
F_1	2.67E-04	1.32E-03	6.65E-03

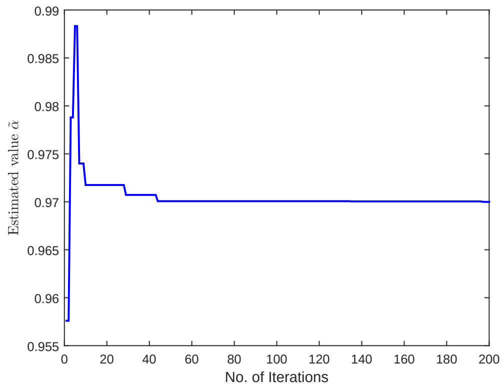

(a) Identified parameter value α

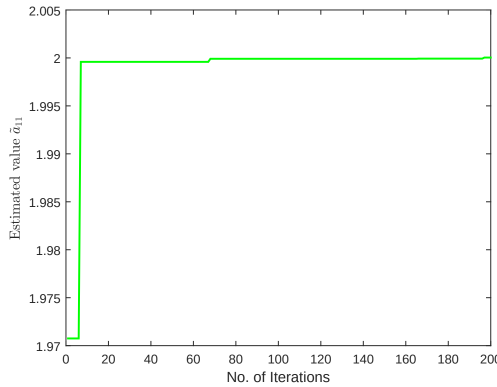

(b) Identified parameter value a_{11}

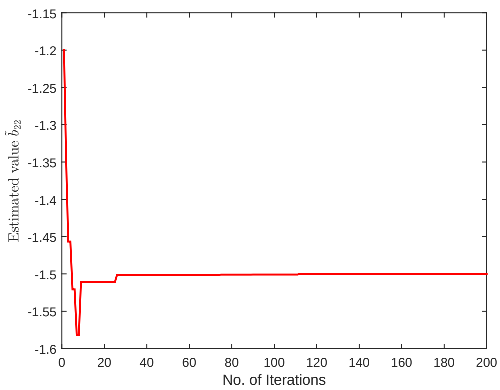

(c) Identified parameter value b_{22}

Fig. 4.3. Evolutionary curve of the identified parameters values with ABC on system (4.52) in a single run in Case 1

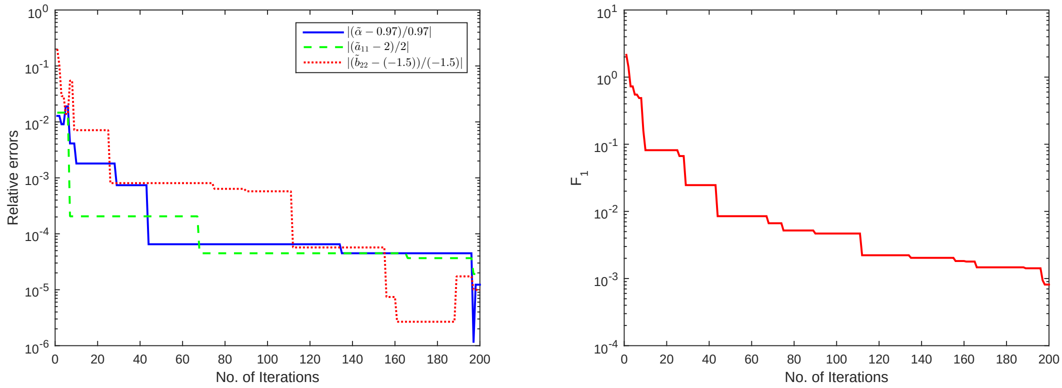

(a) Relative error values

(b) Objective function values

Fig. 4.4. Evolutionary curve in terms of the relative errors and objective function values with ABC on system (4.52) in a single run in Case 1

- **Case 2:** $\alpha = 0.65$

In order to test the efficiency of the ABC algorithm in identifying different fractional derivative order, in this case we assume that the real fractional order α in system (4.52) is 0.65, which need to be identified. The other experimental setup is the same with that in Case 1.

Similarly, 30 independent runs are performed. The statistical results in terms of the best, the mean and the worst identified parameters obtained by ABC algorithm are given in Table 4.2, which demonstrates that the unknown parameters of system (4.52) can be well identified by ABC algorithm. Figs. 4.5 and 4.6 display the convergence profile of the evolutionary processes in terms of identified values, the corresponding relative error values and the fitness values in a single run, which further illustrate the effectiveness of the proposed ABC algorithm-based parameter identification method.

4.5.2 Simulation results on distributed consensus tracking

In this subsection, we will achieve the distributed consensus tracking based on the identified parameters. We assume that the real FOMASs are modeled as Case 1. Based on the identified values obtained in Table 4.1, the identified value can be approximated as $\tilde{\alpha} = 0.97$, $\tilde{a}_{11} = 2.0$, $\tilde{b}_{22} = -1.5$, thus the dynamics of the six

Table 4.2: Statistical results for system (4.52) over 30 independent runs in Case 2

	Best	Mean	Worst
$\tilde{\alpha}$	0.649999999996805	0.649999999279857	0.650000009077807
$\lvert\frac{\tilde{\alpha}-0.65}{0.65}\rvert$	4.92E-12	4.57E-09	1.40E-08
$\tilde{a}_{11}$	1.999999999967040	2.000000003700050	2.000000030544100
$\lvert\frac{\tilde{a}_{11}-2}{2}\rvert$	1.65E-11	3.12E-09	1.53E-08
$\tilde{b}_{22}$	-1.500000002447100	-1.500000001810420	-1.500000492509220
$\lvert\frac{\tilde{b}_{22}-(-1.5)}{-1.5}\rvert$	1.63E-09	3.07E-08	3.28E-07
F_1	2.62E-08	3.04E-07	2.76E-06

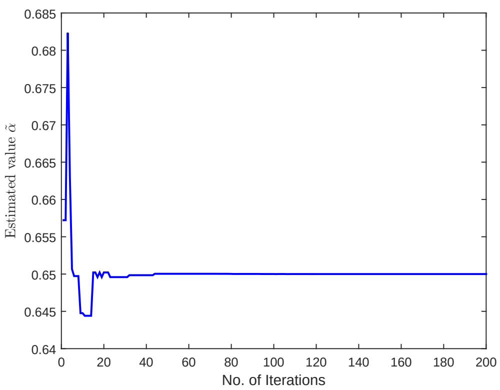

(a) Identified parameter value α

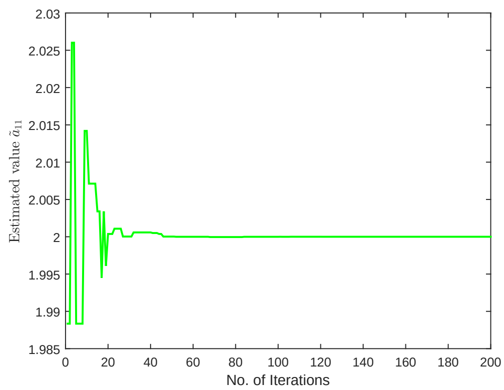

(b) Identified parameter value a_{11}

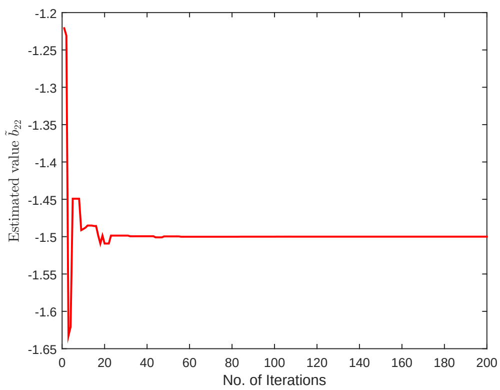

(c) Identified parameter value b_{22}

Fig. 4.5. Evolutionary curve of the identified parameters values with ABC on system (4.52) in a single run in Case 2

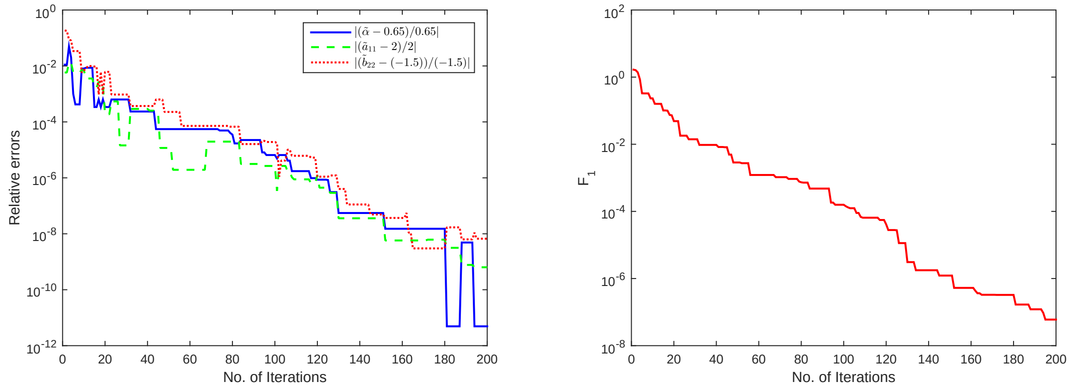

(a) Relative error values **(b)** Objective function values

Fig. 4.6. Evolutionary curve in terms of the relative errors and objective function values with ABC on system (4.52) in a single run in Case 2

followers can be modeled as

$$x_i^{(\bar{\alpha})}(t) = -\bar{C}x_i(t) + \bar{A}f(x_i(t)) + \bar{B}f(x_i(t-\tau)) + u_i(t) + w_i(t), \quad i = 1, 2, \cdots, 6, \tag{4.55}$$

and the dynamic of the leader can be written as

$$x_0^{(\bar{\alpha})}(t) = -\bar{C}x_0(t) + \bar{A}f(x_0(t)) + \bar{B}f(x_0(t-\tau)), \tag{4.56}$$

where $\bar{\alpha} = 0.97, \bar{C} = I_2$,

$$\bar{A} = [\bar{a}_{ij}]_{2\times 2} = \begin{bmatrix} 2.0 & -0.1 \\ -5.0 & 2.0 \end{bmatrix}, \quad \bar{B} = [\bar{b}_{ij}]_{2\times 2} = \begin{bmatrix} -1.5 & -0.1 \\ -0.2 & -1.5 \end{bmatrix},$$

other definitions in (4.55) and (4.56) are the same as those of (4.52).

The initial conditions are selected as $x_0 = [2, 1.5]^T, x_1 = [4, -2.5]^T, x_2 = [1, -1.2]^T, x_3 = [3, -3.4]^T$, $x_4 = [2.5, -3.7]^T, x_5 = [1.5, 4]^T, x_6 = [2, 3]^T$. The external disturbances are given as: $w_{1j}(t) = 0.3\cos(t+2), w_{2j}(t) = 0.6\sin(t-2), w_{3j}(t) = 0.25\cos(3t-5), w_{4j}(t) = 0.55\sin(4t+4), w_{5j}(t) = 0.5\sin(-3t-1), w_{6j}(t) = 0.7\cos(6t-3)$, for $j = 1, 2$. Based on Theorems 4.8 and 4.12, we choose $a = 21, \beta = 2, \lambda = 0.3, \delta = 0.28$, then the LMIs (4.15),(4.16) and (4.33), (4.34) hold.

Firstly, the state trajectories of consensus tracking by nonlinear discontinuous control protocol (4.13) are shown in Fig. 4.7, which shows that the six followers can track the leader's states quickly. Besides the phase portraits are also displayed in Fig. 4.8, from which we can find that all agents can successfully synchronize to the chaotic attractor of the leader, which can further verify the feasibility of Theorem 4.8. The corresponding control inputs are also given in Fig. 4.9.

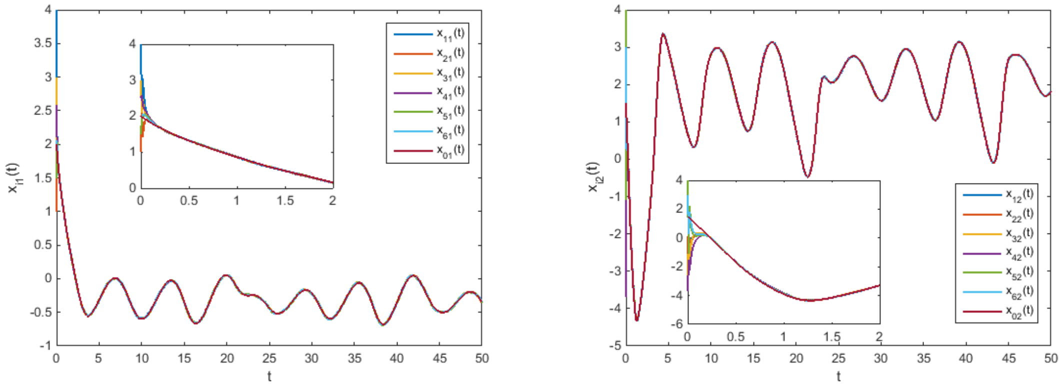

(a) State trajectories of $x_{i1}(i = 0, 1, \cdots, 6)$ **(b)** State trajectories of $x_{i2}(i = 0, 1, \cdots, 6)$

Fig. 4.7. State trajectories of FOMASs (4.55) and (4.56) by control protocol (4.13)

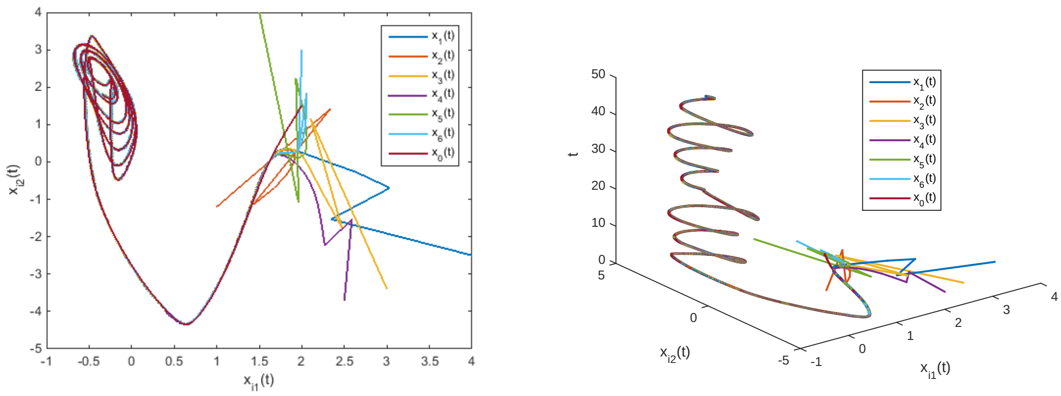

(a) Phase portraits in 2D **(b)** Phase portraits in 3D

Fig. 4.8. Phase portraits for all agents $(i = 0, 1, \cdots, 6)$ by control protocol (4.13)

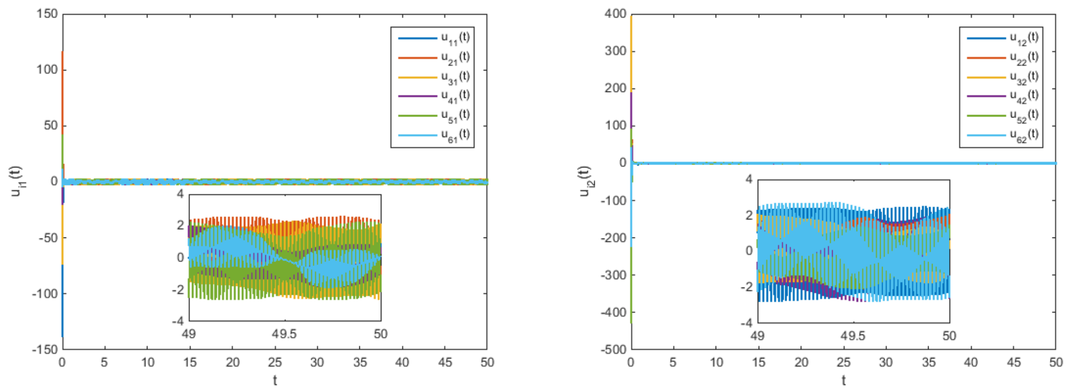

(a) Control inputs of $u_{i1}(i = 1, \cdots, 6)$ **(b)** Control inputs of $u_{i2}(i = 1, \cdots, 6)$

Fig. 4.9. Control inputs for control protocol (4.13)

Then, for boundary layers widths d_i in Eq. (4.32), in order to study the influence of the parameters d_i, two cases are considered as: $d_i = 0.6, (i = 1, 2, \cdots, 6)$ and $d_i = 0.1, (i = 1, 2, \cdots, 6)$. The evolutionary trajectories of consensus tracking by nonlinear continuous control protocol (4.31) are given in Figs. 4.10 and 4.13, where the consensus tracking errors can become smaller if the value of the boundary layers widths d_i are smaller. Besides, the corresponding phase portrait are given in Figs. 4.11 and 4.14, where all agents can successfully synchronize to the chaotic attractor of the leader. Furthermore, the chattering behavior can be avoided which can be verified in Figs. 4.12 and 4.15. Therefore, Theorem 4.12 is validated.

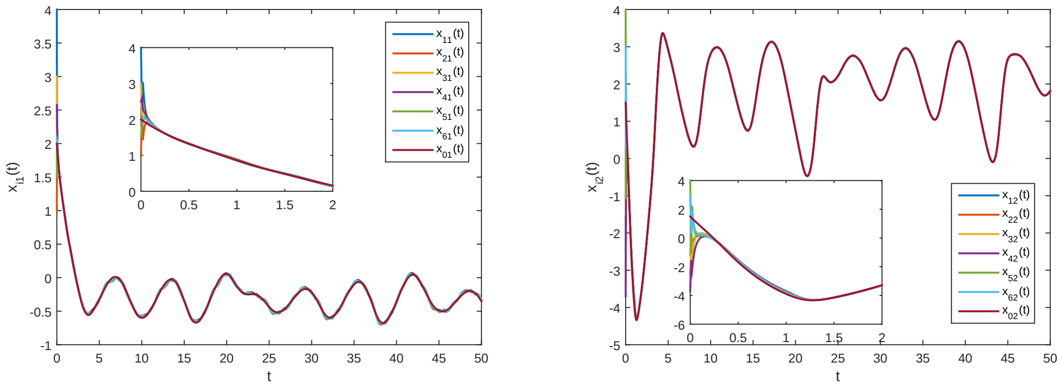

(a) State trajectories of $x_{i1}(i = 0, 1, \cdots, 6)$ **(b)** State trajectories of $x_{i2}(i = 0, 1, \cdots, 6)$

Fig. 4.10. State trajectories of FOMAS (4.55) and (4.56) by control protocol (4.31) with $d_i = 0.6(i = 1, 2, \cdots, 6)$

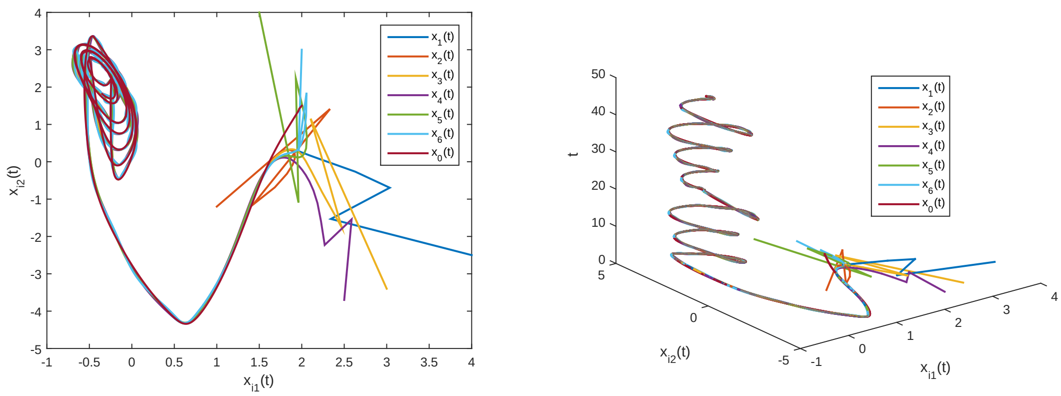

(a) Phase portraits in 2D **(b)** Phase portraits in 3D

Fig. 4.11. Phase portraits for all agents $(i = 0, 1, \cdots, 6)$ by control protocol (4.31) with $d_i = 0.6(i = 1, 2, \cdots, 6)$

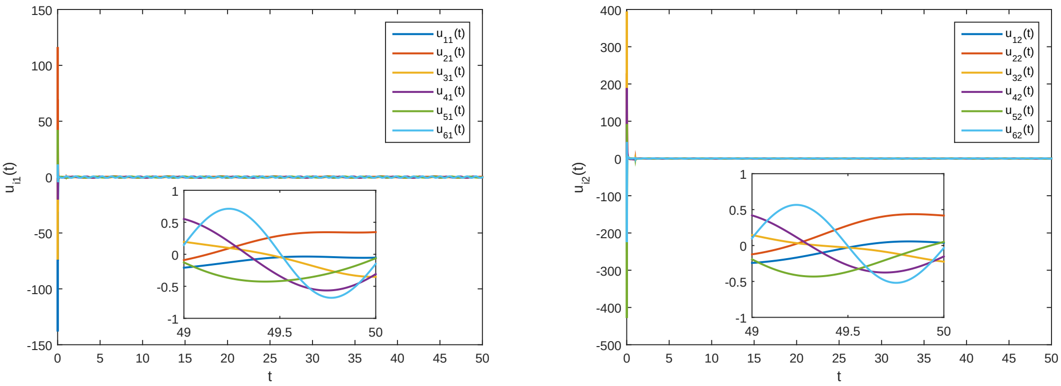

(a) Control inputs of $u_{i1}(i = 1, \cdots, 6)$ **(b)** Control inputs of $u_{i2}(i = 1, \cdots, 6)$

Fig. 4.12. Control inputs for control protocol (4.31) with $d_i = 0.6(i = 1, 2, \cdots, 6)$

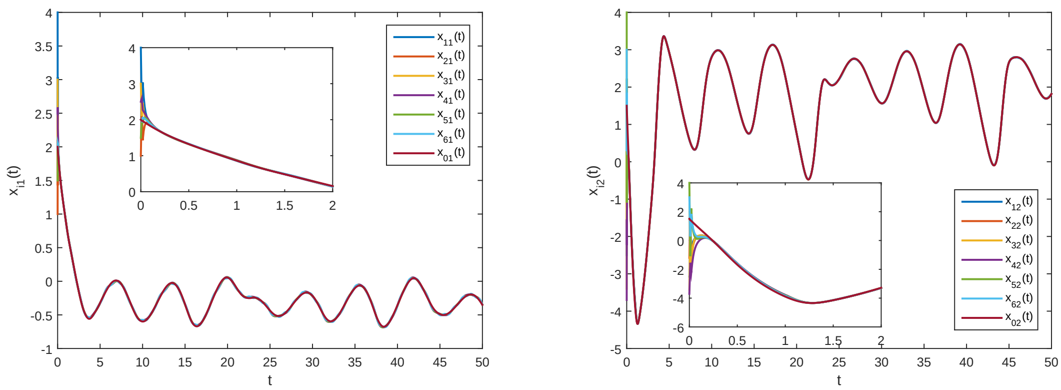

(a) State trajectories of $x_{i1}(i = 0, 1, \cdots, 6)$ **(b)** State trajectories of $x_{i2}(i = 0, 1, \cdots, 6)$

Fig. 4.13. State trajectories of FOMAS (4.55) and (4.56) by control protocol (4.31) with $d_i = 0.1(i = 1, 2, \cdots, 6)$

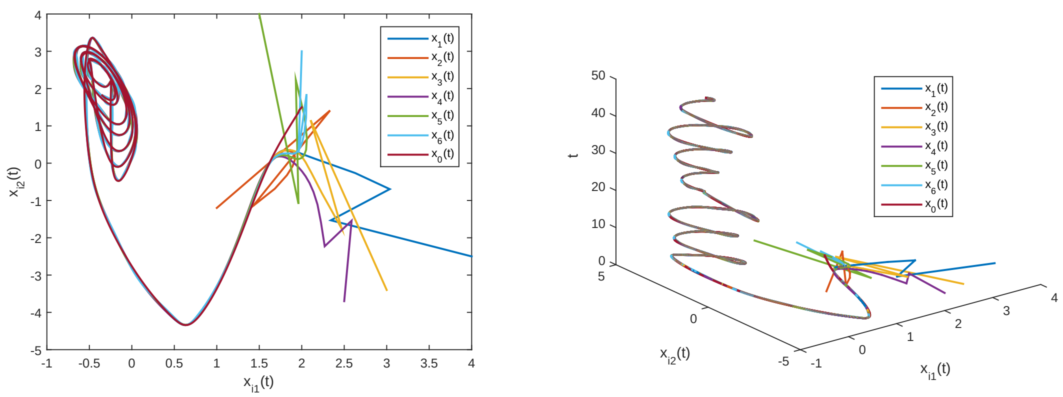

(a) Phase portraits in 2D **(b)** Phase portraits in 3D

Fig. 4.14. Phase portraits for all agents ($i = 0, 1, \cdots, 6$) by control protocol (4.31) with $d_i = 0.1(i = 1, 2, \cdots, 6)$

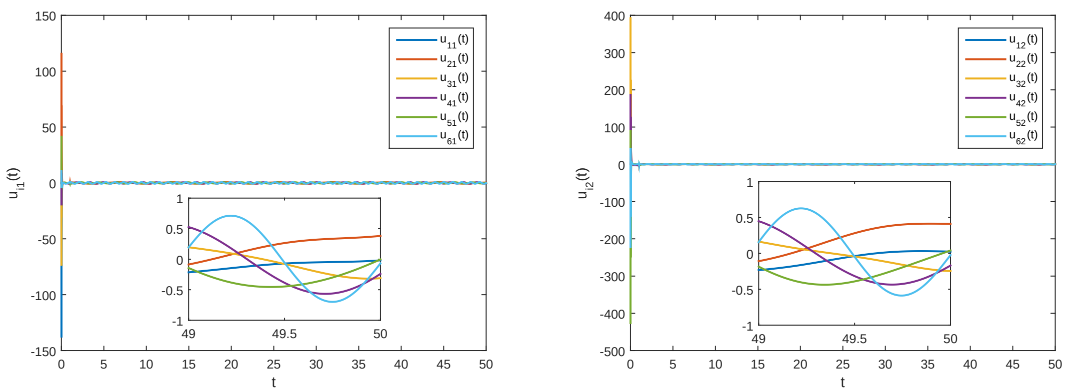

(a) Control inputs of $u_{i1}(i = 1, \cdots, 6)$ **(b)** Control inputs of $u_{i2}(i = 1, \cdots, 6)$

Fig. 4.15. Control inputs for control protocol (4.31) with $d_i = 0.1(i = 1, 2, \cdots, 6)$

4.6 Conclusion

In this chapter, the distributed consensus tracking of unknown nonlinear delayed FOMASs with external disturbances is investigated. Firstly, the parameter identification of the unknown nonlinear delayed FOMASs is converted into a functional optimization problem by treating the unknown fractional orders as additional decision variables. Then ABC algorithm-based parameter identification method is proposed to solve the functional optimization problem. Secondly, based on the identified parameters, a discontinuous control protocol is put forward to solve the consensus tracking problem by applying the inequalities of the fractional derivative and the comparison principle of the linear fractional equation with delay, and a new sufficient condition is established. Thirdly, in order to eliminate the chattering behavior caused by the above discontinuous control protocol, a continuous control protocol is further designed, and the UUB tracking errors can be obtained which can be tuned as small as enough by selecting proper parameters. Simulations are provided to show the efficiencies of the proposed parameter identification scheme and the two control protocols.

Chapter 5

Distributed cooperative synchronization of heterogenous uncertain nonlinear delayed FOMASs with unknown leader based on DE algorithm

Contents

5.1 Introduction

Note that the results obtained in Chapters 2, 3 and 4 assume that the control input of a leader is either equal to zero or available to all the followers, which has some limitations and lacks flexibility. More specifically, for the purpose of leading the followers to achieve special tasks, the leader's input need to be nonzero or time-varying. Furthermore, it is impossible for all the followers to know the leader's control input, when they are in an uncooperative scenario. Therefore, it is significant and essential to consider the leader with nonzero input, although it is difficult to address because of the limited information accessibility. Recently, some works have been done to overcome this difficulty in different distributed cooperative control problems. For example, in Yuan & He (2017), a leader of bounded input was considered in the cooperative output regulation of MASs. In Yu *et al.* (2018), a leader with bounded input was taken into account for the time-varying formation tracking. However, for distributed cooperative synchronization of FOMASs, a few researchers have considered the leader with bounded input. Gong (2017) studied the distributed synchronization of FOMAS with a leader of bounded input, while the time delay was not considered which is unavoidable in practice as mentioned Chapters 2 and 4. Therefore, in this chapter, it is full of challenge and meaningful to consider the leader's bounded input and the time delay simultaneously.

Recently, the investigation of heterogeneous MASs has become a hot topic in distributed cooperative control. Heterogeneity may occur because of the diverse designs and operating factors. For example, Li *et al.* (2018) considered heterogeneous input disturbances in the rendezvous problem. Jain & Ghose (2017a,b) studied the formation control of multi-vehicles with heterogenous control gains. In addition, MASs with heterogenous dynamics were also investigated in Devasia (2017); Guo *et al.* (2018); Meng *et al.* (2018). However, most results about the heterogeneous MASs are based on the integer-order models, a few results have been obtained based on the fractional-order models (Gong, 2017). Therefore, in this chapter, we consider the delayed nonlinear FOMASs with heterogenous control gains, which is more reasonable and practical.

As mentioned in Chapter 4, there may exist different kinds of uncertainties and nonlinearities in practical MASs, distributed cooperative control of uncertain nonlinear MASs has attracted much attentions. For instance, the MASs with uncertain parameters were considered in Yazdani & Haeri (2017). Khalili *et al.* (2018) studied the MASs with modelling uncertainty and known nonlinearity. In Chen *et al.* (2017), unknown control directions were taken into account in the consensus of nonlinear MASs. In addition, Gong & Lan (2018a,b) investigated the unknown nonlinear FOMASs using neural network-based robust adaptive control algorithm. However, all the results mentioned above are based on the known differential orders, while in some situations, the structure of the MASs may be known and the differential orders and system parameters are unknown, which need to be identified beforehand. Thus, based on a similar spirit, the unknown fractional orders and system parameters are further considered in the distributed cooperative synchronization of heterogenous nonlinear delayed FOMASs with unknown leader.

Differential evolution (DE), as an efficient AIOAs, was proposed in 1995 (Storn & Price, 1997). Many researches have demonstrated that DE can successfully tackle various optimization problems appeared in different fields, such as economic dispatch, controller design and tuning, and data clustering (Das & Suganthan, 2011). Compared to other AIOAs, the concept of DE is simple enough to be implemented easily, and it owns quick convergence. Therefore, in this chapter, the DE is employed to identify the unknown fractional orders and system parameters of the nonlinear delayed FOMASs, which not only can broad the application fields of the DE, but also can offer a promising parameter identification method for the FOMASs at the same time.

Under the above discussions, in this chapter, distributed cooperative synchronization of uncertain nonlinear delayed FOMASs with unknown leader and heterogenous control gains is addressed. Firstly, an efficient DE-based parameter identification scheme is put forward to identify the unknown nonlinear delayed FOMASs. Then based on the identified fractional orders and system parameters, a discontinuous distributed control protocol is designed to achieve the distributed cooperative synchronization by using the fractional-order derivative inequality and comparison principle of the linear fractional equation with delay. Thirdly, for the purpose of overcoming the chattering phenomenon resulting from the discontinuous controller, a continuous control protocol is further put forward, where the UUB tracking errors can be obtained and tuned small enough with appropriate parameters.

Compared with the existing works, our contribution are as follows. Firstly, different with Cui *et al.* (2017); Ma *et al.* (2016); Wen *et al.* (2013) which considered the integer-order MASs, this chapter considers the delayed MASs with fractional-order dynamics, moreover the unknown leaders, uncertain parameters, and the heterogenous control gains are also considered. Secondly, different from Chen *et al.* (2018c); Gong *et al.* (2019); Shen & Cao (2012); Yang *et al.* (2014a); Yu *et al.* (2017b) which considered linear FOMASs without/with time delay, due to the nonlinear dynamics is inevitable in practice, this chapter considers nonlinear FOMASs with time delay. Thirdly, different from Chen *et al.* (2018c); Cui *et al.* (2017); Hu *et al.* (2019c); Ma *et al.* (2016); Shen & Cao (2012); Wen *et al.* (2013); Yang *et al.* (2014a); Yu *et al.* (2017b); Zhu *et al.* (2017) which have not considered the leader's control input, in this chapter we consider the situation that the leader owns unknown bounded input, which could be more flexible and general in the distributed cooperative synchronization. Fourthly, different from Chen *et al.* (2017); Gong & Lan (2018a,b); Khalili *et al.* (2018); Yazdani & Haeri (2017) where the differential orders were assumed to be known, while in this chapter differential orders and system parameters are both considered to be unknown, then a DE-based parameter identification method is proposed to identity the unknown parameters of the delayed heterogenous nonlinear FOMASs. Fifthly, different from Ahandani *et al.* (2018); Panahi *et al.* (2016), which only considered the parameter identification problem, this chapter also applies it to the distributed cooperative synchronization. Furthermore, it is worth noting that this chapter makes a promising link between the artificial intelligent technique and distributed cooperative synchronization of FOMASs or other control fields.

The rest of this chapter is organized as following. In Section 5.2, the description of distributed cooperative synchronization is given. In Section 5.3, a DE-based parameter identification scheme for unknown nonlinear delayed FOMASs is put forward. In Section 5.4, based on the identified parameters, two powerful nonlinear control protocols are proposed to deal with the distributed cooperative synchronization. Finally, the efficiencies of the proposed DE-based parameter identification method and the designed control algorithms are both verified based on the simulation experiments.

5.2 Problem description for synchronization of FOMASs

Given FOMASs with one leader labeled as 0 and N followers labeled as 1 to N, the dynamics of FOMASs are described as

$$x_i^{(\alpha)}(t) = -Cx_i(t) + Af(x_i(t)) + Bf(x_i(t-\tau)) + u_i(t), \quad i = 0, 1, \cdots, N, \quad (5.1)$$

where $\alpha \in (0, 1]$, $x_i(t) = [x_{i1}(t), \cdots, x_{in}(t)]^T \in R^n$ denotes state vector of the ith agent. The nonlinear vector function $f(x_i(t)) = [f_1(x_{i1}(t)), \cdots, f_n(x_{in}(t))]^T \in R^n$ and constant time delay $\tau > 0$. $C = [c_{ij}]_{n\times n}$, $A = [\hat{a}_{ij}]_{n\times n}$ and $B = [\hat{b}_{ij}]_{n\times n}$ denote the corresponding weight matrices. $u_i(t) \in R^n$ is the control input vector for agent i.

Definition 5.1 *Considered any initial conditions of FOMASs (5.1), the distributed cooperative synchronization is obtained, if*

$$\lim_{t\to\infty} \|x_i(t) - x_0(t)\| = 0, \quad \forall\ i = 1, 2, \cdots, N.$$

To achieve the distributed cooperative synchronization, the following Assumptions and Lemmas are needed.

Assumption 5.2 *The nonlinear functions f_i are Lipschitz continuous with Lipschitz constants $\theta_i > 0$, such that*

$$|f_i(\mu) - f_i(\nu)| < \theta_i |\mu - \nu|, \quad \forall\ \mu, \nu \in R, \quad i = 1, \cdots, n.$$

Assumption 5.3 *The leader's control input $u_0(t)$ satisfies $\|u_0(t)\| \le \rho < +\infty$, where $\rho \ge 0$.*

Assumption 5.4 *The communication topology $\bar{\mathcal{G}}$ among the followers and leader has a directed spanning tree with the leader as the root node.*

5.3 DE-based parameter identification for FOMASs

5.3.1 Differential evolution

Differential evolution (DE), belonging to AIOAs, was reported by Storn and Price in 1995 (Das & Suganthan, 2011; Storn & Price, 1997). Contrasted with other AIOAs, DE has the nice properties with simple idea, easy fulfillment and fast searching speed. Therefore, DE has wide applications in complex continuous optimization problems appeared in various fields (Das & Suganthan, 2011). In addition, diverse searching equations of DE have been designed. In this chapter, DE/rand/1/bin version is used. The detailed information of DE can be referred to Das & Suganthan (2011); Storn & Price (1997). The main operators are as following:

Mutation operator: A mutated individual V_i is produced as

$$V_i = X_{r1} + F(X_{r2} - X_{r3}), \tag{5.2}$$

where $r1, r2, r3$ are three different integers randomly chosen from 1 to SN (the size of the population), $F > 0$ denotes the scale factor.

Crossover operator: A trial vector T_i is generated by recombination of X_i and V_i as

$$t_{i,j} = \begin{cases} \nu_{i,j}, & if \quad r \leq CR \quad or \quad j = j_{rand}, \\ x_{i,j}, & otherwise, \end{cases} \tag{5.3}$$

where $i = 1, 2, \cdots, SN$, $j = 1, 2, \cdots, D$, $t_{i,j}$ denotes the jth element of the trial vector T_i, r is a uniformly random value between 0 and 1, $CR \in [0, 1]$ is to control the ratio of selection between the parent and mutated vectors, and j_{rand} is a random integer from 1 to D to guarantee that at least one element of V_i will be inherited.

Selection operator: Comparison between the trail vector T_i and X_i is conducted and the superior one will be kept to the next generation, namely

$$X_i = \begin{cases} T_i, \qquad if \quad f(X_i) > f(T_i) \\ (for \ minimization \ problem, \ vice \ versa), \\ X_i, \qquad otherwise. \end{cases} \tag{5.4}$$

5.3.2 The proposed DE-based parameter identification scheme

Based on the above efficient DE and the parameter identification model introduced in Subsection 4.3.1, the following parameter identification scheme for FOMASs is proposed as Algorithm 3 (Hu *et al.*, 2019b).

Algorithm 3 DE-based parameter identification scheme

1: Initialize the parameters for DE and FOMASs (5.1)
2: Create the initial population based on the feasible domain Ω defined in subsection 4.3.1
3: **repeat**
4: Call the mutation operator based on (5.2)
5: Call the crossover operator based on (5.3)
6: Call the selection operator based on (4.6) and (5.4)
7: **until** Maximum iteration is met
8: Return the best parameter identification values

Remark 5.5 *In this chapter, DE is specially applied to the parameter identification of unknown nonlinear delayed FOMASs, which both can expand the applications of DE and can provide a meaningful approach for identifying the unknown nonlinear delayed FOMASs.*

5.4 Distributed cooperative synchronization of FOMASs based on DE

By applying Algorithm 3, we assume that system parameters C, A, B and fractional order α of the unknown FOMASs (5.1) are identified as $\bar{\alpha}, \bar{C} = [\bar{c}_{ij}]_{n\times n}, \bar{A} = [\bar{a}_{ij}]_{n\times n}$ and $\bar{B} = [\bar{b}_{ij}]_{n\times n}$. Then the dynamics of FOMASs can be reformulated as

$$x_i^{(\bar{\alpha})}(t) = -\bar{C}x_i(t) + \bar{A}f(x_i(t)) + \bar{B}f(x_i(t-\tau)) + u_i(t), \quad i = 0, 1, \cdots, N, \tag{5.5}$$

where $\bar{\alpha}, \bar{C} = [\bar{c}_{ij}]_{n\times n}, \bar{A} = [\bar{a}_{ij}]_{n\times n}$ and $\bar{B} = [\bar{b}_{ij}]_{n\times n}$ are the corresponding estimated values. Other definitions in (5.5) are the same as those of (5.1).

Denote the synchronization errors as $e_{x_i} = x_i(t) - x_0(t)$, and $e_{f_i} = f(x_i(t)) - f(x_0(t))$, $e_{x_{i\tau}} = x_i(t-\tau) - x_0(t-\tau)$, $e_{f_{i\tau}} = f(x_i(t-\tau)) - f(x_0(t-\tau))$. Let $e_x, e_f, e_{x_\tau}, e_{f_\tau}$ and $u(t)$ be the column vectors of $e_{x_i}, e_{f_i}, e_{x_{i\tau}}, e_{f_{i\tau}}$ and $u_i(t)$, respectively. Based on (5.5), the synchronization errors e_x can be obtained as:

$$\begin{aligned} e_x^{(\bar{\alpha})}(t) = & -(I_N \otimes \bar{C})e_x + (I_N \otimes \bar{A})e_f \\ & + (I_N \otimes \bar{B})e_{f_\tau} - \mathbf{1}_N \otimes u_0(t) + u(t). \end{aligned} \tag{5.6}$$

According to Assumption 5.4, v_0 is a global reachable node. Let $M = \mathcal{L} + \mathcal{B} = [m_{ij}]_{N\times N}$, then matrix M is positive definite based on Lemma 1.2.

In the following, based on the identified FOMASs (5.5), two kinds of distributed controllers are designed to tackle the distributed cooperative synchronization under the directed communication topology.

5.4.1 Discontinuous distributed control algorithm

To achieve the distributed cooperative synchronization, a nonlinear discontinuous control protocol is designed for each follower as

$$u_i(t) = -ay_i - \beta h(y_i), \qquad i = 1, 2, \cdots, N, \tag{5.7}$$

where $y_i = \gamma_i \sum_{j=0}^{N} a_{i,j}(x_i - x_j)$, and $a, \beta, \gamma_i > 0$ are constant coupling gains. $h(y_i)$ is a nonlinear discontinuous function defined as

$$h(y_i) = \begin{cases} \frac{y_i}{\|y_i\|}, & \|y_i\| \neq 0, \\ \mathbf{0}_n, & \|y_i\| = 0. \end{cases} \tag{5.8}$$

Based on the graph theory introduced in Chapter 1, it can be easily verified that $y_i = \gamma_i \sum_{j=0}^{N} a_{i,j}(e_{x_i} - e_{x_j}) = \gamma_i \sum_{j=1}^{N} m_{ij} e_{x_j}$, which means $y = (\Lambda M \otimes I_n)e_x$, where $\Lambda = diag\{\gamma_1, \gamma_2, \cdots, \gamma_N\}$, $\tilde{M} = M \otimes I_n$ and y is the column vector of y_i .

Theorem 5.6 *(Hu et al., 2019b) Given Assumptions 5.2-5.4, with the nonlinear discontinuous control algorithm (5.7), the distributed cooperative synchronization of delayed nonlinear FOMASs (5.5) can be reached, if $\beta \geq \rho$, and there exist some constants $\lambda > \delta > 0, a > 0$ and positive definite matrixes Ξ_1 and Ξ_2 such the following LMIs hold:*

$$\Phi = \begin{bmatrix} \Phi_1 & \Lambda^{-1} \otimes \Theta \\ * & -\Xi_1 \end{bmatrix} < 0, \tag{5.9}$$

$$\Psi = \begin{bmatrix} -\lambda_{min}(\tilde{G})\delta I_{Nn} & \Lambda^{-1} \otimes \Theta \\ * & -\Xi_2 \end{bmatrix} < 0, \tag{5.10}$$

where $\Phi_1 = -G\Lambda^{-1} \otimes (\bar{C} + \bar{C}^T) + (G \otimes \bar{A})\Xi_1(G \otimes \bar{A})^T + (G \otimes \bar{B})\Xi_2(G \otimes \bar{B})^T - a(Q \otimes I_n) + \lambda_{max}(\tilde{G})\lambda I_{Nn}$, $\tilde{G} = G\Lambda^{-1} \otimes I_n$. $\Theta = diag\{\theta_1, \cdots, \theta_n\}$ *with* θ_i *defined in Assumption 5.2.*

Proof: Substitute the protocol (5.7) into synchronization errors system (5.6) as

$$\begin{aligned} e_x^{(\bar{\alpha})}(t) = &-(I_N \otimes \bar{C})e_x + (I_N \otimes \bar{A})e_f \\ &+ (I_N \otimes \bar{B})e_{f_\tau} - \mathbf{1}_N \otimes u_0(t) - ay - \beta H(y), \end{aligned} \tag{5.11}$$

where $H(y) = [h^T(y_1), \cdots, h^T(y_N)]^T \in R^{Nn}$.

In order to verify the stability of the errors system (5.6), construct the Lyapunov function as

$$V(t) = y^T(G\Lambda^{-1} \otimes I_n)y = y^T\tilde{G}y. \tag{5.12}$$

Then based on Lemma 1.19, we have

$$\begin{aligned} V^{(\bar{\alpha})}(t) &\le 2y^T\tilde{G}y^{(\bar{\alpha})} \\ &= 2y^T(G\Lambda^{-1} \otimes I_n)(\Lambda M \otimes I_n)e_x^{(\bar{\alpha})} \\ &= 2y^T(GM \otimes I_n)e_x^{(\bar{\alpha})} \\ &= 2y^T(GM \otimes I_n)\big(-(I_N \otimes \bar{C})e_x + (I_N \otimes \bar{A})e_f \\ &\quad + (I_N \otimes \bar{B})e_{f_\tau} - \mathbf{1}_N \otimes u_0(t) - ay - \beta H(y)\big). \end{aligned} \tag{5.13}$$

With the properties of Kronecker product, one has

$$\begin{aligned} 2y^T(GM \otimes I_n)\big(-(I_N \otimes \bar{C})e_x\big) &= -2y^T(GM \otimes \bar{C})(\Lambda M \otimes I_n)^{-1}y \\ &= -2y^T(G\Lambda^{-1} \otimes \bar{C})y \\ &= -y^T\big(G\Lambda^{-1} \otimes (\bar{C} + \bar{C}^T)\big)y. \end{aligned} \tag{5.14}$$

Based on Lemma 1.22, let $\Xi = \Xi_1, \xi = 1$, it yields

$$\begin{aligned}
&2y^T(GM \otimes I_n)(I_N \otimes \bar{A})e_f \\
&\quad = 2y^T(GM \otimes \bar{A})e_f \\
&\quad = 2y^T(G \otimes \bar{A})(M \otimes I_n)e_f \\
&\quad \leq y^T(G \otimes \bar{A})\Xi_1(G \otimes \bar{A})^T y + e_f^T(M \otimes I_n)^T \Xi_1^{-1}(M \otimes I_n)e_f \\
&\quad \leq y^T(G \otimes \bar{A})\Xi_1(G \otimes \bar{A})^T y + e_x^T(I_N \otimes \Theta)(M \otimes I_n)^T \Xi_1^{-1}(M \otimes I_n)(I_N \otimes \Theta)e_x \\
&\quad = y^T(G \otimes \bar{A})\Xi_1(G \otimes \bar{A})^T y + y^T(\Lambda M \otimes I_n)^{-T}(I_N \otimes \Theta)(M \otimes I_n)^T \Xi_1^{-1}(M \otimes I_n) \\
&\qquad \times (I_N \otimes \Theta)(\Lambda M \otimes I_n)^{-1} y \\
&\quad = y^T(G \otimes \bar{A})\Xi_1(G \otimes \bar{A})^T y + y^T(\Lambda^{-1} \otimes \Theta)\Xi_1^{-1}(\Lambda^{-1} \otimes \Theta)y.
\end{aligned} \tag{5.15}$$

Based on Lemma 1.22, let $\Xi = \Xi_2, \xi = 1$, it yields

$$\begin{aligned}
&2y^T(GM \otimes I_n)(I_N \otimes \bar{B})e_{f_\tau} \\
&\quad = 2y^T(GM \otimes \bar{B})e_{f_\tau} \\
&\quad = 2y^T(G \otimes \bar{B})(M \otimes I_n)e_{f_\tau} \\
&\quad \leq y^T(G \otimes \bar{B})\Xi_2(G \otimes \bar{B})^T y + e_{f_\tau}^T(M \otimes I_n)^T \Xi_2^{-1}(M \otimes I_n)e_{f_\tau} \\
&\quad \leq y^T(G \otimes \bar{B})\Xi_2(G \otimes \bar{B})^T y + e_{x_\tau}^T(I_N \otimes \Theta)(M \otimes I_n)^T \Xi_2^{-1}(M \otimes I_n)(I_N \otimes \Theta)e_{x_\tau} \\
&\quad = y^T(G \otimes \bar{B})\Xi_2(G \otimes \bar{B})^T y + y_\tau^T(\Lambda M \otimes I_n)^{-T}(I_N \otimes \Theta)(M \otimes I_n)^T \Xi_2^{-1}(M \otimes I_n) \\
&\qquad \times (I_N \otimes \Theta)(\Lambda M \otimes I_n)^{-1} y_\tau \\
&\quad = y^T(G \otimes \bar{B})\Xi_2(G \otimes \bar{B})^T y + y_\tau^T(\Lambda^{-1} \otimes \Theta)\Xi_2^{-1}(\Lambda^{-1} \otimes \Theta)y_\tau.
\end{aligned} \tag{5.16}$$

Due to $M\mathbf{1}_N = (\mathcal{L} + \mathcal{B})\mathbf{1}_N = [a_{10}, a_{20}, \cdots, a_{N0}]^T$, one has

$$\begin{aligned}
2y^T(GM \otimes I_n)(-\mathbf{1}_N \otimes u_0) &= -2y^T(GM\mathbf{1}_N \otimes u_0) \\
&= -2\sum_{i=1}^{N} g_i a_{i0} y_i^T u_0 \\
&\leq 2\sum_{i=1}^{N} g_i a_{i0} \|y_i\| \|u_0\| \\
&\leq 2\rho \sum_{i=1}^{N} g_i a_{i0} \|y_i\|.
\end{aligned} \tag{5.17}$$

According to Lemma 1.2, one obtains

$$
\begin{aligned}
&2y^T(GM\otimes I_n)(-ay)\\
&\quad= -2ay^T(GM\otimes I_n)y\\
&\quad= -a\big(y^T(GM\otimes I_n)y + y^T(GM\otimes I_n)^T y\big)\\
&\quad= -ay^T\Big(\big(GM+(GM)^T\big)\otimes I_n\Big)y\\
&\quad= -ay^T(Q\otimes I_n)y.
\end{aligned}
\tag{5.18}
$$

Due to $y_i^T h(y_i) = \|y_i\|$ and $y_i^T h(y_j) \le \|y_i\|\|h(y_j)\| = \|y_i\|$, one has

$$
\begin{aligned}
&2y^T(GM\otimes I_n)(-\beta H(y))\\
&= -2\beta\sum_{i=1}^{N} g_i y_i^T\Big(a_{i0}h(y_i) + \sum_{j=1}^{N} a_{ij}\big(h(y_i)-h(y_j)\big)\Big)\\
&\le -2\beta\sum_{i=1}^{N} g_i a_{i0}\|y_i\|.
\end{aligned}
\tag{5.19}
$$

Then according to $\beta > \rho$, (5.9),(5.10), and (5.14)-(5.19), it yields

$$
\begin{aligned}
&V^{(\bar{\alpha})}(t)\\
&\le y^T\Big(-G\Lambda^{-1}\otimes(\bar{C}+\bar{C}^T) + (G\otimes\bar{A})\Xi_1(G\otimes\bar{A})^T\\
&\quad + (\Lambda^{-1}\otimes\Theta)\Xi_1^{-1}(\Lambda^{-1}\otimes\Theta) + (G\otimes\bar{B})\Xi_2(G\otimes\bar{B})^T - a(Q\otimes I_n)\Big)y\\
&\quad + y_\tau^T(\Lambda^{-1}\otimes\Theta)\Xi_2^{-1}(\Lambda^{-1}\otimes\Theta)y_\tau - 2\beta\sum_{i=1}^{N} g_i a_{i0}\|y_i\| + 2\rho\sum_{i=1}^{N} g_i a_{i0}\|y_i\|\\
&\le y^T\Big(-G\Lambda^{-1}\otimes(\bar{C}+\bar{C}^T) + (G\otimes\bar{A})\Xi_1(G\otimes\bar{A})^T + (\Lambda^{-1}\otimes\Theta)\Xi_1^{-1}(\Lambda^{-1}\otimes\Theta)\\
&\quad + (G\otimes\bar{B})\Xi_2(G\otimes\bar{B})^T - a(Q\otimes I_n) + \tilde{\lambda}I_{Nn}\Big)y\\
&\quad + y_\tau^T\Big((\Lambda^{-1}\otimes\Theta)\Xi_2^{-1}(\Lambda^{-1}\otimes\Theta) - \tilde{\delta}I_{Nn}\Big)y_\tau - \tilde{\lambda}y^Ty + \tilde{\delta}y_\tau^T y_\tau\\
&= y^T\Phi y + y_\tau^T\Psi y_\tau - \tilde{\lambda}y^Ty + \tilde{\delta}y_\tau^T y_\tau\\
&\le -\tilde{\lambda}y^Ty + \tilde{\delta}y_\tau^T y_\tau\\
&\le -\frac{\tilde{\lambda}}{\lambda_{max}(\tilde{G})}y^T\tilde{G}y + \frac{\tilde{\delta}}{\lambda_{min}(\tilde{G})}y_\tau^T\tilde{G}y_\tau\\
&= -\lambda V(t) + \delta V(t-\tau),
\end{aligned}
\tag{5.20}
$$

where $\tilde{\lambda} = \lambda_{max}(\tilde{G})\lambda$, $\tilde{\delta} = \lambda_{min}(\tilde{G})\delta$.

Now, consider the fractional-order linear delayed system as

$$\begin{cases} Z^{(\bar{\alpha})}(t) = -\lambda Z(t) + \delta Z(t-\tau), \bar{\alpha} \in (0,1], \\ Z(t) = \phi(t), t \in [-\tau, 0], \end{cases} \tag{5.21}$$

which has the same initial condition with system (5.20). According to Lemma 1.18, if $\lambda > \delta$ and there exists no purely imaginary root for the following characteristic equation of system (5.21)

$$s^{\bar{\alpha}} + \lambda - \delta e^{-s\tau} = 0, \tag{5.22}$$

then, the zero solution of system (5.21) is Lyapunov globally asymptotically stable, which implies that $Z(t) \to 0$ as $t \to +\infty$. For (5.22), suppose there exists a pure imaginary root $s = \eta i, \eta \in R$. If $\eta > 0, s = \eta i = |\eta|(\cos\frac{\pi}{2} + i\sin\frac{\pi}{2})$, and if $\eta < 0, s = \eta i = |\eta|(\cos\frac{\pi}{2} - i\sin\frac{\pi}{2})$. Then substituting $s = \eta i = |\eta|(\cos\frac{\pi}{2} \pm i\sin\frac{\pi}{2})$ into (5.22) generates

$$|\eta|^{\bar{\alpha}}\big(\cos\frac{\bar{\alpha}\pi}{2} + i\sin(\pm\frac{\bar{\alpha}\pi}{2})\big) + \lambda - \delta(\cos\eta\tau - i\sin\eta\tau) = 0. \tag{5.23}$$

Separate (5.23) into real and imaginary parts as

$$\begin{cases} |\eta|^{\bar{\alpha}}\cos\frac{\bar{\alpha}\pi}{2} + \lambda = \delta\cos\eta\tau, \\ |\eta|^{\bar{\alpha}}\sin(\pm\frac{\bar{\alpha}\pi}{2}) = -\delta\sin\eta\tau. \end{cases} \tag{5.24}$$

From (5.24), it can be conducted as

$$|\eta|^{2\bar{\alpha}} + 2\lambda|\eta|^{\bar{\alpha}}\cos\frac{\bar{\alpha}\pi}{2} + \lambda^2 - \delta^2 = 0. \tag{5.25}$$

Since $|\eta|^{\bar{\alpha}} > 0, \cos\frac{\bar{\alpha}\pi}{2} > 0, \lambda^2 > \delta^2$, so (5.25) cannot hold. Therefore, the pure imaginary root does not exist in characteristic equation (5.22). According to Lemma 1.18, $Z(t)$ is Lyapunov globally asymptotically stable. With Lemmas 1.2 and 1.17, we have $\lambda_{min}(\tilde{G})\|y\|^2 \le V(t) \le Z(t) \to 0, t \to +\infty$, which means that $\|e_x\|^2 \to 0, t \to +\infty$. Therefore, the proof is completed. ■

5.4.2 Continuous distributed control algorithm

In subsection 5.4.1, the discontinuous control protocol (5.7) can result in the undesirable chattering phenomenon in practice. Therefore, to compensate this drawback, a continuous distributed control protocol is further designed to solve the distributed cooperative synchronization. According to the boundary layer technique (Young *et al.*, 1999), the continuous control protocol is designed as

$$u_i(t) = -ay_i - \beta\bar{h}_i(y_i), \qquad i = 1, 2, \cdots, N, \tag{5.26}$$

where $y_i = \gamma_i \sum_{j=0}^{N} a_{i,j}(x_i - x_j)$, and $a, \beta, \gamma_i > 0$ are constant coupling gains. $\bar{h}_i(y_i)$ is a nonlinear continuous function defined as

$$\bar{h}_i(y_i) = \begin{cases} \frac{y_i}{\|y_i\|}, & \|y_i\| > d_i, \\ \frac{y_i}{d_i}, & \|y_i\| \leq d_i, \end{cases} \tag{5.27}$$

where $d_i > 0$ denotes the width of the boundary layers.

Theorem 5.7 *(Hu* et al.*, 2019b) Given Assumptions 5.2-5.4, the synchronization errors of FOMASs (5.5) are UUB with the continuous control algorithm (5.26), if $\beta \geq \rho$, and there exist some constants $\lambda > \delta > 0, a > 0$ and positive definite matrixes Ξ_1 and Ξ_2 such the LMIs (5.9) and (5.10) hold. Moreover, the tracking error e_x asymptotically converges to the following bounded region*

$$\mathcal{D} = \left\{ e_x : \|e_x\|^2 \leq \frac{2\sum_{i=1}^{N} d_i g_i(\rho a_{i0} + \beta l_{ii})}{\lambda_{min}(M^T \Lambda^2 M)\lambda_{min}(\tilde{G})(\lambda - \delta)} \right\}. \tag{5.28}$$

Proof: Substituting the protocol (5.26) into the synchronization errors system (5.6), one obtains that

$$\begin{aligned} e_x^{(\bar{\alpha})}(t) = & -(I_N \otimes \bar{C})e_x + (I_N \otimes \bar{A})e_f \\ & + (I_N \otimes \bar{B})e_{f_\tau} - \mathbf{1}_N \otimes u_0(t) - ay - \beta\bar{H}(y), \end{aligned} \tag{5.29}$$

where $\bar{H}(y) = [\bar{h}_1^T(y_1), \cdots, \bar{h}_N^T(y_N)]^T \in R^{Nn}$.

The $\bar{\alpha}$-order derivative of Lyapunov function candidate (5.12) with errors system (5.29) is

$$\begin{aligned}
V^{(\bar{\alpha})}(t) &\leq 2y^T\tilde{G}y^{(\bar{\alpha})} \\
&= 2y^T(G\Lambda^{-1}\otimes I_n)(\Lambda M\otimes I_n)e_x^{(\bar{\alpha})} \\
&= 2y^T(GM\otimes I_n)e_x^{(\bar{\alpha})} \\
&= 2y^T(GM\otimes I_n)\big(-(I_N\otimes\bar{C})e_x+(I_N\otimes\bar{A})e_f \\
&\quad +(I_N\otimes\bar{B})e_{f_\tau}-\mathbf{1}_N\otimes u_0(t)-ay-\beta\bar{H}(y)\big).
\end{aligned}\tag{5.30}$$

Based on the property of (5.27), the following three cases are discussed.

(i) $\|y_i\|>d_i,\quad i=1,2,\cdots,N.$

In this case, based on (5.17) and (5.19), one has

$$\begin{aligned}
&2y^T(GM\otimes I_n)\big(-\mathbf{1}_N\otimes u_0(t)-\beta\bar{H}(y)\big) \\
&\quad\leq 2(-\beta+\rho)\sum_{i=1}^{N}g_ia_{i0}\|y_i\|<0.
\end{aligned}\tag{5.31}$$

Substituting (5.14)-(5.16), (5.18) and (5.31) into (5.30) yields

$$V^{(\bar{\alpha})}(t)<-\lambda V(t)+\delta V(t-\tau).\tag{5.32}$$

(ii) $\|y_i\|\leq d_i,\quad i=1,2,\cdots,N.$

Based on (5.17), one has

$$2y^T(GM\otimes I_n)(-\mathbf{1}_N\otimes u_0)\leq 2\rho\sum_{i=1}^{N}d_ig_ia_{i0}.\tag{5.33}$$

Note that for any $i,j=1,2,\cdots,N$,

$$\begin{aligned}
&y_i^T\bar{h}_i(y_i)=\|y_i\|^2/d_i\geq 0, \\
&y_i^T\bar{h}_i(y_j)\leq\|y_i\|\|\bar{h}_i(y_j)\|\leq\|y_i\|\leq d_i,
\end{aligned}$$

one has

$$\begin{aligned}
&2y^T(GM\otimes I_n)\big(-\beta\bar{H}(y)\big)\\
&=2\beta\sum_{i=1}^{N}g_iy_i^T\Big(-a_{i0}\bar{h}_i(y_i)+\sum_{j=1}^{N}a_{ij}\big(\bar{h}_j(y_j)-\bar{h}_i(y_i)\big)\Big)\\
&\leq 2\beta\sum_{i=1}^{N}d_ig_i\sum_{j=1}^{N}a_{ij}\\
&=2\beta\sum_{i=1}^{N}d_ig_il_{ii}.
\end{aligned}\tag{5.34}$$

Therefore, it can be obtained that

$$2y^T(GM\otimes I_n)\big(-\mathbf{1}_N\otimes u_0-\beta\bar{H}(y)\big)\leq 2\sum_{i=1}^{N}d_ig_i(\rho a_{i0}+\beta l_{ii}).\tag{5.35}$$

Substituting (5.14)-(5.16) and (5.35) into (5.30) yields

$$V^{(\bar{\alpha})}(t)<-\lambda V(t)+\delta V(t-\tau)+2\sum_{i=1}^{N}d_ig_i(\rho a_{i0}+\beta l_{ii}).\tag{5.36}$$

(iii) y satisfies neither Case (i) nor Case (ii).

Without loss of generality, we suppose $||y_i||>d_i, i=1,2,\cdots,\kappa$, and $||y_i||\leq d_i, i=\kappa+1,\kappa+2,\cdots,N$, $(1<\kappa<N)$. For this case, according to (5.31) and (5.35), one derive that

$$2y^T(GM\otimes I_n)\big(-\mathbf{1}_N\otimes u_0-\beta\bar{H}(y)\big)\leq 2\sum_{i=\kappa+1}^{N}d_ig_i(\rho a_{i0}+\beta l_{ii}).\tag{5.37}$$

Thus, from (5.14)-(5.16) and (5.37), one has

$$V^{(\bar{\alpha})}(t)<-\lambda V(t)+\delta V(t-\tau)+2\sum_{i=\kappa+1}^{N}d_ig_i(\rho a_{i0}+\beta l_{ii}).\tag{5.38}$$

Therefore, based on the above three discussed cases, for all $y\in R^{Nn}$, we have

$$V^{(\bar{\alpha})}(t)<-\lambda V(t)+\delta V(t-\tau)+d,\tag{5.39}$$

where $d = 2\sum_{i=1}^{N} d_i g_i(\rho a_{i0} + \beta l_{ii})$.

Consider the following system:

$$Z^{(\bar{\alpha})}(t) = -\lambda Z(t) + \delta Z(t-\tau) + d, \tag{5.40}$$

where $Z(t) \geq 0 (Z(t) \in R)$, and has the same initial conditions with $V(t)$. Based on Lemma 1.17, one can obtain that $0 < V(t) < Z(t)$. With Properties 1.7 and 1.8, we have

$$(Z(t) - \bar{d})^{(\bar{\alpha})}(t) = -\lambda(Z(t) - \bar{d}) + \delta(Z(t-\tau) - \bar{d}), \tag{5.41}$$

where $\bar{d} = d/(\lambda - \delta)$. Taking $\bar{Z}(t) = Z(t) - \bar{d}$, then system (5.41) can be transformed into

$$\bar{Z}^{(\bar{\alpha})}(t) = -\lambda \bar{Z}(t) + \delta \bar{Z}(t-\tau). \tag{5.42}$$

Applying the similar proof procedure in Theorem 5.6, we can obtain that $\bar{Z}(t) = Z(t) - \bar{d} \to 0$, as $t \to +\infty$, which implies that

$$\lambda_{min}(\tilde{G})\|y\|^2 \leq V(t) \leq Z(t) \to \bar{d},\ t \to +\infty. \tag{5.43}$$

Due to $y = (\Lambda M \otimes I_n)e_x$, one has

$$\|y\|^2 = y^T y = e_x^T(M^T\Lambda^2 M \otimes I_n)e_x \geq \lambda_{min}(M^T\Lambda^2 M)\|e_x\|^2. \tag{5.44}$$

Therefore, according to (5.43) and (5.44), the synchronization errors can asymptotically converge to the following bounded region

$$\begin{aligned} \|e_x\|^2 &\leq \frac{\bar{d}}{\lambda_{min}(M^T\Lambda^2 M)\lambda_{min}(\tilde{G})} \\ &= \frac{2\sum_{i=1}^{N} d_i g_i(\rho a_{i0} + \beta l_{ii})}{\lambda_{min}(M^T\Lambda^2 M)\lambda_{min}(\tilde{G})(\lambda - \delta)}, \quad (t \to +\infty), \end{aligned} \tag{5.45}$$

which can be made small enough by choosing proper parameter d_i. ■

Corollary 5.8 *If the widths d_i of the boundary layers are the same in controller (5.26), i.e., $d_1 = d_2 = \cdots = d_N = d$, the bounded region in Theorem 5.7 can be* *simplified as*

$$\mathcal{D} = \left\{ e_x : \|e_x\|^2 \leq \frac{2d \sum_{i=1}^{N} g_i(\rho a_{i0} + \beta l_{ii})}{\lambda_{min}(M^T \Lambda^2 M)\lambda_{min}(\tilde{G})(\lambda - \delta)} \right\}. \tag{5.46}$$

Remark 5.9 *Compared with the synchronization of delayed fractional-order coupled systems where there are only a single master and a single slave system (Bao et al., 2015; Chen et al., 2018a, 2015b; Zhang & Yang, 2018), this chapter studies synchronization for a single mater and multiple slaves delayed FOMASs, where the multiple salves systems are coupled with a connected directed communication topology. Different from the single master and a single slave system (Bao et al., 2015; Chen et al., 2018a, 2015b; Zhang & Yang, 2018), in this chapter, to verify the effectiveness of the proposed synchronization controller in theory, the design of the Lyapunov function should depend on the graph communication topology and heterogenous control gains, which are full of challenge due to the structure of the graph and the heterogeneities.*

Remark 5.10 *In this chapter, the distributed cooperative synchronization of nonlinear delayed FOMASs with unknown leader is investigated based on directed communication topology. In fact, the results are also effective for distributed cooperative synchronization of FOMASs with any nonlinear dynamics as*

$$\begin{cases} x_0^{(\alpha)}(t) = f(x_0(t), x_0(t-\tau)) + u_0(t), & leader, \\ x_i^{(\alpha)}(t) = f(x_i(t), x_i(t-\tau)) + u_i(t), & followers, \end{cases}$$

where nonlinear function $f(\cdot)$ satisfies Assumption 5.2, and leader's control input $u_0(t)$ satisfies Assumption 5.3.

Remark 5.11 *When the number of the followers is assumed as $N = 1$, the synchronization methods studied in this chapter will degenerate into the case of single mater-single slave synchronization between two delayed fractional-order nonlinear systems (Bao et al., 2015; Chen et al., 2018a, 2015b; Zhang & Yang, 2018). That is to say, this chapter is an extension of the classical master-slave synchronization to the more general case of FOMASs.*

Remark 5.12 *When the fractional order $\bar{\alpha} = 1$, the distributed cooperative synchronization studied in this chapter will reduce to the case of integer-order MASs*

(Cui et al., 2017; Ma et al., 2016) as

$$\begin{cases} \dot{x}_0(t) = -Cx_0(t) + Af(x_0(t)) + Bf(x_0(t-\tau)) + u_0(t), & leader, \\ \dot{x}_i(t) = -Cx_i(t) + Af(x_i(t)) + Bf(x_i(t-\tau)) + u_i(t), & followers, \end{cases}$$

which is a special case of this chapter.

5.5 Simulations

5.5.1 DE-based parameter identification results

5.5.1.1 Parameter identification without noise

For the initialization of Algorithm 3, the number of sample points is chosen as $K = 100$ and the step size is $h = 0.01$. For DE algorithm, $SN = 100$, maximum iteration is 200, $F = 0.5, CR = 0.7$.

- **Case 1:** $\alpha = 0.98$

Consider FOMASs with one leader and six followers. The communication topology is given as Fig. 5.1. Assume that the leader and followers have homogenous nonlinear dynamics with two-dimensional fractional-order delayed neural networks as

$$\begin{aligned} x_i^{(\alpha)}(t) = -Cx_i(t) + Af(x_i(t)) + Bf(x_i(t-\tau)), \\ i = 0, 1, \cdots, 6, \end{aligned} \tag{5.47}$$

where $x_i(t) = [x_{i1}(t), x_{i2}(t)]^T, \alpha = 0.98, C = I_2, \tau = 0.9$, $f(x_i(t)) = [f_1(x_{i1}(t)), f_2(x_{i2}(t))]^T$, and $f_j(x_{ij}(t)) = \frac{1}{2}(|x_{ij}+1| - |x_{ij}-1|), j = 1, 2$. Obviously, from Assumption 5.2, it is easily obtained that $\Theta = I_2$. The feedback matrixes A and B are respectively given as

$$A = [\hat{a}_{ij}]_{2\times 2} = \begin{bmatrix} 1+\frac{\pi}{4} & 20 \\ 0.1 & 1+\frac{\pi}{4} \end{bmatrix},$$

$$B = [\hat{b}_{ij}]_{2\times 2} = \begin{bmatrix} -1.3\frac{\sqrt{2}}{4}\pi & 0.1 \\ 0.1 & -1.3\frac{\sqrt{2}}{4}\pi \end{bmatrix}.$$

With the above parameters, each agent has a chaotic attractor, which is shown in Fig. 5.2.

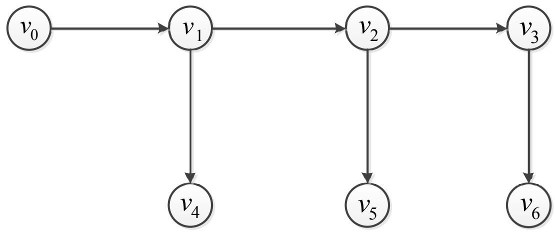

Fig. 5.1. The communication topology with one leader and six followers

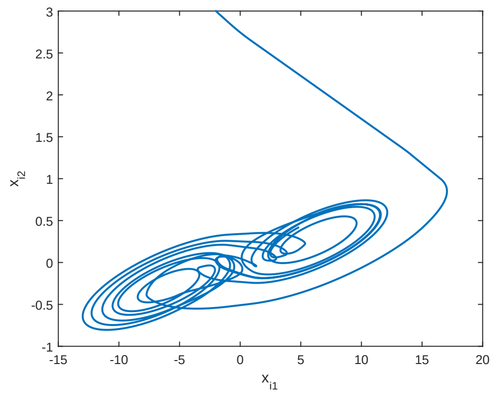

Fig. 5.2. Chaotic behavior of agent i with initial value $[-2, 3]^T$

Since the nonlinear dynamics of all the agents are homogenous, we just need identify one agent. Without loss of generality, we select agent 1 as the identified object. In order to reflect the performance of Algorithm 3 more clearly in terms of tables and figures, we randomly assume the fractional order $\alpha = 0.98$, system parameters $\hat{a}_{12} = 20, \hat{b}_{21} = 0.1$ as unknown parameters which need to be identified. Then the corresponding identified system is

$$\tilde{x}_1^{(\tilde{\alpha})}(t) = -\tilde{C}\tilde{x}_1(t) + \tilde{A}f(\tilde{x}_1(t)) + \tilde{B}f(\tilde{x}_1(t-\tau)), \tag{5.48}$$

with $\tilde{C} = I_2$, and

$$\tilde{A} = [\tilde{a}_{ij}]_{2\times 2} = \begin{bmatrix} 1+\frac{\pi}{4} & \tilde{a}_{12} \\ 0.1 & 1+\frac{\pi}{4} \end{bmatrix},$$

$$\tilde{B} = [\tilde{b}_{ij}]_{2\times 2} = \begin{bmatrix} -1.3\frac{\sqrt{2}}{4}\pi & 0.1 \\ \tilde{b}_{21} & -1.3\frac{\sqrt{2}}{4}\pi \end{bmatrix}.$$

Other definitions in (5.48) are the same as those of (5.47). The searching space Ω is set as $(\tilde{\alpha}, \tilde{a}_{12}, \tilde{b}_{21}) \in [0.01, 1] \times [19, 21] \times [0.01, 2]$. The corresponding objective

Table 5.1: Statistical results for system (5.47) over 30 independent runs without noise in Case 1

	Best	Mean	Worst
$\tilde{\alpha}$	0.98000000000000	0.980000000000000	0.980000000000000
$\lvert\frac{\tilde{\alpha}-0.98}{0.98}\rvert$	0.00E+00	0.00E+00	0.00E+00
$\tilde{a}_{12}$	20.00000000000000	20.000000000000000	19.999999999999900
$\lvert\frac{\tilde{a}_{12}-20}{20}\rvert$	0.00E+00	6.28E-16	2.84E-15
$\tilde{b}_{21}$	0.10000000000000	0.100000000000000	0.100000000000037
$\lvert\frac{\tilde{b}_{21}-0.1}{0.1}\rvert$	1.72E-14	1.36E-13	3.69E-13
F_1	1.98E-14	8.69E-14	2.54E-13

function is

$$F_1(\tilde{\alpha}, \tilde{a}_{12}, \tilde{b}_{21}) = \sum_{k=0}^{K} \|x_{1k} - \tilde{x}_{1k}\|. \tag{5.49}$$

Thus, the parameter identification problem of systems (5.47) can be converted into a functional optimization problem where the objective function is (5.49). Obviously, the smaller the objective function value F_1 is, the better combination of parameters $(\tilde{\alpha}, \tilde{a}_{12}, \tilde{b}_{21})$ is.

The Algorithm 3 is operated with 30 independent runs. Firstly, the statistical results in terms of the best, the mean and the worst identified parameters obtained by DE algorithm are given in Table 5.1. Table 5.1 demonstrates that the unknown fractional order and system parameters of system (5.47) can be well identified by Algorithm 3, even though the worst identified values can also have a high accuracy. Secondly, Figs. 5.3 and 5.4 show the convergence processes in terms of identified parameters, their relative errors values and the objective function values in a single run, which further verifies the effectiveness of the proposed DE-based parameter identification method.

- **Case 2:** $\alpha = 0.6$

To test the performance of the DE algorithm in identifying different fractional derivative order, in this case the real fractional order α in system (5.47) is assumed as 0.6, which needs to be identified. The other experimental setup is the same with that in Case 1.

Similarly, 30 independent runs are executed. The statistical results in terms of

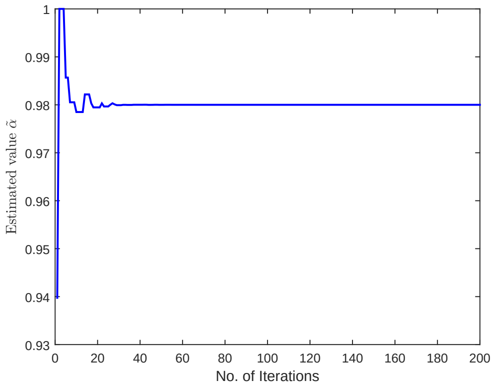

(a) Identified parameter value α

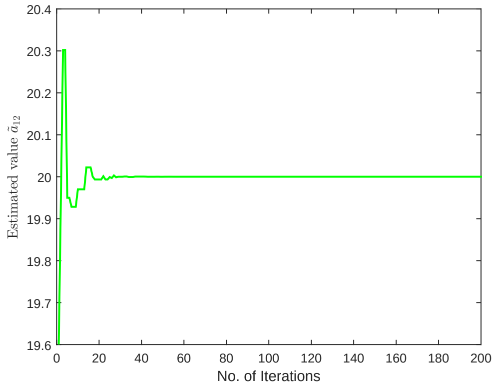

(b) Identified parameter value a_{12}

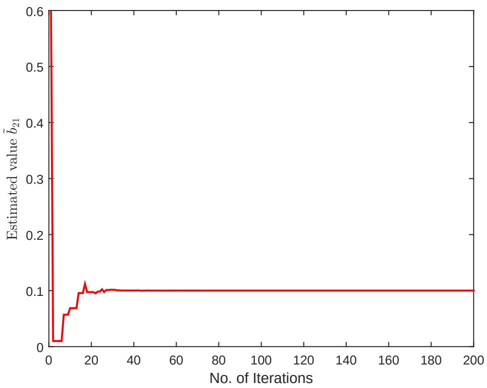

(c) Identified parameter value b_{21}

Fig. 5.3. Evolutionary curve of the identified parameters values with DE on system (5.47) in a single run without noise in Case 1

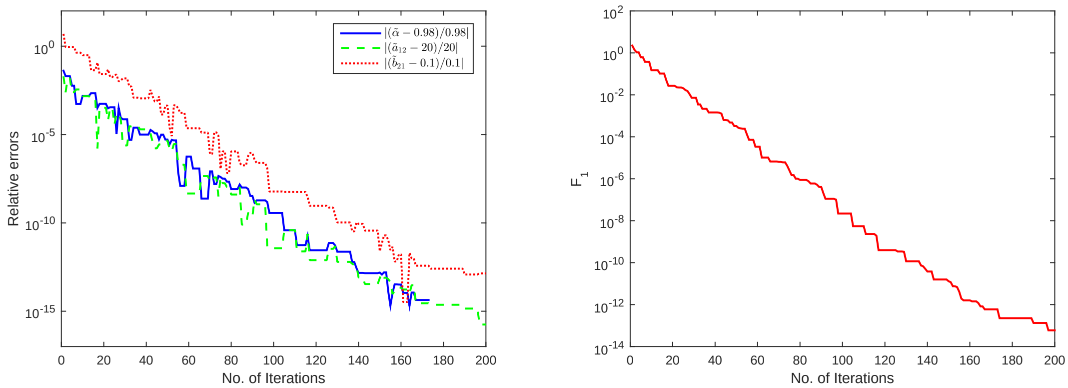

(a) Relative error values **(b)** Objective function values

Fig. 5.4. Evolutionary curve in terms of the relative errors and objective function values with DE on system (5.47) in a single run without noise in Case 1.

Table 5.2: Statistical results for system (5.47) over 30 independent runs without noise in Case 2

	Best	Mean	Worst
$\tilde{\alpha}$	0.600000000000000	0.600000000000005	0.600000000000011
$\lvert\frac{\tilde{\alpha}-0.6}{0.6}\rvert$	0.00E+00	8.70E-15	1.91E-14
$\tilde{a}_{11}$	20.000000000000000	20.000000000000300	20.000000000000500
$\lvert\frac{\tilde{a}_{11}-20}{20}\rvert$	1.07E-15	1.24E-14	2.65E-14
$\tilde{b}_{22}$	0.100000000000004	0.100000000000003	0.100000000000084
$\lvert\frac{\tilde{b}_{22}-0.1}{0.1}\rvert$	3.84E-14	2.72E-14	8.36E-13
F_1	1.57E-13	6.56E-13	7.87E-13

the best, the mean and the worst identified parameters obtained by DE algorithm are showed in Table 4.2, which demonstrates that the unknown parameters of system (5.47) can be well identified by DE algorithm. Figs. 5.5 and 5.6 display the convergence profile of the evolutionary processes in terms of identified values, the corresponding relative error values and the fitness values in a single run, which further illustrate the effectiveness of the proposed DE algorithm-based parameter identification method.

5.5.1.2 Parameter identification with noise

In real situations, the measured real data usually contains certain noise. Thus, in this subsection, we add the additive white Gaussian noise ($AWGN$) to orbits in

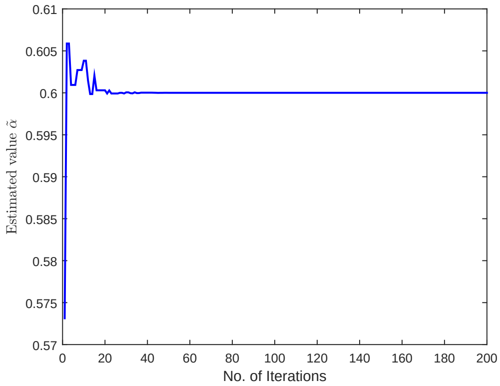

(a) Identified parameter value α

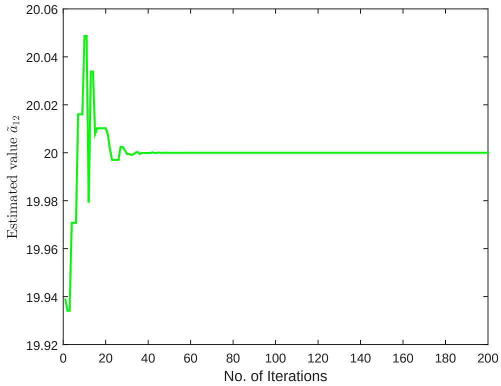

(b) Identified parameter value a_{12}

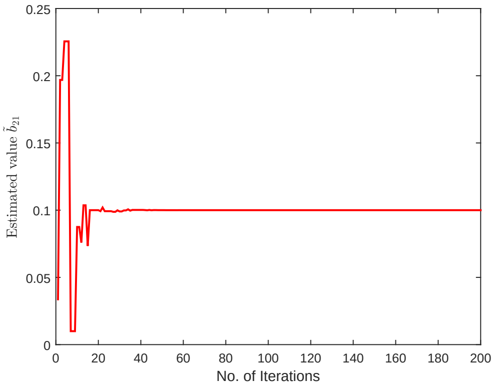

(c) Identified parameter value b_{21}

Fig. 5.5. Evolutionary curve of the identified parameters values with DE on system (5.47) in a single run without noise in Case 2

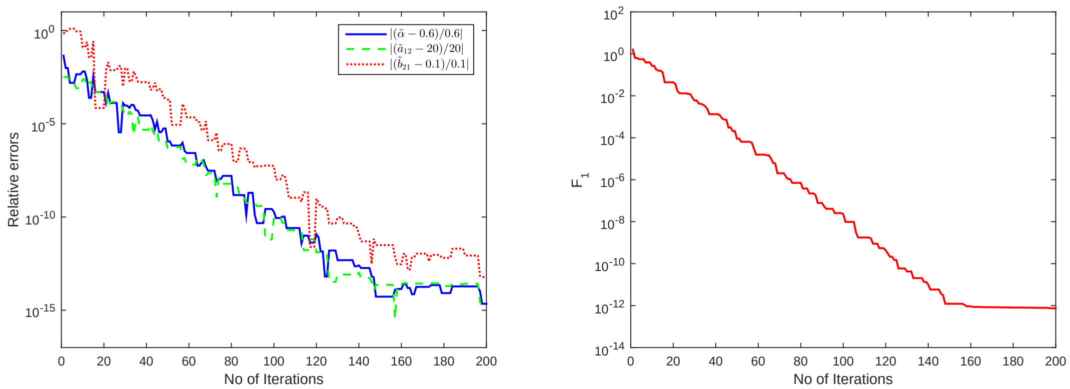

(a) Relative error values

(b) Objective function values

Fig. 5.6. Evolutionary curve in terms of the relative errors and objective function values with DE on system (5.47) in a single run without noise in Case 2.

the original system (5.47) and the identified system (5.48). Besides, the signal-to-noise ratio (SNR) probably the most common and well understood performance measure used in science and engineering that compares the level of a desired signal to the level of background noise. It is a term for the power ratio between a signal and the background noise: $SNR = P_s/P_n$, where P_s is the average signal power and P_n is average noise power (Yuan & Yang, 2019). Here the SNR is set as 50.

- **Case 1:** $\alpha = 0.98$

The other experimental setup is the same with the Case 1 in Subsection 5.5.1.1. The Algorithm 3 is executed with 30 independent runs. Firstly, the statistical results in terms of the best, the mean and the worst identified parameters obtained by DE algorithm are given in Table 5.3, which illustrates that the unknown fractional order and system parameters of system (5.47) can still be well identified by Algorithm 3 under the measurement noise. Secondly, Fig. 5.7 shows the convergence processes of the identified values in a single run, which further verifies the effectiveness of the proposed DE-based parameter identification method.

- **Case 2:** $\alpha = 0.6$

To test the performance of the DE algorithm in identifying different fractional derivative order, in this case the real fractional order α in system (5.47) is assumed as 0.6, which needs to be identified. The other experimental setup is the same with the Case 1 in Subsection 5.5.1.1. 30 independent runs are executed.

Table 5.3: Statistical results for system (5.47) over 30 independent runs with noise in Case 1

	Best	Mean	Worst
$\tilde{\alpha}$	0.980000946887114	0.980094598025661	0.980236062265603
$\lvert\frac{\tilde{\alpha}-0.98}{0.98}\rvert$	9.66E-07	9.65E-05	2.41E-04
$\tilde{a}_{12}$	20.000337557599700	20.001390039300400	20.002943132678700
$\lvert\frac{\tilde{a}_{12}-20}{20}\rvert$	1.69E-05	6.95E-05	1.47E-04
$\tilde{b}_{21}$	0.100171306525072	0.100425767521111	0.098146838686302
$\lvert\frac{\tilde{b}_{21}-0.1}{0.1}\rvert$	1.71E-03	4.26E-03	1.85E-02
F_1	4.04E-02	4.22E-02	4.31E-02

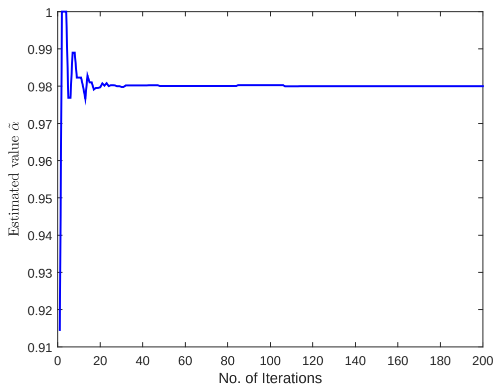

(a) Identified parameter value $\tilde{\alpha}$

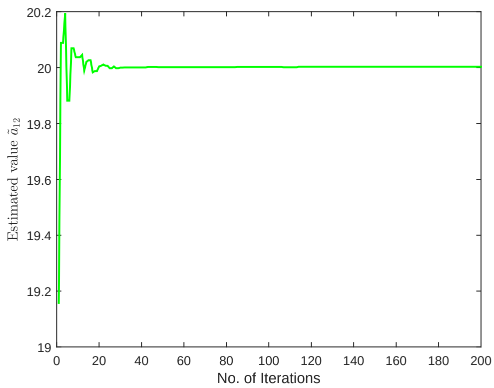

(b) Identified parameter value $\tilde{a}_{12}$

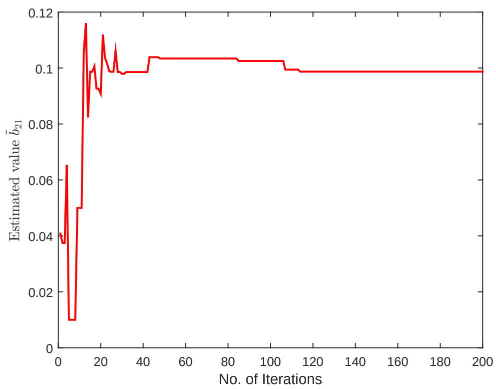

(c) Identified parameter value $\tilde{b}_{21}$

Fig. 5.7. Evolutionary curve of the identified parameters values with DE on system (5.47) in a single run with noise in Case 1.

Table 5.4: Statistical results for system (5.47) over 30 independent runs with noise in Case 2

	Best	Mean	Worst
$\tilde{\alpha}$	0.600005935258439	0.599872950311652	0.599724951293683
$\lvert\frac{\tilde{\alpha}-0.6}{0.6}\rvert$	9.89E-06	2.12E-04	4.58E-04
$\tilde{a}_{12}$	20.000028486039900	19.999571285840600	19.997228191011500
$\lvert\frac{\tilde{a}_{12}-20}{20}\rvert$	1.42E-06	2.14E-05	1.39E-04
$\tilde{b}_{21}$	0.100250428262669	0.100707665018889	0.103818248094096
$\lvert\frac{\tilde{b}_{21}-0.1}{0.1}\rvert$	2.50E-03	7.08E-03	3.82E-02
F_1	3.97E-02	4.07E-02	4.17E-02

The statistical results in terms of the best, the mean and the worst identified parameters obtained by DE algorithm are showed in Table 5.4, which demonstrates that the unknown parameters of system (5.47) can be well identified by DE algorithm under the measurement noise. Secondly, Fig. 5.8 shows the convergence processes of the identified values in a single run, which further verifies the effectiveness of the proposed DE-based parameter identification method.

5.5.2 Simulation results on distributed cooperative synchronization

In this subsection, we will achieve the distributed consensus tracking based on the identified parameters. We assume that the real FOMASs are modeled as Case 1. Based on the identified values obtained by Algorithm 3, which are given in Subsection 5.5.1, the identified parameters values are approximated as: $\bar{\alpha} = 0.98$, $\bar{a}_{12} = 20$, and $\bar{b}_{21} = 0.1$, thus the dynamics of FOMASs can be reformulated as

$$\begin{aligned} x_i^{(\bar{\alpha})}(t) = -\bar{C}x_i(t) + \bar{A}f(x_i(t)) + \bar{B}f(x_i(t-\tau)) + u_i(t), \\ i = 0, 1, \cdots, 6, \end{aligned} \tag{5.50}$$

where $\bar{\alpha} = 0.98, \bar{C} = I_2$,

$$\bar{A} = [\bar{a}_{ij}]_{2\times 2} = \begin{bmatrix} 1+\frac{\pi}{4} & 20 \\ 0.1 & 1+\frac{\pi}{4} \end{bmatrix}, \quad \bar{B} = [\bar{b}_{ij}]_{2\times 2} = \begin{bmatrix} -1.3\frac{\sqrt{2}}{4}\pi & 0.1 \\ 0.1 & -1.3\frac{\sqrt{2}}{4}\pi \end{bmatrix}.$$

Other definitions in (5.50) are the same as those of (5.47).

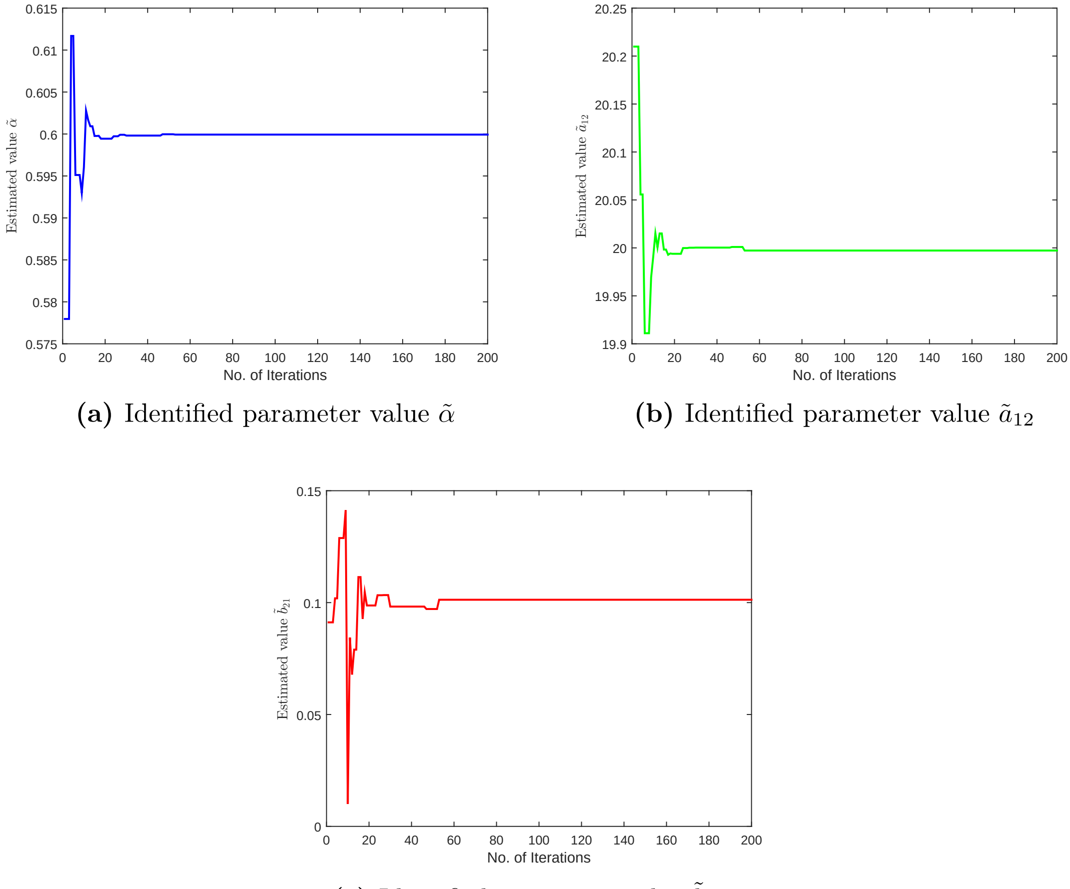

(a) Identified parameter value $\tilde{\alpha}$

(b) Identified parameter value $\tilde{a}_{12}$

(c) Identified parameter value $\tilde{b}_{21}$

Fig. 5.8. Evolutionary curve of the identified parameters values with DE on system (5.47) in a single run with noise in Case 2.

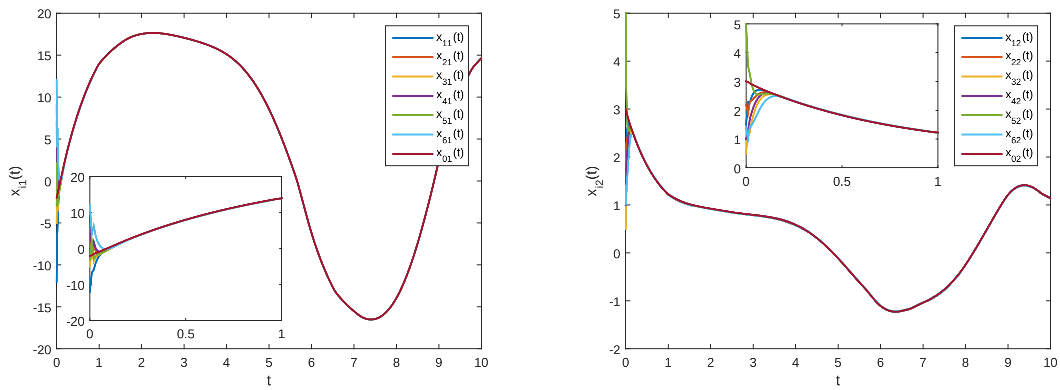

(a) State trajectories of $x_{i1}(i = 0, 1, \cdots, 6)$ **(b)** State trajectories of $x_{i2}(i = 0, 1, \cdots, 6)$

Fig. 5.9. State trajectories of FOMASs (5.50) by control protocol (5.7)

The initial conditions are selected as $x_0 = [-2, 3]^T$, $x_1 = [-12, 1.5]^T, x_2 = [7, 2.2]^T, x_3 = [-5, 0.5]^T$, $x_4 = [9, 1]^T, x_5 = [-3, 5]^T, x_6 = [12, 1.4]^T$. The leader's control input is given as: $u_0(t) = [0.3\cos(t),\ 0.4\sin(t-1)]^T$. The heterogenous control gains are set as $\Lambda = diag\{1.10, 0.95, 1.05, 0.90, 1.10, 1.00\}$. Based on Theorems 5.6 and 5.7, we choose $a = 42, \beta = 1, \lambda = 1.6, \delta = 1.58$, then the LMIs (5.9) and (5.10) hold.

Firstly, the state trajectories of distributed cooperative synchronization by nonlinear discontinuous control protocol (5.7) are displayed in Fig. 5.9, which shows that the six followers can track the leader's states quickly which can verify Theorem 5.6. The corresponding control inputs are also given in Fig. 5.10.

Then, for boundary layers widths d_i in Eq. (5.27), in order to study the influence of the parameters d_i, two cases are considered as: $d_i = 2, (i = 1, 2, \cdots, 6)$ and $d_i = 0.2, (i = 1, 2, \cdots, 6)$. The evolutionary trajectories of distributed cooperative synchronization by nonlinear continuous control protocol (5.26) are given in Figs. 5.11 and 5.13. From Figs. 5.11 and 5.13, it can be found that the synchronization errors will be smaller if the value of the boundary layers widths d_i are smaller. Furthermore, the chattering behavior can be avoided which can be verified in Figs. 5.12 and 5.14. Therefore, Theorem 5.7 is validated.

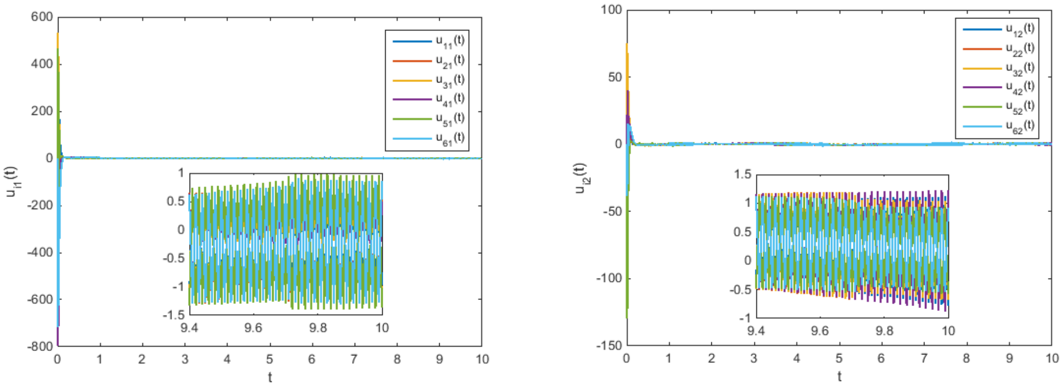

(a) Control inputs of $u_{i1}(i = 1, \cdots, 6)$ **(b)** Control inputs of $u_{i2}(i = 1, \cdots, 6)$

Fig. 5.10. Control inputs for control protocol (5.7)

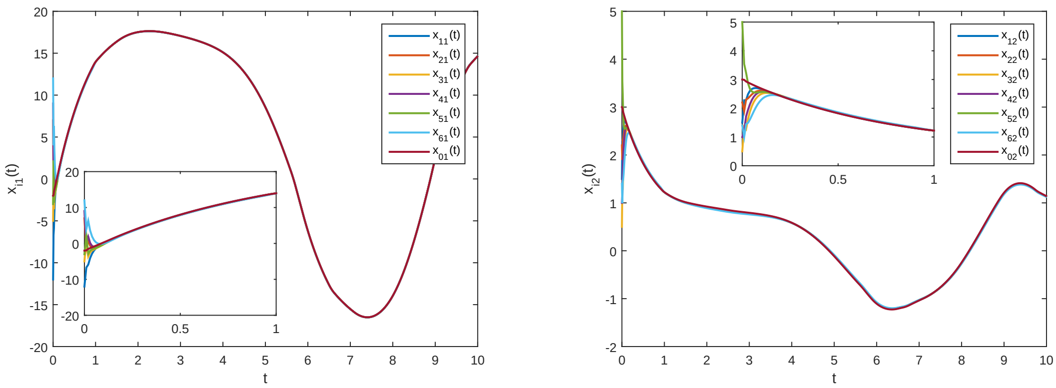

(a) State trajectories of $x_{i1}(i = 0, 1, \cdots, 6)$ **(b)** State trajectories of $x_{i2}(i = 0, 1, \cdots, 6)$

Fig. 5.11. State trajectories of FOMAS (5.50) by control protocol (5.26) with $d_i = 2(i = 1, 2, \cdots, 6)$

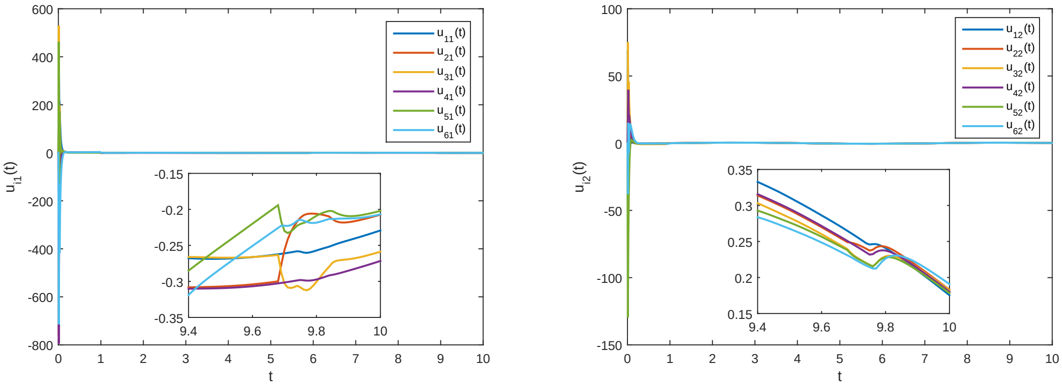

(a) Control inputs of $u_{i1}(i = 1, \cdots, 6)$ **(b)** Control inputs of $u_{i2}(i = 1, \cdots, 6)$

Fig. 5.12. Control inputs for control protocol (5.26) with $d_i = 2(i = 1, 2, \cdots, 6)$

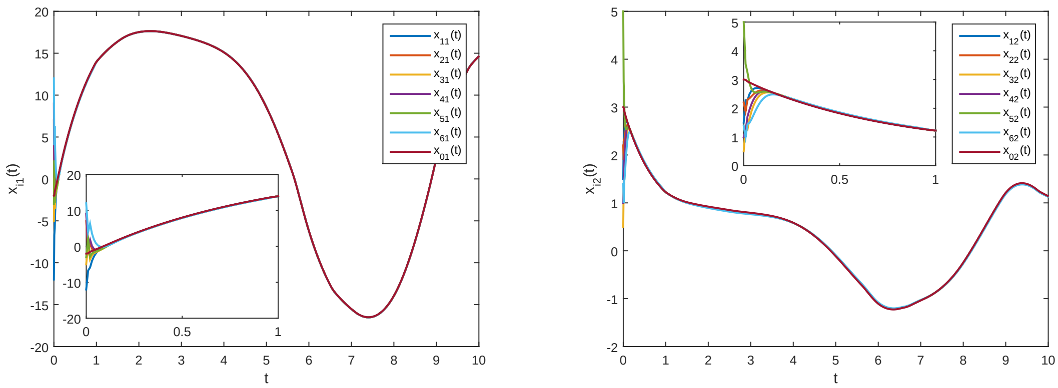

(a) State trajectories of $x_{i1}(i = 0, 1, \cdots, 6)$ **(b)** State trajectories of $x_{i2}(i = 0, 1, \cdots, 6)$

Fig. 5.13. State trajectories of FOMAS (5.50) by control protocol (5.26) with $d_i = 0.2(i = 1, 2, \cdots, 6)$

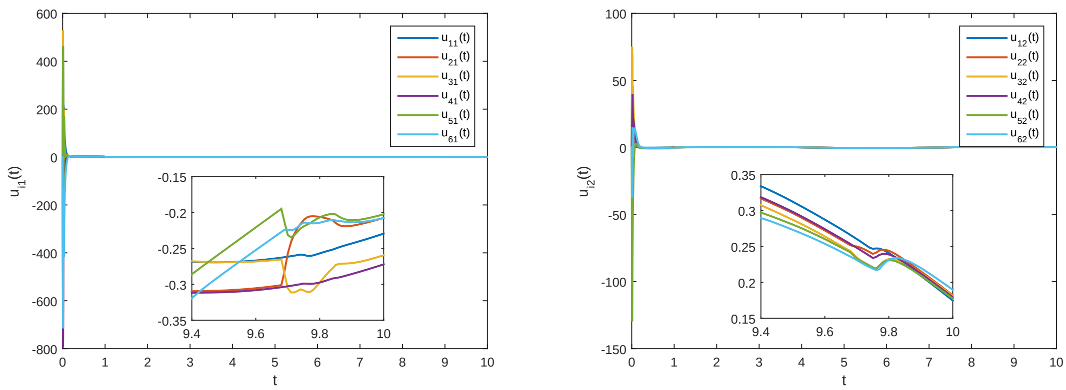

(a) Control inputs of $u_{i1}(i = 1, \cdots, 6)$ (b) Control inputs of $u_{i2}(i = 1, \cdots, 6)$

Fig. 5.14. Control inputs for control protocol (5.26) with $d_i = 0.2(i = 1, 2, \cdots, 6)$

5.6 Conclusion

In this chapter, the distributed cooperative synchronization of uncertain nonlinear delayed FOMASs with unknown leader and heterogeneous control gains is investigated. Firstly, a DE-based parameter identification method is proposed to identify the unknown nonlinear delayed FOMASs by transforming it into a functional optimization problem. Secondly, under the identified parameters, a discontinuous control protocol is designed to solve the distributed cooperative synchronization by employing the inequalities of the fractional derivative and the comparison principle of the linear fractional equation with delay, and a new sufficient conditions is obtained. Thirdly, for the purpose of eliminating the chattering behavior originated from the discontinuous control protocol, a continuous control protocol is further proposed, and the UUB synchronization errors can be obtained which can be adjusted small enough by choosing proper parameters. Finally, simulations are given to demonstrate the efficiencies of the proposed parameter identification scheme and the two control protocols.

Chapter 6

Parameter identification of unknown nonlinear FOMASs by a modified artificial bee colony algorithm

Contents

6.1 Introduction

As mentioned in Chapters 4 and 5, most consensus control algorithms are valid only for the FOMASs whose system parameters and fractional orders are known in advance. However, in practice, the FOMASs are usually partly known. That is, the form of the fractional-order differential equations are known, while some or all of the fractional orders and system parameters are unknown. Therefore, in order to control and utilize the FOMASs, identifying the unknown fractional orders and system parameters are really important. In Chapter 4, an efficient artificial bee colony algorithm (ABC) is used to identify the unknown FOMASs. In Chapter 5, the differential evolution (DE) is selected to identify the unknown FOMASs. However, although the AIOAs, such as ABC and DE, have demonstrated superior features compared to other traditional methods, there is no specific algorithm that can achieve the best solution for all optimization problems. Namely, as far as most algorithms are concerned, it is difficult to simultaneously manage the tradeoff between exploration and exploitation successfully for all the optimization problems. Similarly, there are no exceptions for ABC and DE.

As introduced in Chapter 4, artificial bee colony (ABC) algorithm, which is belong to the family of the population-based AIOAs, was put forward by Karaboga motivated by the foraging behavior of honeybees (Karaboga *et al.*, 2014). Due to its nice properties, it has been widely utilised in diverse real-world optimization problems (Karaboga *et al.*, 2014) and a lot of ABC variants have been put forwards (Gao *et al.*, 2018, 2019; Ji *et al.*, 2019; Yurtkuran *et al.*, 2018). Although it was reported that ABC algorithm owns wonderful performance, the randomness of the searching equation brings about the strong exploration and weak exploitation. Thus it's necessary to find a balance between the two contradictory aspects for the original ABC algorithm.

To improve the exploitation performance of ABC algorithm, many researchers have concentrated on the study of searching strategies as they can control the balance between exploration and exploitation. Nowadays, there are two approaches mostly preferred by the researchers to improve the existing ABC algorithm, known as hybridization and modification.

The former (hybridization) is the process of mixing with other AIOAs-based methods or traditional algorithms. For instance, in Kang *et al.* (2009), a hybrid simplex ABC was proposed by combining the Nelder-Mead simplex method. In Hsieh *et al.* (2012), a new hybrid algorithm was put forward by combining the ABC with PSO. In Ozturk *et al.* (2015), a novel ABC algorithm was proposed based on genetic operator. In Kefayat *et al.* (2015), a hybrid of ant colony algorithm and ABC algorithm was proposed. In Zhou & Yao (2017), a hybrid approach combining ABC algorithm and cuckoo search algorithm was put forwards. In Jadon *et al.* (2017), a hybrid ABC algorithm with DE was designed. In Gao *et al.* (2019), parzen window method and two different neighborhood mechanisms were applied to the ABC algorithm.

The latter (modification) is the process of integrating an operator of an existing algorithm into the ABC. For example, in Zhu & Kwong (2010), a global-best guided ABC was introduced, which used the global best individual's information within the searching rule similar to PSO. In Gao *et al.* (2014), two new searching equations were presented to generate candidate solutions in the employed bees phase and onlooker bees phase in respect. In Imanian *et al.* (2014), inspired by PSO, a modified ABC algorithm is proposed by applying a new searching equation in the onlooker bees phase, which used the PSO searching strategy to guide the search for candidate solutions. In Kiran *et al.* (2015), variable search strategies were used in the proposed ABC algorithm. In Sharma *et al.* (2016), a Lévy flight inspired search strategy was proposed and integrated with ABC algorithm. In Xue *et al.* (2018), a self-adaptive ABC algorithm based on the global best candidate was proposed. However, the studies, are not restricted to the above mentioned two aspects, for an extensive literature review of the ABC, it can be referred to Karaboga *et al.* (2014).

In this chapter, to enhance the exploration and the exploitation abilities, the above mentioned two approaches (hybridization and modification) are both considered together. As a result, a modified artificial bee colony algorithm, called mABC algorithm, is put forward. Namely, in terms of modification, two new searching equations based on the chaotic map, adaptive parameter updating law and elite learning strategy are proposed respectively. In terms of hybridization, the opposite-based learning mechanism is added to be hybridized with the modified ABC algorithm. Then, the proposed mABC algorithm is applied to the parameter identification of nonlinear FOMASs.

The rest of this chapter is organised as follows. In Section 6.2, the proposed mABC algorithm is introduced. In Section 6.3, the problem formulation for parameters identification is described based on mABC algorithm. In Section 6.4, experiment results are provided. Finally, conclusions are given.

6.2 The proposed mABC algorithm

Based on the original ABC algorithm introduced in Subsection 4.3.2 in Chapter 4, in order to make well balance between exploration and exploitation abilities, in this section, the mABC algorithm is put forward. In the mABC algorithm, two novel searching equations are designed based on the chaotic map, adaptive parameter updating law and elite learning strategy. Then to further avoid premature, the opposite-based learning is utilised based on a perturbation rate.

6.2.1 Chaos map-based random parameter generator

Most of the random parameters appeared in AIOAs are generated by uniform or Gaussian distribution. Currently, due to the pseudo-randomness of the chaotic maps, the random parameters can be replaced with chaotic maps for the purpose of utilizing their nice statistical performance (Yousri *et al.*, 2019). In this chapter, the Logistic map is used, which is described as

$$z_{k+1} = az_k(1 - z_k), \quad a = 4. \tag{6.1}$$

The distributed values for 300 iterations under random initial values are displayed in Fig. 6.1.

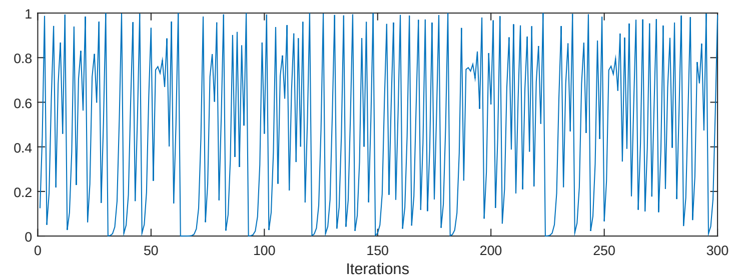

Fig. 6.1. The distributed values of the Logistic map.

6.2.2 Opposition-based generation jumping

Opposition-based learning (OBL), as a new scheme for machine intelligence, has been widely applied to AIOAs to improve their performance (Tizhoosh, 2005), the consideration of the opposite point of the current point is the core of OBL. Denote a current point as $X = (x_1, x_2, \cdots, x_D)$, where $x_j \in R$ and $x_j \in [a_j, b_j]$. The opposite point $V = (v_1, v_2, \cdots, v_D)$ is defined by $v_j = a_j + b_j - x_j$.

Different from OBL, the opposition-based generation jumping (OGJ) generates the opposite point dynamically along with searching process. The opposite value of each variable will be generated as

$$ox_{i,j} = x^P_{min}(j) + x^P_{max}(j) - x_{i,j}, \tag{6.2}$$

where $x^P_{min}(j)$ and $x^P_{max}(j)$ are the minimum and maximum values of the jth variable in the current population P respectively.

6.2.3 Two new searching equations

New searching equation for employed bees: Inspired by the mutation operator of DE, a modified searching equation is proposed as

$$V_i = X_{r1} + ch(X_{r2} - X_{r3}), \tag{6.3}$$

where $r1, r2, r3$ ($r1 \neq r2 \neq r3 \neq i$) are three different indexes chosen randomly from $\{1, 2, \cdots, SN/2\}$, ch is a random value generated based on Eq. (6.1).

Then the OGJ is conducted under the perturbation or jumping rate (J_r) which is described in Subsection 6.2.2. Thus, the combinatorial searching strategy in the employed bees phase can be given as

$$V_i = \begin{cases} X_{r1} + ch(X_{r2} - X_{r3}), & if \quad rand > Jr, \\ X^P_{min} + X^P_{max} - X_i, & \quad otherwise, \end{cases} \tag{6.4}$$

where $X^P_{min} = (x^P_{min}(1), x^P_{min}(2), \cdots, x^P_{min}(D))$ and $X^P_{max} = (x^P_{max}(1), x^P_{max}(2), \cdots, x^P_{max}(D))$.

New searching equation for onlooker bees: Since Eq. (6.3) pays more emphasis on the exploration, to enhance the exploitation performance, the following searching equation based on adaptive elite learning strategy is proposed as

$$V_i = X_{r1} + \eta(t)(X_{best} - X_{r2}), \tag{6.5}$$

$$\eta(t) = (\xi_{max} - \xi_{min}) \cdot \sqrt{1 - \frac{t}{T}} + \xi_{min}, \tag{6.6}$$

where X_{best} represents the best solution obtained so far, $r1$ and $r2$ denote two different indexes chosen randomly from $\{1, 2, \cdots, SN/2\}$. t and T represent the current and total iterations in respect. In Eq. (6.5), with the help of the best-so-far solution X_{best}, Eq. (6.5) focuses more on the exploitation ability, which can compensate the disadvantage of Eq. (6.3). In addition, the adaptive parameter adjusting law in Eq. (6.6) is employed. From Eq. (6.6), it can be found that at the early iteration process, the value of $\eta(t)$ is large, so the searching direction is more toward the best-so-far solution, which can enhance the searching speed. As the iteration increases, the value $\eta(t)$ decreases gradually, the influence of the best-so-far solution weakens at the same time, which can avoid premature.

Then the OGJ is also considered under the perturbation or jumping rate (J_r). The combinatorial searching strategy in the onlooker bees phase can be written as

$$V_i = \begin{cases} X_{r1} + \eta(t)(X_{best} - X_{r2}), & if \;\; rand > Jr, \\ X^P_{min} + X^P_{max} - X_i, & otherwise. \end{cases} \tag{6.7}$$

6.2.4 The proposed mABC algorithm

Under above discussion, the mABC algorithm is put forward. In mABC algorithm, two novel searching equations are put forward based on the chaotic maps, adaptive parameter adjusting law and elite learning strategy. Then the opposite-based learning is utilised based on a perturbation rate. The main process of the mABC algorithm is given as follows. After initialization, the following searching process is repeated. Firstly, the employed bees use the new combinatorial searching strategy (6.4) to produce the novel candidate solutions. Then greedy selection is employed. When all the employed bees finish the tasks, the probability $p_i (i = 1, 2, \cdots, SN/2)$ are calculated using (4.9). Then, each onlooker bee selects a food position with p_i, the new combinatorial searching strategy (6.7) is employed to produce the new candidate solutions. Then the greedy selection is conducted again. Finally, the scout process is called. Then, the algorithm goes back to the employed bee phase and repeat the loop until stop condition is met. The main flowchart of the mABC algorithm is shown in **Algorithm** 4.

6.3 The proposed mABC algorithm-based parameter identification approach

6.3.1 Problem formulation for the parameter identification

In order to identify the parameters of unknown FOMASs, consider the original systems as

$$x_i^{(\alpha)}(t) = f(x_i(t), \theta), \quad i \in \mathcal{N} \cup \{0\}, \tag{6.8}$$

where the fractional order $\alpha \in (0, 1]$, $\theta = (\theta_1, \theta_2, \cdots, \theta_m)$ are the system parameters; $x_i(t) \in R^n$ are the ith agent's state; $f(x_i(t), \theta) \in R^n$ is the intrinsic nonlinearity.

Consider the identified systems as

$$\tilde{x}_i^{(\tilde{\alpha})}(t) = f(\tilde{x}_i(t), \tilde{\theta}), \quad i \in \mathcal{N} \cup \{0\}, \tag{6.9}$$

where $\tilde{\alpha}$ is the identified fractional order, $\tilde{\theta} = (\tilde{\theta}_1, \tilde{\theta}_2, \cdots, \tilde{\theta}_m)^T$ denotes the identified system parameters, $\tilde{x}_i(t) \in R^n$ denotes the state of systems (6.9). Besides, systems (6.8) and (6.9) have the same initial conditions.

To identify FOMASs (6.8), it is converted into the following functional optimization model as

$$\begin{aligned} J_i(\tilde{\alpha}\tilde{\theta}) &= arg \min_{(\tilde{\alpha},\tilde{\theta})\in\Omega} F_i \\ &= arg \min_{(\tilde{\alpha},\tilde{\theta})\in\Omega} \sum_{k=1}^{K} \|x_{ik} - \tilde{x}_{ik}\|, \quad i \in \mathcal{N} \cup \{0\}, \end{aligned} \tag{6.10}$$

where K is the size of the sampling data. x_{ik} and $\tilde{x}_{ik}$ represent respectively the ith agent's state of systems (6.8) and (6.9) at time kh, where h is the step size (Diethelm *et al.*, 2002). Ω denotes the searching space for $\tilde{\alpha}, \tilde{A}$ and $\tilde{\theta}$. Therefore,

Algorithm 4 Framework of the mABC algorithm (Hu *et al.*, 2019d)

Step 0) Predefine some parameters: SN (population size number), D (searching dimension), $LOWER$ (lower bound), $UPPER$ (upper bound), $limit$ (control parameter), MCN (maximum cycle number), $trail = 0$.
Step 1) The population initialization phase:
  Step 1.1) Randomly generate $0.5 * SN$ points in the search space to form an initial population via Eq. (4.7).
  Step 1.2) Evaluate the objective function values of population.
  Step 1.3) cycle=1;
Step 2) The employed bees phase:
  For $i = 1$ **to** $0.5 * SN$ **do**
    Step 2.1)
      Step 2.1.1) Generate a candidate solution V_i by **Eq. (6.4)**.
      Step 2.1.2) Evaluate $f(V_i)$.
    Step 2.2) If $f(V_i) < f(X_i)$, set $X_i = V_i$, otherwise, set $trial_i = trial_i + 1$.
  End For
Step 3) Calculating the probability values p_i by Eq. (4.9), set $t = 0, i = 1$.
Step 4) The onlooker bees phase:
  While $t \leq 0.5 *$ SN, **do**
    Step 4.1)
      If $rand(0, 1) < p_i$
        Step 4.1.1) Searching the candidate solution V_i via **Eq. (6.7)**.
        Step 4.1.4) Set $t = t + 1$.
      End If
    Step 4.2) Set $i = i + 1$, if $i = 0.5 * SN$, set $i = 1$.
  End While
Step 5) The scout bees phase:
  If $max(trial_i) > limit$, replace X_i with a new candidate solution generated via Eq. (4.7).
Step 6) Set $cycle = cycle + 1$, and **if** $cycle > MCN$, then stop and output the best solution achieved so far, otherwise, go to **Step 2**.

FOMASs (6.8) can be identified by searching suitable $\tilde{\alpha}, \tilde{A}$ and $\tilde{\theta}$ in the region Ω by minimizing function (6.10).

6.3.2 The mABC algorithm-based parameter identification approach

Using the proposed mABC algorithm introduced in Section 6.2, and the function optimization model (6.10), the following mABC algorithm-based parameter identification approach is presented as Algorithm 5.

Algorithm 5 mABC algorithm-based parameter identification scheme

1: Initialize parameters for Algorithm 4 and FOMASs (6.9)
2: Produce the initial population in the feasible region Ω defined in Subsection 6.3.1
3: **repeat**
4: Optimize the function (6.10) with employed bees based on (6.4)
5: Optimize the function (6.10) with onlooker bees based on (6.7)
6: Optimize the function (6.10) with scout bees based on (4.7)
7: **until** Maximum iteration is met
8: Return the best parameter identification values

6.4 Experimental setup and results

6.4.1 Experimental setup

To test the efficiency of the proposed scheme, the FOMASs modeled with five typical fractional-order chaotic systems are treated as the standard benchmarks which are described in (6.11)-(6.15). Nowadays, these nonlinear systems have been widely utilized as benchmarks for investigations of parameter identification with different algorithms by lots of researchers (Ahandani *et al.*, 2018; Lin & Wang, 2017; Sheng *et al.*, 2014; Wei *et al.*, 2018).

Example 6.1 *The FOMASs are modeled with fractional-order Chua's circuit as*

$$\begin{cases} x_{i1}^{(\alpha)}(t) = p_1(x_{i2}(t) - g(x_{i1}(t))), \\ x_{i2}^{(\alpha)}(t) = x_{i1}(t) - x_{i2}(t) + x_{i3}(t), \\ x_{i3}^{(\alpha)}(t) = -p_2 x_{i2}(t), \end{cases} \tag{6.11}$$

where $i = 0, 1 \cdots, N$, $g(x_{i1}(t)) = m_1 x_{i1}(t) + \frac{1}{2}(m_0 - m_1)(|x_{i1}(t)+1| - |x_{i1}(t)-1|)$, $\alpha = 0.97, p_1 = 10, p_2 = 14.7, m_0 = -0.144, m_1 = 0.256.$

Example 6.2 *The FOMASs are modeled with fractional-order Rössler system as*

$$\begin{cases} x_{i1}^{(\alpha)}(t) = -(x_{i2}(t) + x_{i3}(t)), \\ x_{i2}^{(\alpha)}(t) = x_{i1}(t) + a x_{i2}(t), \\ x_{i3}^{(\alpha)}(t) = b + x_{i3}(t)(x_{i1}(t) - c), \end{cases} \tag{6.12}$$

where $i = 0, 1 \cdots, N$, $\alpha = 0.90, a = 0.4, b = 0.2, c = 10.$

Example 6.3 *The FOMASs are modeled with fractional-order financial system as*

$$\begin{cases} x_{i1}^{(\alpha)}(t) = x_{i3}(t) + x_{i1}(t)(x_{i2}(t) - a), \\ x_{i2}^{(\alpha)}(t) = 1 - b x_{i2}(t) - x_{i1}^2(t), \\ x_{i3}^{(\alpha)}(t) = -x_{i1}(t) - c x_{i3}(t), \end{cases} \tag{6.13}$$

where $i = 0, 1 \cdots, N$, $\alpha = 0.95, a = 3, b = 0.1, c = 1.$

Example 6.4 *The FOMASs are modeled with fractional-order Lorenz system as*

$$\begin{cases} x_{i1}^{(\alpha)}(t) = a(x_{i2}(t) - x_{i1}(t)), \\ x_{i2}^{(\alpha)}(t) = c x_{i1}(t) - x_{i2}(t) - x_{i1}(t) x_{i3}(t), \\ x_{i3}^{(\alpha)}(t) = -b x_{i3}(t) + x_{i1}(t) x_{i2}(t), \end{cases} \tag{6.14}$$

where $i = 0, 1 \cdots, N$, $\alpha = 0.99, a = 10, b = 8/3, c = 28.$

Example 6.5 *The FOMASs are modeled with fractional-order neural networks as*

$$\begin{cases} x_{i1}^{(\alpha)}(t) = a_1 x_{i1}(t) + b_{11} tanh(x_{i1}(t)) + b_{12} tanh(x_{i2}(t)) + b_{13} tanh(x_{i3}(t)), \\ x_{i2}^{(\alpha)}(t) = a_2 x_{i2}(t) + b_{21} tanh(x_{i1}(t)) + b_{22} tanh(x_{i2}(t)) + b_{23} tanh(x_{i3}(t)), \\ x_{i3}^{(\alpha)}(t) = a_3 x_{i3}(t) + b_{31} tanh(x_{i1}(t)) + b_{32} tanh(x_{i2}(t)) + b_{33} tanh(x_{i3}(t)), \end{cases} \tag{6.15}$$

where $i = 0, 1 \cdots, N,\ A = diag\{a_1, a_2, a_3\} = -I_3,$

$$B = [b_{ij}]_{3\times 3} = \begin{bmatrix} 2 & -1.2 & 0 \\ 1.8 & 1.71 & 1.15 \\ -4.75 & 0 & 1.1 \end{bmatrix}.$$

In the following experiments, to show convinced results, the mABC algorithm is compared with the standard ABC and some other typical AIOAs, such as DE (Storn & Price, 1997), PSO (Eberhart & Shi, 2000) and CS (Yang & Deb, 2009). In order to execute the same function evaluation numbers, the population size are all set as $SN = 100$, To calculate the objective function, the $K = 100$ and $h = 0.01$. 30 runs are conducted for each algorithm in each example, and all runs are stopped when the predefined iteration T is met. Some other special parameters of the compared algorithms and identified FOMASs are set as Tables 6.1 and 6.2 respectively. Here, the homogeneous FOMASs are considered, therefore we just need to randomly choose one agent to identify.

Table 6.1: Parameters setting for the compared algorithms

Algorithms	Parameters
mABC	$limit = 15, \xi_{max} = 0.5, \xi_{min} = 0.005, J_r = 0.1$
ABC	$limit = 15$
DE	$F = 0.5, CR = 0.7$
PSO	$vmax = 1, vmin = -1, w = 0.7298, c1 = c2 = 1.49618$
CS	$pa = 0.25$

Table 6.2: Parameters setting for the considered FOMASs

FOMASs	Unknown parameters	Lower bound	Upper bound	Initial condition	T
System (6.11)	$(\alpha, p_1, p_2, m_0, m_1)$	(0.01,9,13,-1,0.01)	(1,11,16,0,1)	(-2,0.5,3)	150
System (6.12)	(α, a, b, c)	(0.01,0.01,0.01,9)	(1,1,1,11)	(3,2,5)	100
System (6.13)	(α, a, b, c)	(0.01,2,0.01,0.5)	(1,4,1,1.5)	(2,3,2)	100
System (6.14)	(α, a, b, c)	(0.01,9,2,27)	(1,11,4,29)	(12,-5,-13)	100
System (6.15)	$(\alpha, b_{11}, b_{22}, b_{33})$	(0.01,1,1,0.5)	(1,3,3,2)	(1,2,0.5)	100

6.4.2 Parameter identification results

To illustrate the superiority of the proposed mABC algorithm, firstly the mean value of the identified parameters with 30 times and the corresponding relative errors are given, and the mean objective function values and the standard derivation are also provided, which can be found in Tables 6.3-6.7. Tables 6.3-6.7 show the identified parameter values obtained by the proposed mABC algorithm are more accurate, the relative errors obtained with mABC algorithm are much smaller than those obtained by other algorithms, and the standard derivation of the mABC algorithm is much smaller than others, which shows that the mABC algorithm is more robust than others. Secondly, Fig. 6.2 displays the evolutionary curves of the objective function values in a single run, which further shows that the searching speed of the mABC algorithm is faster than others.

Besides, the box plots of the experimental results in terms of the best objective function values in 30 runs are given in Fig. 6.3. In Fig. 6.3, the box plots, which are also called as box and whisker plots, display five-number summary of a set of data. The five-number summary includes the minimum, first quartile, median, third quartile, and maximum. In a box plot, a box is drawn from the first quartile to the third quartile. A vertical line goes through the box at the median. The whiskers go from each quartile to the minimum or maximum. In fact, the five-number summary divides the data into sections that each contain approximately 25% of the data in that set. Besides, the box plot can display the outliers and what their values are, which are marked with +. It can also reflect if the data is symmetrical, how tightly the data is grouped, and if and how the data is skewed. Therefore, based on the characteristics of Fig. 6.3, it can be found that the performance of the mABC algorithm are the best among all the compared algorithms for all the systems.

Table 6.3: Statistical results in terms of mean values for parameter identification of FOMASs (6.11)

	mABC	ABC	DE	PSO	CS
α	0.969999999963962	0.969108668929158	0.970011498248518	0.971399332871050	0.970859819985801
$\lvert\frac{\alpha-0.97}{0.97}\rvert$	**3.72E-11**	9.19E-04	1.19E-05	1.44E-03	8.86E-04
p_1	9.999999999601490	9.979946641501790	9.999507186165270	9.867773856560690	9.969646494300770
$\lvert\frac{p_1-10}{10}\rvert$	**3.99E-11**	2.01E-03	4.93E-05	1.32E-02	3.04E-03
p_2	14.699999999162200	14.672235192216800	14.699954465408900	14.535336437671600	14.673050072167500
$\lvert\frac{p_2-14.7}{14.7}\rvert$	**5.70E-11**	1.89E-03	3.10E-06	1.12E-02	1.83E-03
m_0	-0.144000000236786	-0.141631851239487	-0.144028449128557	-0.097038353733713	-0.154428547836811
$\lvert\frac{m_0-(-0.144)}{-0.144}\rvert$	**1.64E-09**	1.64E-02	1.98E-04	3.26E-01	7.24E-02
m_1	0.256000000745335	0.256293252258667	0.256197124637012	0.152550078593795	0.296178225732747
$\lvert\frac{m_1-0.256}{0.256}\rvert$	**2.91E-09**	1.15E-03	7.70E-04	4.04E-01	1.57E-01
J_1	**1.29E-09**	2.11E-01	2.75E-03	4.97E-01	1.69E-01
Std	**7.04E-09**	6.02E-02	9.06E-04	4.48E-01	4.00E-02

Table 6.4: Statistical results in terms of mean values for parameter identification of FOMASs (6.12)

	mABC	ABC	DE	PSO	CS
α	0.900000000000007	0.900000934702510	0.899999992812217	0.900476029743134	0.899325519605760
$\lvert\frac{\alpha-0.9}{0.9}\rvert$	**7.52E-15**	1.04E-06	7.99E-09	5.29E-04	7.49E-04
a	0.399999999999985	0.399998667169488	0.399999978894998	0.400022388034355	0.399631561857637
$\lvert\frac{a-0.4}{0.4}\rvert$	**3.76E-14**	3.33E-06	5.28E-08	5.60E-05	9.21E-04
b	0.200000000000662	0.200199173089204	0.199998917658505	0.226667228634665	0.192492576454752
$\lvert\frac{b-0.2}{0.2}\rvert$	**3.31E-12**	9.96E-04	5.41E-06	1.33E-01	3.75E-02
c	10.000000000000400	10.000112683062500	10.000000357589200	10.020928948380600	10.004189705708300
$\lvert\frac{c-10}{10}\rvert$	**4.23E-14**	1.13E-05	3.58E-08	2.09E-03	4.19E-04
J_1	**6.61E-13**	0.002569746	6.60E-06	0.014593375	0.060988296
Std	**1.89E-13**	1.31E-03	3.60E-06	7.99E-02	2.47E-02

Table 6.5: Statistical results in terms of mean values for parameter identification of FOMASs (6.13)

	mABC	ABC	DE	PSO	CS
α	0.950000000000007	0.950507527589402	0.949999918469961	0.951637304166363	0.949477786745610
$\lvert\frac{\alpha-0.95}{0.95}\rvert$	**7.13E-15**	5.34E-04	8.58E-08	1.72E-03	5.50E-04
a	3.000000000000000	3.001983645276290	3.000000274350410	3.005143486624690	2.998774196816740
$\lvert\frac{a-3}{3}\rvert$	**1.48E-16**	6.61E-04	9.15E-08	1.71E-03	4.09E-04
b	0.100000000000003	0.101314738721886	0.100000162046569	0.103998985147500	0.100060538054273
$\lvert\frac{b-0.1}{0.1}\rvert$	**3.23E-14**	1.31E-02	1.62E-06	4.00E-02	6.05E-04
c	1.000000000000020	1.001421295824540	0.999999630314067	1.007189155678480	0.997241336982322
$\lvert\frac{c-1}{1}\rvert$	**1.75E-14**	1.42E-03	3.70E-07	7.19E-03	2.76E-03
J_1	**1.87E-13**	2.37E-02	3.43E-05	2.35E-02	4.59E-02
Std	**3.44E-13**	1.31E-02	1.39E-05	9.81E-02	2.16E-02

Table 6.6: Statistical results in terms of mean values for parameter identification of FOMASs (6.14)

	mABC	ABC	DE	PSO	CS
α	0.990000000000001	0.989883631443830	0.990000024541688	0.990333336667774	0.990180502717956
$\lvert\frac{\alpha-0.99}{0.99}\rvert$	**5.61E-16**	1.18E-04	2.48E-08	3.37E-04	1.82E-04
a	10.000000000000100	9.990975625810070	10.000000746310500	10.017643275039700	10.003000177964100
$\lvert\frac{a-10}{10}\rvert$	**1.24E-14**	9.02E-04	7.46E-08	1.76E-03	3.00E-04
b	2.666666666666730	2.664549397031520	2.666667555596440	2.675131218483940	2.669360589181400
$\lvert\frac{b-8/3}{8/3}\rvert$	**2.31E-14**	7.94E-04	3.33E-07	3.17E-03	1.01E-03
c	27.999999999999900	27.998858480608700	27.999999923100800	28.005999451836900	28.007120911522200
$\lvert\frac{c-28}{28}\rvert$	**4.82E-15**	4.08E-05	2.75E-09	2.14E-04	2.54E-04
J_1	**7.80E-12**	7.14E-01	2.76E-04	3.93E-01	2.62E+00
Std	**1.09E-11**	5.34E-01	1.35E-04	2.15E+00	1.07E+00

Table 6.7: Statistical results in terms of mean values for parameter identification of FOMASs (6.15)

	mABC	ABC	DE	PSO	CS
α	0.980000000000000	0.980023386901886	0.980000061882073	0.991333360939757	0.979963140355235
$\lvert\frac{\alpha-0.98}{0.98}\rvert$	**3.40E-16**	2.39E-05	6.31E-08	1.16E-02	3.76E-05
b_{11}	2.000000000000000	2.000026001223250	1.999999983660480	1.994394995097900	1.999952086912340
$\lvert\frac{b_{11}-2}{2}\rvert$	**5.55E-16**	1.30E-05	8.17E-09	2.80E-03	2.40E-05
b_{22}	1.710000000000000	1.710061372444070	1.709999966869790	1.702292760073590	1.710333544567430
$\lvert\frac{b_{22}-1.71}{1.71}\rvert$	**0.00E+00**	3.59E-05	1.94E-08	4.51E-03	1.95E-04
b_{33}	1.100000000000000	1.099763987541540	1.099999738101140	1.109231196578470	1.100505113623240
$\lvert\frac{b_{33}-1.1}{1.1}\rvert$	**8.07E-16**	2.15E-04	2.38E-07	8.39E-03	4.59E-04
J_1	**6.48E-14**	8.40E-03	9.94E-06	1.17E-01	1.49E-02
Std	**3.84E-14**	4.06E-03	3.89E-06	1.04E-01	5.62E-03

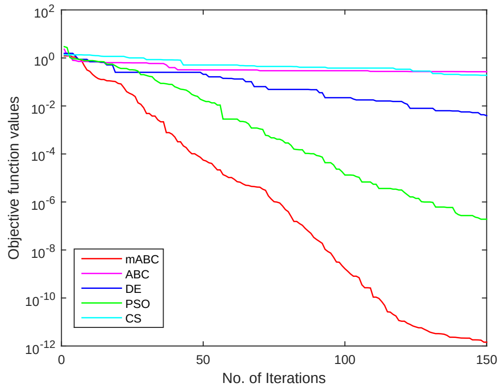

(a) FOMASs (6.11)

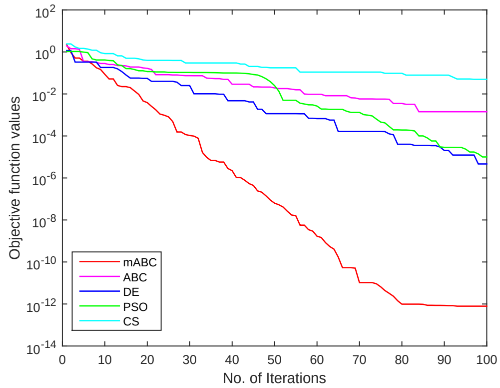

(b) FOMASs (6.12)

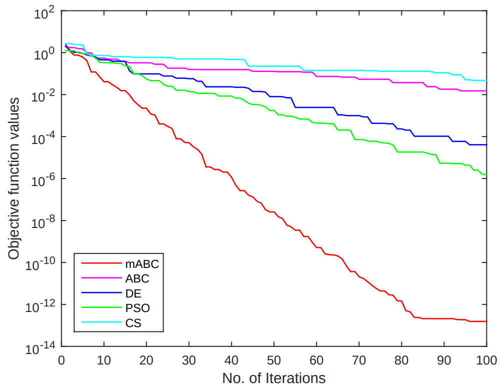

(c) FOMASs (6.13)

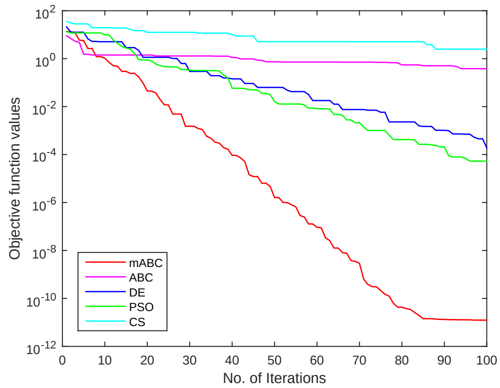

(d) FOMASs (6.14)

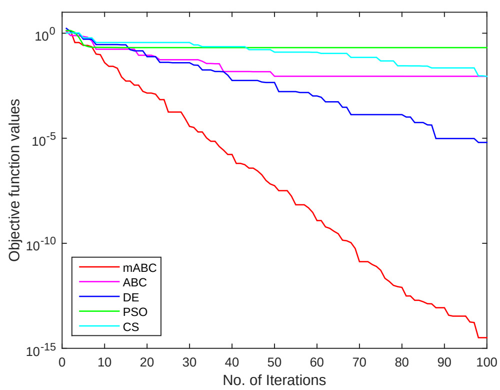

(e) FOMASs (6.15)

Fig. 6.2. Searching processes of the objective function values for different FOMASs with the compared AIOAs in a single run.

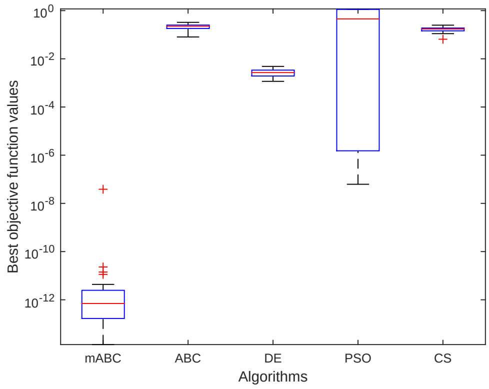

(a) FOMASs (6.11)

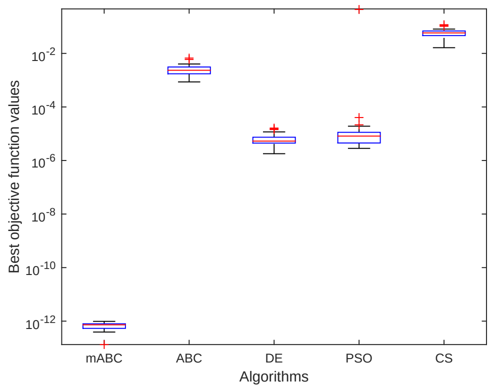

(b) FOMASs (6.12)

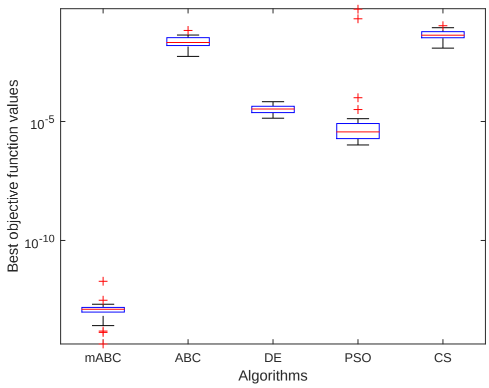

(c) FOMASs (6.13)

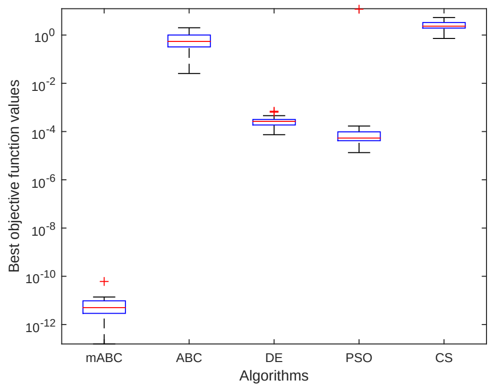

(d) FOMASs (6.14)

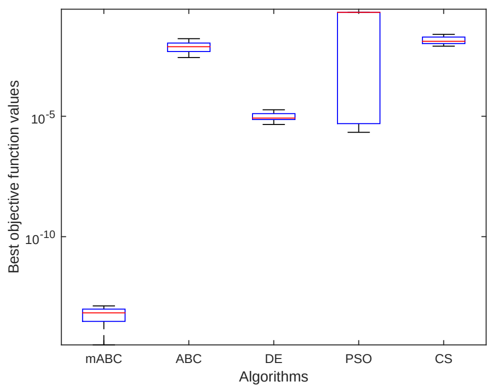

(e) FOMASs (6.15)

Fig. 6.3. Box plots of the objective function values in 30 independent runs for different FOMASs with the compared AIOAs.

To further evaluate the performance of mABC algorithm, Wilcoxon signed rank test with respect to the best objective function values in 30 runs is used between the compared algorithms as showed in Tables 6.8-6.12. In Tables 6.8-6.12, R^+ denotes the sum of ranks for runs where the right algorithm outperform the left one, R^- denotes the sum of ranks for runs where the left algorithm outperform the right one; $p-value$ reflects the significance of the results in a statistical hypothesis test, where the smaller the $p-value$, the stronger evidences against the null hypothesis. If $h = 1$, this means the null hypothesis is rejected with $100*0.05\%$ significance level, If $h = 0$, this means the null hypothesis is failed to be rejected with $100*0.05\%$ significance level. Therefore, from Tables 6.8-6.12, it can be found that the proposed mABC algorithm significantly outperforms other algorithms. Furthermore, the Friedman test is also carried out on the relative errors in Tables 6.3-6.7 among the compared algorithms. The p-value is $3.9447e-16$, which further confirms that there exists significant difference among the compared algorithms. Meanwhile, the mABC algorithm obtains the highest rank, which can be clearly seen in Fig. 6.4.

Table 6.8: Wilcoxon signed ranks test results for FOMASs (6.11)

Algorithms	R+	R-	p-value	h	Algorithms	R+	R-	p-value	h
mABC vs ABC	0	465	1.73E-06	1	DE vs PSO	55	410	2.61E-04	1
mABC vs DE	0	465	1.73E-06	1	DE vs CS	0	465	1.73E-06	1
mABC vs PSO	0	465	1.73E-06	1	PSO vs ABC	365	100	6.42E-03	1
mABC vs CS	0	465	1.73E-06	1	PSO vs CS	398	67	6.64E-04	1
DE vs ABC	0	465	1.73E-06	1	CS vs ABC	97	368	5.32E-03	1

Table 6.9: Wilcoxon signed ranks test results for FOMASs (6.12)

Algorithms	R+	R-	p-value	h	Algorithms	R+	R-	p-value	h
mABC vs ABC	0	465	1.73E-06	1	DE vs PSO	98	367	5.67E-03	1
mABC vs DE	0	465	1.73E-06	1	DE vs CS	0	465	1.73E-06	1
mABC vs PSO	0	465	1.73E-06	1	PSO vs ABC	30	435	3.11E-05	1
mABC vs CS	0	465	1.73E-06	1	PSO vs CS	30	435	3.11E-05	1
DE vs ABC	0	465	1.73E-06	1	CS vs ABC	465	0	1.73E-06	1

Table 6.10: Wilcoxon signed ranks test results for FOMASs (6.13)

Algorithms	R+	R-	p-value	h	Algorithms	R+	R-	p-value	h
mABC vs ABC	0	465	1.73E-06	1	DE vs PSO	378	87	2.77E-03	1
mABC vs DE	0	465	1.73E-06	1	DE vs CS	0	465	1.73E-06	1
mABC vs PSO	0	465	1.73E-06	1	PSO vs ABC	59	406	3.59E-04	1
mABC vs CS	0	465	1.73E-06	1	PSO vs CS	59	406	3.59E-04	1
DE vs ABC	0	465	1.73E-06	1	CS vs ABC	417	48	1.48E-04	1

Table 6.11: Wilcoxon signed ranks test results for FOMASs (6.14)

Algorithms	R+	R-	p-value	h	Algorithms	R+	R-	p-value	h
mABC vs ABC	0	465	1.73E-06	1	DE vs PSO	435	30	3.11E-05	1
mABC vs DE	0	465	1.73E-06	1	DE vs CS	0	465	1.73E-06	1
mABC vs PSO	0	465	1.73E-06	1	PSO vs ABC	30	435	3.11E-05	1
mABC vs CS	0	465	1.73E-06	1	PSO vs CS	30	435	3.11E-05	1
DE vs ABC	0	465	1.73E-06	1	CS vs ABC	459	6	3.18E-06	1

Table 6.12: Wilcoxon signed ranks test results for FOMASs (6.15)

Algorithms	R+	R-	p-value	h	Algorithms	R+	R-	p-value	h
mABC vs ABC	0	465	1.73E-06	1	DE vs PSO	72	393	9.63E-04	1
mABC vs DE	0	465	1.73E-06	1	DE vs CS	0	465	1.73E-06	1
mABC vs PSO	0	465	1.73E-06	1	PSO vs ABC	374	91	3.61E-03	1
mABC vs CS	0	465	1.73E-06	1	PSO vs CS	374	91	3.61E-03	1
DE vs ABC	0	465	1.73E-06	1	CS vs ABC	415	50	1.74E-04	1

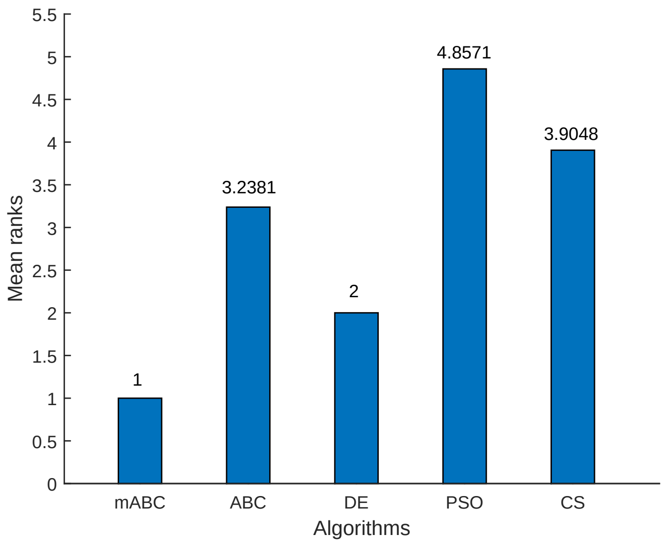

Fig. 6.4. The Friedman test among the compared algorithms

6.5 Conclusion

In this chapter, the parameter identification of unknown nonlinear FOMASs is addressed based a modified ABC algorithm. Firstly, the mABC algorithm is put forward. Then it is applied to identify the unknown parameters of the nonlinear FOMASs, where the parameter identification is converted into a functional optimization issue. Finally, experimental results demonstrate that the proposed mABC-based parameters identification approach owns higher accuracy, stronger robustness and faster searching speed than other compared algorithms.

Conclusions and Perspectives

Summary of main results

This thesis deals with the parameter identification from the viewpoint of optimization and distributed tracking control of fractional-order multi-agent systems (FOMASs) considering time delays, external disturbances, inherent nonlinearity, parameters uncertainties, and heterogeneity under fixed undirected/directed communication topology.

Firstly, in Chapter 2, over fixed directed communication topology, the leader-following consensus of heterogenous FOMASs is investigated with respect to input delays based on the frequency domain analysis approach, where the fractional orders between leader and followers are heterogenous, which is more general. The main contributions are as following: firstly, different from the leaderless consensus of FOMASs and leader-following consensus of FOMASs with homogeneous orders between leader and followers, the leader-following consensus of FOMASs with heterogenous orders between leader and followers is investigated and a novel control algorithm with a fractional-order estimator is designed. Secondly, in contrast with leaderless consensus of delayed FOMASs and leader-following consensus of FOMASs without time delays, the leader-following consensus of HFOMASs under input delays is considered based on the proposed control algorithm.

Secondly, in Chapter 3, the inherent nonlinear dynamics and external disturbances are further considered into the FOMASs, and the distributed consensus tracking is studied based on the fractional Lyapunov direct method over fixed undirected communication topology. Compared with the existing results, There are four main differences. Firstly, different from the most results studying the integer-order models, the MASs with fractional dynamics are studied. Secondly, in contrast with most results about the consensus tracking of FOMASs without considering the external disturbances, the external disturbances are considered into the FOMASs in this Chapter. Thirdly, different from most results where the style of the external disturbances are known, in this Chapter we do not known the style of the external disturbances beforehand. Fourthly, different from most results using a linear control protocol, we propose two effective nonlinear control algorithms.

Thirdly, in Chapter 4, the unknown parameters are further considered, the distributed consensus tracking of unknown nonlinear delayed FOMASs with external disturbances is addressed based on ABC algorithm, where the parameter identification problem is tackled from the viewpoint of optimization. Compared with the existing works, the contribution are as follows. Firstly, compared with most results concerning the integer-order MASs, the delayed MASs with fractional-order dynamics, external disturbances are considered. Secondly, different from the results about the time delays with linear case, the time delay under nonlinear case is further investigated. Thirdly, most results about the FOMASs only considered the external disturbances, but have not taken the time delays into account at the same time. Fourthly, most existing results are supposed that the fractional orders and system parameters of the nonlinear FOMASs are known beforehand, while in this Chapter, the parameters are considered to be unknown, and the ABC algorithm is employed to identify the unknown parameters of the unknown delayed FOMASs. Furthermore, it should be pointed out that this Chapter provides a promising link between the artificial intelligent technique and distributed cooperative control of FOMASs or other control fields.

Fourthly, the results obtained above assume that the control input of a leader is either equal to zero or available to all the followers, which has some limitations and lacks flexibility. More specifically, for the purpose of leading the followers to achieve special tasks, the leader's input need to be nonzero or time-varying. Besides, the controller gains may be heterogenous due to imperfect implementation. Thus in Chapter 5, under a fixed directed graph, the distributed cooperative synchronization of heterogenous uncertain nonlinear delayed FOMASs with a leader of bounded unknown input is further investigated based on DE algorithm. Compared with the existing works, our contribution are as follows. Firstly, compared with most results concerning the integer-order MASs, the delayed MASs with fractional-order dynamics, unknown leaders and parameters, and heterogenous control gains are involved. Secondly, different from some results studied the time delays with linear FOMASs, the time delay with nonlinear dynamics is further studied; Thirdly, different from most results without considering the leader's control input, we assume that the leader owns bounded unknown input, which could be more flexible and general in the distributed cooperative synchronization. Fourthly, different from most results, where the differential orders are assumed to be known, while in this Chapter, differential orders and system parameters are both considered to be unknown, and a DE-based parameter estimation method is proposed to identify the unknown parameters of the delayed heterogenous nonlinear FOMASs.

Fifthly, in Chapter 4, an efficient ABC algorithm is used to identify the unknown FOMASs. In Chapter 5, the DE algorithm is selected to identify the unknown FOMASs. However, although the AIOAs, such as ABC and DE, have demonstrated superior features compared to other traditional methods, there is no specific algorithm that can achieve the best solution for all optimization problems. Namely, as far as most algorithms are concerned, it is difficult to simultaneously manage the tradeoff between exploration and exploitation successfully for all the optimization problems. Similarly, there are no exceptions for ABC and DE. Therefore, in Chapter 6, to enhance the exploration and the exploitation abilities, a hybrid adaptive artificial bee colony algorithm, named as mABC, is put forward. Then, the proposed mABC algorithm is applied to the parameters identification of nonlinear FOMASs, experiment results demonstrate that the proposed mABC algorithm can identify the unknown parameters more accurately, efficiently and robustly. Compared with the existing works, our contribution are as follows. Firstly, a novel modified ABC algorithm is proposed. Secondly, a novel parameter identification scheme based on the modified ABC algorithm is put forward. Thirdly, non-parametric statistic tests are employed to demonstrate the performance of the proposed algorithm.

Future works

The following directions will be explored in the future

- This thesis mainly investigates the continuous-time fractional-order multi-agent systems (FOMASs) by using the Caputo fractional-order derivative as the initial conditions of the Caputo fractional-order differential equations are the same with those of the integer-order one, which is more reasonable in practice. To the best of authors' knowledge, for the study of the discrete-time FOMASs, few results have been reported where only the Grünwald-Letnikov fractional-order derivative has been used because of definition of fractional order derivative (Shahamatkhah & Tabatabaei, 2018; Wyrwas *et al.*, 2018). In the authors' future works, the authors will try to extend their results to the discrete-time versions.

- The proportional-integral-derivative (PID) controller is perhaps the most widely used controller in the world, it is easy to design and implement and has been applied well in most control systems. While control theory has been developed significantly, the PID controllers are used in a wide range of process control, motor drives, magnetic and optic memories, automotive control, flight control, instrumentation, and so on. In industrial applications, more than 90% of all control loops are PID type. Besides, Podlubny proposed a generalization of the PID controller, namely the fractional-order PID controller (FOPID or $\mathrm{PI}^{\lambda}\mathrm{D}^{\delta}$), where λ and δ are integers. However, it is difficult and complicated to design the FOPID controller by analytical method because of using fraction calculus. In the future, we plan to use the AIOAs for tuning of FOPID controller in the distributed coordination of FOMASs.

- As we have mentioned before, there is no specific AIOAs that can achieve the best solution for all optimization problems. Therefore, we will continue to improve the existing AIOAs to manage the tradeoff between exploration and exploitation.

- Note that most existing results are focus on the fixed communication topology, constant time delays. In the future, we will try to extend our results to switched communication topology, and time-varying time delays.

- Our obtained results mainly focus on the the theoretical aspects. Only the numerical simulations have been conducted to test the effectiveness of our results. In the future, we plan to verify our results using a practical experimental platform.

Bibliography

Ahandani, M.A., Ghiasi, A.R. & Kharrati, H. (2018). Parameter identification of chaotic systems using a shuffled backtracking search optimization algorithm. *Soft Computing*, **22**, 8317–8339. 114, 151

Andersson, M. & Wallander, J. (2004). Kin selection and reciprocity in flight formation? *Behavioral Ecology*, **15**, 158–162. 12

Bai, J. & Yu, Y. (2018). Neural Networks Based Adaptive Consensus for a Class of Fractional-Order Uncertain Nonlinear Multiagent Systems. *Complexity*, **2018**. 9

Bai, J., Wen, G., Rahmani, A. & Yu, Y. (2015a). Distributed formation control of fractional-order multi-agent systems with absolute damping and communication delay. *International Journal of Systems Science*, **46**, 2380–2392. 18

Bai, J., Wen, G., Rahmani, A. & Yu, Y. (2015b). Formation tracking of fractional-order multi-agent systems based on error predictor. In *The 27th Chinese Control and Decision Conference (2015 CCDC)*, 279–284, IEEE. 19

Bai, J., Wen, G., Rahmani, A., Chu, X. & Yu, Y. (2016). Consensus with a reference state for fractional-order multi-agent systems. *International Journal of Systems Science*, **47**, 222–234. 12

Bai, J., Wen, G., Rahmani, A. & Yu, Y. (2017a). Consensus Problem with a Reference State for Fractional-Order Multi-Agent Systems. *Asian Journal of Control*, **19**, 1009–1018. 11, 12

Bai, J., Wen, G., Rahmani, A. & Yu, Y. (2017b). Distributed consensus tracking for the fractional-order multi-agent systems based on the sliding mode control method. *Neurocomputing*, **235**, 210–216. 38, 39, 58, 59

Bai, J., Wen, G., Song, Y., Rahmani, A. & Yu, Y. (2017c). Distributed formation control of fractional-order multi-agent systems with relative damping and communication delay. *International Journal of Control, Automation and Systems*, **15**, 85–94. 16, 18

Bai, J., Wen, G. & Rahmani, A. (2018). Leaderless consensus for the fractional-order nonlinear multi-agent systems under directed interaction topology. *International Journal of Systems Science*, **49**, 954–963. 11, 39

Bao, H., Park, J.H. & Cao, J. (2015). Adaptive synchronization of fractional-order memristor-based neural networks with time delay. *Nonlinear Dynamics*, **82**, 1343–1354. 83, 92, 97, 127

Bhalekar, S. & Daftardar-Gejji, V. (2011). A predictor-corrector scheme for solving nonlinear delay differential equations of fractional order. *Journal of Fractional Calculus and Applications*, **1**, 1–9. 84

Cao, J., Li, H.X. & Ho, D.W. (2005). Synchronization criteria of LurâĂŹe systems with time-delay feedback control. *Chaos, Solitons & Fractals*, **23**, 1285–1298. 29

Cao, Y. & Ren, W. (2010). Distributed formation control for fractional-order systems: Dynamic interaction and absolute/relative damping. *Systems & Control Letters*, **59**, 233–240. 4, 7, 39, 59

Cao, Y., Li, Y., Ren, W. & Chen, Y. (2010). Distributed coordination of networked fractional-order systems. *IEEE Transactions on Systems, Man, and Cybernetics, Part B (Cybernetics)*, **40**, 362–370. 18

Cao, Y., Yu, W., Ren, W. & Chen, G. (2013). An overview of recent progress in the study of distributed multi-agent coordination. *IEEE Transactions on Industrial informatics*, **9**, 427–438. 2, 3, 18

Chen, C., Wen, C., Liu, Z., Xie, K., Zhang, Y. & Chen, C.P. (2017). Adaptive consensus of nonlinear multi-agent systems with non-identical partially unknown control directions and bounded modelling errors. *IEEE Transactions on Automatic Control*, **62**, 4654–4659. 113, 114

Chen, J., Guan, Z.H., Li, T., Zhang, D.X., Ge, M.F. & Zheng, D.F. (2015a). Multiconsensus of fractional-order uncertain multi-agent systems. *Neurocomputing*, **168**, 698–705. 9, 12

Chen, J., Guan, Z.H., Yang, C., Li, T., He, D.X. & Zhang, X.H. (2016). Distributed containment control of fractional-order uncertain multi-agent systems. *Journal of the Franklin Institute*, **353**, 1672–1688. 16

Chen, J., Chen, B. & Zeng, Z. (2018a). Global Asymptotic Stability and Adaptive Ultimate Mittag-Leffler Synchronization for a Fractional-Order Complex-Valued Memristive Neural Networks With Delays. *IEEE Transactions on Systems, Man, and Cybernetics: Systems*, 1–17. 83, 127

Chen, L., Wu, R., Cao, J. & Liu, J.B. (2015b). Stability and synchronization of memristor-based fractional-order delayed neural networks. *Neural Networks*, **71**, 37–44. 28, 83, 92, 97, 127

Chen, L., Wang, Y.W., Yang, W. & Xiao, J.W. (2018b). Robust consensus of fractional-order multi-agent systems with input saturation and external disturbances. *Neurocomputing*, **303**, 11–19. 13

Chen, Y., Wen, G., Peng, Z. & Rahmani, A. (2018c). Consensus of Fractional-Order Multiagent System via Sampled-Data Event-Triggered Control. *Journal of the Franklin Institute*. 11, 114

Consolini, L., Morbidi, F., Prattichizzo, D. & Tosques, M. (2008). LeaderâĂŞfollower formation control of nonholonomic mobile robots with input constraints. *Automatica*, **44**, 1343–1349. 3

Crabtree, D.E. & Haynsworth, E.V. (1969). An identity for the Schur complement of a matrix. *Proceedings of the American Mathematical Society*, **22**, 364–366. 29

Cui, B., Zhao, C., Ma, T. & Feng, C. (2017). Leaderless and leader-following consensus of multi-agent chaotic systems with unknown time delays and switching topologies. *Nonlinear Analysis: Hybrid Systems*, **24**, 115–131. 81, 97, 114, 128

Das, S. & Suganthan, P.N. (2011). Differential evolution: a survey of the state-of-the-art. *IEEE transactions on evolutionary computation*, **15**, 4–31. 113, 116

Desoer, C. & Wang, Y.T. (1980). On the generalized Nyquist stability criterion. *IEEE Transactions on Automatic Control*, **25**, 187–196. 43, 46

Devasia, S. (2017). Iterative control for networked heterogeneous multi-agent systems with uncertainties. *IEEE Transactions on Automatic Control*, **62**, 431–437. 112

Diethelm, K., Ford, N.J. & Freed, A.D. (2002). A predictor-corrector approach for the numerical solution of fractional differential equations. *Nonlinear Dynamics*, **29**, 3–22. 149

Dimarogonas, D.V., Frazzoli, E. & Johansson, K.H. (2012). Distributed event-triggered control for multi-agent systems. *IEEE Transactions on Automatic Control*, **57**, 1291–1297. 7

Dong, T. & Wang, A. (2018). Event-Triggered Consensus of Nonlinear Multi-Agent Systems with Unknown External Disturbance. *Asian Journal of Control*, **20**, 1928–1937. 58, 59

Du, H., Li, S. & Shi, P. (2012). Robust consensus algorithm for second-order multi-agent systems with external disturbances. *International Journal of Control*, **85**, 1913–1928. 7

Du, H., He, Y. & Cheng, Y. (2014). Finite-time synchronization of a class of second-order nonlinear multi-agent systems using output feedback control. *IEEE Transactions on Circuits and Systems I: Regular Papers*, **61**, 1778–1788. 7

Duarte-Mermoud, M.A., Aguila-Camacho, N., Gallegos, J.A. & Castro-Linares, R. (2015). Using general quadratic Lyapunov functions to prove Lyapunov uniform stability for fractional order systems. *Communications in Nonlinear Science and Numerical Simulation*, **22**, 650–659. 28, 58

Eberhart, R.C. & Shi, Y. (2000). Comparing inertia weights and constriction factors in particle swarm optimization. In *Evolutionary Computation, 2000. Proceedings of the 2000 Congress on*, vol. 1, 84–88, IEEE. 153

Fan, Y., Huang, X., Wang, Z. & Li, Y. (2018). Nonlinear dynamics and chaos in a simplified memristor-based fractional-order neural network with discontinuous memductance function. *Nonlinear Dynamics*, 1–17. 83

Gao, H., Shi, Y., Pun, C.M. & Kwong, S. (2018). An Improved Artificial Bee Colony Algorithm with its Application. *IEEE Transactions on Industrial Informatics*. 144

Gao, W., Wei, Z., Luo, Y. & Cao, J. (2019). Artificial bee colony algorithm based on Parzen window method. *Applied Soft Computing*, **74**, 679–692. 144, 145

Gao, W.F., Liu, S.Y. & Huang, L.L. (2014). Enhancing artificial bee colony algorithm using more information-based search equations. *Information Sciences*, **270**, 112–133. 145

Girejko, E., Mozyrska, D. & Wyrwas, M. (2018). Behaviour of fractional discrete-time consensus models with delays for summator dynamics. *Bulletin of the Polish Academy of Sciences. Technical Sciences*, **66**. 15

Gong, P. (2016). Distributed consensus of non-linear fractional-order multi-agent systems with directed topologies. *IET Control Theory & Applications*, **10**, 2515–2525. 15

Gong, P. (2017). Distributed tracking of heterogeneous nonlinear fractional-order multi-agent systems with an unknown leader. *Journal of the Franklin Institute*, **354**, 2226–2244. 12, 16, 38, 39, 59, 112

GONG, P. & LAN, W. (2018a). Adaptive robust tracking control for multiple unknown fractional-order nonlinear systems. *IEEE transactions on cybernetics*, 1–12. 14, 113, 114

GONG, P. & LAN, W. (2018b). Adaptive robust tracking control for uncertain nonlinear fractional-order multi-agent systems with directed topologies. *Automatica*, **92**, 92–99. 14, 113, 114

GONG, Y., WEN, G., PENG, Z., HUANG, T. & CHEN, Y. (2019). Observer-based time-varying formation control of fractional-order multi-agent systems with general linear dynamics. *IEEE Transactions on Circuits and Systems–II: Express Briefs*. 19, 114

GU, Y., YU, Y. & WANG, H. (2017). Synchronization-based parameter estimation of fractional-order neural networks. *Physica A: Statistical Mechanics and its Applications*, **483**, 351–361. 19, 80, 86

GUEDES, J.J., CASTOLDI, M.F., GOEDTEL, A., AGULHARI, C.M. & SANCHES, D.S. (2018). Parameters estimation of three-phase induction motors using differential evolution. *Electric Power Systems Research*, **154**, 204–212. 20, 81

GUO, S., MO, L. & YU, Y. (2018). Mean-square consensus of heterogeneous multi-agent systems with communication noises. *Journal of the Franklin Institute*, **355**, 3717–3736. 112

HORN, R.A., HORN, R.A. & JOHNSON, C.R. (1990). *Matrix analysis*. Cambridge university press. 29

HSIEH, T.J., HSIAO, H.F. & YEH, W.C. (2012). Mining financial distress trend data using penalty guided support vector machines based on hybrid of particle swarm optimization and artificial bee colony algorithm. *Neurocomputing*, **82**, 196–206. 145

HU, W., WEN, G., RAHMANI, A., BAI, J. & YU, Y. (2019a). Leader-following consensus of heterogenous fractional-order multi-agent systems under input delays. *Asian journal of control, DOI:10.1002/asjc.2137*. 36, 40, 42, 45

Hu, W., Wen, G., Rahmani, A. & Yu, Y. (2019b). Differential evolution-based parameter estimation and synchronization of heterogeneous uncertain nonlinear delayed fractional-order multi-agent systems with unknown leader. *Nonlinear Dynamics*, **97**, 1087–1105. 36, 117, 118, 123

Hu, W., Wen, G., Rahmani, A. & Yu, Y. (2019c). Distributed consensus tracking of unknown nonlinear chaotic delayed fractional-order multi-agent systems with external disturbances based on ABC algorithm. *Communications in Nonlinear Science and Numerical Simulation*, **71**, 101–117. 36, 86, 89, 93, 114

Hu, W., Wen, G., Rahmani, A. & Yu, Y. (2019d). Parameters estimation using mABC algorithm applied to distributed tracking control of unknown nonlinear fractional-order multi-agent systems. *Communications in Nonlinear Science and Numerical Simulation*, **79**, 104933. 36, 61, 150

Hu, W., Wen, G., Rahmani, A. & Yu, Y. (2019e). Robust consensus tracking based on DE with parameters identification for uncertain nonlinear fractional-order multi-agent systems with external disturbances. In *2019 International Conference on Fractional Calculus Theory and Applications (ICFCTA 2019), 25-26 April 2019, Bourges, France*. 36, 63

Huang, X., Zhao, Z., Wang, Z. & Li, Y. (2012). Chaos and hyperchaos in fractional-order cellular neural networks. *Neurocomputing*, **94**, 13–21. 83

Hummel, D. (1995). Formation flight as an energy-saving mechanism. *Israel Journal of Zoology*, **41**, 261–278. 12

Imanian, N., Shiri, M.E. & Moradi, P. (2014). Velocity based artificial bee colony algorithm for high dimensional continuous optimization problems. *Engineering Applications of Artificial Intelligence*, **36**, 148–163. 145

Jadon, S.S., Tiwari, R., Sharma, H. & Bansal, J.C. (2017). Hybrid artificial bee colony algorithm with differential evolution. *Applied Soft Computing*, **58**, 11–24. 145

Jain, A. & Ghose, D. (2017a). Stabilization of collective formations with speed and controller gain heterogeneity and saturation. *Journal of the Franklin Institute*, **354**, 5964–5995. 112

JAIN, A. & GHOSE, D. (2017b). Synchronization of multi-agent systems with heterogeneous controllers. *Nonlinear Dynamics*, **89**, 1433–1451. 112

JI, J., SONG, S., TANG, C., GAO, S., TANG, Z. & TODO, Y. (2019). An artificial bee colony algorithm search guided by scale-free networks. *Information Sciences*, **473**, 142–165. 144

KANG, F., LI, J. & XU, Q. (2009). Structural inverse analysis by hybrid simplex artificial bee colony algorithms. *Computers & Structures*, **87**, 861–870. 145

KARABOGA, D., GORKEMLI, B., OZTURK, C. & KARABOGA, N. (2014). A comprehensive survey: artificial bee colony (ABC) algorithm and applications. *Artificial Intelligence Review*, **42**, 21–57. 20, 81, 85, 144, 145

KASLIK, E. & SIVASUNDARAM, S. (2012). Nonlinear dynamics and chaos in fractional-order neural networks. *Neural Networks*, **32**, 245–256. 83

KEFAYAT, M., ARA, A.L. & NIAKI, S.N. (2015). A hybrid of ant colony optimization and artificial bee colony algorithm for probabilistic optimal placement and sizing of distributed energy resources. *Energy Conversion and Management*, **92**, 149–161. 145

KENNEDY, J. (2010). Particle swarm optimization. *Encyclopedia of machine learning*, 760–766. 20

KHALILI, M., ZHANG, X., POLYCARPOU, M.M., PARISINI, T. & CAO, Y. (2018). Distributed adaptive fault-tolerant control of uncertain multi-agent systems. *Automatica*, **87**, 142–151. 113, 114

KIRAN, M.S., HAKLI, H., GUNDUZ, M. & UGUZ, H. (2015). Artificial bee colony algorithm with variable search strategy for continuous optimization. *Information Sciences*, **300**, 140–157. 145

KONNUR, R. (2003). Synchronization-based approach for estimating all model parameters of chaotic systems. *Physical Review E*, **67**, 027204. 19, 80

LAKSHMANAN, S., PRAKASH, M., LIM, C.P., RAKKIYAPPAN, R., BALASUBRAMANIAM, P. & NAHAVANDI, S. (2018). Synchronization of an inertial neural network with time-varying delays and its application to secure communication.

IEEE transactions on neural networks and learning systems, **29**, 195–207. 83, 92, 97

Li, H. (2012). Observer-type consensus protocol for a class of fractional-order uncertain multiagent systems. In *Abstract and Applied Analysis*, vol. 2012, Hindawi. 9

Li, P., Xu, S., Chen, W., Wei, Y. & Zhang, Z. (2018). A connectivity preserving rendezvous for unicycle agents with heterogenous input disturbances. *Journal of the Franklin Institute*, **355**, 4248–4267. 112

Li, Y., Chen, Y. & Podlubny, I. (2010a). Stability of fractional-order nonlinear dynamic systems: Lyapunov direct method and generalized MittagâĂŞLeffler stability. *Computers & Mathematics with Applications*, **59**, 1810–1821. 12, 26, 27, 58

Li, Y., Yu, W., Wen, G., Yu, X. & Yao, L. (2014). Observer design for consensus of general fractional-order multi-agent systems. In *2014 IEEE international symposium on circuits and systems (ISCAS)*, 1792–1795, IEEE. 12

Li, Z., Duan, Z., Chen, G. & Huang, L. (2010b). Consensus of multiagent systems and synchronization of complex networks: A unified viewpoint. *IEEE Transactions on Circuits and Systems I: Regular Papers*, **57**, 213–224. 81

Li, Z., Wen, G., Duan, Z. & Ren, W. (2015). Designing fully distributed consensus protocols for linear multi-agent systems with directed graphs. *IEEE Transactions on Automatic Control*, **60**, 1152–1157. 23

Lin, J. & Wang, Z.J. (2017). Parameter identification for fractional-order chaotic systems using a hybrid stochastic fractal search algorithm. *Nonlinear Dynamics*, **90**, 1243–1255. 151

Lin, J., Morse, A.S. & Anderson, B.D. (2007). The multi-agent rendezvous problem. Part 2: The asynchronous case. *SIAM Journal on Control and Optimization*, **46**, 2120–2147. 3

Lin, P. & Jia, Y. (2010). Robust HâĹđ consensus analysis of a class of second-order multi-agent systems with uncertainty. *IET control theory & applications*, **4**, 487–498. 7

Liu, H., Cheng, L., Tan, M. & Hou, Z.G. (2018a). Exponential Finite-Time Consensus of Fractional-Order Multiagent Systems. *IEEE Transactions on Systems, Man, and Cybernetics: Systems*, 1–10. 10, 39

Liu, H., Xie, G. & Gao, Y. (2019a). Consensus of fractional-order double-integrator multi-agent systems. *Neurocomputing*, **340**, 110–124. 11

Liu, H., Xie, G. & Yu, M. (2019b). Necessary and sufficient conditions for containment control of fractional-order multi-agent systems. *Neurocomputing*, **323**, 86–95. 16

Liu, J., Chen, W., Qin, K. & Li, P. (2018b). Consensus of Fractional-Order Multiagent Systems with Double Integral and Time Delay. *Mathematical Problems in Engineering*, **2018**. 8, 9

Liu, J., Chen, W., Qin, K. & Li, P. (2018c). Consensus of Multi-Integral Fractional-Order Multiagent Systems with Nonuniform Time-Delays. *Complexity*, **2018**. 8, 9

Liu, J., Qin, K., Chen, W. & Li, P. (2018d). Consensus of Delayed Fractional-Order Multiagent Systems Based on State-Derivative Feedback. *Complexity*, **2018**. 8, 9

Liu, J., Qin, K., Chen, W., Li, P. & Shi, M. (2018e). Consensus of fractional-order multiagent systems with nonuniform time delays. *Mathematical Problems in Engineering*, **2018**. 8, 9

Liu, J., Qin, K., Li, P. & Chen, W. (2018f). Distributed consensus control for double-integrator fractional-order multi-agent systems with nonuniform time-delays. *Neurocomputing*, **321**, 369–380. 8, 9

Liu, J., Li, P., Chen, W., Qin, K. & Qi, L. (2019c). Distributed formation control of fractional-order multi-agent systems with relative damping and nonuniform time-delays. *ISA Transactions*. 19

Liu, J., Li, P., Qi, L., Chen, W. & Qin, K. (2019d). Distributed formation control of double-integrator fractional-order multi-agent systems with relative damping and nonuniform time-delays. *Journal of the Franklin Institute*, **356**, 5122–5150. 19

LIU, P., ZENG, Z. & WANG, J. (2018g). Global Synchronization of Coupled Fractional-Order Recurrent Neural Networks. *IEEE transactions on neural networks and learning systems*. 83

LIU, S., YANG, R., ZHOU, X.F., JIANG, W., LI, X. & ZHAO, X.W. (2019e). Stability analysis of fractional delayed equations and its applications on consensus of multi-agent systems. *Communications in Nonlinear Science and Numerical Simulation*. 8, 13

LIU, X. & XU, B. (2012). Distributed containment control of networked fractional-order systems with multiple leaders. In *Proceedings of the 10th World Congress on Intelligent Control and Automation*, 3987–3992, IEEE. 16

LIU, X., XU, B. & XIE, L. (2012). Distributed Containment Control of Networked Fractional-Order Systems with Delay-Dependent Communications. 16

LIU, X., HO, D.W., CAO, J. & XU, W. (2017a). Discontinuous observers design for finite-time consensus of multiagent systems with external disturbances. *IEEE transactions on neural networks and learning systems*, **28**, 2826–2830. 58, 59

LIU, X., ZHANG, Z. & LIU, H. (2017b). Consensus control of fractional-order systems based on delayed state fractional order derivative. *Asian Journal of Control*, **19**, 2199–2210. 7, 8, 9

LUO, D., WANG, J. & SHEN, D. (2018). Learning formation control for fractional-order multiagent systems. *Mathematical Methods in the Applied Sciences*, **41**, 5003–5014. 19

MA, T. (2015). Synchronization of multi-agent stochastic impulsive perturbed chaotic delayed neural networks with switching topology. *Neurocomputing*, **151**, 1392–1406. 81, 97

MA, T., LEWIS, F.L. & SONG, Y. (2016). Exponential synchronization of nonlinear multi-agent systems with time delays and impulsive disturbances. *International Journal of Robust and Nonlinear Control*, **26**, 1615–1631. 81, 97, 114, 128

MA, T., LI, T. & CUI, B. (2018). Coordination of fractional-order nonlinear multi-agent systems via distributed impulsive control. *International Journal of Systems Science*, **49**, 1–14. 15, 38, 39

MA, X., SUN, F., LI, H. & HE, B. (2017). The consensus region design and analysis of fractional-order multi-agent systems. *International Journal of Systems Science*, **48**, 629–636. 12

MALINOWSKA, A.B. & ODZIJEWICZ, T. (2018). Optimal control of discrete-time fractional multi-agent systems. *Journal of Computational and Applied Mathematics*, **339**, 258–274. 10

MATIGNON, D. (1996). Stability results for fractional differential equations with applications to control processing. In *Computational engineering in systems applications*, vol. 2, 963–968, IMACS, IEEE-SMC Lille, France. 12, 27

MENG, X., XIE, L. & SOH, Y.C. (2018). Event-Triggered Output Regulation of Heterogeneous Multiagent Networks. *IEEE Transactions on Automatic Control*, **63**, 4429–4434. 112

MO, L., YUAN, X. & YU, Y. (2019). Neuro-adaptive Leaderless Consensus of Fractional-order Multi-agent Systems. *Neurocomputing*. 9

NI, J., LIU, L., LIU, C. & LIU, J. (2017). Fixed-Time Leader-Following Consensus for Second-Order Multiagent Systems With Input Delay. *IEEE Transactions on Industrial Electronics*, **64**, 8635–8646. 38

OLFATI-SABER, R. (2006). Flocking for multi-agent dynamic systems: Algorithms and theory. *IEEE Transactions on automatic control*, **51**, 401–420. 3

OZTURK, C., HANCER, E. & KARABOGA, D. (2015). A novel binary artificial bee colony algorithm based on genetic operators. *Information Sciences*, **297**, 154–170. 145

PAN, H., YU, X. & GUO, L. (2018). Admissible leader-following consensus of fractional-order singular multi-agent system via observer-based protocol. *IEEE Transactions on Circuits and Systems II: Express Briefs*. 14

PANAHI, S., JAFARI, S., PHAM, V.T., KINGNI, S.T., ZAHEDI, A. & SEDIGHY, S.H. (2016). Parameter identification of a chaotic circuit with a hidden attractor using Krill herd optimization. *International Journal of Bifurcation and Chaos*, **26**, 1650221. 114

PARLITZ, U. (1996). Estimating model parameters from time series by autosynchronization. *Physical Review Letters*, **76**, 1232. 19, 80

PENG, Z., WEN, G., RAHMANI, A. & YU, Y. (2013). LeaderâĂŞfollower formation control of nonholonomic mobile robots based on a bioinspired neurodynamic based approach. *Robotics and autonomous systems*, **61**, 988–996. 3

PENG, Z., WEN, G., YANG, S. & RAHMANI, A. (2016). Distributed consensus-based formation control for nonholonomic wheeled mobile robots using adaptive neural network. *Nonlinear Dynamics*, **86**, 605–622. 3

PODLUBNY, I. (1998). *Fractional differential equations: an introduction to fractional derivatives, fractional differential equations, to methods of their solution and some of their applications*, vol. 198. Academic press. 4, 25

RAKKIYAPPAN, R., CAO, J. & VELMURUGAN, G. (2015). Existence and uniform stability analysis of fractional-order complex-valued neural networks with time delays. *IEEE Transactions on Neural Networks and Learning Systems*, **26**, 84–97. 83

REN, G. & YU, Y. (2016). Robust consensus of fractional multi-agent systems with external disturbances. *Neurocomputing*, **218**, 339–345. 9, 13, 58, 59, 82

REN, G. & YU, Y. (2017a). Consensus of Fractional Multi-Agent Systems Using Distributed Adaptive Protocols. *Asian Journal of Control*, **19**, 2076–2084. 39

REN, G. & YU, Y. (2017b). Robust consensus for fractional nonlinear multi-agent systems with external disturbances. In *Control Conference (CCC), 2017 36th Chinese*, 11401–11407, IEEE. 9, 58, 59

REN, G., YU, Y. & ZHANG, S. (2015). Leader-following consensus of fractional nonlinear multiagent systems. *Mathematical Problems in Engineering*, **2015**. 12

Ren, G., Yu, Y., Xu, C. & Hai, X. (2019). Consensus of fractional multi-agent systems by distributed event-triggered strategy. *Nonlinear Dynamics*, **95**, 541–555. 11

Ren, W. & Beard, R.W. (2008). *Distributed consensus in multi-vehicle cooperative control*. Springer, London. 23

Shahamatkhah, E. & Tabatabaei, M. (2018). Leader-following consensus of discrete-time fractional-order multi-agent systems. *Chinese Physics B*, **27**, 010701. 15, 168

Shariati, A. & Tavakoli, M. (2017). A descriptor approach to robust leader-following output consensus of uncertain multi-agent systems with delay. *IEEE Transactions on Automatic Control*, **62**, 5310–5317. 38

Sharma, H., Bansal, J.C., Arya, K.V. & Yang, X.S. (2016). LÃĺvy flight artificial bee colony algorithm. *International Journal of Systems Science*, **47**, 2652–2670. 145

Shen, J. & Cao, J. (2012). Necessary and Sufficient Conditions for Consensus of Delayed Fractional-order Systems. *Asian Journal of Control*, **14**, 1690–1697. 7, 8, 9, 38, 39, 81, 114

Shen, J., Cao, J. & Lu, J. (2012). Consensus of fractional-order systems with non-uniform input and communication delays. *Proceedings of the Institution of Mechanical Engineers, Part I: Journal of Systems and Control Engineering*, **226**, 271–283. 7, 8, 9

Shen, S., Li, W. & Zhu, W. (2017). Consensus of fractional-order multiagent systems with double integrator under switching topologies. *Discrete Dynamics in Nature and Society*, **2017**. 10

Sheng, Z., Wang, J., Zhou, S. & Zhou, B. (2014). Parameter estimation for chaotic systems using a hybrid adaptive cuckoo search with simulated annealing algorithm. *Chaos: An Interdisciplinary Journal of Nonlinear Science*, **24**, 013133. 151

Shi, M., Yu, Y. & Teng, X. (2018). Leader-following consensus of general fractional-order linear multi-agent systems via event-triggered control. *The Journal of Engineering*, **2018**, 199–202. 14

Shi, M., Qin, K., Liang, J. & Liu, J. (2019a). Distributed control of uncertain multiagent systems for tracking a leader with unknown fractional-order dynamics. *International Journal of Robust and Nonlinear Control*. 14

Shi, M., Yu, Y. & Xu, Q. (2019b). Delay-dependent consensus condition for a class of fractional-order linear multi-agent systems with input time-delay. *International Journal of Systems Science*, 1–10. 8, 9

Shi, Y. & Zhang, J. (2015). Networked convergence of fractional-order multiagent systems with a leader and delay. *Mathematical Problems in Engineering*, **2015**. 15

Simon, D. (2008). Biogeography-based optimization. *IEEE transactions on evolutionary computation*, **12**, 702–713. 20

Slotine, J.J. & Sastry, S.S. (1983). Tracking control of non-linear systems using sliding surfaces, with application to robot manipulators. *International journal of control*, **38**, 465–492. 63

Socha, K. & Dorigo, M. (2008). Ant colony optimization for continuous domains. *European journal of operational research*, **185**, 1155–1173. 20

Song, C., Cao, J. & Liu, Y. (2015). Robust consensus of fractional-order multi-agent systems with positive real uncertainty via second-order neighbors information. *Neurocomputing*, **165**, 293–299. 9, 39

Soorki, M.N. & Tavazoei, M.S. (2014). Adaptive consensus tracking for fractional-order linear time invariant swarm systems. *Journal of Computational and Nonlinear Dynamics*, **9**, 031012. 15

Soorki, M.N. & Tavazoei, M.S. (2016). Constrained swarm stabilization of fractional order linear time invariant swarm systems. *IEEE/CAA Journal of Automatica Sinica*, **3**, 320–331. 10

Soorki, M.N. & Tavazoei, M.S. (2017). Asymptotic swarm stability of fractional-order swarm systems in the presence of uniform time-delays. *International Journal of Control*, **90**, 1182–1191. 7, 8, 9

Soorki, M.N. & Tavazoei, M.S. (2018). Adaptive robust control of fractional-order swarm systems in the presence of model uncertainties and external disturbances. *IET Control Theory & Applications*, **12**, 961–969. 10

Storn, R. & Price, K. (1997). Differential evolutionâĂŞa simple and efficient heuristic for global optimization over continuous spaces. *Journal of global optimization*, **11**, 341–359. 20, 113, 116, 153

Sun, F., Zhu, W., Li, Y. & Liu, F. (2016). Finite-time consensus problem of multi-agent systems with disturbance. *Journal of the Franklin Institute*, **353**, 2576–2587. 59

Sun, W., Li, Y., Li, C. & Chen, Y. (2011). Convergence speed of a fractional order consensus algorithm over undirected scale-free networks. *Asian Journal of Control*, **13**, 936–946. 59

Tam, K.Y. (1992). Genetic algorithms, function optimization, and facility layout design. *European Journal of Operational Research*, **63**, 322–346. 20

Tian, Y.P. & Liu, C.L. (2008). Consensus of multi-agent systems with diverse input and communication delays. *IEEE Transactions on Automatic Control*, **53**, 2122–2128. 3, 7

Tizhoosh, H.R. (2005). Opposition-based learning: a new scheme for machine intelligence. In *Computational intelligence for modelling, control and automation, 2005 and international conference on intelligent agents, web technologies and internet commerce, international conference on*, vol. 1, 695–701, IEEE. 147

Vaseghi, B., Pourmina, M.A. & Mobayen, S. (2017). Secure communication in wireless sensor networks based on chaos synchronization using adaptive sliding mode control. *Nonlinear Dynamics*, **89**, 1689–1704. 92, 93, 97

Wang, A., Liao, X. & Dong, T. (2018a). Fractional-order follower observer design for tracking consensus in second-order leader multi-agent systems: Periodic sampled-based event-triggered control. *Journal of the Franklin Institute*, **355**, 4618–4628. 15

Wang, F. & Yang, Y. (2017a). Leader-following consensus of nonlinear fractional-order multi-agent systems via event-triggered control. *International Journal of Systems Science*, **48**, 571–577. 15

Wang, F. & Yang, Y. (2017b). Leader-following exponential consensus of fractional order nonlinear multi-agents system with hybrid time-varying delay: A heterogeneous impulsive method. *Physica A: Statistical Mechanics and its Applications*, **482**, 158–172. 15

Wang, H., Yu, Y., Wen, G., Zhang, S. & Yu, J. (2015). Global stability analysis of fractional-order Hopfield neural networks with time delay. *Neurocomputing*, **154**, 15–23. 28, 83

Wang, X. & Su, H. (2018). Self-Triggered Leader-Following Consensus of Multi-Agent Systems with Input Time Delay. *Neurocomputing*. 38

Wang, Y., Cao, J., Wang, H., Alsaedi, A. & Alsaadi, F.E. (2018b). Exponential Consensus for Nonlinear Multi-Agent Systems with Communication and Input Delays via Hybrid Control. *Asian Journal of Control*. 38

Wei, J. & Yu, Y. (2018). An Effective Hybrid Cuckoo Search Algorithm for Unknown Parameters and Time Delays Estimation of Chaotic Systems. *IEEE Access*, **6**, 6560–6571. 20, 81

Wei, J., Yu, Y. & Cai, D. (2018). Identification of uncertain incommensurate fractional-order chaotic systems using an improved quantum-behaved particle swarm optimization algorithm. *Journal of Computational and Nonlinear Dynamics*, **13**, 051004. 151

Wen, G., Yu, W., Zhao, Y. & Cao, J. (2013). Pinning synchronisation in fixed and switching directed networks of Lorenz-type nodes. *IET Control Theory & Applications*, **7**, 1387–1397. 114

WEN, G., ZHANG, Y., PENG, Z., YU, Y. & RAHMANI, A. (2019). Observer-based output consensus of leader-following fractional-order heterogeneous nonlinear multi-agent systems. *International Journal of Control*, 1–9. 14

WEN, Y., ZHOU, X.F., ZHANG, Z. & LIU, S. (2015). Lyapunov method for nonlinear fractional differential systems with delay. *Nonlinear dynamics*, **82**, 1015–1025. 13

WYRWAS, M., MOZYRSKA, D. & GIREJKO, E. (2018). Fractional discrete-time consensus models for single-and double-summator dynamics. *International Journal of Systems Science*, **49**, 1212–1225. 15, 168

XU, G.H., CHI, M., HE, D.X., GUAN, Z.H., ZHANG, D.X. & WU, Y. (2014). Fractional-order consensus of multi-agent systems with event-triggered control. In *11th IEEE International Conference on Control & Automation (ICCA)*, 619–624, IEEE. 11

XUE, Y., JIANG, J., ZHAO, B. & MA, T. (2018). A self-adaptive artificial bee colony algorithm based on global best for global optimization. *Soft Computing*, 1–18. 145

YANG, H., HAN, F., LIU, F., LIU, H. & ZHAO, M. (2014a). Distributed coordination of fractional dynamical systems with exogenous disturbances. *Mathematical Problems in Engineering*, **2014**. 38, 39, 58, 59, 81, 82, 114

YANG, H., WANG, F. & HAN, F. (2018). Containment control of fractional order multi-agent systems with time delays. *IEEE/CAA Journal of Automatica Sinica*, **5**, 727–732. 16

YANG, H.Y., GUO, L., XU, B. & GU, J.Z. (2013a). Collaboration control of fractional-order multiagent systems with sampling delay. *Mathematical Problems in Engineering*, **2013**. 10

YANG, H.Y., GUO, L., ZHU, X.L., CAO, K.C. & ZOU, H.L. (2013b). Consensus of compound-order multi-agent systems with communication delays. *Open Physics*, **11**, 806–812. 7, 8, 9

Yang, H.y., Zhu, X.l. & Cao, K.c. (2014b). Distributed coordination of fractional order multi-agent systems with communication delays. *Fractional Calculus and Applied Analysis*, **17**, 23–37. 7, 8, 9

Yang, H.Y., Yang, Y., Han, F., Zhao, M. & Guo, L. (2019a). Containment control of heterogeneous fractional-order multi-agent systems. *Journal of the Franklin Institute*, **356**, 752–765. 16

Yang, R., Liu, S., Tan, Y.Y., Zhang, Y.J. & Jiang, W. (2019b). Consensus analysis of fractional-order nonlinear multi-agent systems with distributed and input delays. *Neurocomputing*, **329**, 46–52. 13

Yang, S., Liao, X., Liu, Y., Chen, X. & Ge, D. (2017). Consensus of Delayed Multi-agent Systems via Intermittent Impulsive Control. *Asian Journal of Control*, **19**, 941–950. 10

Yang, X.S. & Deb, S. (2009). Cuckoo search via LÃľvy flights. In *2009 World Congress on Nature & Biologically Inspired Computing (NaBIC)*, 210–214, IEEE. 153

Yazdani, S. & Haeri, M. (2017). Robust adaptive fault-tolerant control for leader-follower flocking of uncertain multi-agent systems with actuator failure. *ISA transactions*, **71**, 227–234. 113, 114

Ye, Y. & Su, H. (2018). Leader-following consensus of general linear fractional-order multiagent systems with input delay via event-triggered control. *International Journal of Robust and Nonlinear Control*, **28**, 5717–5729. 15

Ye, Y. & Su, H. (2019). Leader-following consensus of nonlinear fractional-order multi-agent systems over directed networks. *Nonlinear Dynamics*, 1–13. 13

Ye, Y., Su, H. & Sun, Y. (2018). Event-triggered consensus tracking for fractional-order multi-agent systems with general linear models. *Neurocomputing*, **315**, 292–298. 15

Yin, X. & Hu, S. (2013). Consensus of Fractional-Order Uncertain Multi-Agent Systems Based on Output Feedback. *Asian Journal of Control*, **15**, 1538–1542. 9, 10, 12

YIN, X., YUE, D. & HU, S. (2013). Consensus of fractional-order heterogeneous multi-agent systems. *IET Control Theory & Applications*, **7**, 314–322. 39

YOUNG, K.D., UTKIN, V.I. & OZGUNER, U. (1999). A control engineer's guide to sliding mode control. *IEEE transactions on control systems technology*, **7**, 328–342. 93, 123

YOUSRI, D., ALLAM, D. & ETEIBA, M.B. (2019). Chaotic whale optimizer variants for parameters estimation of the chaotic behavior in Permanent Magnet Synchronous Motor. *Applied Soft Computing*, **74**, 479–503. 146

YU, J., DONG, X., LI, Q. & REN, Z. (2018). Time-varying formation tracking for high-order multi-agent systems with switching topologies and a leader of bounded unknown input. *Journal of the Franklin Institute*, **355**, 2808–2825. 112

YU, S. & LONG, X. (2015). Finite-time consensus for second-order multi-agent systems with disturbances by integral sliding mode. *Automatica*, **54**, 158–165. 58, 59

YU, W., LI, Y., WEN, G., YU, X. & CAO, J. (2017a). Observer design for tracking consensus in second-order multi-agent systems: Fractional order less than two. *IEEE Transactions on Automatic Control*, **62**, 894–900. 14

YU, Z., JIANG, H. & HU, C. (2015). Leader-following consensus of fractional-order multi-agent systems under fixed topology. *Neurocomputing*, **149**, 613–620. 12, 15, 37, 39

YU, Z., JIANG, H., HU, C. & YU, J. (2017b). Necessary and sufficient conditions for consensus of fractional-order multiagent systems via sampled-data control. *IEEE Transactions on Cybernetics*, **47**, 1892–1901. 11, 59, 114

YUAN, C. & HE, H. (2017). Cooperative output regulation of heterogeneous multi-agent systems with a leader of bounded inputs. *IET Control Theory & Applications*, **12**, 233–242. 112

YUAN, L. & YANG, Q. (2019). Parameter identification of fractional-order chaotic systems without or with noise: Reply to comments. *Communications in Nonlinear Science and Numerical Simulation*, **67**, 506–516. 134

YUAN, X., MO, L. & YU, Y. (2019). Observer-based quasi-containment of fractional-order multi-agent systems via event-triggered strategy. *International Journal of Systems Science*, 1–17. 16

YURTKURAN, A., YAGMAHAN, B. & EMEL, E. (2018). A novel artificial bee colony algorithm for the workforce scheduling and balancing problem in sub-assembly lines with limited buffers. *Applied Soft Computing*, **73**, 767–782. 144

ZHANG, L. & YANG, Y. (2018). Lag synchronization for fractional-order memristive neural networks with time delay via switching jumps mismatch. *Journal of the Franklin Institute*, **355**, 1217–1240. 83, 127

ZHANG, W., CAO, J., WU, R., ALSAEDI, A. & ALSAADI, F.E. (2018a). Projective synchronization of fractional-order delayed neural networks based on the comparison principle. *Advances in Difference Equations*, **2018**, 73. 92, 93, 97, 98

ZHANG, Y., WEN, G., PENG, Z., YU, Y. & RAHMANI, A. (2018b). Group multiple lags consensus of fractional-order nonlinear leader-following multi-agent systems via adaptive control. *Transactions of the Institute of Measurement and Control*, 0142331218777570. 16

ZHAO, D., ZOU, T., LI, S. & ZHU, Q. (2012). Adaptive backstepping sliding mode control for leaderâĂŞfollower multi-agent systems. *IET Control Theory & Applications*, **6**, 1109–1117. 7

ZHOU, J. & YAO, X. (2017). A hybrid approach combining modified artificial bee colony and cuckoo search algorithms for multi-objective cloud manufacturing service composition. *International Journal of Production Research*, **55**, 4765–4784. 145

ZHOU, L. & TAN, F. (2019). A chaotic secure communication scheme based on synchronization of double-layered and multiple complex networks. *Nonlinear Dynamics*, 1–15. 83

ZHU, G. & KWONG, S. (2010). Gbest-guided artificial bee colony algorithm for numerical function optimization. *Applied mathematics and computation*, **217**, 3166–3173. 145

ZHU, W., WANG, M. & YANG, C. (2014). Leader-following consensus of fractional-order multi-agent systems with general linear models. In *Proceeding of the 11th World Congress on Intelligent Control and Automation*, 3493–3496, IEEE. 12

ZHU, W., CHEN, B. & YANG, J. (2017). Consensus of fractional-order multi-agent systems with input time delay. *Fractional Calculus and Applied Analysis*, **20**, 52–70. 8, 9, 12, 13, 38, 39, 59, 80, 114

ZOU, W. & XIANG, Z. (2017). Containment control of fractional-order nonlinear multi-agent systems under fixed topologies. *IMA Journal of Mathematical Control and Information*, **35**, 1027–1041. 16

Résumé Etendu

Cette thèse traite de l'identification des paramètre du point de vue de l'optimisation et du contrôle de suivi distribué des systèmes multi-agents d'ordre fractionnaire (FOMASs) en tenant compte des délais, des perturbations externes, de la non-linéarité inhérente, des incertitudes des paramètres et de l'hétérogénéité dans le cadre d'une communication fixe non dirigée/dirigée topologie. Plusieurs contrôleurs efficaces sont conçus pour réaliser avec succès le contrôle de suivi distribué des FOMASs dans différentes conditions. Plusieurs types d'algorithmes d'optimisation de l'intelligence artificielle et leurs versions modifiées sont appliqués pour identifier les paramètres inconnus des FOMASs avec une précision élevée, une convergence rapide et une grande robustesse. Il est à noter que cette thèse fournit un lien prometteur entre la technique d'intelligence artificielle et le contrôle distribué.

Tout d'abord, au chapitre 2, sur la topologie de communication dirigée fixe, le consensus des FOMASs hétérogènes suivant le leader est étudié en ce qui concerne les retards d'entrée sur la base de l'approche par analyse du domaine fréquentiel, où les ordres fractionnaires entre leader et suiveurs sont hétérogènes, ce qui est plus général. Les principales contributions sont les suivantes: premièrement, différent du consensus sans leader des FOMASs et du consensus suivant des leaders avec des ordres homogènes entre leader et suiveurs, le consensus des leaders suivant des FOMASs avec des ordres hétérogènes est étudié et un roman algorithme de contrôle avec un estimateur d'ordre fractionnel est conçu. Deuxièmement, contrairement au consensus sans leader des FOMASs retardés et au consensus des FOMASs suivant les dirigeants sans délai, le consensus des leaders HFOMASs suivant les retards d'entrée est pris en compte sur la base de l'algorithme de contrôle proposé.

Deuxièmement, au chapitre 3, la FOMASs prend en compte la dynamique non linéaire inhérente et les perturbations externes, et le suivi du consensus distribué est étudié sur la base de la méthode directe fractionnelle de Lyapunov sur une topologie de communication fixe non dirigée. Par rapport aux résultats existants, il existe quatre différences principales. Premièrement, différents des principaux résultats concernant les modèles d'ordre entier, les MAS à dynamique fractionnelle sont étudiés. Deuxièmement, contrairement à la plupart des résultats concernant le suivi par consensus des FOMASs sans prendre en compte les perturbations externes, les perturbations externes sont prises en compte dans les FOMASs dans le présent chapitre. Troisièmement, différents de la plupart des résultats où le style des perturbations externes sont connus, nous ne connaissons pas auparavant le style des perturbations externes. Quatrièmement, différents de la plupart des résultats utilisant un protocole de contrôle linéaire, nous proposons deux algorithmes de contrôle non linéaires efficaces.

Troisièmement, au chapitre 4, les paramètres inconnus sont également pris en compte, le suivi distribué par consensus de FOMASs inconnus à retard non linéaire avec perturbations externes est traité sur la base de l'algorithme ABC, où le problème d'identification de paramètre est traité du point de vue de l'optimisation. Par rapport aux travaux existants, la contribution est la suivante. Premièrement, par rapport à la plupart des résultats concernant les MASs d'ordre entier, les MASs différés à dynamique d'ordre fractionnel, les perturbations externes sont prises en compte. Deuxièmement, différents des résultats concernant les retards dans le cas linéaire, le retard dans le cas non linéaire fait l'objet d'une enquête plus approfondie. Troisièmement, la plupart des résultats concernant les FOMASs ne prenaient en compte que les perturbations externes, mais n'ont pas tenu compte des retards en même temps. Quatrièmement, la plupart des résultats existants supposent que les ordres fractionnaires et les paramètres système des FOMASs non linéaires sont connus à l'avance. Dans ce chapitre, les paramètres sont considérés comme inconnus et l'algorithme ABC est utilisé pour identifier les paramètres inconnus de l'inconnu retardé. FOMASs. En outre, il convient de souligner que ce chapitre constitue un lien prometteur entre la technique intelligente artificielle et le contrôle coopératif distribué des FOMASs ou d'autres champs de contrôle.

Quatrièmement, les résultats obtenus ci-dessus supposent que l'entrée de contrôle d'un leader est égale à zéro ou disponible pour tous les suiveurs, ce qui présente certaines limites et manque de flexibilité. Plus précisément, pour amener les suiveurs à accomplir des tâches spéciales, la contribution du responsable doit être non nulle ou variable dans le temps. En outre, les gains du contrôleur peuvent être hétérogènes en raison d'une mise en œuvre imparfaite. Ainsi, au chapitre 5, sous un graphe dirigé fixe, la synchronisation coopérative distribuée de FOMASs hétérogènes incertains, à retard retardé non linéaire, avec un chef de file d'entrée inconnue liée est approfondie sur la base de l'algorithme DE. Par rapport aux travaux existants, notre contribution est la suivante. Premièrement, comparés à la plupart des résultats concernant les MASs d'ordre entier, les MASs retardés avec une dynamique d'ordre fractionnaire, des leaders et paramètres inconnus et des gains de contrôle hétérogènes entrent en jeu. Deuxièmement, les résultats différés avec les FOMASs linéaires sont différents de certains résultats. Le retard temporel avec la dynamique non linéaire est ensuite étudié; Troisièmement, différent de la plupart des résultats sans tenir compte de l'entrée de contrôle du leader, nous supposons que le leader possède une entrée inconnue limitée, ce qui pourrait être plus flexible et plus général dans la synchronisation coopérative distribuée. Quatrièmement, il est différent de la plupart des résultats, où les ordres différentiels sont supposés connus, tandis que dans ce chapitre, les ordres différentiels et les paramètres système sont tous deux considérés comme inconnus, et une méthode d'estimation des paramètres basée sur l'algorithme DE est proposée pour identifier les paramètres inconnus de les FOMASs non linéaires hétérogènes retardés.

Cinquièmement, au chapitre 4, un algorithme ABC efficace est utilisé pour identifier les FOMASs inconnus. Au chapitre 5, l'algorithme DE est sélectionné pour identifier les FOMASs inconnus. Cependant, bien que les AIOAs, telles que ABC et DE, aient démontré des fonctionnalités supérieures à celles des autres méthodes traditionnelles, il n'existe aucun algorithme spécifique permettant d'obtenir la meilleure solution pour tous les problèmes d'optimisation. À savoir, autant que la plupart En ce qui concerne les algorithmes, il est difficile de gérer simultanément le compromis entre exploration et exploitation pour tous les problèmes d'optimisation. De même, il n'y a pas d'exception pour ABC et DE. Par conséquent, au chapitre 6, pour améliorer les capacités d'exploration et d'exploitation, un algorithme hybride adaptatif de colonies d'abeilles artificielles, appelé mABC, est proposé. Ensuite, l'algorithme mABC proposé est appliqué à l'identification des paramètres de FOMASs non linéaires. Les résultats de l'expérience démontrent que l'algorithme mABC proposé permet d'identifier les paramètres inconnus de manière plus précise, efficace et robuste. Par rapport aux travaux existants, notre contribution est la suivante. Tout d'abord, un nouvel algorithme ABC modifié est proposé. Deuxièmement, un nouveau schéma d'identification de paramètre basé sur l'algorithme ABC modifié est proposé. Troisièmement, des tests statistiques non paramétriques sont utilisés pour démontrer les performances de l'algorithme proposé.

Titre: Identification de Paramètre basée sur l'Optimisation de l'Intelligence Artificielle et le Contrôle de Suivi Distribué des Systèmes Multi-agents d'Ordre Fractionnaire

Résumé: Cette thèse traite de l'identification des paramètres du point de vue de l'optimisation et du contrôle de suivi distribué des systèmes multi-agents d'ordre fractionnaire (FOMASss) en tenant compte des délais, des perturbations externes, de la non-linéarité inhérente, des incertitudes des paramètres et de l'hétérogénéité sous une topologie de communication fixée non dirigée/dirigée. Plusieurs contrôleurs efficaces sont con?us pour permettre le contrôle de suivi distribué de FOMASss avec succès dans différentes conditions. Plusieurs types d'algorithmes d'optimisation de l'intelligence artificielle et leurs versions modifiées sont appliqués pour identifier les paramètres inconnus du FOMAS avec une précision élevée, une convergence rapide et une grande robustesse. Il est Íď noter que cette thèse fournit un lien prometteur entre la technique d'intelligence artificielle et le contrôle distribué.

Mots-clés: Identification des paramètres, optimisation de l'intelligence artificielle, suivi du consensus distribué/suivi du leader/synchronisation, retard, perturbations externes, dynamique non linéaire, paramètres inconnus, hétérogénéité.

Title: Parameter Identification based on Artificial Intelligence Optimization and Distributed Tracking Control of Fractional-order Multi-agent Systems

Abstract: This thesis deals with the parameter identification from the viewpoint of optimization and distributed tracking control of fractional-order multi-agent systems (FOMASss) considering time delays, external disturbances, inherent nonlinearity, parameters uncertainties, and heterogeneity under fixed undirected/directed communication topology. Several efficient controllers are designed to achieve the distributed tracking control of FOMASss successfully under different conditions. Several kinds of artificial intelligence optimization algorithms and their modified versions are applied to identify the unknown parameters of the FOMASss with high accuracy, fast convergence and strong robustness. It should be noted that this thesis provides a promising link between the artificial intelligence technique and distributed control.

Keywords: Parameter identification, artificial intelligence optimization, distributed consensus tracking/leader-following consensus/synchronization, time delays, external disturbances, nonlinear dynamics, unknown parameters, heterogeneity.